Effect of different biochars on inorganic nitrogen availability

Makhosazana Princess Aghoghovwia

Dissertation presented for the degree of
Doctor of Philosophy in Soil Science at
Stellenbosch University

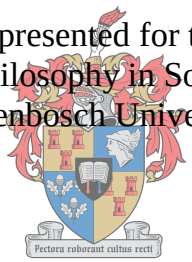

Supervisor: Dr Ailsa G. Hardie
Co-supervisor: Dr Andrei B. Rozanov

Faculty of AgriSciences
Department of Soil Science

March 2018

Declaration

By submitting this dissertation electronically, I declare that the entirety of the work contained therein is my own, original work, that I am the sole author thereof (save to the extent explicitly otherwise stated), that reproduction and publication thereof by Stellenbosch University will not infringe any third party rights and that I have not previously in its entirety or in part submitted it for obtaining any qualification.

March 2018

Abstract

Biochar (a fine pyrolysed organic material) is an amendment used to increase and sustain productivity, reduce environmental pollution and sequester carbon (C) in soils. Successes were reported in improving acidic, sandy and highly weathered soil. However, the effects are strongly influenced by biochar physico-chemical characteristics, which vary widely depending on feedstock and pyrolysis conditions. The main objective of this study was to determine the effects of six biochars (commercially-produced in South Africa under various pyrolysis conditions from maize stover, grape pip, grape skin, pine wood, rubber tyre and sugarcane pith) on nitrogen (N) interactions in a sandy soil. The physico-chemical properties of the above biochars were characterised, three main experiments were conducted to study the effects of biochar addition to soil on (1) inorganic (ammonium and nitrate) N adsorption and desorption of added ammonium and nitrate in aqueous solution; (2) soil C and N mineralisation; and (3) leaching of inorganic N fertiliser.

Maize stover and grape skin chars were suggested to be imperfect biochars due to low total C contents. Characterisation suggested that the sugarcane pith char was either not a suitable raw material for biochar or it was not actually a biochar due to its low stability and high chemical reactivity. However, its high ash content (66%) suggests good nutrient delivery as a soil amendment. Pine wood biochar was the most recommendable because of its low ash (3.5%), high total C (80%) and high surface area (344 m^2 g^{-1}), which all aid nutrient and water holding. However, the grape pip biochar had a low surface area (9.8 m^2 g^{-1}) and the highest fixed-C content (87%) which can be good for soil C storage.

This work shows that despite many positive effects of biochar application to soil reported in literature, the negative effects of such applications on N availability are clear. All six biochars had a stronger nitrate removal affinity (82-89%) compared to ammonium (33-39%). It was also shown that adsorbed nitrate was not desorbable (0.01-0.23%) compared to adsorbed ammonium removal which was around 50% desorbable with KCl. Based on the shape of the adsorption isotherms, physisorption was the suggested mechanism for this behaviour. Competing reactions such as redox reactions in nitrate adsorption and volatilisation of ammonium were also suggested to have influenced the adsorption study results.

Laboratory incubation studies showed that biochars enhanced N immobilisation along with increase in absolute and suppression of relative soil respiration. Pine wood and sugarcane pith biochars were found to reduce inorganic N availability the most due to net N immobilisation. The following biochar property may be linked to N immobilisation: inherent inorganic N in the soil-biochar system. Suppression of relative soil respiration may be due to biochar fixed-C content. Sugarcane pith char had the least effect

on relative respiration because of its low fixed-C content (15.6%). However, the remaining biochars were substantially limiting the relative CO_2 emissions. Rubber tyre char was the best performer in this regard with 75% lower cumulative relative CO_2 emissions compared to the control. Among the plant-derived biochars, grape pip had the lowest CO_2 released with 59% lower cumulative relative CO_2 release.

The leaching column experiment showed that application of biochars at 2.5% (w/w) to sandy soil reduced cumulative leaching of NH_4^+ and NO_3^- by 15-26% and 11-54%, respectively, compared to unamended soil. Using ^{15}N labelled ammonium nitrate, it was found that 0.77-10.81% of applied fertiliser N remained in soil-biochar treatments after leaching. Only the pine wood and sugarcane pith biochar treatments significantly increased N fertiliser retention by 136 and 157% compared to the control soil. Whereas, the rubber tyre biochar treatment significantly reduced N fertiliser retention by 81%. The study concludes that all six biochars make inorganic N less available by mechanisms such as nitrate capture which is related to aromaticity and metal content of the chars and by enhancing biological immobilisation.

Opsomming

Biohoutskool (‘n fyn gepiroliseerde organiese materiaal) is ‘n grondverbeteringsmiddel wat gebruik word om produktiwiteit te verhoog en vol te hou, omgewingsbesoedeling te verminder en koolstof (C) in gronde te sekwestreer. Sukses was aangetoon in die verbetering van suur-, sanderige- en hoogs verweerde grond. Maar, die effekte word egter sterk beïnvloed deur die biohoutskool fisies-chemiese eienskappe, wat hoogs wissellend is, afhangende van biomassa en pirolise toestande. Die hoof doel van hierdie studie was om die effekte van ses houtskole (wat kommersieël in Suid Afrika onder verskillende pirolise toestande vanuit mieliestoppels, druiwepitte, druiweskille, dennehout, rubberbande en suikerriet-sponsweefsel geproduseer word) op stikstof (N) interaksies in die sandground te bepaal. Die fisies-chemiese eienskappe van die bogenoemde biohoutskole was karakteriseer, drie hoof eksperimente was onderneem om die effek van biohoutskool byvoeging op grond op (1) anorganiese (ammonium en nitraat) N adsorpsie en desorpsie van bygevoeg ammonium en nitraat in waterige oplossing te bestuurder; (2) grond C en N mineralisering; en (3) uitloging van anorganiese N kunsmis te bepaal.

Mieliestoppel- en druiweskille houtskole was voorgestel as grensgeval biohoutskole as gevolg van die lae totale-C inhoud. Die eienskappe van suikerriet-sponsweefsel houtskool het aangedui dat dit nie ‘n geskikte rou materiaal vir biohoutskool was nie of dat dit nie eintlik ‘n biohoutskool was nie as gevolg van die lae stabiliteit en hoë chemiese reaktiwiteit. Maar, sy hoë as inhoud (66%) dui egter op goeie voedingstof-lewering as ‘n grondverberingsmiddel. Dennehout biohoutskool was die meeste aanbevelende weens sy lae as (3.5%), hoë totale C (80%) en hoë oppervlakarea (344 m^2 g^{-1}), wat goeie voedingstof- en waterhuishouding bevorder. Maar die druiwepit biohoutskool het ‘n lae oppervlakarea (9.8 m^2 g^{-1}) en die hoogste vaste-C inhoud (87%) wat goed vir C-berging en as ‘n mikrobiese voedselbron kan wees.

Hierdie werk toon dat ten spyte van die baie positiewe effekte van biohoutskool wat in die literatuur aangetoon is, die negatiewe effekte van sulke toediening op N beskikbaarheid ook duidelik is. Hierdie effekte sluit in N immobilisasie en onderdrukking van grondrespirasie. Hierdie effekte was gekwantifiseer en meganismes was ondersoek vir biohoutskole vir van verskillende kwaliteit. Dennehout en suikerriet-sponsweefsel biohoutskole was die beste om anorganiese N beskik baarheid te verminder as gevolg van netto N immobilisasie. Die volgende biohoutskooleienskap kan aan N immobilisasie gekoppel word: inherente anorganiese N in die grond-biohoutskool-stelsel. Onderdrukking van grondrespirasie kan wees as gevolg van biohoutskool vaste-C inhoud. Suikerriet-sponsweefsel houtskool was nie vir die onderdrukking

van koolstofdioksied (CO_2) respirasie as gevolg van sy lae vaste-C inhoud geskik nie. Maar, die biohoutskole wat oorbly het as goeie CO_2-sorbente gedien, wat die CO_2-vrystelling beperk. Rubberband houtskool was die bes-presterende biohoutskool met 75% laer kumulatiewe CO_2 as die kontrole. Tussen die plant-afgeleide biohoutskole, het druiwepit die laagste CO_2 vrygestel met 59% laer kumulatiewe CO_2.

Die logingskolom-eksperiment het gewys dat biohoutskole die kumulatiewe loging van ammonium en nitraat met 15-26% en 11-54%, relatief tot suiwer sand, verminder. Biohoutskole het betekenisvol N kunsmis behou met 0.77-10.81% in die grond-biohoutskool behandelings na uitloging. Die N kunsmis wat oorgebly het was dubbel in die dennehout en suikerriet-sponsweefsel houtskole. Daar was 18-24% totale uitruilbare N wat in die grond oorgebly het na uitloging. Die studie het tot die gevolgtrekking gekom dat al ses biohoutskole die anorganiese N kunsmis onbeskikbaar gemaak het as gevolg van sy hoë nitraat vasleggingsvermoë weens hoë biohoutskool-aromatisiteit, wat nitraat kan verminder en redoks toestande kan bevorder.

Dedication

To

Kesiena Nadeagh Aghoghovwia, my daughter;

and to

Adora, Aphiwe, Brorhie, Dwayne, Dylan, Eguono, Ese, Fejiro, John-Paul, Khanya, Khanyisile, Kutloano, Lethokuhle, Mamuyovwi A., Mamuyovwi E., Melusi, Musawenkosi B., Musawenkosi M., Ngozi, Nhlanhla, Nokukhanya, Nomangwe, Nompumelelo, Nqobile, Ogheneochuko E., Ogheneochuko O., Ogaga, Olanna, Omonuvie, Phumelele, Romeo, Sibonelelwe, Sibongile, Sinenhlanhla, Sinethemba, Sinothile, Siphelelo, Tejiri, Tobore, Tshepang, Ufuoma, Zanele:

May you always use your **IMAGINATION** and be unflinchingly committed to your dreams.
Remember that your best asset is your mind. Develop, expand and nurture it.

Acknowledgements

This project could not have been completed without the diligent guidance of my supervisor, Dr Ailsa Hardie. Her patience and belief in me made all the difference. I wish to also express gratitude to my co-supervisor, Dr Andrei Rozanov, for his strategic interventions.

Thanks to the staff, colleagues and fellow students at the Department of Soil Science, including Dr Marion Carrier, Nigel Robertson† and Charlo Scheepers, for the collegial atmosphere in which to do productive work. Prof Chris du Preez was extremely kind in reading a chapter and giving useful suggestions, and thanks to Prof Cornie van Huyssteen for editing the Afrikaans version of the abstract. Thanks also to Palo Loke for assistance with statistics.

A study on biochar would not have been possible without the supply of biochar! Thanks to Brenn-O-Kem (Pty) Ltd, Department of Process Engineering (Stellenbosch University), PaceOil (Pty) Ltd, and S&P Carbon (Pty) Ltd, Kareedouw (Eastern Cape, South Africa) for donating the biochars used in this study.

Samples on which this study was based were analysed in laboratories across the country. Thanks to Bemlab. The Central Analytical Facilities (CAF) staff assisted with various aspects of sample analysis; many thanks to Dr Cynthia Sanchez-Garrido, Matt Gordon, Herschel Achilles, Riana Rossouw, Madelaine Frazenburg, and Donovan Lombard. The Department of Horticultural Science gave unmitigated access to their lab: many thanks to Renate Smit. My samples were analysed for specific surface area in the Department of Process Engineering, many thanks to Hanlie Botha. Thanks to Dr Paul Verhoeven of the Department of Chemistry for assistance with FTIR. Mike Butler of iThemba LABS was extremely generous in analysing my isotope samples. Warm salutation to the memory of Dr Sven Kaehler who helped with the initial isotope analysis.

The financial assistance of the National Research Foundation (NRF) towards this research is hereby acknowledged. Opinions expressed and conclusions arrived at, are those of the author and are not necessarily to be attributed to the NRF. I also thank the Ernst and Ethel Eriksen Trust for their generous support throughout the project.

† The affable Department of Soil Science lab technician who sadly passed away in January 2018.

My husband, Onoriode, has been a treasure! Thank you for your constant love, patience, firmness and support. Thank you for being my sounding board. Thank you for being my first reader and offering me instrumental advice throughout my dissertation writing process. I am blessed to have you as my companion and to share this life with you. *Meiguo!* Kesiena, my darling daughter, I love you unconditionally. Thank you for teaching me how to be brave, tenacious and stronger than I ever could.

I have been blessed with wonderful parents and siblings whose unwavering faith and moral support have been my strength. Thanks also to my in-laws for their prayers and encouragement.

My stay in Matieland has afforded me the joy of enduring friendship. Ilse Snyman, the “soil-a-thons” and skype-visits-over-tea made this journey less solitary. Thank you for that Christmas Eve when you came to “steal” me away from the lab for a few hours. Hanging out with you and Izak that day has remained unforgettable! You two hold a very special place in my heart. My running sisters and dear friends, Nonjabulo Gule and Welmarie van Schalkwyk, thank you for this sisterhood and more.

And finally, to Jehovah God be all the glory. I am grateful for the gift He has blessed me with and for His daily sustenance.

Table of Contents

List of Figures

List of Tables

List of Abbreviations and Acronyms

AN	Ammonium nitrate
$BaCl_2$	Barium chloride
C	Carbon
CEC	Cation exchange capacity
C/N	Carbon-to-nitrogen ratio
CO_2	Carbon dioxide
d	day
EBC	European biochar certificate
EC	Electrical conductivity
EDTA	Ethylenediaminetetraacetic acid
FWC	Field water capacity
H	Hydrogen
H/C	Hydrogen-to-carbon ratio
HCl	Hydrochloric acid
H_2O	Water
HNO_3	Nitric acid
IBI	International biochar initiative
KBr	Potassium bromide
KCl	Potassium chloride
kHz	kilo Hertz
m	metre

M	Molar
ms	milliseconds
N	Nitrogen
N_2	Dinitrogen (nitrogen gas)
Na_2EDTA	Disodium salt of ethylene diamine tetra acetic acid
NaOH	Sodium hydroxide
NH_3	Ammonia
NH_4^+	Ammonium
NH_4-N	Ammonium-nitrogen
nm	nanometres
NO_3^-	Nitrate
NO_3-N	Nitrate-nitrogen
O/C	Oxygen-to-carbon ratio
S	Sulfur
SEM	Scanning electron microscopy
SOC	Soil organic carbon
SOM	Soil organic matter
TGA	Thermogravimetric analysis
w/v	weight per volume
w/w	weight per weight

Chapter 1
General Introduction

1.1 Background information

Agriculture carries the burden and responsibility to feed the growing global human population, which is expected to reach 8.5 billion people by 2030 (United Nations 2015). To meet the growing food demand farmers have to continuously maintain and improve the soil quality. Biochar is a fine pyrolysed organic material often suggested as a soil amendment (Wu et al 2012; Hansen et al 2014; Butnan et al 2015) to increase and sustain soil productivity as an alternative to organic amendments. It has unique physical and chemical characteristics, such as a high porosity, which enable it to act as an adsorbent (Ahmad et al 2014; Mohan et al 2014; Uras-Postma et al 2014; Umeugochukwu 2016), improve the water retention of biochar amended soils (Pietikäinen et al 2000; Laird et al 2010a) and also increase the nutrient holding capacity of soils (Glaser et al 2002). The biochar characteristics responsible for increasing the nutrient holding capacity of soils are an increase in the quantity of exchangeable cations and carboxylic groups and a high surface area (Ding et al 2016). Any naturally occurring feedstock can be used as the substrate to produce biochar. To make biochar, the feedstock needs to undergo pyrolysis. Pyrolysis is a thermochemical process where biomass is heated at extremely high temperatures under oxygen limited conditions. The product obtained is a black, carbonised product that can then be applied as a soil amendment. Pyrolysis is central to producing biochar since it is during pyrolysis that the carbon (C) is locked into a more recalcitrant form – the black carbon.

Biochar quality not only depends on the feedstock sources, but also varies due to pyrolysis conditions, such as temperature (Laird et al 2009; Manyà 2012). The final biochar product has unique properties depending on the precursor and the production conditions. For example, nutrient retention can be directly affected by biochar pyrolysis temperature. Biochars produced at low temperatures (temperatures up to 400 °C) often have high hydrogen-to-carbon (H/C) ratios, high oxygen contents and a lower surface area. In comparison, high temperature biochars (temperatures up to 700 °C) would be highly carbonised and have low H/C and oxygen and a higher surface area (Chan and Xu 2009; Novak et al 2009).

Carbon sequestration is seen as one of the most important ways to counteract global climate change and its impact of life on earth. There is currently a global interest in the use of biochar as a soil amendment to permanently sequester carbon in soils, as biochar is estimated to persist in soil for hundreds to thousands of years (Laird 2008). Furthermore, research has shown that biochar has beneficial effects on soil fertility of sandy and highly weathered soils (Sohi et al 2010; Laird et al 2010c), which are common in subtropical climates like South Africa. The use of biochar as a soil amendment has the

added benefit of decreasing environmental pollution caused by inorganic fertilisers by enhancing fertiliser retention (Laird et al 2010d).

Recent studies have shown that biochars can adsorb nutrients from applied fertilisers and that sometimes these nutrients can reversibly be released. This characteristic of biochar might give biochar the potential to act as a slow-release fertiliser (Ding et al 2016). In a study by Zhang et al (2015), two oak wood-derived biochars produced at 400 °C and 600 °C adsorbed ammonium (NH_4^+) by 81% and 75%, respectively. The mechanism proposed for NH_4^+ adsorption was π-π electron donor-acceptor interactions associated with fused aromatic carbon rings interacting with ammonia. Furthermore, the biochars were desorbed using a 2 M potassium chloride (KCl) solution and it was found that 18% and 31% NH_4^+ was desorbed from the biochar produced at 600 °C and 400 °C, respectively.

1.2 Motivation

The foundation for this research is built on my Masters study which demonstrated the potential of pine wood biochar as an amendment of acidic, sandy soil (Sika 2012). It was found that biochar improved the nutrient holding capacity of a sandy soil and thereby improved its fertility. Biochar is a highly porous material while the carboxylate groups found in biochar provide cation exchange capacity (CEC), and are an important source of biochar's high nutrient retention ability (Glaser et al 2001). It was also reported that pine wood biochar can significantly retard inorganic nitrogen (N) fertiliser leaching from a sandy soil (Sika and Hardie 2014). This is important in reducing environmental pollution caused by leaching of chemical fertilisers. However, it was also found that the biochar reduced the amount of exchangeable inorganic nitrogen, especially nitrate, in the sandy soil. To better understand this phenomenon, six contrasting, locally-produced biochars were investigated in the current study to quantify the potential of biochar to behave in any particular manner as affected by feedstock and pyrolysis conditions. The nutrient sorption characteristics (Yao et al 2012) of individual biochars, the nutrient cycling potential (Gaskin et al 2008) and other characteristics should be investigated prior to use as a soil amendment.

Soil carbon and nitrogen mineralisation rates are influenced by biochar application because they determine the C and N pools microorganisms have access to. The biochar C/N ratio is one key characteristic that determines whether N mineralisation or N immobilisation will occur after biochar is applied to soil. It has been reported that when a fresh biochar with a high C/N ratio undergoes microbial decomposition, then decreased mineralisation and increased immobilisation of soil N occurs (Bruun et al 2012). Biochar in soils generally have low carbon dioxide-C respiration rates compared to the control due to lower amounts of labile C (Lehmann et al 2011). Since biochar properties affect soil C and N mineralisation, they too need to be investigated.

Acidic sandy soils and highly weathered soils can be a bane. The latter are often associated with low CEC due to the presence of low activity kaolinitic clays (Bronick and Lal 2005) and low soil organic carbon (SOC) levels (Chan and Xu 2009; Novak et al 2009; Van Zwieten et al 2010b). The use of biochar to ameliorate acidic sandy soil has been shown as a way to optimising yields (Chan et al 2007; Gaskin et al 2008; Van Zwieten et al 2010b) and long-term storage of carbon in soils.

1.3 Problem statement

The effect of reduced N leaching upon application of biochar to soils is known (Sika and Hardie 2014). However, it remains to be established what mechanisms of interaction exist between biochar, soils and fertilisers to achieve enhanced productivity and long-term capture and storage of carbon in soils. Furthermore, although biochar can be made from a variety of sources, feedstock that are commonly used to produce biochar in South Africa are invasive tree species such as *Acacia* and *Eucalyptus* (Lusiba et al 2016), *Pinus* (Sika and Hardie 2014), black wattle and vineyard prunings (Uras et al 2012), and sugar cane bagasse (Carrier et al 2012). Different companies manufacture these biochars found in the South African market and they use various feedstocks and pyrolysis conditions to produce the biochars. The effectiveness of these commercially available biochars on inorganic N retention in soil is not clearly understood, especially because various feedstocks and pyrolysis conditions are used.

1.4 Objectives and key questions

The main goal of this research was to establish the effects of various locally-produced and readily-available biochars manufactured from different feedstocks and under different pyrolysis conditions on nitrogen dynamics in an acidic, sandy soil. The objectives of the study were therefore:

- To determine variation in characteristics of commercially produced biochars in South Africa.
- To determine the inorganic N sorption characteristics of the different biochar types. What mechanisms and processes are responsible for retaining N?
- To investigate which biochar properties influence carbon and nitrogen mineralisation in biochar amended soil.
- To assess the effect of biochars on leaching of mineral N fertiliser in soil. To what extent does leaching occur and how much exchangeable N remains in the soil after leaching?

1.5 Expected significance

The research is expected to help build a sound scientific knowledge base of locally produced biochars that can be used in South Africa and across the continent. The knowledge generated from this research can further be used to compile recommendations for biochars in South Africa similar to the guidelines

set by international organisations that provide information, data and clear definitions for industrially-produced biochars to help establish criteria for the utilisation of biochars in agricultural development and carbon sequestration projects. This study will contribute to our understanding of the mechanisms and processes involved in biochar-soil-fertiliser interactions. An understanding of these interactions will help to improve methods for sustainable, environmentally friendly, and improved agricultural management practices of highly weathered and sandy soils. This can lead to greater economic and environmental successes of commercial and subsistence farming. Biochar production can assist in waste management by using agricultural wastes to produce biochar, create business and employment opportunities, and even generate electricity due to the intense energy release during the production of biochar. Furthermore, biochar application to soils in South Africa gives prospects for wider roll-out of pyrolysis plants (including mobile units) – a current technology driven by research and development, where industry and agriculture can collaborate.

1.6 Structure of dissertation

The dissertation comprises of seven chapters as outlined in Figure 1.1. In Chapter 1, a brief introduction into biochar is given. This chapter also highlights the motivation for this study. An overall review of the fundamental literature of this study is given in Chapter 2. Chapter 3 marks the beginning of the four research units discussed in this study. A physical and chemical characterisation of the six biochar materials is reported in Chapter 3. The methods used in this research were primarily based on the information from scientific literature. In Chapter 4, the properties investigated from the characterisation of the biochars are examined by way of a sorption-desorption experiment. This research unit focuses on the ability of biochar to sorb mineral N from solution and also to desorb the N with 2 M KCl. The short-term effect of the biochars on soil C and N mineralisation is investigated in Chapter 5. Each biochar was mixed with the topsoil sandy soil at the same rate and incubated. Chapter 6 demonstrates the effect of the six biochars on the leaching of ^{15}N-labeled ammonium nitrate and post-leaching mineral N availability in sandy soil. General conclusions from the study are summarised in Chapter 7. The second part of this chapter highlights recommendations for future research in this field.

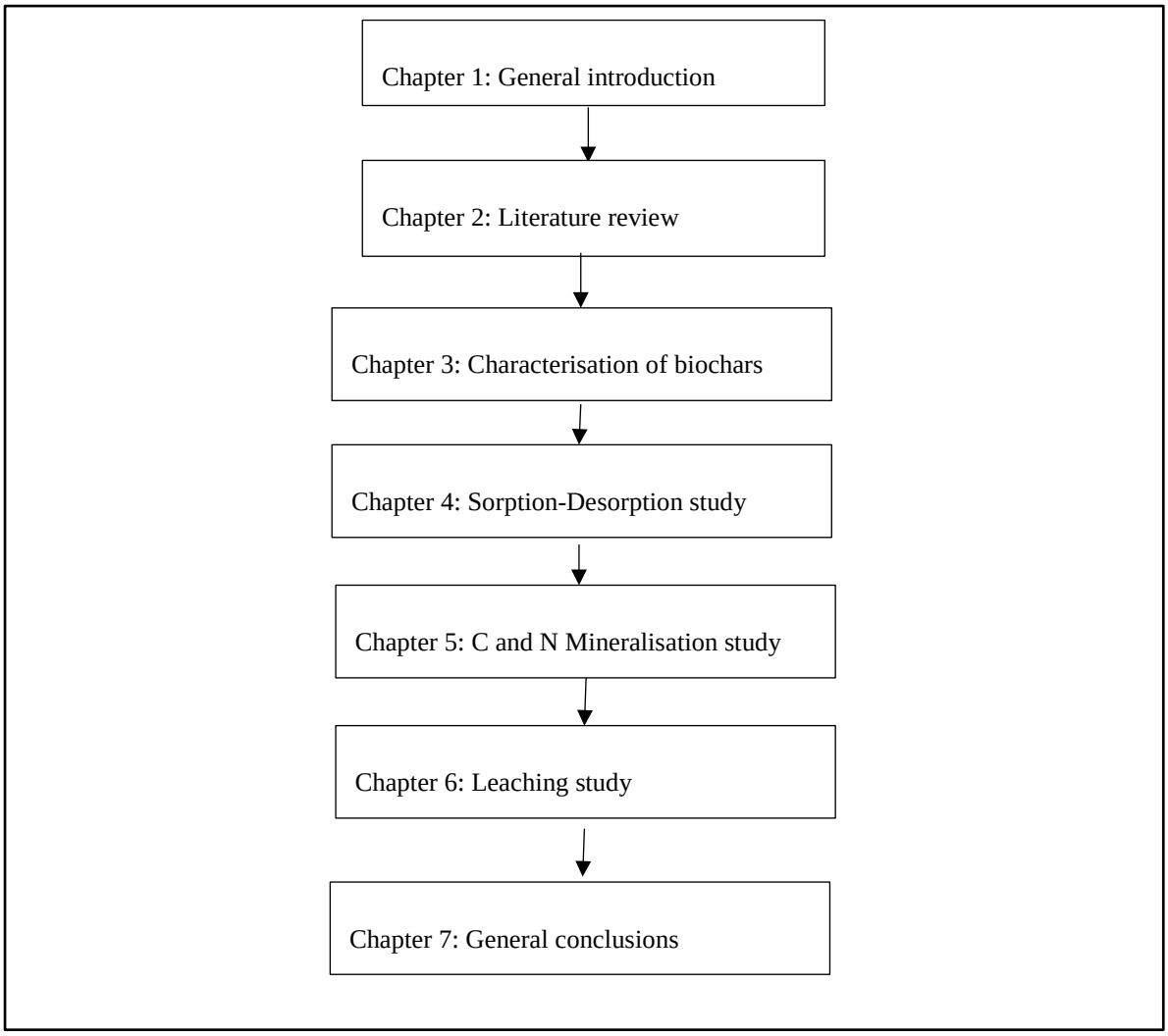

Figure 1. 1: Layout of the dissertation.

Chapter 2
Literature Review

2.1 Introduction

Interest into the use of biochar has become increasingly popular. Most notably, the use of biochar in agricultural soils has been suggested as a long-term strategy to promote soil C sequestration due to its recalcitrant nature (Glaser 2007; Steiner et al 2008b; Vaccari et al 2011). When biochar is added to soil, the first most common noticeable chemical change is that the pH increases, thus biochar limes soil (Yuan et al 2011). Biochar is chemically and microbially stable in soil environments (Conz et al 2017). It provides soil with a persistent soil organic matter (SOM) rich pool. In addition, studies have found that biochar can combat nutrient leaching (losses) especially of nitrate, a highly mobile macronutrient (Laird et al 2010b; Sika and Hardie 2014), and also decrease the uptake of potentially toxic elements (Choppala et al 2012; Khan et al 2014; Puga et al 2015). The synonyms for biochar include char, charcoal, black carbon, and carbon black.

Biochar stems from an extensive history. In the pre-Columbian era, nomads in central Amazonia would slash and burn artefacts instead of carrying them to their next destination to ease the load. Examples of the types of artefacts they would burn are organic wastes, wood, excrements and animal bones (Neves et al 2003; Glaser 2007). This ancient practice is an early example of the formation of anthropogenic soils. In particular, this practice led to the formation of the commonly known Amazonian Dark Earth or *Terra Preta* soils (Woods and McCann 1999; Glaser and Woods 2004; Glaser 2007). It is from this concept that modern-day biochar arises. Biochar is the pulverised charcoal applied to the soil for crop production. The idea behind the technology is based on the recreation of *Terra Preta*. The term *Terra Preta* loosely translates to dark earth and this means to create soils that are mostly dark in colour, high in organic matter and therefore nutrient rich (Glaser and Birk 2012).

Unlike the outdated slash and burn practices where biomass was converted to ash through combustion, modern day biomass undergoes slash and char processes to produce biochar (Lehmann et al 2002) which is produced industrially by pyrolysis. Pyrolysis is the umbrella term representing various technologies responsible for the conversion of biomass to biochar.

Similar to the black carbon rich *Terra Preta* soils of the Amazon, biochar should ideally remain in the soil long enough to provide long-term chemical, physical and biological changes in soil (Hammes and Schmidt 2009). An understanding of the stability of biochar application in soil is important because it allows for better maintenance of the global C budget (Czimczik and Masiello 2007; Major et al 2010). This allows for a determination of the duration that C may remain sequestered in the soil and thereby

influence the reduction of greenhouse gas emissions to aid in the alleviation of climate change (Lehmann et al. 2009). In effect, this would aid in managing the application of black carbon for increasing its potential as a long-term C sink of atmospheric CO_2 (Lehmann et al 2006). The application of biochar to a soil system appears to create a carbon sink because there is an increase in the soil organic carbon content over time due to C moving into a soil system (Powlson et al 2011).

Lehmann and Joseph (2009) suggested that for biochar to contribute to climate change mitigation, two prerequisites should be fulfilled. The first is that vegetative biomass had to be cultivated at the same rate as it was being pyrolysed. This is because photosynthesis in plants is responsible for the conversion from atmospheric CO_2 to an organic C form. The second prerequisite is that the biochar product had to be considerably more stable than the initial feedstock material from which it was produced.

2.2 Biomass for pyrolysis

Since the industrial revolution there has been an overwhelming increase in fossil fuel products consumption and wastage. It is estimated that by the year 2025 there will be 4.3 billion urban residents who will generate 1.42 kg of municipal solid waste per person per day (Hoornweg and Bhada-Tata 2012). Clearly waste build up is inevitable. However, when the solid wastes comprise of plant-derived and reusable resources, innovative solutions such as pyrolysis technology can be used to handle these wastes, and thus manage their build-up.

Plant biomass is made up of a combination of low molecular weight substances (such as organic extractives and ash) and macromolecular substances (such as polysaccharides and lignin) (Mohan et al 2006). The polysaccharides comprise of cellulose and hemicelluloses. During pyrolyisis, the degradation of each component of plant biomass occurs at different rates and by different pathways (Bridgwater et al 1999). Schematic representations of the main reactions that occur and the products formed over the temperature ranges during pyrolysis are shown for cellulose (Figure 2.1), xylan (the major component of angiosperm hemicelluloses) (Figure 2.2), and lignin (Figure 2.3). Results from KBr-pelletised FTIR spectra of celluloses, hemicelluloses and lignin indicate the main functional groups found (Table 2.1). In summary, the cellulose had the strongest O-H and C-O stretches; while the hemicelluloses had the highest C=O compounds, and lignin was highest in methoxyl-O-CH_3, C-O-C stretching and aromatic ring containing compounds (Yang et al 2007).

Virtually any organic biomass can be pyrolysed to produce biochar. Studies have been done on over 100 types of biomass that have been made into biochar from various sources ranging from agricultural residues such as poultry litter and peanut hulls (Gaskin et al 2008), and rice husk and rice straw (Fu et al 2011; Jindo et al 2014); forestry wastes such as poplar (Conte et al 2014) and pine (Gaskin et al 2008; Alburquerque et al 2014) wood chips; as well as sewages sludge (Yuan et al 2013; Srinivasan et al

2015). An obvious positive knock-on effect of pyrolysing biomass is that it helps to reduce and reuse wastes which would ordinarily be discarded.

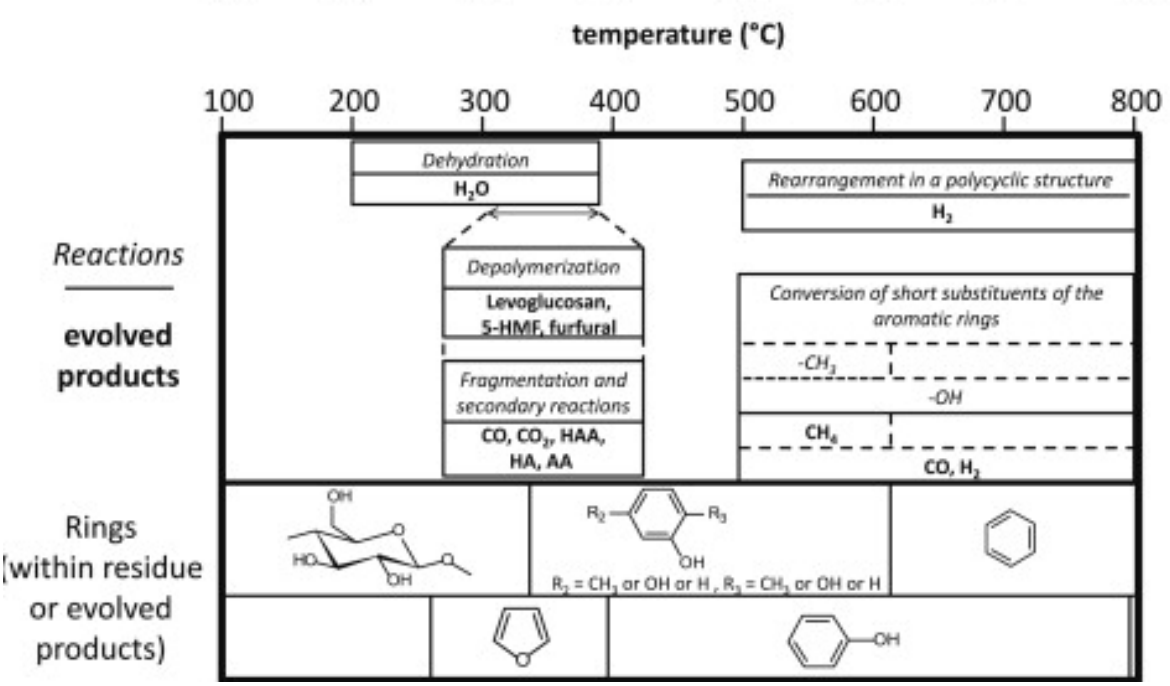

Figure 2. 1: Reactions that take place during pyrolysis of cellulose and the formation of chemical structures with increasing temperature; HAA: hydroxyacetaldehyde, HA: hydroxyacetone, and AA: acetaldehyde.[2]

[2] Reprinted from Renewable and Sustainable Energy Reviews, Vol. 38, Collard, F. and Blin, J., A review on pyrolysis of biomass constituents: Mechanisms and composition of the products obtained from the conversion of cellulose, hemicelluloses and lignin, Pages 594-608, Copyright 2014, with permission from Elsevier.

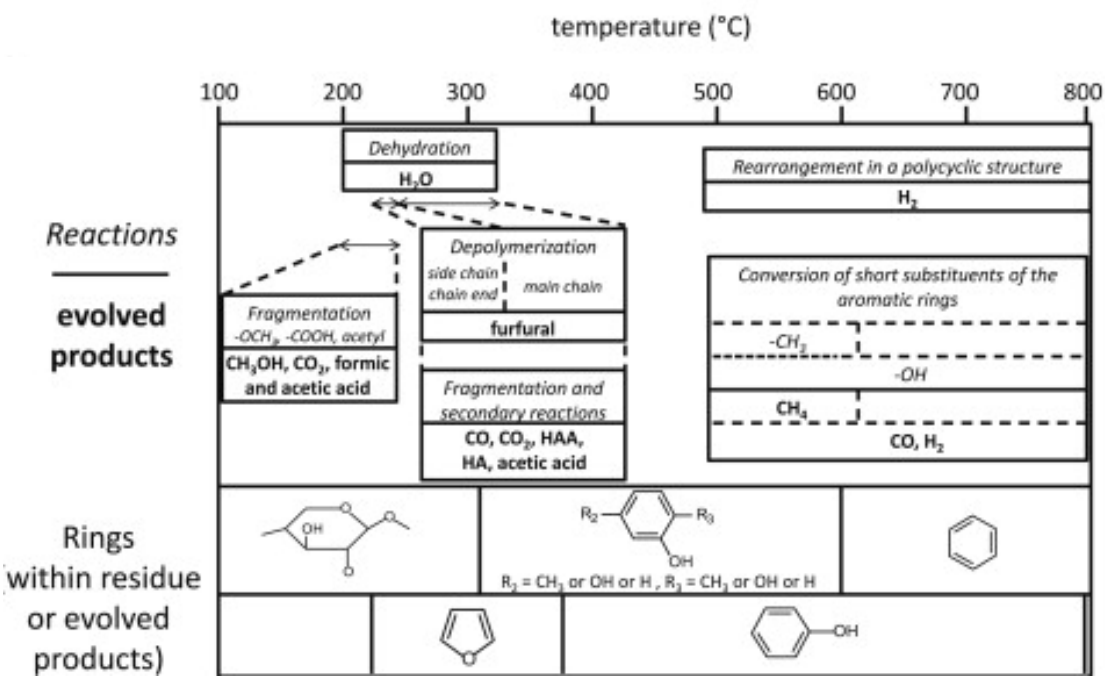

Figure 2. 2: Reactions that take place during pyrolysis of the hemicellulose xylan and the formation of chemical structures with increasing temperature; HAA: hydroxyacetaldehyde, HA: hydroxyacetone, and AA: acetaldehyde.[3]

[3] Reprinted from Renewable and Sustainable Energy Reviews, Vol. 38, Collard, F. and Blin, J., A review on pyrolysis of biomass constituents: Mechanisms and composition of the products obtained from the conversion of cellulose, hemicelluloses and lignin, Pages 594-608, Copyright 2014, with permission from Elsevier.

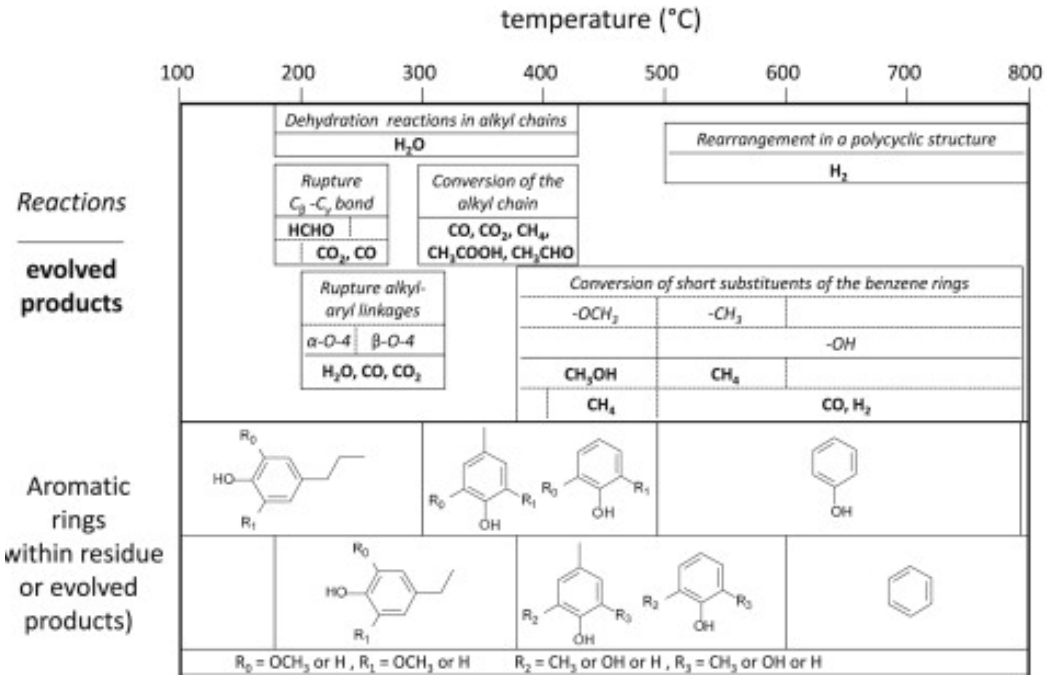

Figure 2. 3: Reactions that take place during pyrolysis of the lignin and the formation of chemical structures with increasing temperature; HAA: hydroxyacetaldehyde, HA: hydroxyacetone, and AA: acetaldehyde.[4]

[4] Reprinted from Renewable and Sustainable Energy Reviews, Vol. 38, Collard, F. and Blin, J., A review on pyrolysis of biomass constituents: Mechanisms and composition of the products obtained from the conversion of cellulose, hemicelluloses and lignin, Pages 594-608, Copyright 2014, with permission from Elsevier.

Table 2. 1: Functional groups of celluloses, hemicelluloses and lignin from FTIR spectra (Redrawn from Yang et al 2007)

Wave number (cm^{-1})[a]	Functional groups	Compounds
3600-3000 (s)	OH stretching	Acid, methanol
2860-2970 (m)	C-H stretching	Alkyl, aliphatic, aromatic
1700-1730 (m)		
1510-1560 (m)	C=O stretching	Ketone and carbonyl
1632 (m)	C=C	Benzene stretching ring
1613 (w), 1450 (w)	C=C stretching	Aromatic skeletal mode
1470-1430 (s)	O-CH_3	Methoxyl-O-CH_3
1440-1400 (s)	OH bending	Acid
1402 (m)	CH bending	
1232 (s)	C-O-C stretching	Aryl-alkyl ether linkage
1215 (s)	C-O stretching	Phenol
1170 (s), 1082 (s)	C-O-C stretching vibration	Pyranose ring skeletal
1108 (m)	OH association	C-OH
1060 (w)	C-O stretching and C-O deformation	C-OH ethanol
700-900 (m)	C-H	Aromatic hydrogen
700-400 (w)	C-C stretching	

[a] s: strong, m: middle, w: weak

2.2.1 Maize stover

Maize is the most important grain crop and staple food produced in South Africa. Eight million tons of maize grain are grown annually (du Plessis 2013). The crop residues that remain in the field after harvesting maize consisting of cobs, husks, leaves and stalks, are referred to as the maize stover. Pyrolysing maize stover is a good way of handling the residues and recovering the nutrients in it. In addition, choosing the ideal pyrolysis conditions is important to achieve the ideal biochar properties in relation to soil amendment. A study comparing the differences between maize stover biochar produced by fast pyrolysis at 450° C and another made by gasification at 700 °C found that the lower pyrolysis temperature of 450 °C produces biochar with a CEC twice as much as the high pyrolytic char. Therefore, when the fast pyrolysis biochar is added to soil, it can improve soil CEC and contribute to C sequestration (Lee et al 2010).

2.2.2 Grape pip and Grape skin

The grape wine and table grape industries are a thriving global market. World wine production was estimated at 28 billion liters in 2015 (OIV 2015). On the other hand, the global table grape industry has an economic value of about US$11.2 billion (Fernandez-Stark et al 2016). Winemaking cellars and juice factories generate large amounts of grape residues (such as unfermented seeds from the making of white wine, and grape skins from juice processing) that usually go to waste. This creates disposal problems of agricultural residue that has no nutritional value. To date, very little literature on grape pip (seed) and grape skin biochars is available. This research aims to fill this knowledge gap.

2.2.3 Pine wood

Wood is generally a composite material made from 65-75% carbohydrate polymers and oligomers, 18-35% lignin and 4-10% of low molecular weight compounds. The specific weight percent of cellulose, hemicellulose and lignin differs with each wood species (Mohan et al 2006). Pine wood (*Pinus* spp.) biochars produced at similar temperatures have consistent results. Angst et al (2014) studied a pine wood biochar produced at 550 °C and found that the pH was 7.9, ash 17.0% and BET 5.0 m^2 g^{-1}. Similar properties were reported by Mukome et al (2013) where pine wood pyrolysed between 500-650 °C had a pH of 7.9, ash at 17% and BET 4.9 m^2 g^{-1}. For wood-derived biochars, a low pyrolysis temperature is associated with a low surface area (Mukome et al 2013). Although pine wood biochars are usually alkaline, Chintala et al (2014) found that pine wood biochar made using microwave pyrolysis was acidic (pH 5.80) because of incomplete oxygenation of the feedstock and low ash content (14.5%).

2.2.4 Rubber tyre

Annually, an estimated 1.5 billion tyres are produced (Williams 2013), while 11 million tyres become waste (end-of-life scrap) tyres (REDISA 2011). Given that vehicle owners replace their tyres periodically, it is unsurprising that rubber tyres constantly feed landfills. Waste tyres are non-biodegradable and can cause harm if ignited because of the noxious gases released to the environment. Rubber tyres are a source of energy and chemical compounds, and when they undergo thermal decomposition, it is possible to recover useful products (Roy et al 1990). Therefore, pyrolysis technology can be used to recycle used vehicle tyres.

In a study conducted by Shah et al (2006), waste tyres were pyrolysed at 450 °C with the aim of determining its adsorption capacity of methylene blue. After pyrolysis, the carbon black was found to be contaminated with inorganic additives. It was then decided to demineralise the carbon black with acid and activate it at 900 °C. When compared to a commercial activated carbon, the results of this

experiment revealed that the adsorption capacity of methylene blue on acid-treated carbon black was greater.

2.2.5 Sugarcane pith

The sugarcane industry in South Africa is worth R12 billion and falls within the top 15 sugar producing countries out of an estimated 120 countries worldwide (SASA 2017). When the sugarcane plant is harvested, the sugarcane stalks are pressed to extract juice that is taken to sugar factories and what remains is the sugarcane bagasse (Kameyama et al 2012). Sugarcane bagasse is made up of the inner pith, which is a soft spongy component; and the outer rind which is a hard fibrous substance (Wirawan et al 2010). In the 1960s, Miller and Tilby invented sugarcane separation which involves separating the long rind fibres from the short internal fibres and pith (Donefer 1986). When sugarcane bagasse is depithed, the fibres from the rind are often used for paper or manufacturing of boards, while the pith is used as livestock feed (Donefer 1986). Pyrolysis of sugarcane bagasse is commonly done, but it is not common to find biochar made from the sugarcane bagasse pith. This research aims to study sugarcane pith biochar.

2.3 Pyrolysis

The word “pyrolysis” is derived from the Greek words ‘*pyr’* which means fire, and ‘*lye’* which means separating (Sarma 2004). It describes an exothermic and irreversible process that involves the thermochemical transformation of organic waste products under oxygen deprived conditions (Lehmann and Joseph 2009). The process of pyrolysis essentially requires a solid product, the biomass feedstock (such as wood), and heat energy as inputs. The outputs or products of the pyrolytic process are: a solid, charcoal; liquid which is the bio-oil and; non-condensable gases, the biogas (also called syngas). Ultimately, biomass feedstock that undergoes pyrolysis changes in both its physical nature and chemical composition.

The chemical nature of the initial organic biomass is a precursor for the degree of reactivity of the biochar produced (Downie et al 2009). During thermal degradation of biomass, the organic matter composition undergoes a series of structural, physical and chemical changes. Cellulose and lignin structures are destroyed first, then aromatic structures appear (Paris et al 2005), and furan-like compounds become visible (Baldock and Smernik 2002). In general, pyrolysis causes aliphatic C to be converted to aromatic C, followed by a decline in organic C mineralisation rates (Chan and Xu 2009).

During pyrolysis, structural changes to the hemicellulose, celluloses and lignin take place. Temperature is one of the factors responsible for the condition of the final biochar product formed (Lua et al 2004; Brown et al 2006). When temperatures reach 120 °C, the organic materials lose their chemically bound moisture. At temperatures between 200 and 260 °C, hemicelluloses are degraded, while cellulose is broken down between 240 and 350 °C and lignin between 280 and 500 °C (Sjöström 1993).

Once the charcoal produced during pyrolysis is crushed to smaller sizes and applied to soil, it becomes known as biochar. Bio-oil is a hydrophilic and oleophobic liquid mixture of polar organics and water (Bridgwater et al 1999). The bio-oil produced from pyrolysis has multiple uses. It can be used as a biofuel instead of using conventional fuels, such as in existing industrial boilers, or it can also be used as a chemical feedstock (Bridgwater et al 1999; Laird et al 2009). The biogas (or syngas) also provides a source for energy production. The bio-oil and charcoal can each be used as a fuel or feedstock, and the gas can be recycled back into the system, therefore, no waste is generated from pyrolysis (Mohan et al 2006).

The quantities and quality (in terms of morphology, structure, properties) of charcoal, bio-oil and biogas that are produced during pyrolysis are primarily dependent on the materials and methodology used. The materials refer to the biomass feedstock, which strongly influences the initial biochar characteristics (Gaskin et al 2008). The methodology refers to the technology used and pyrolysis conditions of pyrolysis peak temperature, length of time, heating rate, etc. which give rise to pyrolysis products, such as biochar, that have different physico-chemical properties (Brown 2009). Mechanised systems have replaced old ways of making biochar and the advantage is that modern systems are highly energy efficient compared to traditional kilns. As different pyrolysis conditions exist, there is no precise definition of the various pyrolysis methodologies by way of specific pyrolysis peak temperatures, particle residence times, heat transfer, heating rates, etc. and therefore the terms used to describe the different pyrolysis methods are broad and arbitrary (Mohan et al 2006). The most common of these pyrolysis methods are slow pyrolysis, fast pyrolysis and vacuum pyrolysis.

2.3.1 Slow pyrolysis

Slow pyrolysis is a common pyrolysis method that is primarily used for the production of charcoal (Mohan et al 2006). Slow pyrolysers are usually batch systems known as charcoal kilns (Laird et al 2009), or continuous systems such as drum pyrolysers, or screw pyrolysers (Brown 2009). They use slow heating (minutes to hours) of biomass to temperatures of approximately 400 °C (Laird et al 2009), with an ideal temperature of 500 °C (Lee et al 2013) in an anoxic environment. A long residence time of biomass during slow pyrolysis results in a completely pyrolysed biochar with little labile C and smaller possibility of causing microbial immobilisation of soil N (Bruun et al 2012). In addition, slow

pyrolysis is described by long solid and gas particle residence times that range from several minutes to hours (Mohan et al 2006).

2.3.2 Fast pyrolysis

There are some considerable differences between fast and slow pyrolysis. The foremost difference is that the technology used for fast pyrolysis is generally more complicated than that used for slow pyrolysis precisely because fast pyrolysis technology is optimised for bio-oil production (Mohan et al 2006; Laird et al 2009). The working principle of fast pyrolysis is well described by Mohan et al (2006): (1) biomass is finely ground to withstand the very high heating and heat transfer rates used; (2) the pyrolysis reaction temperature is carefully controlled to remain in the range of 425-500 °C; (3) thereafter, short vapour residence times of about < 2 s are employed; (4) and lastly, the pyrolysis vapours and aerosols are cooled rapidly, resulting in the formation of bio-oil, primarily, as well as some charcoal. Fast pyrolysis can be manipulated to give even higher oil yields by using even higher heating rates and reaction times of about 500 °C as well as short residence times to minimise secondary reactions (Bridgwater et al 1999). The amounts of fast pyrolysis products produced range between 60 and 75 wt % of bio-oil, 15-25 wt % of charcoal, and 10-20 wt % of gases, depending on the feedstock used (Mohan et al 2006).

Preparation for producing fast pyrolysis biochars is very important. If the pyrolysis temperature is too low, or if the biomass feedstock particles are too big, then a partially pyrolysed biochar may result, and the consequence of that would be a reduced potential for soil C sequestration because of the increased labile C (Bruun et al 2011). Furthermore, application of a partially pyrolysed biochar may result in microbial immobilisation of soil N (Laird et al 2009).

2.3.3 Vacuum pyrolysis

Vacuum pyrolysis is a type of fast pyrolysis that differs because it has slow heating rates and requires large biomass particles (Bridgwater et al 1999). It is unique from the other pyrolysis methods discussed because its installation has a vacuum pump where an inert gas such as nitrogen is used to remove volatile gaseous residues and minimise the extent of secondary reaction products (such as aromatisation and recondensation reactions, thermal cracking, and gas phase collision) (Roy et al 1999). Thus, vacuum pyrolysis produces a biochar of high quality and very little bio-oil and gas.

2.4 Physico-chemical properties of biochar

The production of two biochars that are the same, physico-chemically, is only possible when the biomass and pyrolysis conditions are precisely the same. Any change in biomass, handling, or pyrolytic

processing, no matter how seemingly small, will result in a completely different biochar. This makes it important to understand what type of biochar has been produced by examining its various physical and chemical properties.

2.4.1 Elemental contents of biochar

During pyrolysis of the starting organic matter (biomass) used to produce biochar, the biochar volume is reduced and its mass is primarily lost in the form of volatile organics. The biochar that is formed retains the mineral and C framework of the starting biomass (Downie et al 2009). Pyrolysing organic matter renders the C in the biomass significantly higher than fresh, unpyrolysed organic matter. This causes an increase in the recalcitrance of C in the biomass due to the changes in the composition of the biomass induced by pyrolysis (Lehmann et al. 2009). And because biochar contains large amounts of C, macro- and micro-nutrients, it may directly supply a source of plant-available nutrients once applied to soil (Gaskin et al 2007). Sollins et al. (1996) identified certain mechanisms responsible for stabilising organic matter applied to the soil, and thereby increasing its residence time. These include its inherent recalcitrance, spatial separation of decomposers and substrate and the interaction of organic matter with mineral surfaces.

Soil carbon sequestration is a term that describes an increase in soil organic carbon content resulting from a change in land management practices (Powlson et al 2011). Biochar has been shown to provide potential long-term C sequestration (Lehmann et al 2006). This suggests that soils amended with biochar increase the soil C storage and thereby contribute to the mitigation of climate change (Lehmann et al 2006; Gaunt and Cowie 2009). However, Powlson et al. (2011) argues that climate change mitigation is only valid in soils when the land management practices result in an additional net transfer of C from atmospheric CO_2 to land (soil and vegetation).

The labile carbon fraction refers to the portion of biochar that undergoes short-term abiotic or biotic mineralisation to carbon dioxide. The labile fraction in biochar is present in a number of forms. These include mineral carbonates, organic molecules and microcrystalline structure carbon. Mineral carbonates are water soluble and occur on the biochar surface or associated with biochar pores. Organic molecules contain H and O, are water soluble and mineralised by soil fauna. The amorphous or microcrystalline structure of biochar is the more stable fraction of biochar and is mineralised on particle surfaces. This surface oxidation means that oxidised functional groups are formed, or that clay complexes form (Joseph et al 2009).

Several reasons are deemed necessary for classifying black carbon by its labile fraction. Firstly, according to C accounting, it allows for the determination of the rate of biochar decay (Gaunt and Cowie 2009). Secondly, it allows for the determination of the organic C available fraction as a source of C for

microorganisms (Thies and Rillig 2009). Some biochars have been found to possess toxic metals that may inhibit germination or maturity of plants (Girard et al 2006). Also, because the labile fraction is generally unstable, knowing its C composition allows for the determination of germination facilitation (Flematti et al 2004) and energy provision for microorganisms (Steiner et al 2008a). The pyrolysis conditions and biomass parent material influence the (predicted) behaviour (or stability) of biochar. For example, increasing pyrolysis temperatures leads to lower H/C and O/C ratios (Spokas 2010), making biochars less prone to degradation. This trend is seen in Mukome et al (2013) where 12 commercially available (non-wooded- and wood-derived) biochars demonstrate that pyrolysis temperature is responsible for the decreasing H/C ratios, indicating demethylation, and decreasing O/C ratios, showing decarboxylation (Figure 2.4). The schematic representation of this effect is known as the Van Krevelen diagram and it represents the O/C and H/C ratios of charred materials plotted against each other based on their elemental composition to understand their structural changes.

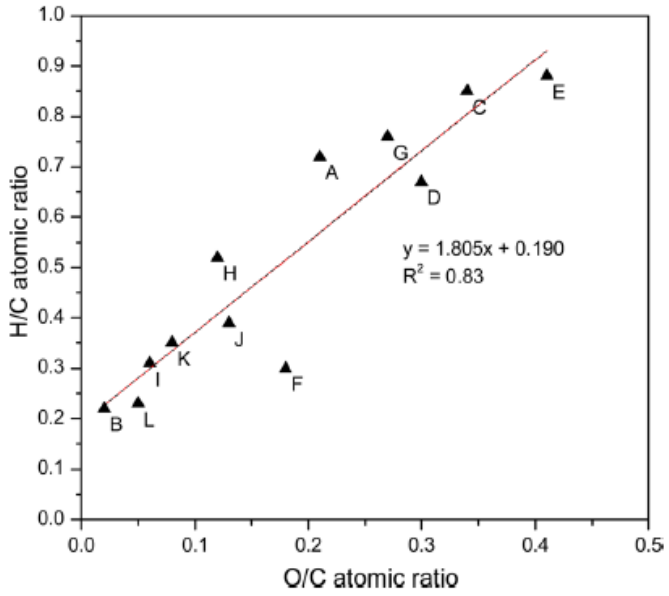

Figure 2. 4: Van Krevelen diagram of 12 commercially available biochars derived from a range of non-wooded and wooded materials produced at varying temperatures.[5]

[5] Reprinted (adapted) with permission from Journal of Agricultural and Food Chemistry, Vol. 61, Mukome et al., Use of chemical and physical characteristics to investigate trends in biochar feedstocks, Pages 2196-2204. Copyright (2013) American Chemical Society.

2.4.2 Surface chemistry of biochar

Biochar processes and physico-chemical properties are often interconnected. An example of this is evident when long-term natural oxidation of biochar occurs. Cheng et al (2008) found that biochar in soils for 130 years resulted in the formation of carboxylic and phenolic functional groups compared to new biochar or biochar incubated for one year. The reason for the increase in the oxygen-containing functional groups is due to the changes in the elemental composition of the biochar over time where the amount of oxygen was for the new biochar increased from 7.2% to 24.8% for the long-term oxidised biochar. Biochar oxidation was also responsible for the decrease in the C content from 90.8% to 70.5%. These effects cumulatively led to the biochar having an increased adsorption capacity, increased CEC, and after one year of incubation, the development of surface negative charge.

Biochar surface area and pore size distribution is also affected by pyrolysis temperature and feedstock type. High temperature biochars (600-700 °C) generally produce high surface area biochars compared to low temperature biochars (< 400 °C (Novak et al 2009; Lehmann et al 2011). A comparison of biochars produced at 600 °C made from plant material (maize stover and oak wood) and a manure-derived biochar (from poultry litter) showed that the plant-derived biochars had higher total surface area (527 and 642 m^2 g^{-1}, respectively) than the poultry litter biochar (94 m^2 g^{-1}) (Lehmann et al 2011). A high biochar surface area has practical implications in agriculture because when it is applied to a soil with large amounts of macropores (Glaser et al 2002), then the retention of soil water (and consequently nutrients) is improved.

2.4.3 Spectroscopic analysis of biochar

Biochar may also be characterised as having unordered or ordered graphene layers (Lehmann et al. 2009). The unordered graphene layers are classified as amorphous structures and as turbostratic crystallites. These unordered structures are typically found at pyrolysis temperatures less than 600° C and show a high stability of biochar (Paris et al 2005). Ordered sheets of biochar have been found to dominate at pyrolysis temperatures above 600 °C (Kercher and Nagle 2003). Although little research has been conducted on the importance of the crystal structure of biochar for its recalcitrance, some studies have shown that biochar is widely characterised by unordered graphene layers as amorphous structures and turbostratic crystallites (Lehmann et al. 2009). In addition, highly stable chemical configurations that are also present in biochar are fullerenes. Fullerenes are spherical structures that have hexagonal and pentagonal rings (Harris 2005). It is suggested that fullerene-type structures contribute to the high recalcitrance of biochar because of their folded structure.

In a study using black carbon produced from *Pinus resinosa* (Red pine) sapwood, Baldock and Smernik (2002) compared the changes in chemical shift regions of the black carbon using solid-state CP and DP

^{13}C NMR spectra. It was found that the chemical shift values of the resonances and the proportion of the total signal intensity found in each chemical shift region increased with increasing heating temperature. At 200°C, certain signal intensities associated with (lignin and cellulose) displayed unique characteristics. The cellulose and hemicelluloses structures of the O-alkyl and di-O-alkyl chemical shift regions were reduced from 70 – 46 %. Conversely, increases of 15 – 30% in aryl and O-aryl and 1 -5 % in carbonyl C chemical shift regions were observed with lignin structures (Baldock and Smernik 2002).

Since cellulose is a major component of wood, Baldock and Smernik (2002) showed that thermal alteration of *Pinus resinosa* sapwood cellulose at temperatures ≥ 300 °C resulted in the presence of O-aryl C. Aryl C is the most dominant C found in charred structures. Studies generally employ aryl C as the basis upon which the chemical changes associated with pyrolysis is concerned (Baldock and Smernik 2002). It has been shown that the quantity of aryl C increases with increasing heating temperatures (Czimczik et al 2002).

2.5 Application of biochar

Several experiments using biochar alone and biochar incorporated into soil have been conducted to investigate the behaviour of biochar and the mechanisms responsible. This section aims give a concise review of the literature on the application of biochar, with special attention to the sorption behaviour of nitrogen to biochar, the C and N dynamics of soil applied biochar and leaching of nitrogen in biochar amended soil.

2.5.1 Inorganic N adsorption

Current biochar sorption research aims to understand whether the N not accounted for in some studies remains in the biochar. One way of doing this is to perform a sorption experiment where adsorption or absorption is investigated and then followed by a desorption experiment to try account for the reverse process.

A recent study, that explored this issue was conducted by Wang et al (2015) where a maple wood biochar pyrolysed at 500 °C was used to assess the completion of desorption and to see if ammonium was lost during the experiment. The study went a step further by assessing the biochar at different pH values. The inherent pH of the biochar was used (pH 8.7), another batch of biochar was adjusted to pH 7, while the final batch of biochar was adjusted to pH values ranging between 3.7 and 8.1. A batch adsorption experiment (0.5 g biochar and 40 mL solution at concentrations between 0 and 100 mg NH_4 L^{-1}) was conducted at room temperature (16-h extraction time) and ^{15}N labelling was used to observe whether the ammonium not recovered was still in the biochar. Desorption was determined using both

water and a 2 M KCl extraction. It was found that leaving the biochar at its inherent pH did not increase ammonium adsorption. However, the biochar adjusted to pH 7 showed a distinct increase in ammonium adsorption with increasing oxidation. The reason this occurred is because after the pH adjustment, deprotonation of the carboxyl and phenolic groups occurred while free Al and Fe precipitated, thus creating the main adsorption sites for ammonium (Brady and Weil 2002). Furthermore, this would lead to a decreased C content and surface positive charge and thus also contribute to an increased CEC (Cheng et al 2008b).

In addition, the desorption results showed that both biochar types (inherent pH and pH-adjusted) had very good ammonium retention potential. After 2 extractions using ultrapure water, there was near complete recovery of the remaining adsorbed ammonium by KCl at the low pH biochars. Potassium chloride extraction from the high pH biochars recovered 41-89% of the adsorbed ammonium. These findings demonstrated that the ammonium sorption of maple wood biochar is readily reversible and that the mechanism responsible for the sorption is ion exchange. Further, the study confirmed that the adsorption capacity of maple wood biochar, in particular, was influenced by oxygen-containing functional groups and pH. The ^{15}N tracer study revealed that the ammonium not recovered during desorption was not in the biochar. It was reasoned that the incomplete recovery of adsorbed NH_4^+ in the biochar after all extractions at higher pH was because of ammonia volatilisation losses (Wang et al 2015a).

Biochar adsorption of ammonium has been examined using several feedstocks and at various pyrolytic temperatures. Yao et al (2012) evaluated 13 biochar materials (bamboo, Brazilian pepperwood, peanut hull, and sugarcane bagasse, including a hydrochar made using peanut hull at 300 °C) that had been produced by slow pyrolysis at 350, 450 or 600 °C, to determine their potential to remove inorganic N from solution. The biochars had a wide pH range between 5.2 and 9.1. It was found that 9 of the 13 biochars tested could remove ammonium from solution. The biochars had removal rates between 1.8% and 15.7% and varied widely with feedstock and no apparent pyrolysis temperature trend was evident.

In a study by Hale et al (2013), the potential of biochar to retain N fertilisers and then release them when necessary was investigated in a batch sorption experiment. Cacao shell biochar produced at 350 °C and maize cob biochar produced at 400 °C were used in the study. The experiment evaluated biochars that were unwashed and compared them to biochars rinsed with Millipore water. The study concluded that the cacao shell and maize cob biochars can add and slowly release ammonium to soil. This finding has significance to crop production because the exchange of NH_4^+ allows for the biochars to adsorb ammonium-nitrogen fertilsers and also release them by cation exchange.

An earlier study by Mizuta (2004) found that bamboo powder charcoal (produced at 900 °C) was approximately 15% more effective than a commercial activated carbon in removing nitrate from contaminated drinking water. Although, the surface area of the bamboo char (400 m^2 g^{-1}) was half that of the activated carbon (850 m^2 g^{-1}), the bamboo biochar was far better at sorbing nitrate than the activated carbon. A similar observation of the surface area not matching the expected sorbing potential was made by Yao et al (2012).

The ability of a high temperature biochar to remove nitrate is consistent with recent findings. Dempster et al (2012a) found that *Eucalyptus* sp. biochar produced at 600 °C used by adsorbed up to 80% nitrate when the nitrate concentration in solution was between 2.5 mg L^{-1} and 5 mg L^{-1}, and had an adsorption rate of 0.02-0.04 mg NO_3^- per g biochar. However, the amount of nitrate adsorbed was reduced to 38% at the highest treatment level of 50 mg L^{-1}, although the adsorption rate had increased to 0.19 mg NO_3^- per g biochar. In another study, Yao et al (2012) reported that Brazilian pepperwood, bamboo, peanut hull and sugarcane bagasse biochars produced at 600 °C had a high nitrate adsorption capacity. The biochars removed between 0.12% and 3.7% nitrate from solution during a sorption investigation.

Kameyama et al (2012) performed a study using sugarcane bagasse, where they determined nitrate adsorption properties of bagasse biochar manufactured at 5 different pyrolysis temperatures in the range of 400-800 °C. They found that significant NO_3^- adsorption occurred at pyrolysis temperatures greater than or equal to (≥) 700 °C. Also, at high pyrolysis temperatures the biochars had high pH (pH 8.7-9.8). It was reasoned that the adsorption of nitrate was a result of base functional groups and not a result of physical adsorption since surface area and micropore volumes followed different trends when compared to observed nitrate adsorption.

Previous studies indicate that there has been very small or no retention of nitrate to biochars (Knowles et al 2011; Jones et al 2012; Kameyama et al 2012; Hale et al 2013; Hollister et al 2013; Gai et al 2014), but they have also reported small release of nitrate from biochars (DeLuca et al 2006; Castaldi et al 2011; Hale et al 2013). A characteristic feature that has been reported for biochars exhibiting no sorption of nitrate is that they were produced at up to 550 °C (DeLuca et al 2006; Castaldi et al 2011; Jones et al 2012; Hollister et al 2013). In contrast, the biochars that have demonstrated sorption of nitrate were produced between 600 and 900 °C (Mizuta 2004; Knowles et al 2011; Kameyama et al 2012; Kameyama et al 2016). This clearly indicates that the nitrate adsorption of biochar is influenced by the pyrolysis temperature and biomass feedstock. Kameyama et al (2016) reported that wood-derived biochars produced at higher temperatures had greater nitrate adsorption than non-wood derived biochars.

2.5.2 Carbon and nitrogen cycling dynamics

Adding biochar to a soil increases the C/N ratio of the soil (Liu et al 2014) due to the higher availability of carbon. This may cause an increased immobilisation of mineral (inorganic) N within the microbial biomass (Case et al 2012). Therefore it is suggested that microbial or physical immobilisation of nitrate in soil following biochar addition may significantly contribute to the suppression of soil nitrous oxide emissions (Case et al 2012).

It has been suggested that soil microorganisms may have the potential to degrade biochar as several wood-decaying fungi have been shown to degrade (or solubilize) low grade charcoal (Hofrichter et al 1999). Fungal strains of *Trichoderma* were found to degrade biochar produced from both low and high grades (Laborda et al 1995). Several incubation studies have been performed to investigate the effect of microbial degradation where biochar is used as the primary carbon source (Cheng et al 2008a; Liang et al 2008; Kuzyakov et al 2009). During a 60-day incubation trial with microbial inoculants and using biochars produced from maize, oak and rye, Hamer et al (2004) found that 0.8, 0.7 and 0.3 % of carbon was lost as CO_2. Currently, very little information is available on quantifying biochar degradation by microbial transformations. Kuzyakov et al (2009) attributes this limitation of estimating the decomposition rate of biochar to ensure quantitative transformations to the long periods needed to perform these experiments.

2.5.3 Inorganic N leaching

In addition to investigating the effects of inorganic (mineral) N sorption capacity of biochar, recent research has gone further by asking what the practical implications of adding N retentive biochar would be to soil when it comes to reducing mineral N fertiliser leaching. This idea demonstrates that using biochar to retain N and the reduction of N leaching are inextricably linked. The mechanisms that have been proposed to explain this relationship between sorption of N in biochar-amended soils and the reduction of N leaching in these soils are: adsorption of NO_3^- by high temperature biochars produced at a minimum temperature of 600 °C (Kameyama et al 2012; Yao et al 2012; Dempster et al 2012b); immobilisation of N due to the enhanced portion of labile C (Steiner et al 2008b); and cation exchange reactions (Liang et al 2006; Mukherjee et al 2011).

It is widely known that biochar amendment can provide good ion retention capacity (Lehmann et al 2003; Liang et al 2006; Cheng et al 2008b). Yao et al (2012) used this knowledge to investigate the potential of two high sorbing biochars to reduce ammonium and nitrate leaching in biochar-amended soil. It was found that Brazilian pepperwood biochar reduced ammonium and nitrate leaching by 34.7% and 34.0%, respectively; and peanut hull biochar was reported to reduce the leaching of nitrate by 14.4% and ammonium by 34.3% (Yao et al 2012). Ding et al (2010) showed that bamboo biochar sorbed

ammonium by cation exchange and reduced cumulative ammonium leaching losses by 15.2% at 20 cm depth. Kameyama et al (2012) reported that the sugarcane bagasse biochar produced at 800 °C was highly effective in adsorbing NO_3^- and it reduced nitrate leaching by 5%. Furthermore, our previous study reported that biochar reduced the cumulative leaching of ammonium between 12% and 86%, and between 26% and 96% for nitrate (Sika and Hardie 2014).

The Eucalyptus sp. biochar (CEC 10 $cmol_c\ kg^{-1}$) that Dempster et al (2012a) found to adsorb ammonium and nitrate was placed in lysimeter pots holding an acidic sandy soil (CEC 2 $cmol_c\ kg^{-1}$), fertilised with ammonium sulfate and irrigated over 21 days. When compared to the control treatment, it was found that the biochar reduced the cumulative ammonium leached by 20% and the cumulative nitrate leached by 25%. In addition to the remarkable retentive properties of the biochar, another reason given for the reduced leaching was the relatively low biochar CEC.

2.6 Gaps in knowledge

In my Masters study (Sika 2012), it was found that biochar significantly reduced the leaching of mineral fertilisers. However, the exact mechanisms and processes behind this were not known, nor was the extent of this retention established. That study was limited to pine wood biochar application on an acidic sandy soil. In recent years, more biochars have been produced in South Africa and are commercially available. The chemical and physical reactions of these new, locally produced biochars remains to be elucidated. Therefore, this research aims to perform a detailed physico-chemical characterisation of the biochars. Biochar interactions with nitrogen are important to understand because biochar is added to soil together with N or multi-nutrient fertilisers. The ammonium and nitrate sorption potential of biochars influences mineral nitrogen leaching and this area of soil nitrogen dynamics research requires serious attention. Mineralisation of carbon and nitrogen of sandy soil with various biochars are also not well documented. Based on these gaps in knowledge, this study merits attention especially because characterisation of the different locally produced biochars will form part of a knowledge database for commercially available biochars in South Africa and this has the potential of improving how soils are managed for crop growth.

Chapter 3

Physico-chemical Characterisation of Biochars

3.1 Introduction

Biochars are produced from different biomass feedstocks using various pyrolysis methods and thus exhibit a complex range in composition and chemistry. Sugarcane bagasse biochar, produced using vacuum pyrolysis, was shown to possess high BET surface area (259 m^2 g^{-1}) and high micropore volume (0.088 cm^3 g^{-1}) (Uras et al 2012). On the other hand, biochars made under fast pyrolysis were shown to have low BET surface areas (Zhang et al 2004; Boateng 2007). Uras et al (2012) also found that biochar from vineyard prunings produced using vacuum pyrolysis had high surface alkalinity (1.67 mmol g^{-1}) and high aromatic C, thus showing potential to improving soil C sequestration. Biomass feedstocks with high inorganic elemental contents typically produce a concentrated mineral ash fraction in their biochars. Most notably, biochars from maize stover, grass, and manure, which have relatively high concentrations of inorganic elements and metals, tend to have higher ash contents compared to wood biochars (Spokas et al 2012). It has been found that ash content is affected by peak pyrolysis temperature and feedstock. The general trend is that as the peak pyrolysis temperature increases, organic components are volatilised, giving rise to a proportionally high ash content. Therefore, herbaceous biomass and manure derived biochars have higher ash contents than wood biochars (Amonette and Joseph 2009).

Currently, two research bodies have set out standard guidelines on the properties of biochars that may be used for soil amendment. They are the International Biochar Initiative (IBI) and the European Biochar Certificate (EBC). The standard characterisation tests that these research bodies require to be performed on biochar samples are total elemental and nutrient contents, thermal gravimeteric analysis, heavy metals and organic compounds determination, specific surface area and other basic chemical analytical methods such as biochar pH determination. Recommendations for biochars produced in South Africa are urgently needed.

Our previous study investigated the application of slow-pyrolysis pine wood biochar to an acidic, sandy soil on ammonium and nitrate leaching and subsequent availability in the soil (Sika and Hardie 2014).

3.2 Objectives

The main goal of this chapter was to investigate the physical, chemical and morphological characteristics of six locally produced biochars available on the South African market. A complete characterisation of the biochar materials was performed to assess their differences and thereby determine their potential for use as soil amendments.

3.3 Materials

3.3.1 Biochars

Six local biochars produced using three different pyrolysis systems were used for this study. The biochars used were: maize stover produced by fast pyrolysis; grape pip, grape skin, pine wood and rubber tyre, all produced by slow pyrolysis; and sugarcane pith produced by vacuum pyrolysis. The maize stover and sugarcane pith biochars were produced and donated by the Department of Process Engineering, Stellenbosch University; grape pip and grape skin biochars were supplied by Brenn-O-Kem (Pty) Ltd.; pine wood biochar was donated by S & P Carbon (Pty) Ltd.; and the rubber tyre biochar was provided by PaceOil (Pty) Ltd.

3.3.2 Preparation of materials

The biochars used in this study were thoroughly mixed and homogenised prior to analysis. The grape pip and grape skin biochars were initially ground by mortar and pestle to reduce their particle size. All biochars were sieved to <2 mm, and, depending on the experiment performed, the biochar samples were also ball-milled to <1 mm when required. Biochar samples were air-dried, the oven-dry weight equivalent was determined and used for the analyses.

3.4 Physico-chemical characterisation of biochars

3.4.1 Total C, N, H, S and O

Total C, N, H and S contents of the biochar samples were determined by dry combustion using the EuroVector Elemental Analyzer 3000 series (EuroVector, Italy) (Nelson and Sommers 1996). The O content was determined by subtracting the C, N, H, S contents, ash and moisture from the total sample mass. All samples were determined using the oven dry weight equivalent of the biochars.

3.4.2 Total elemental analysis

Total inorganic elemental analysis of both major and trace elements (consisting of P, Ca, Mg, K, Fe, Mn, Cu, Zn, Co, B, Mo, Na, Al, Se, Cr, As, Ni, Pb, Cd, Sr, Ba and Si) of the biochar materials was performed by microwave assisted acid digestion followed by analysis on an inductively coupled plasma mass spectrometer (ICP-MS). A 0.3 g biochar sample was weighted and digested with 10 mL HCl/HNO_3 and 40 mL deionised water and then microwaved. The microwave was used at a 1600 W power level at 100%, a 25 minute ramp time, pressure at 800 psi, temperature of 210°C and a holding time of 30 minutes. The ICP-MS equipment used to analyse the samples was the Mars240/50 model (CEM Corporation, USA).

3.4.3 Proximate analysis (TGA)

Thermogravimetric analysis of the biochar samples was performed on the biochar materials to determine the moisture (at 105 °C), volatile matter (at 900 °C) content, ash (at 750 °C) and fixed C (by subtraction) contents (ASTM standard 1762-84 2007). Each biochar sample was heated from 20 °C – 600°C at 10°C min^{-1}, nitrogen gas was then used at a flow rate of 20.0 mL min^{-1}, and this was followed by heat at 600 – 900 ° C at 20°C min^{-1}. There were two holding times at 900°C for 7 minutes and 30 minutes each. Lastly, oxygen gas was introduced at a flow rate of 20 mL min^{-1} for the combustion process. All samples were reported using the oven dry weight equivalent of the biochars.

3.4.4 Biochar pH

The inherent biochar pH was measured in a 1:20 w/v ratio using distilled water and 1 M KCl solution. Two grams (oven-dry equivalent) of the <2 mm sieved biochar samples and 40 mL solution were used. The samples were shaken for 30 min and allowed to settle before pH readings were performed (Cheng and Lehmann 2009).

3.4.5 Biochar surface acidity and alkalinity

Biochar surface acidity and alkalinity were determined using the Boehm titration method (Cheng and Lehmann 2009). In summary, a 0.15 g biochar sample was added to 15 mL each of 0.1 M NaOH and 0.1 M HCl solution, and placed on a shaker for 30 hours. The resulting slurry was filtered by gravitation using Whatman no. 42 filter paper. For the determination of surface acidity, the unreacted base was neutralised by taking an aliquot of 5 mL of the NaOH filtrate and transferring it to 10 mL of a 0.1 M HCl solution. The solution was back-titrated with 0.1 M NaOH using phenolphthalein as an indicator. Surface alkalinity was determined similarly to surface acidity, except that a 5 mL aliquot of the HCl filtrate was used and back-titrated with the acid. Lastly, the base and uptake of the biochar sample were converted to the content of surface acidity and surface alkalinity (mmol g^{-1}), respectively. The solutions were prepared using deionised water. The 0.1 M NaOH solution used was prepared using a standardised solution and calibrated with an autotitrator. The 0.1 M HCl solution used was also prepared using a standardised solution, followed by manual back titration. Surface acidity and alkalinity were calculated using the following equations:

$$\text{Surface acidity } (mmol/g) = \frac{\text{mmol NaOH uptake}}{\text{g biochar}} = \frac{1.5 \text{ mmol NaOH } - [(1 \text{ mmol-x})] \times \frac{15 \text{ mL}}{5 \text{ mL}}}{0.15 \text{ g}}$$

$$\text{Surface alkalinity } (mmol/g) = \frac{\text{mmol HCl uptake}}{\text{g biochar}} = \frac{1.5 \text{ mmol HCl } - [(1 \text{ mmol-x})] \times \frac{15 \text{ mL}}{5 \text{ mL}}}{0.15 \text{ g}}$$

3.4.6 Fourier Transform Infrared Spectroscopy

Fourier Transform Infrared (FTIR) spectroscopy is a vibrational spectroscopy technique used for identifying the distribution of chemical bonds on mineral surfaces. In this research, it was used to investigate the crystalline and poorly crystalline functional group minerals on biochar surfaces. The instrument was purged with N_2 gas prior to measurements to prevent interference from H_2O and CO_2. Biochar samples were carefully sampled and finely ground by ball-milling to limit sample heterogeneity. In addition, biochar samples and KBr (Sigma Aldrich, reagent grade) were oven dried prior to use. The spectrophotometer was fitted with a diamond crystal and measurements were taken in the 400 cm^{-1} to 4000 cm^{-1} infrared range at a resolution of 6 cm^{-1}. The FTIR scans were carried out with 128 scans on a 0.004% (oven dry weight equivalent) pressed KBr pellet. The spectra were read on a Thermo Nicolet Nexus FTIR spectrophotometer (Thermo Fisher Scientific Inc., USA), and processed using the OMNIC version 7.2 software.

3.4.7 BET specific surface area

The Brunauer-Emmet-Teller (BET) specific surface area (SSA) of the biochars was determined using N_2 gas on a Micromeritics ASAP2010 (Accelerated Surface Area and Porosimetry) system (Micromeritics Instrument Corp., USA). The biochar samples were degassed on the VacPrep 061 at 90°C for 60 min, then at 300°C for approximately 16 hours. Thereafter, they were kept at 200°C on the VacPrep until analysis. No degassing was performed on the instrument itself.

3.4.8 Scanning Electron Microscopy

Imaging of the <2 mm sieved biochar samples was accomplished using a Leo® 1430VP Scanning Electron Microscope (ZEISS, Germany) at Stellenbosch University. Prior to imaging, the samples were mounted on a stub with double sided carbon tape. The samples were then coated with a thin layer of gold in order to make the sample surface electrically conducting. The Scanning Electron images show the surface structure of the material. Beam conditions during surface analysis were 7 kV and approximately 1.5 nA, with a spot size of 150.

3.4.9 Statistical analysis

The total C, N, H, S, O and ash content of biochars was analysed using the general linear model univariate analysis of variance (ANOVA) in order to determine statistically significant differences between the treatments. The data was tested for normal distribution and homogeneity before statistical analysis. For comparison of means, Fischer's Least Significant Difference (LSD) post hoc test with a P

< 0.05 level of significance was used. Statistical analysis was performed using IBM SPSS (IBM SPSS Statistics for Windows, Version 24.0. Armonk, NY: IBM Corp.).

3.5 Results and Discussion

3.5.1 Total C, N, H and S analysis

The biochars mostly had a high total C content, with the exception of sugarcane pith, which was statistically significant ($P < 0.05$) compared to the other chars (Table 3.1). The pine wood biochar had significantly the highest total C amount of 80.31%. This corresponds with reports that biochars produced from hardwood have higher C amounts than those obtained from herbaceous feedstocks (Streubel and Pierce 2011; Jindo et al 2014).

Using the guidelines of the EBC, sugarcane pith char should not be classified as biochar, but as pyrogenic carbonaceous material (EBC 2012). This is due to its low C content <50%. Although such a material is not biochar, it may contribute as a valuable fertiliser additive due to its high ash content (Table 3.3).

Furthermore, a comparison of the maize stover and grape skin biochars suggest that they may be borderline pyrogenic carbonaceous materials (EBC 2012). This is because of their total C and ash contents of 50 and 41%, as well as 59 and 30%, respectively. However, since the maize stover char has 50% total C and the grape skin char has a total C contents >50%, they may still be marginally acceptable as biochar.

The C/N mass ratio between the biochars is in the range 38 – 373. This parameter is important because a wide C/N ratio greater than 30:1 has adverse effects which may lead to net N immobilisation when applied to soils (Stevenson and Cole 1999; Havlin et al 2014). Therefore, all the biochars studied may potentially decrease mineral (inorganic) N reserves due to net N immobilisation. However, it would also be a function of the black C content, which is generally difficult to degrade.

Table 3. 1: Total C, N, H, S, O and ash content of biochars (expressed as dry wt basis). Means in the same column followed by the same letter are not significantly different at P < 0.05 level based on the Least Significant Difference test.

Biochar	%C	%N	%H	%S	%O	%Ash	C/N[a]	H/C[b]	O/C[b]
Maize stover	50.05 d	0.20 c	1.90 a	0 b	16.18 a	41.36 b	244.53 b	0.45 b	0.24 a
Grape pip	74.70 b	1.27 a	1.21 b	2.00 a	14.92 ab	5.91 de	58.73 cd	0.19 d	0.15 b
Grape skin	59.20 c	0.73 b	0.58 c	2.20 a	6.88 c	30.43 c	81.43 c	0.12 e	0.09 c
Pine wood	80.31 a	0.22 c	2.11 a	1.87 a	11.97 b	3.52 e	372.29 a	0.31 c	0.11 bc
Rubber tyre	75.09 b	1.18 a	1.71 a	2.10 a	12.39 b	7.52 d	63.56 cd	0.27 cd	0.12 bc
Sugarcane pith	27.90 e	0.73 b	1.74 a	0 b	3.64 c	65.99 a	38.01 d	0.74 a	0.10 c

[a] = Mass ratio

[b] = Molar ratio

The H/C molar ratio was in the range of 0.12 and 0.74; while the O/C molar ratio of the biochars was in the range 0.10 – 0.24 (Table 3.1). Reporting of the ideal H/C and O/C ratios of biochar is inconsistent in the literature. According to the recommendation of the IBI, the H/C ratio of biochar must be less than 0.7 to distinguish it from other thermochemically processed biomasses that are not biochar (IBI 2015). A limit for the O/C ratio is not specified. The EBC recommends a maximum threshold value of 0.7 for the H/C ratio and 0.4 for the O/C ratio (EBC 2012). Hedges et al (2000) reports that along the combustion continuum, charcoal in particular, or in comparison to other combustion products, has an O/C ratio of 0.2 – 0.4. The findings in Table 3.1 are low in O and high in C and are thus considered in the well-pyrolysed range. It has been suggested that if materials fall above this O/C range, then it may be due to incomplete combustion or thermally undegraded cellulose of the organic materials during pyrolysis (Masiello 2004; Podgorski et al 2012). However, it is also suggested that O/C below 0.2 is a good indication that a biochar may provide a half-life of at least 1000 years (Spokas 2010), showing promising potential for long-term C sequestration (Lehmann et al 2006).

With the exception of the sugarcane pith char, all the other biochars have both low H/C and O/C ratios. This means that these biochars are more aromatic and highly condensed. Thus, the biochars in this study are less prone to degradation (Masiello 2004), compared to uncharred biomass, which typically possess high H/C and O/C values. This suggests that the H/C and O/C ratios of the sugarcane pith char point to lower stability and higher chemical reactivity in soils. Therefore, according to the recommendation of the IBI, the sugarcane pith char is described as thermochemically altered. This is in contrast to thermochemically converted biomass with H/C ratios below 0.7 which have larger proportions of fused aromatic rings (IBI 2015).

The H/C molar ratio informs about the aromaticity of the biochar, i.e., its degree of carbonisation (Krull et al 2009). This means that a low H/C is highly carbonised, exhibits a highly aromatic structure and generally high C contents which is characterised by stable, condensed aromatic structures (Van Zwieten et al 2010b). Therefore, the order of carbon stability from the results in Table 3.1 are: grape skin>grape pip>rubber tyre>pine wood>maize stover>sugarcane pith. This shows that the grape chars are more highly carbonised; while sugarcane pith biochar contains more of its original structures such as lignin and cellulose (Streubel 2011). This finding confirms that the sugarcane pith char may only be partially thermochemically altered (IBI Biochar Standards).

3.5.2 Total inorganic elemental analysis

The biochars varied quite widely in their inorganic elemental composition (Table 3.2) largely because of the differences in feedstock and pyrolysis conditions. The grape skin biochar contained the highest total P (0.74%) and K (4.28%) content of the biochars, whereas, the maize stover contained the highest Ca (2.25%) and Mg (1.14%) contents (Table 3.2). The grape skin and maize stover also had relatively high ash contents which were statistically significant ($P < 0.05$) (30.43 and 41.36%, respectively) (Table 3.1). Thus these chars would provide valuable macronutrients when applied to soils. The sugarcane pith had the highest amounts of Si, Fe, Al and Mn relative to the other biochars (Table 3.2). Sugarcane is known to take up large amounts of Si from the soil. A similar finding was observed in rice husk biochar which had high levels of silicon and mineral elements (Abdulrazzaq et al 2014). These high Si, Fe, Al and Mn elemental concentrations contributed to the highest ash content (66.0%) of the sugarcane pith biochar (Table 3.1). It is also possible that the high Si, Fe and Al in the sugarcane pith biochar was due to clay contamination. The pine wood biochar contained the lowest levels of macro and micronutrients of the plant-derived biochars (Table 3.2) and this correlated well with its low ash contents of 3.53% (Table 3.1). The rubber tyre biochar contained the lowest concentrations of macronutrients (P, Ca, Mg and K) compared to the plant-derived chars, whereas, it contained by far the highest concentration of metals such as Zn (5-20 times higher), Cr, and Pb (Table 3.2). Zinc oxide is one the major additives to synthetic rubber to assist with the vulcanisation process during the production of tyres. These levels of metals could be of concern in soil application, and this was tested in Chapter 5.

Table 3. 2: Total inorganic elemental analysis of the biochar materials.

	Maize stover	Grape pip	Grape skin	Pine wood	Rubber tyre	Sugarcane pith
Macronutrients (%)						
P	0.31	0.41	0.74	0.02	0.00	0.51
Ca	2.25	1.18	1.29	0.32	0.06	1.35
Mg	1.14	0.20	0.31	0.11	0.02	0.69
K	2.95	2.31	4.28	0.24	0.05	0.31
Micronutrients (mg kg^{-1})						
Fe	5051.50	2052.54	4036.67	635.71	7770.11	30968.27
Mn	197.76	102.96	53.52	52.47	24.93	804.50
Cu	19.58	32.06	69.15	5.07	12.63	72.10
Zn	26.22	39.31	13.43	10.18	2205.18	114.23
Co	2.51	0.44	1.33	0.33	13.75	12.95
B	20.76	38.46	83.99	3.86	6.02	4.29
Mo	2.75	0.64	1.39	0.17	1.92	1.62
Non-essential elements and toxins (mg kg^{-1})						
Na	332.51	512.93	952.11	402.16	151.97	522.02
Si	718.19	771.57	814.51	750.63	925.84	1010.82
Al	4768.77	1423.44	5182.91	1567.59	2306.00	19631.82
Se	0.05	1.03	0.18	1.28	0.52	3.09
Ba	32.05	45.30	42.49	9.73	22.52	ND
Sr	78.56	58.16	72.50	28.22	2.95	ND
Cr	117.75	49.28	50.90	10.50	435.52	348.12
As	0.42	5.88	3.73	5.62	1.08	4.24
Ni	40.24	3.60	23.94	0.75	73.59	101.34
Pb	2.08	1.41	0.35	0.60	9.13	37.61
Cd	0.03	0.00	0.00	0.01	0.11	0.83
Sb	0.03					0.04
Hg	0.11					0.11

3.5.3 Proximate analysis (TGA)

Table 3.3 presents the proximate (TGA) results of the six biochars. The volatile matter content refers to the labile fraction of biochar that is regarded as generally more easily degradable by soil microorganisms (Keiluweit et al 2010). The percentage ash refers to the non-combustible mineral fraction of the biochars (Table 3.2). The fixed C content represents the black C fraction in the biochars and is used to estimate the longevity of biochar in soil (Enders et al 2012).

Table 3. 3: Proximate analysis of the biochars (expressed as dry wt basis).

Biochar	% Volatiles	% Ash	% Fixed C
Maize stover	58.64	41.36	0.00
Grape pip	7.52	5.91	86.57
Grape skin	5.78	30.43	63.80
Pine wood	16.37	3.52	80.11
Rubber tyre	24.24	7.52	68.23
Sugarcane pith	18.40	65.99	15.60

Four of the biochars (grape pip, pine wood, rubber tyre and grape skin) have fixed C percentages above 50 and therefore show good potential for carbon sequestration (Table 3.3). The maize stover biochar consists of more than 50% volatile matter and contained no fixed C (Table 3.3). This indicates that it was not properly pyrolysed and is in agreement with the high O/C and H/C ratio of the material (Table 3.1), which indicate less aromatically condensed character. A possible reason for the high volatiles in the maize stover is that some atmospheric O_2 was present during the initial stages of pyrolysis which prevented complete pyrolysis (Amonette and Joseph 2009).

The sugarcane pith char also has a H/C ratio >0.6 which indicates further possibly of not being fully pyrolysed (Schimmelpfennig and Glaser 2012) and therefore showing characteristics of its original feedstock.

3.5.4 Biochar pH

Biochar materials were mostly moderately alkaline to alkaline (8.0 > pH > 11), except for rubber tyre which was acidic with pH 2.4 in water (Table 3.4). The basic pH nature of the biochars corresponds with the high concentration of inorganic soluble salts (Table 3.2). These results are in agreement with studies where biochars have been reported to have an alkaline nature (Chan and Xu 2009; Singh et al 2010). An advantage of alkaline biochar is that when used to amend acidic soil, it has a liming effect (Glaser et al 2002; Zheng et al 2013a). However, when adding alkaline biochar to neutral or alkaline

soils, various concerns arise. For example, how increases in soil pH >8.0 may affect plant growth and the negative effects of the availability of phosphates and micronutrients in plants (Artiola et al 2012). Elemental analysis results (Table 3.2) from the low pH rubber tyre char showed that it contained approximately 5 times lower concentrations of alkali and alkaline elements (Na, Mg, K, Ca) compared to the other biochars. This confirms that the alkali and alkaline earth minerals are the main cause of plant-derived biochars alkaline pH values (Zheng et al 2013a).

Table 3. 4: pH of biochar materials.

Biochar	pH_{H2O}	pH_{KCl}	ΔpH
Maize stover	10.70	10.19	-0.51
Grape pip	10.30	10.18	-0.12
Grape skin	10.31	9.65	-0.66
Pine wood	9.51	8.88	-0.63
Rubber tyre	2.43	2.34	-0.09
Sugarcane pith	8.07	7.40	-0.67

The pH value in distilled water indicates the active acidity in the biochar, while the pH value in 1 M KCl solution indicates the exchangeable acidity or alkalinity (McBride 1994a). The difference between the two readings (delta pH) indicates the net surface charge of the material (Rowell 1994). All of the biochars appear to have a net negative surface charge as indicated by negative delta pH values (Table 3.4). It is well known that surface charge and exchangeable acidity are a function of pH and that deprotonation and hydrolysis reactions are involved. And since the degree of hydrolysis is pH dependent (Essington 2004), it follows that acidic and alkaline solutions will behave differently. In the alkaline biochars, proton activity was low and therefore hydrolysis was favoured. However, in the rubber tyre char pH measurement solution, which was acidic, the proton activity was high and thus the displacement of protons from waters of hydration was not favoured (Essington 2004).

3.5.5 Biochar surface acidity and surface alkalinity

Results from Table 3.5 indicate that both acidic and basic sites coexist on the surface of most of the biochar materials. Generally, a higher surface acidity indicates a higher content of acidic functional groups, such as in the rubber tyre biochar which had the lowest pH (Table 3.4). These acidic functional groups are confirmed on the FTIR spectrum at approximately 1600 and at 1092 cm^{-1} (Figure 3.1e) as carboxylic and phenolic groups, respectively (Carrier et al 2012). The results also show that the biochars

generally had higher surface acidity than surface alkalinity although the pH values were alkaline, with the exception of the sugarcane pith char (Table 3.5).

However, recent studies raise concern regarding the use of the Boehm titration method to measure the quantity of exchangeable acidity of biochars. This is because the Boehm titration was originally developed for the quantification of organic functional groups of carbon blacks and activated carbons (Boehm 1994). Biochars differ from these carbon rich products in that they contain basic and acidic components that may interfere with the titration and thus render the results invalid (Tsechansky and Graber 2014). In particular, biochars differ from carbon blacks and activated carbon in that they have higher ash contents (carbonate and other inorganic alkalis) and greater C solubility (Fidel 2012). Evidence of the carbonates is revealed in the FTIR spectra (Figure 3.1a-f). It has also been found that carbon-rich samples with large concentrations of silica can release dissolved silica when treated with alkali Boehm reactants and may adsorb or release protons when titrated (Fidel et al 2013). This is likely to have occurred during Boehm titration of the biochars in this study given the high Si levels (Table 3.2). Therefore, these results may be partially biased.

Table 3. 5: Surface acidity and alkalinity of the biochar materials.

Biochar	Surface acidity (mmol g^{-1})	Surface alkalinity (mmol g^{-1})
Maize stover	0.60	0.00
Grape pip	0.60	0.30
Grape skin	0.50	0.00
Pine wood	0.50	0.70
Rubber tyre	2.40	1.20
Sugarcane pith	1.40	0.10

It is evident that using the Boehm titration analytical method to determine biochar surface acidity and alkalinity can be problematic unless ash is removed before treatment with the Boehm reactants. Current literature highlights the importance of removing the interference of ash and DOC prior to analysis.

3.5.6 Fourier Transform Infrared Spectroscopy

Previous studies where FTIR have been used to characterise biochars have focused on the changes in the biochar's functional groups as a function of pyrolytic temperature (Chen et al 2008; Keiluweit et al 2010; Angin 2013; Zhao and Nartey 2014). However, this research differs in that various biochar materials produced under different pyrolysis conditions are investigated.

Figure 3.1 shows the FTIR spectra of the biochars in the infrared region (wavenumbers 4000-400 cm^{-1}). The biochars' spectra were characterised by the organic functional group showing intense peaks of

O-H stretching in the 3500-3400 cm^{-1} region (Figures 3.1a-f). These peaks indicate the presence of water, carboxylic acids, phenol and alcohol groups. All the chars also indicated the presence of very weak aliphatic C-H stretching in the 2970-2820 cm^{-1} region (Johnston and Aochi 1996). The sharp peak at 2360 cm^{-1} is due to background CO_2 and this is an artefact. The strong bands in the 1690-1560 cm^{-1} region were found in all the biochars and represent aromatic C=C stretching (Guo and Bustin 1998). This is an indication of good stability of biochars in soil. The weaker shoulder at 1750-1660 cm^{-1} just prior to the C=C bands is typical for stretching C=O vibrations of carboxylic acids (Silverstein et al 1991).

Bands in the 1145-1100 cm^{-1} region were observed in the grape pip (Figure 3.1b) and pine wood (Figure 3.1d) biochars and suggest the presence of C-O and C-C stretching (Chen et al 2008). Other broad bands in the spectra were the asymmetric (1650-1540 cm^{-1}) and symmetric (1450-1360 cm^{-1}) COO- stretching bands. The bands in the 1170-950 cm^{-1} region of the spectra indicate that all the biochars confirm the presence of C-O stretching of polysaccharides, such as cellulose. These peaks appear most intense relative to the aromatic 1620 cm^{-1} peaks in the maize stover (Figure 3.1a) and sugarcane pith (Figure 3b) biochars, which indicates that they were not as well-pyrolysed as the other biochars. The presence of the oxidised functional groups in the biochars was also an indication of an increase in CEC, shown by high O/C (Shenbagavalli and Mahimairaja 2012). Lastly, the most dominant inorganic functional group present in all the spectra are the carbonates (900-670 cm^{-1}) (Johnston and Aochi 1996). The carbonates are part of basic functional groups, which are influenced by the concentration of basic cations in the biochar (Table 3.2). The sharp peak at 1385 cm^{-1} is typical for N-O stretches of nitrates. Interestingly, the char obtained from the pyrolysis of synthetic rubber tires (Figure 3.1e) looks similar to the chars obtained from plant biomass.

Although aromatic C peaks were observed in all the biochars, sugarcane pith biochars' high ash content (Table 3.1) generally causes the ash to protect organic compounds against degradation, especially at increasing pyrolytic temperatures, and thereby prevent the development of aromatic C structures in biochar (Enders et al 2012). On the other hand, in addition to the FTIR spectrum characterisation, pine wood biochar was found to possess good aromatic C due to the high total C content and relatively low H/C ratio (Table 3.1). The maize stover char showed considerable aliphatic character by having an intense FTIR peak and high O/C ratio which indicates possible immobilisation of N when added to soil (Deenik et al 2010).

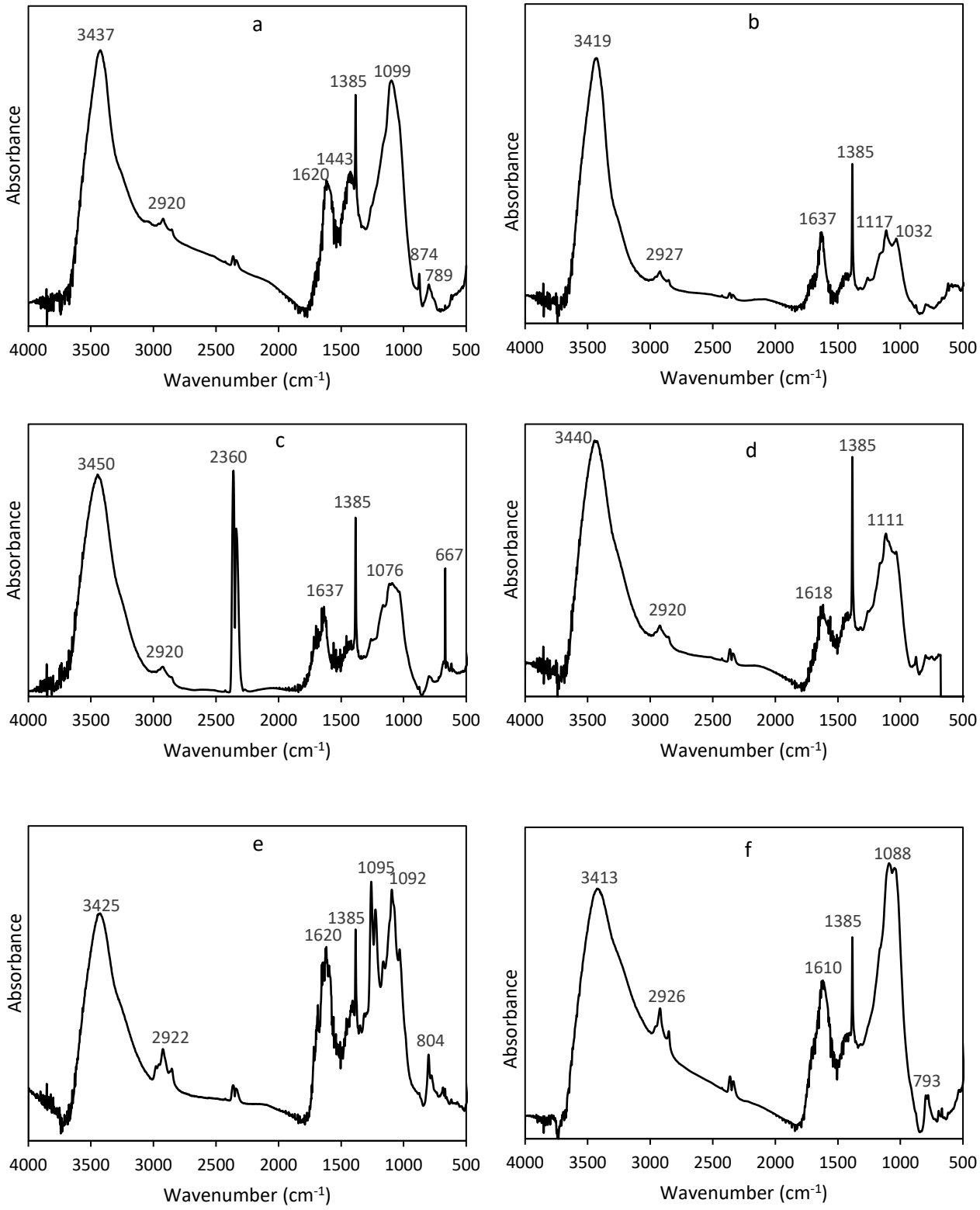

Figure 3. 1: FTIR spectra of the biochar materials: (a) maize stover, (b) grape pip, (c) grape skin, (d) pine wood, (e) rubber tyre, and (f) sugarcane pith.

SURFACE AREA AND POROSITY OF BIOCHAR

3.5.7 Surface area of biochar

The BET specific surface area of biochar gives an indication of the efficiency of its surface morphology in adsorbing various solutes (Lehmann et al 2006). Pine wood biochar had the highest surface area (344.27 m^2 g^{-1}) and therefore can be good for nutrient adsorption; while grape pip biochar had the lowest BET surface area (9.82 m^2 g^{-1}) and thus not suitable for this purpose (Table 3.6). The low BET surface area associated with the grape pip biochar may be due to the high amounts of inorganic alkaline species (Table 3.2), which can decrease the surface area by blocking access to the biochar micropores (Song and Guo 2012). The typical trend is for surface area to increase with pyrolytic temperature and for low mineral ash biochar to have a higher surface area than high mineral ash biochar (Joseph et al 2009). This trend is observed in this study, where the pine wood derived biochar, produced by slow pyrolysis has low ash contents (Table 3.3) and a larger surface area; while the maize stover biochar, a high ash containing char produced by fast pyrolysis, has a smaller surface area (Table 3.6).

Table 3. 6: BET surface area of the biochars determined using liquid N_2 adsorption.

Biochar	Specific surface area (m^2 g^{-1})
Maize stover	160.53
Grape pip	9.82
Grape skin	76.98
Pine wood	344.27
Rubber tyre	82.07
Sugarcane pith	106.59

3.5.8 Scanning electron microscopy (SEM)

Contrasting differences were observed at the surface of the various biochar samples. Scanning electron microscope images of the biochar materials over a wide range of magnifications are shown in Figures 3.2 – 3.7. The structural development of the biochar materials ranged from showing increased proportions of aromatic structures and high disorder in their amorphous mass in maize stover (Figure 3.2) and grape skin (Figure 3.4) biochars. The grape pip (Figure 3.3) and sugarcane pith (Figure 3.7) chars showed growing sheets of conjugated aromatic C, turbostratically arranged; while the pine wood biochar (Figure 3.5) had graphitic structure with order in the third dimension (Downie et al 2009).

Grape pip, grape skin and rubber tyre chars all had lower BET surface areas (Table 3.6) and these results are confirmed by their SEM micrographs (Figures 3.3, 3.4 and 3.6). They show that the interior parts of the biochars were congested and not porous. Similar findings were also reported by Angin (2013) and Zhao and Nartey (2014). Fu et al (2011) suggests that the lower BET surface areas are as a result of the processes of softening, melting, fusing and carbonisation during pyrolysis. These processes prevent the entry of the adsorption gas to the pores and ultimately lead to lower surface areas.

Figure 3.2 shows the SEM images obtained for the maize stover biochar at the 100 µm and 20 µm scales. Figure 3.2a displayed a random arrangement of biochar particles demonstrating the heterogenic nature of pyrolysed materials. Close examination of the SEM image indicated some adhering soil particles (mineral phases) which suggest contamination of the feedstock before pyrolysis. This observation corresponds with maize stover biochar's high volatile matter content (Table 3.3). At the 20 µm magnification scale (Figure 3.2b), signs of longitudinal fibrous structures are visible from the elongated cylindrical structures likely arising from the cellulosic structure of maize which can be broadly grouped into fibrous, prismatic and spherical (Pituello et al 2014).

The grape pip biochar at the 100 µm scale shows the rough texture of the grape seed (pip) with micro-particles (Figure 3.3a). Its texture affirms the low BET SSA of grape pip biochar of 9.82 m^2 g^{-1} (Table 3.6). At 20 µm (Figure 3.3b), the plant cell wall structure pores become visible. It no longer shows the plant cell wall pore-like structure; instead it shows a messy arrangement with micro-particles and some indication of plant cell wall pore structure.

The SEM images of the grape skin biochar are similar to those of grape pip biochar. Figure 3.4a shows large rough materials, at 20 µm (Figure 3.4b) the rough texture shows micro-particles and some pores. At 2 µm (Figure 3.4c), the grape skin biochar exhibits a smooth surface with irregular porosity.

The pine wood biochar SEM images showed the typical fibrous structure of woody plants displayed with elongated fibres (Figure 3.5). A honeycomb-like structure is distinctly observed at the 100 µm

scale (Figure 3.5a), and more clearly seen at the 20 µm (Figure 3.5b) and 10 µm (Figure 3.5c) scales where finer particles are seen inside the large macropores, providing high surface area (Chintala et al 2014). A high biochar surface area is known to enhance soil aeration and improve water and nutrient holding capacities (Glaser et al 2002; Sohi et al 2010; Uzoma et al 2011). Figure 3.5c shows large internal pores which indicate strong potential for the ability of increasing biological activities in biochar-amended soil (Thies and Rillig 2009). This corresponds with the observed high surface area of pine wood (344.27 m^2g^{-1}).

The rubber tyre biochar showed large sphere-like particles at the 100 µm scale (Figure 3.6a). At 20 µm it appeared that the sphere-like particles were adhered to by numerous micro-particles (Figure 3.6b). Sevilla and Fuertes (2009) reported similar microspheres (at a magnification of 10 µm) on maize stover that underwent hydrothermal carbonisation (HTC) to form hydrochar. They found that the sphere-like micro-particles were formed as a result of the degradation of cellulose during low-temperature (170-300°C) HTC which then precipitated as growth spheres. Although this finding supports the observation in Figure 3.6, it contradicts the fact that the rubber tyre char was produced by slow pyrolysis, which occurs at an average temperature of 450°C.

Sugarcane pith biochar showed a heterogeneous random arrangement of biochar materials. At the 20 µm scale, long, tube-like fibrous structures are visible (Figure 7b). At 10 µm, the plant cell wall structure is detected (Figure 7c). This observation is further confirmed by the BET surface area measuring 106.59 $m^2\ g^{-1}$ (Table 3.6)

The SEM images of biochars yielded from pine wood, grape skin and sugarcane pith showed clearly visible plant structure residues, demonstrating that lignin degradation takes place at the high pyrolysis temperatures. This finding is comparable to the findings of Pituello et al (2014) where biochars produced at high pyrolysis temperatures >550 °C from cattle manure and silage digestate, vineyard pruning residues and municipal organic waste digestate behaved similarly.

The SEM images of the biochar materials in the current study clearly show that biochar morphology is complex. The images reflect the heterogeneity of the parent biomass and the differences caused by the various pyrolytic processes.

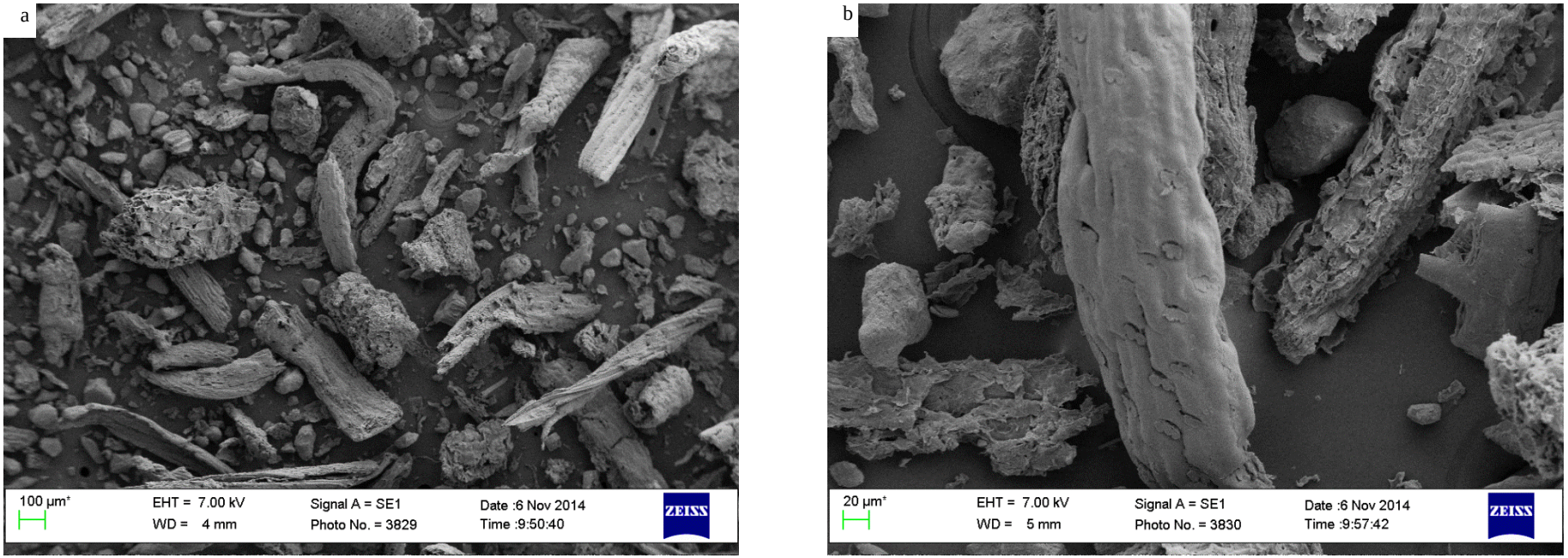

Figure 3. 2: SEM images of biochar from maize stover at (a) 100 µm and (b) 20 µm.

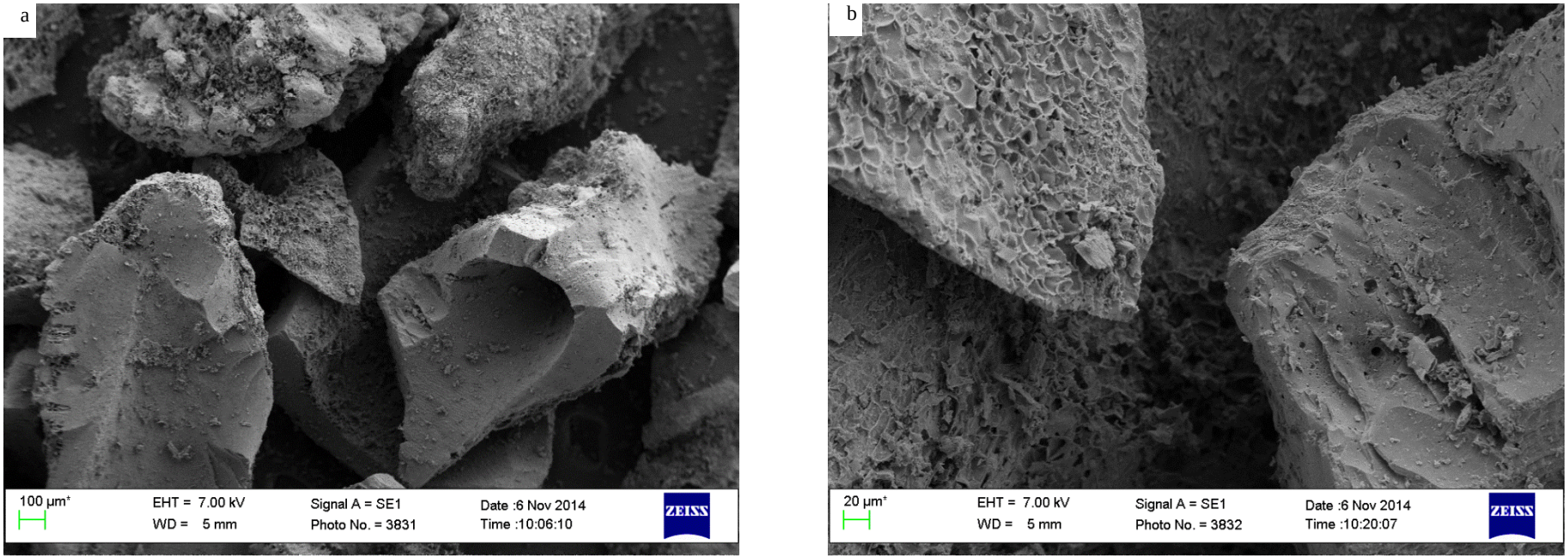

Figure 3. 3: SEM images of biochar from grape pip at (a) 100 µm and (b) 20 µm.

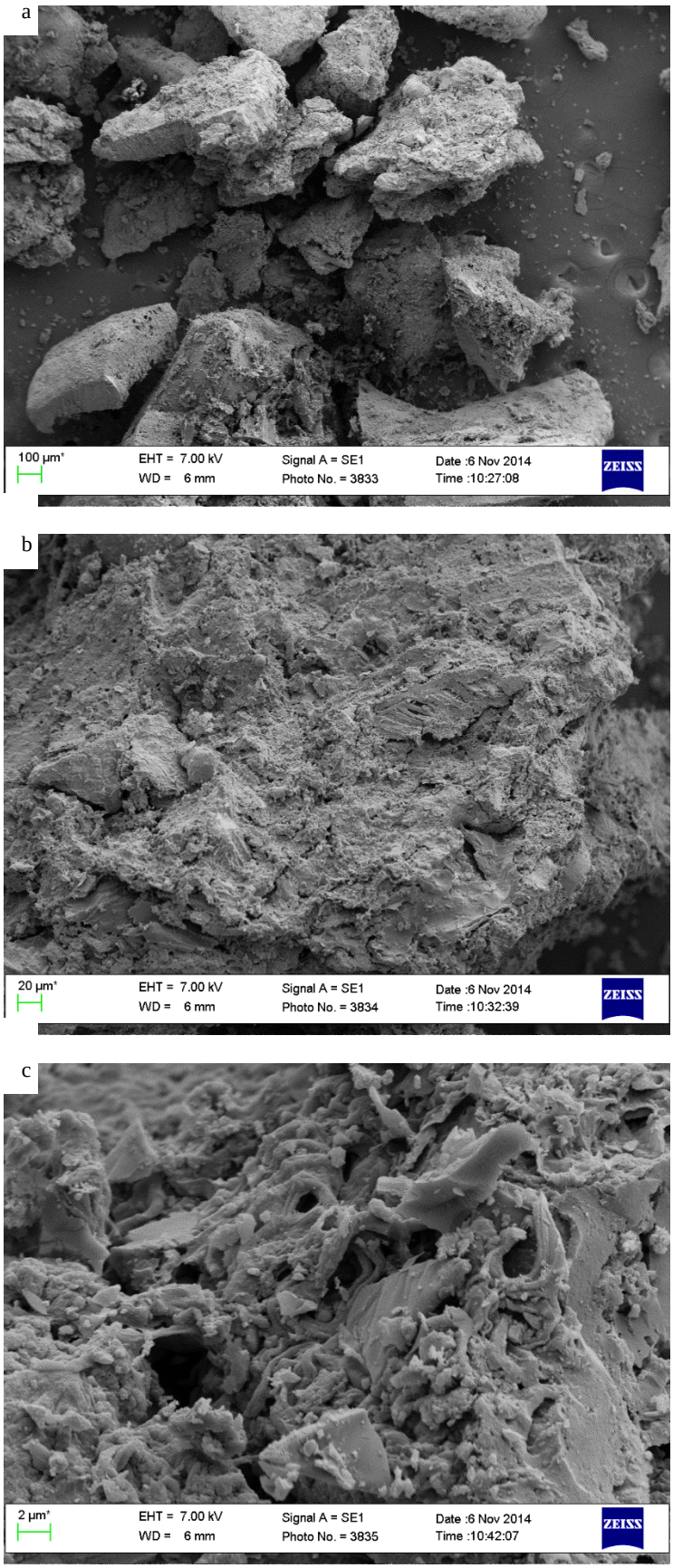

Figure 3. 4: SEM images of biochars from grape skin at (a) 100 µm, (b) 20 µm and (c) 2 µm.

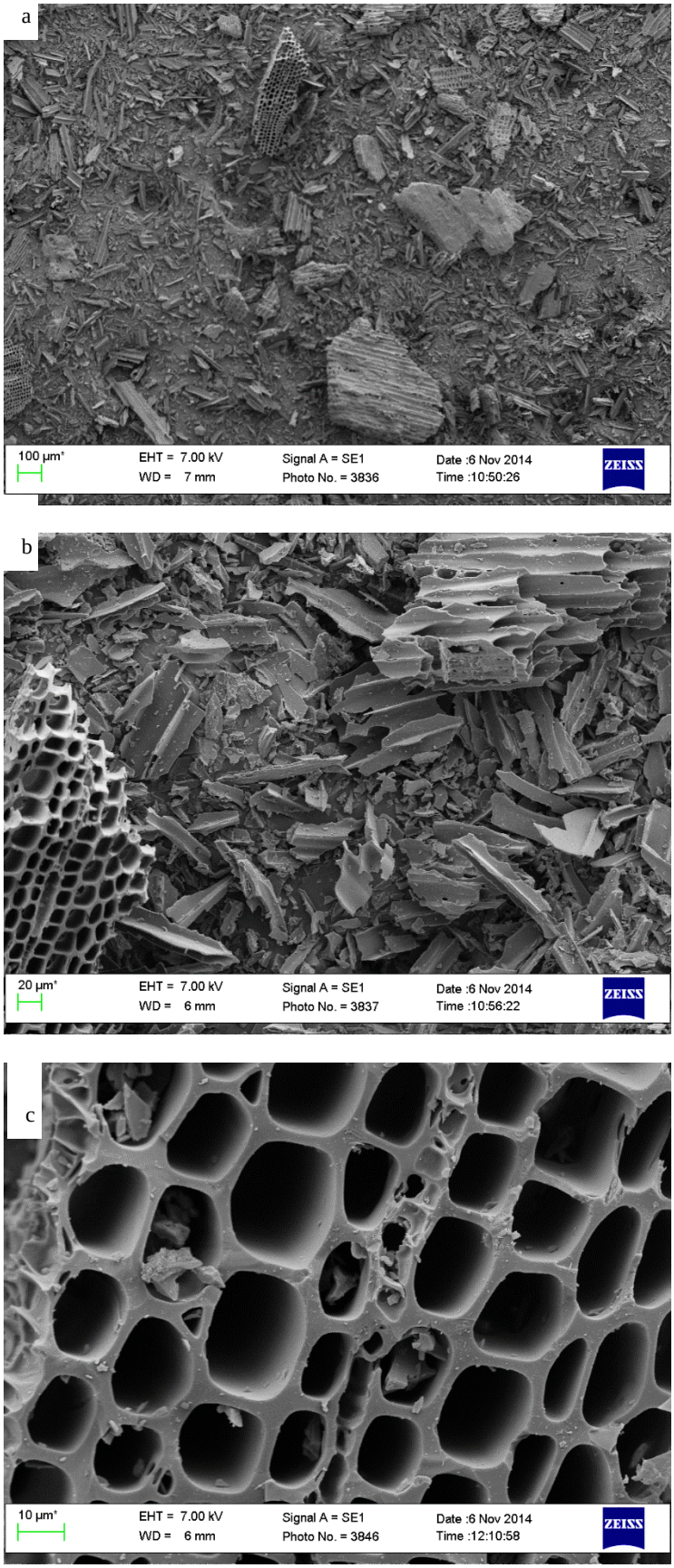

Figure 3. 5: SEM images of biochars from pine wood at (a) 100 µm, (b) 20 µm and (c) 10 µm.

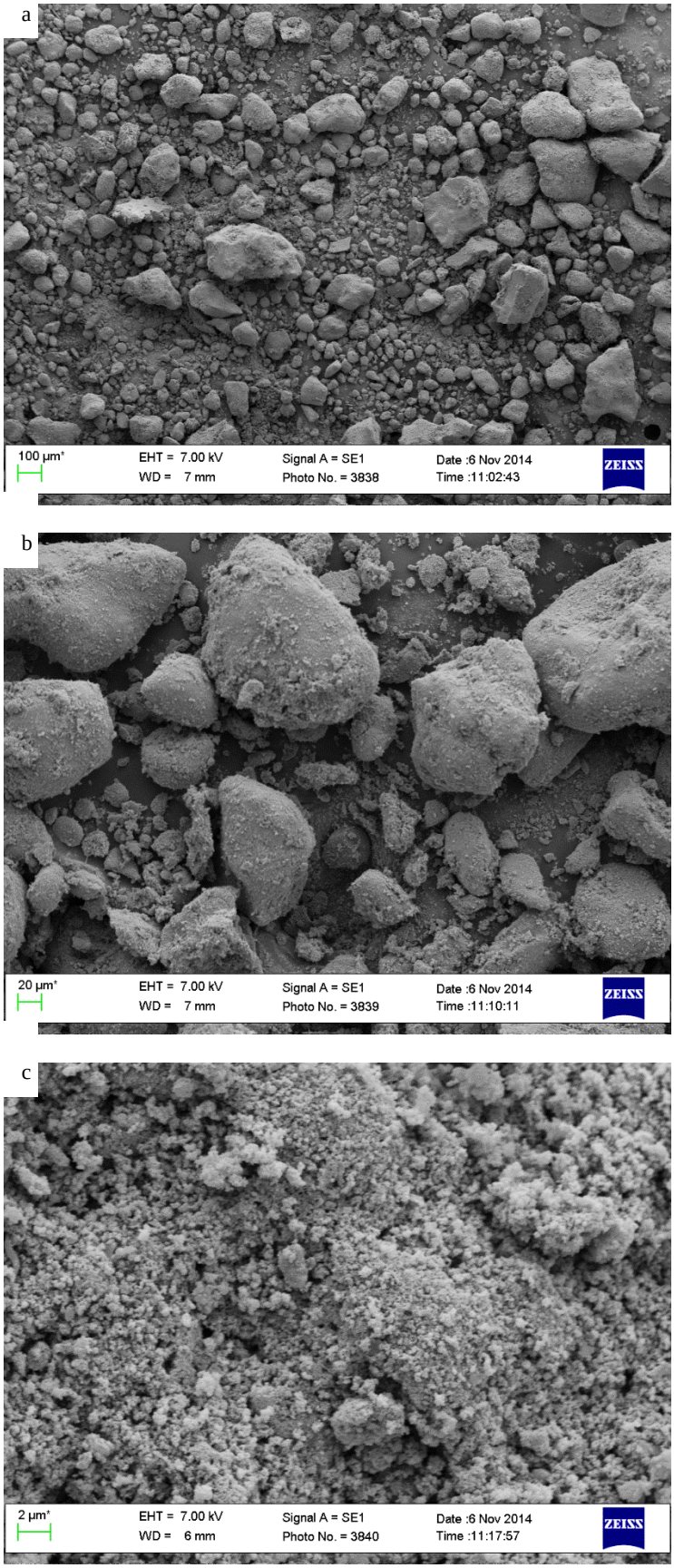

Figure 3. 6: SEM images of biochars from rubber tyre at (a) 100 µm, (b) 20 µm and (c) 2 µm.and (c) 2 µm.

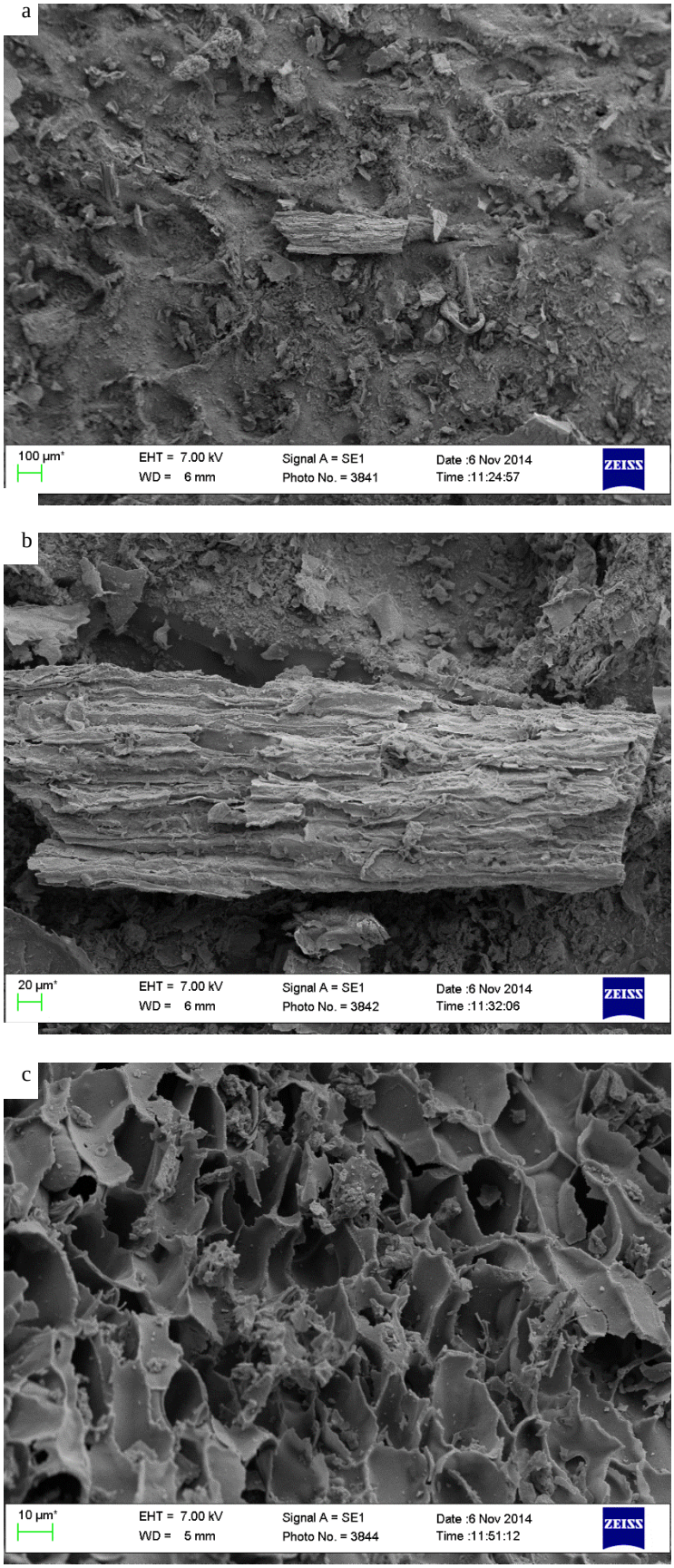

Figure 3. 7: SEM images of biochars from sugarcane pith at (a) 100 µm, (b) 20 µm and (c) 10 µm.

3.6 Conclusions

The physico-chemical and morphological characterisation of the six biochars revealed that they were very different in nature. Both the maize stover and grape skin biochars are marginally accepted as biochars according to the EBC. This is because according to the EBC recommendation, a biochar must have a minimum threshold of 50% total C. The maize stover and grape skin biochars had 50% and 59% total C, respectively. Maize stover also contained more than 50% volatile matter compared to the other chars as a result of soil particles and impurities during pyrolysis. Grape skin biochar had the lowest H/C of 0.12 and consequently was the most highly carbonised relative to the other biochars.

All of the plant-derived biochars were alkaline in nature, with pH readings in water ranging between 8.0-10.7. The rubber tyre biochar was the only acidic char in this research study. Its pH(H_2O) 2.4 reading was better explained by the high content of acidic functional groups and low content of alkali and alkaline earth metals.

The physico-chemical properties revealed from studying the pine wood biochar render it a highly recommendable soil amendment. This is because it had a low ash content, very high total C content of 80%, and a high surface area of 344 m^2 g^{-1} making it ideal for nutrient and water adsorption. It was found that the grape pip derived char had a very low BET surface area (9.8 m^2 g^{-1}) which may not possess adequate characteristics as a biochar. However, this does not preclude its use as a biochar because it can still be applied to soil for C storage (due to the large fixed C content of 87%) and as an inorganic nutrient source.

Of all the biochars studied, the results from the sugarcane pith suggested that perhaps the product produced by vacuum pyrolysis was not in fact a biochar. On the contrary, vacuum pyrolysis may have not been an ideal pyrolysis method to produce biochar from sugarcane pith. This is because the guidelines given by the EBC suggested that it was a pyrogenic carbonaceous material due to its low C content, whereas the IBI described it as thermochemically altered as a result of its lower stability and higher chemical reactivity in soils as revealed by its H/C and O/C. Notwithstanding, the sugarcane pith char may still be used as a soil amendment because it would serve as a valuable nutrient delivery substrate due to its high ash content. Overall, each biochar studied demonstrated its unique characteristics which deem each worthy as a soil amendment due of its specific biomass feedstock and pyrolysis conditions.

Chapter 4

Adsorption and desorption of ammonium and nitrate on biochars

4.1 Introduction

The loss of mineral nutrients in soil is highly problematic in agriculture. Losses are a burden on the economic situation of the farmers who grow crops and on the environment that becomes polluted because of displaced fertilisers. Nitrogen is one of the most highly mobile macronutrients added to soils (Havlin et al 2014). This is the reason why it is prone to lower plant use efficiency. Nitrogen is often lost to surface and groundwater by leaching of NO_3^- (Addiscott 1996). It is also lost through gaseous emissions of dinitrogen gas (N_2), nitrous oxide (N_2O), nitric oxide (NO) and ammonia (NH_3), volatilisation and denitrification (Brady and Weil 2002; Knowles et al 2011; Cameron et al 2013). The greatest advantage of biochar adsorbing applied ammonium (Steiner et al 2008b) and nitrate, is that N leaching is reduced.

Recent findings have shown that physico-chemical properties of biochar such as the surface area and surface charge, as well as biochar microporosity actually affects the retention of ammonium and nitrate (Yao et al 2012; Hale et al 2013; Hollister et al 2013). Soil CEC, which can be increased by biochar application, also plays a critical role in nutrient adsorption/desorption and their availability in soil (Shenbagavalli and Mahimairaja 2012). An example of this was observed where Shenbagavalli and Mahimairaja (2012) reported that the CEC (16 cmol kg^{-1}) of prosopis (wood) biochar adsorbed approximately 2880 NH_4^+ kg^{-1} biochar. Some mechanisms for NH_4^+ sorption by biochar have been described by CEC, acidic and oxygen functional groups (Wang et al 2015b; Yang et al 2017), whereas NO_3^- sorption is controlled by basic functional groups and positive exchange sites on the biochar surface (Cheng and Lehmann 2009; Wang et al 2015b).

Pyrolysis temperature and activation of biochar has also been reported to increase the formation of aromatic C structures for temperatures greater than 400 °C, and increase nitrate sorption capacity (Zhang et al 2017). While several studies investigating the sorption properties of biochars have been conducted, few have studied the potential reversibility of NH_4^+ and NO_3^- sorption on the different biochar types, and this is what this research undertakes.

4.2 Objective

The principal objective of this study was to investigate which biochar properties control NH_4^+ and NO_3^- adsorption (capture) and desorption (release). This was to identify mechanisms for N retention. The rationale for this is that biochars with a low N capturing ability would be most favourable for amending

soil in which to grow plants because that N would be plant available and not adsorbed to the biochar surface. It would also facilitate understanding of how biochar can be managed alongside the use of mineral (inorganic) N fertilisers.

4.3 Materials and Methods

This research unit was carried out by investigating the sorption properties of different biochars in NH_4^+ and NO_3^- aqueous solutions to evaluate for nitrogen release and removal. The biochar properties of elemental and proximate analysis, pH, surface acidity and alkalinity, functional groups from the FTIR results, and BET surface area described in Chapter 3 were used to relate the results.

4.3.1 Adsorption of ammonium and nitrate on biochars

A sorption study of ammonium and nitrate was carried out using batch equilibrium method on the six biochar types described in Chapter 3. Ball-milled biochar samples were used in this research unit to exclude the effect of particle size. The adsorption study was conducted at the pH of each biochar using two separate solutions, NH_4Cl and KNO_3 as adsorbates applied at concentrations of 5, 10, 25, 50 and 100 mg L^{-1}. In addition to the adsorbates, a very weak KCl solution of 0.01 M was used as a background electrolyte. The reason this was done was to minimise ionic strength effects and to suppress exchange reactions. The experiment was performed using a 1:200 biochar to solution ratio where 0.25 g (oven-dry equivalent) biochar was shaken with 50 mL solution. Each treatment was replicated three times. All glass apparatus were soaked in 10% HCl, washed and thoroughly rinsed with deionised water before use.

For the determination of equilibration time, 0.25 g (oven-dry equivalent) biochar was weighed in a series of clean plastic bottles and 50 mL of known concentration of NH_4^+ and NO_3^- solutions were added and shaken on an IKA® KS 260 mechanical shaker (IKA Works, Inc., USA) at different time intervals of 1, 3, 6, 12, 24 and 48 hours. The amount of ammonium and nitrate adsorbed onto the biochars increased with time, but eventually a constant value was reached when no further adsorption took place. Thus the equilibration time was found to be 24 hours and was used in this research unit.

Once the equilibrium period of 24 h of shaking had lapsed, the samples were filtered under vacuum using 0.45 µm nylon membrane filters. The pH and EC of the supernatant solution were measured and the quantity of ammonium and nitrate in solution were determined colorimetrically using the methods described in Section 4.3.3. The amount of NH_4^+ and NO_3^- adsorbed on the biochar surfaces was calculated from the difference in the concentration of ammonium and nitrate in the initial solution before extraction.

4.3.2 Desorption of ammonium and nitrate from biochars

To investigate the release of NH_4^+ and NO_3^- from biochar surfaces, the highest ammonium and nitrate (100 mg L^{-1}) treatment concentrations were used for the desorption experiment. The same methodology used for the adsorption study was used for the adsorption step, except that 1 g of biochar was reacted with 200 ml of solution (still maintaining a 1:200 solid to solution ratio) (Section 4.3.1). Thereafter, the vacuum filtered biochar was collected from the pre-weighed filter membrane and the biochar on the filter paper was weighed. This was then carefully scraped and the total wet mass was recorded, and subsequently corrected for dry mass. The known mass of biochar was then shaken in 200 mL of 2 M KCl for 24 h to allow for desorption reactions to take place (similar 1:200 solid to liquid ratio as adsorption experiment). The reason that 2 M KCl was used is because it is common routine practice for determining mineral N in soils (Mulvaney 1996; Zhang et al 2015). After 24 h of shaking, the samples were membrane filtered (0.45 μm) to separate the biochar from the solution. The concentrations of ammonium and nitrate in the 2 M KCl extraction solution were measured colorimetrically as described in Section 4.3.3. The amount of desorbed ammonium and nitrate was corrected by subtracting the amount of ammonium and nitrate that was calculated to be in the solution entrained in the wet biochar sample used for the desorption experiment.

4.3.3 Determination of mineral N in solution

The concentration of NH_4^+ in the solutions was determined colorimetrically using the salicylate method (Mulvaney 1996). The procedure was undertaken as follows: the aliquot was mixed with a chelating agent, namely disodium salt of ethylenediaminetetraacetic acid (Na_2EDTA), to prevent precipitation; catalyst (sodium nitroprusside) which increases the rate and intensity of colour development; and finally, hypochlorite reagent. The sample was brought up to a volume of 25 mL and the colour was allowed to develop in a water bath set to 37°C. An ultra-violet/visible (UV/VIS) spectrophotometer was used at 667 nm to measure the intensity of the emerald green colour that developed from each sample. The concentration of NH_4^+ was calculated based on the linear regression equation of the calibration curve prepared from the analyses of standards. Nitrate in solution was measured using an auto analyser high resolution digital colorimeter (SANS 13395 1996). In summary, the samples were put through a cadmium column and measured at a wavelength of 520 nm.

4.3.4 Statistical analysis

The ammonium and nitrate adsorption coefficients and all the physico-chemical properties of the six biochars were correlated using Pearson's statistical test. Statistical analysis was performed using IBM SPSS (IBM SPSS Statistics for Windows, Version 24.0. Armonk, NY: IBM Corp.).

4.4 Results and Discussion

4.4.1 Adsorption of ammonium and nitrate by biochars

The ammonium adsorption isotherms showed wide variability between the char samples (Figure 4.1). It was found that the rubber tyre, maize stover and sugarcane pith biochars were non-linear and showed the lowest adsorption affinities (K_p = 0.086, 0.093 and 0.112 resp.) for ammonium. The Freundlich adsorption isotherm best describes these biochars because saturation was reached and they were the weakest adsorbing biochars. The adsorption data of the remaining biochars was best described as linear based on the R^2 values (Figure 4.1). Generally, a straight line is characteristic of a C-curve (McBride 1994b). A C-curve is a linear adsorption isotherm that represents a constant partitioning mechanism. This means that the grape pip, pine wood and grape skin biochar samples had a high affinity for the ammonium ions adsorbed. This finding suggests that weak adsorption known as physical adsorption, or physisorption, took place since saturation was not reached. The grape skin, pine wood and grape pip biochars showed the highest affinity (K_p = 0.173, 0.151 and 0.131, resp.) for ammonium adsorption (Table 4.1). This implies that grape skin, pine wood and grape pip biochars have high NH_4^+ capturing abilities, which might be beneficial for enhancing N fertiliser efficiency, but only if the NH_4^+ is exchangeable.

The biochars demonstrated a much higher affinity (K_p ranging between 0.627-0.788) for nitrate (Figure 4.2 and Table 4.1) compared to ammonium (K_p ranging between 0.086-0.173). The nitrate adsorption isotherms were more linear (Figure 4.2) as indicated by the higher R^2 values for linear regression fitting (Table 4.1). Therefore, the linear adsorption isotherm best fitted the nitrate adsorption data. In contrast to the ammonium adsorption results, the rubber tyre showed the highest affinity (K_p = 0.788) for nitrate adsorption (Table 4.1).

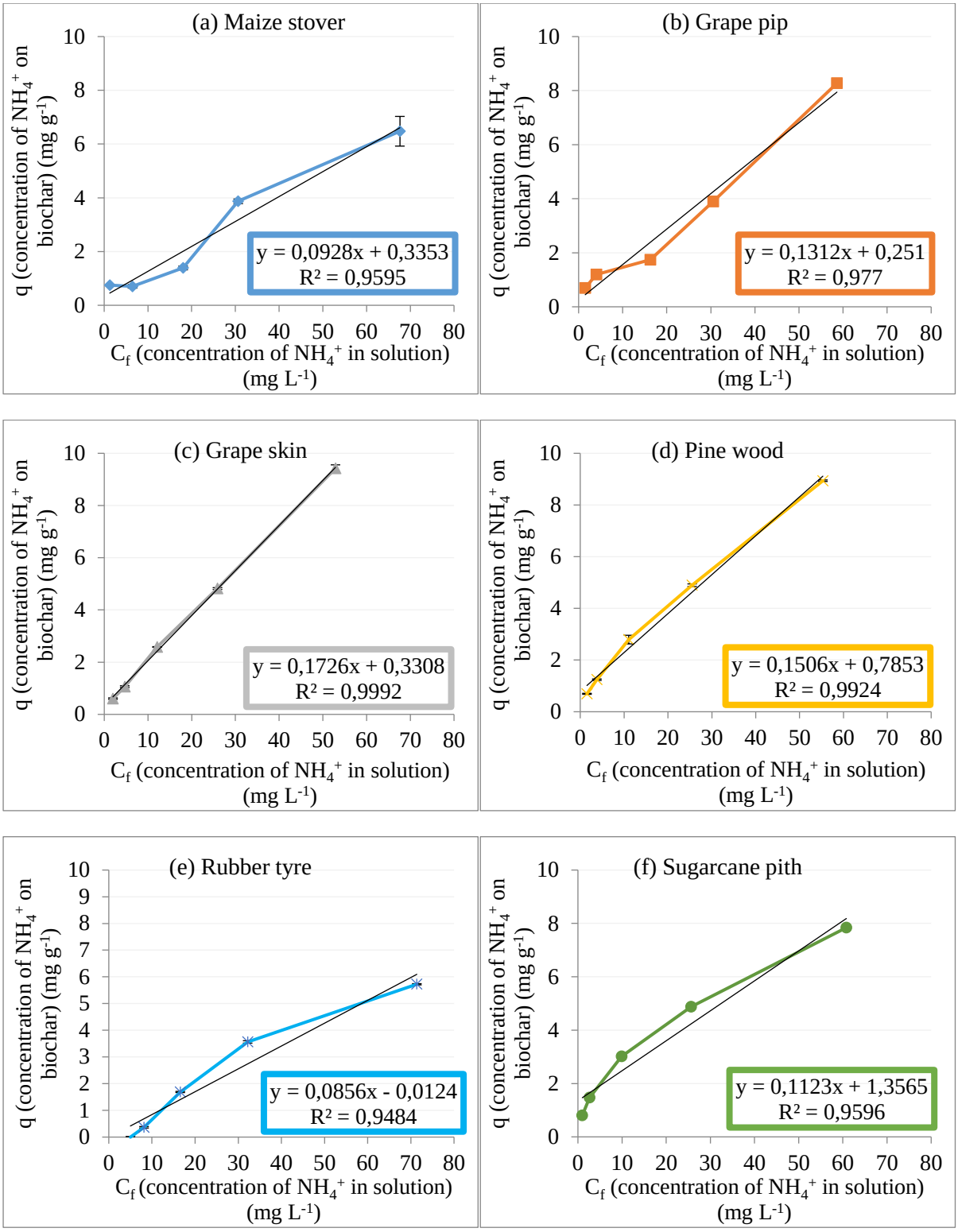

Figure 4. 1: Ammonium adsorption isotherms of the six different biochars (a-f) after 24 hours equilibration with ammonium chloride solution. Error bars represent standard deviation of the mean where n = 3.

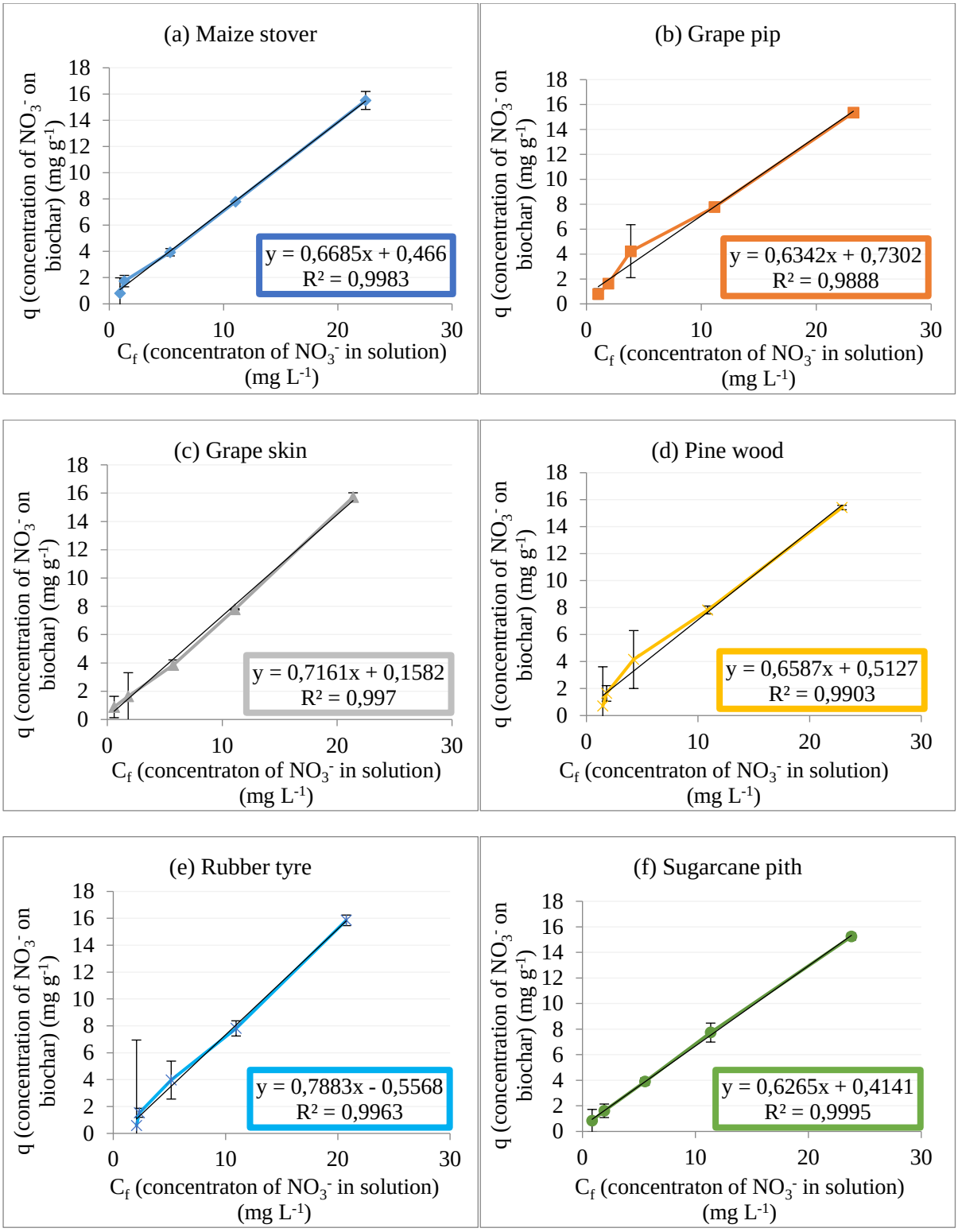

Figure 4. 2: Nitrate adsorption isotherms of the six different biochars (a-f) afte 24 hours equilibration with potassium nitrate solution. Error bars represent standard deviation of the mean where n = 3.

Table 4. 1: Linear adsorption isotherm partitioning constants of ammonium and nitrate on the six biochars arranged in terms of increasing affinity.

Ion sorbed	Biochar	*K_p	R^2
Ammonium	Rubber tyre	0.086	0.948
	Maize stover	0.093	0.960
	Sugarcane pith	0.112	0.960
	Grape pip	0.131	0.977
	Pine wood	0.151	0.992
	Grape skin	0.173	0.999
Nitrate	Sugarcane pith	0.627	0.999
	Grape pip	0.634	0.989
	Pine wood	0.659	0.990
	Maize stover	0.669	0.998
	Grape skin	0.716	0.997
	Rubber tyre	0.788	0.996

*K_p represents the partitioning coefficients obtained from the slope of the linear adsorption isotherms.

The percentage ammonium and nitrate adsorbed of what was added is shown to clarify the relative differences between the treatments (Figures 4.3). It was found that between 46 and 87% of ammonium was adsorbed by the biochars at the (lowest) 5 mg L^{-1} treatment level compared to the 31-48% adsorbed at the (highest) 100 mg L^{-1} treatment (Figure 4.3a). Nitrate adsorption on the other hand achieved near constant adsorption levels between 77 and 88% across the extraction solution treatments, with the exception of the rubber tyre char which adsorbed 64% NO_3^- at the 5 mg L^{-1} treatment level (Figure 4.3b).

Other studies also show that although nitrate capture by biochars does occur, it is subjective. Similar to this study, a study by Kammann et al (2015a) also showed that wood derived biochar produced at 750 °C sorbed nitrate very strongly compared to ammonium. However, it was suggested that the measured NO_3^- capture may have been underestimated because nitrate may be removed in part due to insufficient extraction times (1-2 hours) that do not allow for all the biochar-bound nutrients to be detected. In contrast, in a study by Hollister et al (2013) where maize stover and oak wood biochars were used, it was shown that an extraction time of 16 h was not sufficient for nitrate adsorption to take place. This was observed when the biochars, both rinsed (aged) and non-rinsed, did not develop basic functional groups as expected, although they were in the pyrolytic temperature range of 350-600 °C. These reports demonstrate that nitrate capture by biochar is dynamic and possibly influenced by biochar type and analytical methodology.

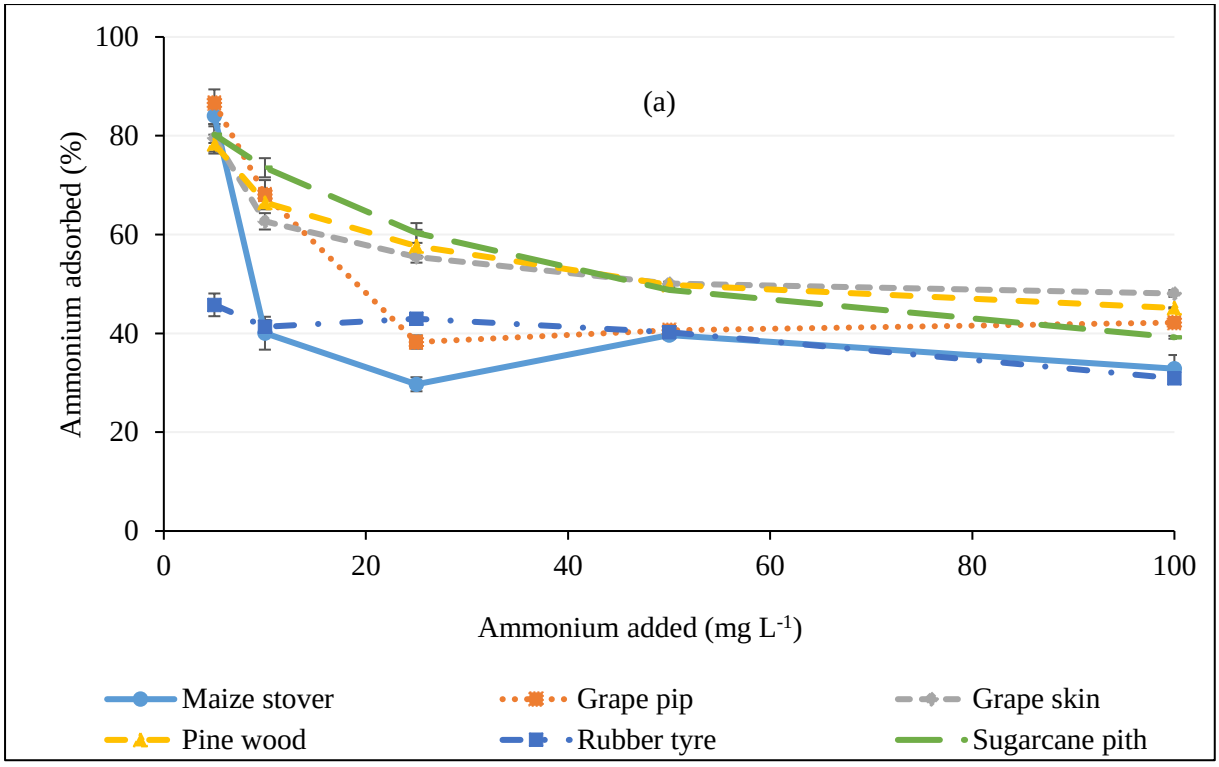

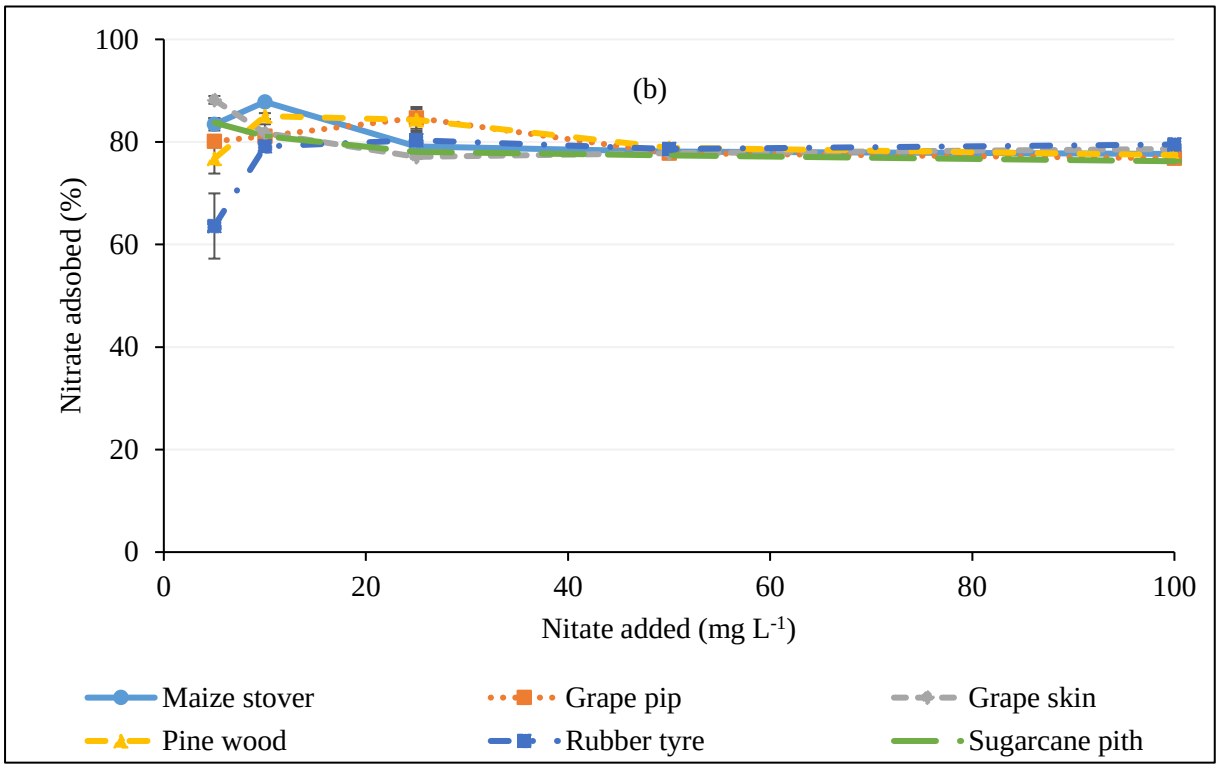

Figure 4. 3: Percentage of (a) ammonium and (b) nitrate adsorbed of what was initially added in the extraction solution treatments by different biochars.

4.4.2 Desorption of ammonium and nitrate from biochars

It was found that the adsorbed ammonium was far more easily desorbed (53.1-60.3% of adsorbed) from the biochars than nitrate (0.02-0.27% of adsorbed), despite the biochars adsorbing far less ammonium (33.1-38.6% of total added) than nitrate (81.8-89.3% of total added) in the 100 mg L^{-1} treatments (Figure 4.4). Accordingly, 53-60% of the calculated adsorbed (q) ammonium was desorbed with 2 M KCl, compared to only 0.02-0.27% of the adsorbed nitrate. This indicates that the NH_4^+ mainly adhered to biochar by electrostatic interactions (cation exchange) as it was largely exchangeable with KCl. This finding correlates with the observed net negative charge (negative ΔpH values in Table 3.4) and the presence of carboxyl groups (Figure 3.1) on the biochars shown in Chapter 3. In contrast, the nitrate was practically not desorbable, which potentially indicates that either it was adsorbed too strongly to be extracted by 2 M KCl in 24 h of shaking or that it possibly could have reacted with biochar and changed speciation and was not longer in the form of nitrate. These findings could possibly indicate that physisorption of NH_4^+ and particularly NO_3^- took place because of the presence of electrostatic and van der Waals forces (Rafatullah et al 2010) in the biochars.

As mentioned above, it could also be possible that nitrate changed speciation, i.e., was reduced, due to reacting with the biochar. Nitrate is a very stable, oxidised form of N, making it unlikely that it spontaneously reduced during the 24 h adsorption experiment. Microbial denitrification requires that all oxygen is removed from solution and would take a considerable period to initiate and is thus also highly unlikely in the short 24 h batch equilibration period. Biochars and black carbons have been shown to be redox reactive and been shown to catalyse the reduction of a number nitrogenous and other organic compounds (Oh et al 2004; Oh and Chiu 2009; Oh et al 2012; Klüpfel et al 2014). This reducing redox reactivity is attributed to the condensed aromatic ring structures in the biochar, which facilitate electron transfer reactions (Oh et al 2012). Biochars produced at pyrolysis temperatures between 400 and 700°C have been shown to have high capacities in accepting (quinone) and donating (aromatic rings) electrons (Klüpfel et al 2014; Yuan et al 2017). Aromatic structures on the biochars were directly supported by evidence from the FTIR (Figure 3.1) and proximate analysis fixed C results (Table 3.3). Thus, it is possible that biochars reduced the nitrate to another form of reduced N, possibly nitrite or even reduced gaseous forms. This requires further investigation in a future study.

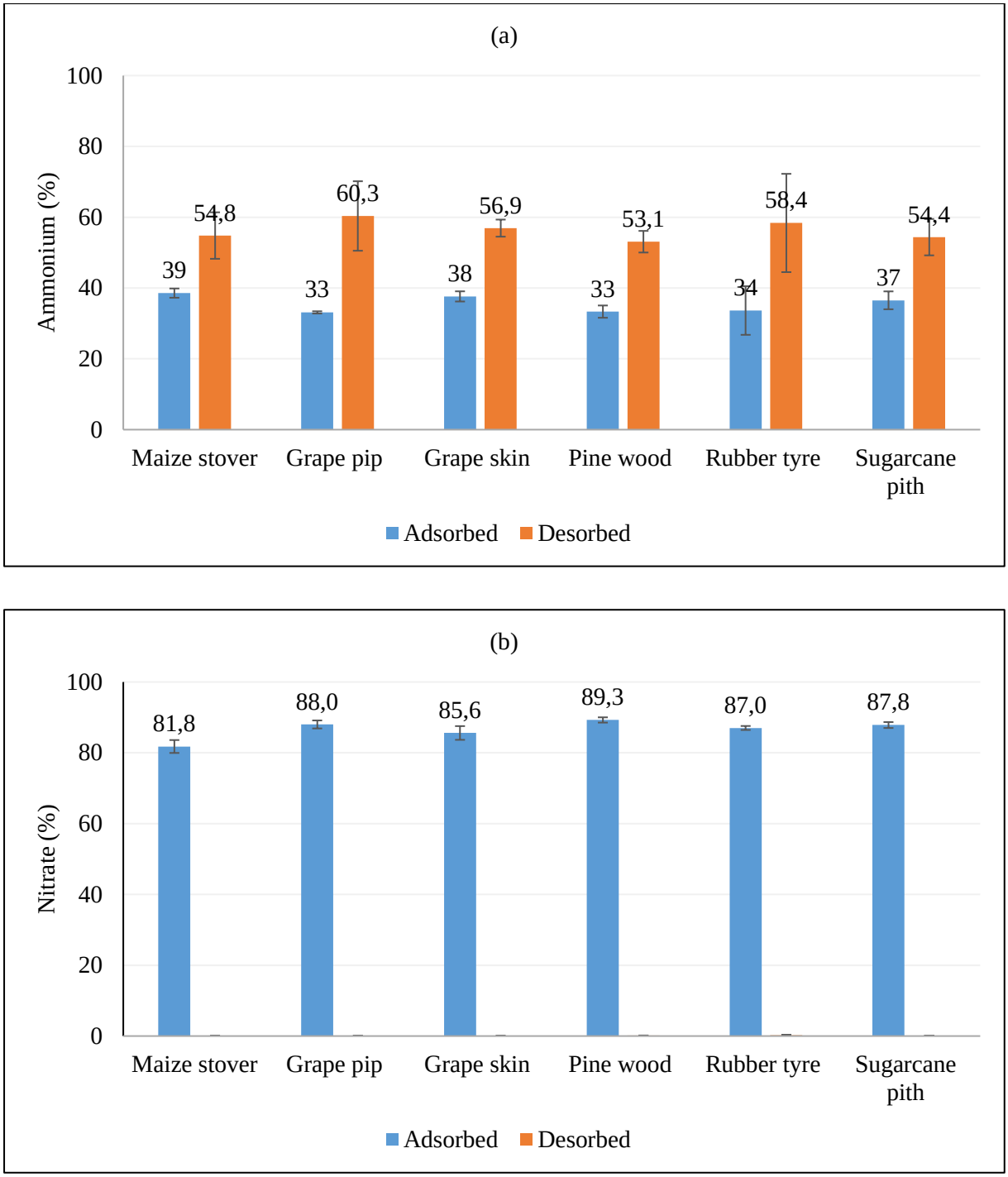

Figure 4. 4: Percentage of (a) ammonium and (b) nitrate initially adsorbed of the total added and the desorbed (2 M KCl) of what was adsorbed in 100 mg L^{-1} treatments by different biochars.

4.4.3 Relationship between K_p and biochar properties

The ammonium and nitrate adsorption partition coefficients of the biochars (Table 4.1) were correlated with all the biochar physico-chemical properties that were characterised in Chapter 3. The correlations are shown in Table 4.2. It was found that the ammonium partition coefficients tended to correlate with more biochar properties than nitrate (Table 4.2). The correlations shown are those with the strongest correlation coefficients (Figures 4.5-4.8). Since the rubber tyre biochar is so distinctly different from the remaining biochars which were produced from plant biomass (Chapter 3), it was interesting to observe how the relationships with mineral N adsorption would differ when compared without the influence of rubber tyre char. Only the correlations that increased when rubber tyre biochar was excluded are discussed here. The remaining correlation results without rubber tyre char are shown in Appendix A.

Sodium had a strong positive correlation with ammonium adsorption (R^2 = 0.69) (Figure 4.5) which was statistically significant ($P < 0.05$) (Appendix A). The correlation demonstrated that more ammonium was adsorbed on biochars with increasing total Na content and this suggests that a cation exchange mechanism is responsible.

There was a strong positive correlation between total sulfur (S) content and ammonium adsorption (R^2 = 0.78) which was statistically significant ($P < 0.05$) (Appendix A) with the plant-derived biochars. The maize stover and sugarcane pith chars measured no total S, while the remaining chars had an average of 2% S (Table 3.1). The correlation showed that more ammonium was adsorbed on high fixed C plant-derived biochars with increasing S contents.

The following highest correlation coefficient was observed between the volatile matter content and ammonium partition coefficients (R^2 = 0.47) (Figure 4.6a). The reason for a decrease in the amount of ammonium adsorbed when the volatile matter content increases may be due to the fact that biochars are usually uncharged and hydrophobic (Das and Sarmah 2015) and would therefore not attract charged ions. Interestingly, when the correlation was redone without the rubber tyre char, the correlation was stronger (R^2 = 0.62) (Figure 4.6b).

Table 4. 2: Correlation coefficients associated with various physico-chemical properties of the six biochars.

Ion sorbed	Biochar properties	*K_p	**R^2	Ion sorbed	Biochar properties	*K_p	**R^2
Ammonium	%C	0.000	0.045	Nitrate	%C	0.001	0.146
	%N	0.010	0.018		%N	0.040	0.088
	%H	0.035	0.329		%H	0.018	0.028
	%S	0.016	0.247		%S	0.028	0.241
	%O	0.002	0.114		%O	0.001	0.009
	%Ash	0.000	0.033		%Ash	0.001	0.132
	C/N	0.000	0.025		C/N	0.000	0.032
	H/C	0.073	0.233		H/C	0.123	0.206
	O/C	0.330	0.309		O/C	0.148	0.019
	%P	0.057	0.234		%P	0.067	0.098
	%Ca	0.003	0.005		% Ca	0.038	0.246
	%Mg	0.028	0.125		% Mg	0.059	0.168
	%K	0.009	0.197		%K	0.001	0.002
	Fe (mg kg^{-1})	0.000	0.098		Fe (mg kg^{-1})	0.000	0.074
	Mn (mg kg^{-1})	0.000	0.057		Mn (mg kg^{-1})	0.000	0.289
	Cu (mg kg^{-1})	0.000	0.128		Cu (mg kg^{-1})	0.001	0.064
	Zn (mg kg^{-1})	0.000	0.332		Zn (mg kg^{-1})	0.000	0.703
	Co (mg kg^{-1})	0.003	0.410		Co (mg kg-1)	0.004	0.140
	B (mg kg^{-1})	0.001	0.439		B (mg kg-1)	0.000	0.012
	Mo (mg kg^{-1})	0.024	0.443		Mo (mg kg-1)	0.021	0.102
	Na (mg kg^{-1})	0.000	0.694		Na (mg kg^{-1})	0.000	0.053
	Si (mg kg^{-1})	0.000	0.085		Si (mg kg^{-1})	0.000	0.028
	Al (mg kg^{-1})	0.000	0.021		Al (mg kg^{-1})	0.000	0.157
	Se (mg kg^{-1})	0.001	0.002		Se (mg kg^{-1})	0.030	0.312
	Ba (mg kg^{-1})	0.000	0.062		Ba (mg kg^{-1})	0.001	0.034
	Sr (mg kg^{-1})	0.000	0.127		Sr (mg kg^{-1})	0.000	0.027
	Cr (mg kg^{-1})	0.000	0.511		Cr (mg kg^{-1})	0.000	0.203
	As (mg kg^{-1})	0.010	0.472		As (mg kg^{-1})	0.016	0.351
	Ni (mg kg^{-1})	0.001	0.368		Ni (mg kg^{-1})	0.000	0.035
	Pb (mg kg^{-1})	0.001	0.111		Pb (mg kg^{-1})	0.001	0.075
	Cd (mg kg^{-1})	0.027	0.071		Cd (mg kg^{-1})	0.065	0.122
	Sb (mg kg^{-1})	0.842	0.209		Sb (mg kg^{-1})	1.562	0.221
	Hg (mg kg^{-1})	0.295	0.246		Hg (mg kg^{-1})	0.471	0.193
	%Volatiles	0.001	0.467		%Volatiles	0.000	0.001
	%Fixed C	0.000	0.245		%Fixed C	0.000	0.054
	pH (H_2O)	0.007	0.298		pH (H_2O)	0.015	0.431
	pH (KCl)	0.006	0.267		pH (KCl)	0.015	0.417
	Surface acidity	0.029	0.445		Surface acidity	0.050	0.389
	Surface alkalinity	0.023	0.110		Surface alkalinity	0.080	0.391
	BET	0.000	0.031		BET	0.000	0.022

*K_p represents the partitioning coefficeints obtained from the slope of the linear adsorption isotherms. **R^2 represents the coefficient of determination that indicates the goodness of fit by a value between 0 and 1.

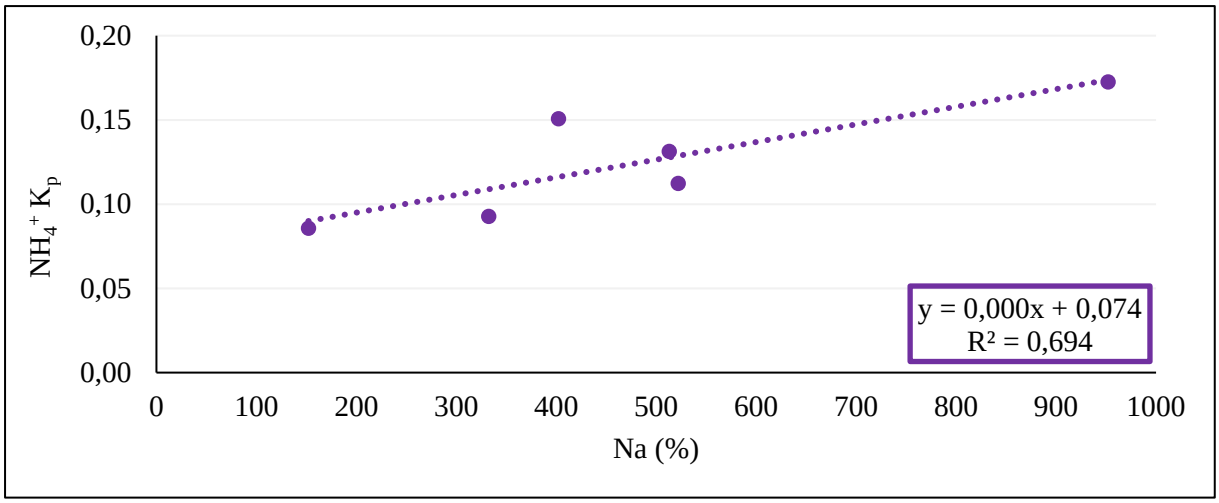

Figure 4. 5: Relationship between biochar total Na content and ammonium partition coefficients.

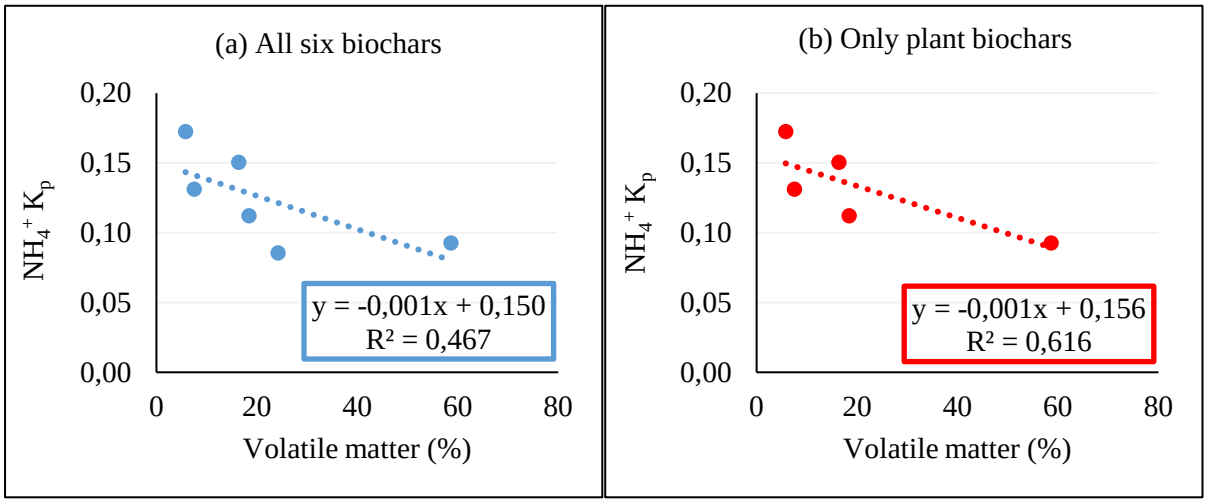

Figure 4. 6: Relationship between biochar volatiles and ammonium partition coefficients comparing (a) all six biochars (including rubber tyre char) with (b) the biochars produced from plant biomass (excluding rubber tyre char).

It was found that the O/C was weakly negatively correlated with ammonium (R^2 = 0.31) (Figure 4.7a). As with the volatiles, when the rubber tyre biochar was excluded from the correlation, the R^2 increased to 0.55 (Figure 4.7b). Theoretically, a higher O/C increases the carboxylic group content of biochar (Mukome et al 2013; Li et al 2017) and this would increase ammonium adsorption. However, since some of the biochars are possibly not completely pyrolysed (Chapter 3), they may still contain cellulose (which is a polysaccharide with a high oxygen content). Therefore, the decrease in ammonium adsorption with an increase in the O/C could explain why higher cellulose results in lower CEC because sugar functional groups do not deprotonate and contribute to CEC.

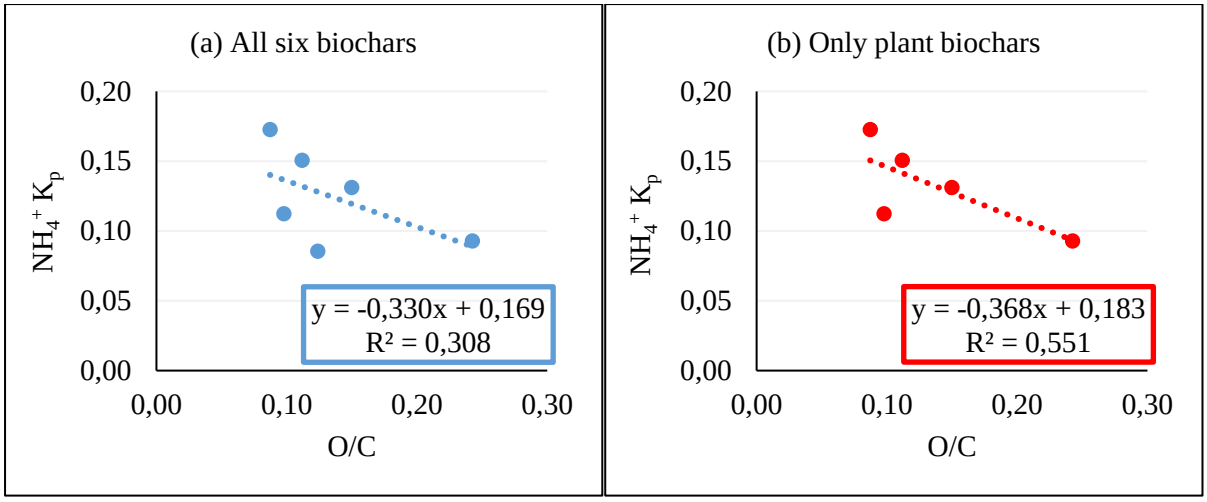

Figure 4. 7: Relationship between biochar O/C and ammonium partition coefficients comparing (a) all six biochars (including rubber tyre char) with (b) the biochars produced from plant biomass (excluding rubber tyre char).

Another noteworthy relationship was between H/C and ammonium adsorption which showed a weak negative correlation (R^2 = 0.23) with all six biochars (Figure 4.8a) and a doubled negative correlation (R^2 = 0.50) with only the plant biochars (Figure 4.8b). The reason for this relationship is that the more aromatic the biochar (lower H/C), the higher its affinity for a cation.

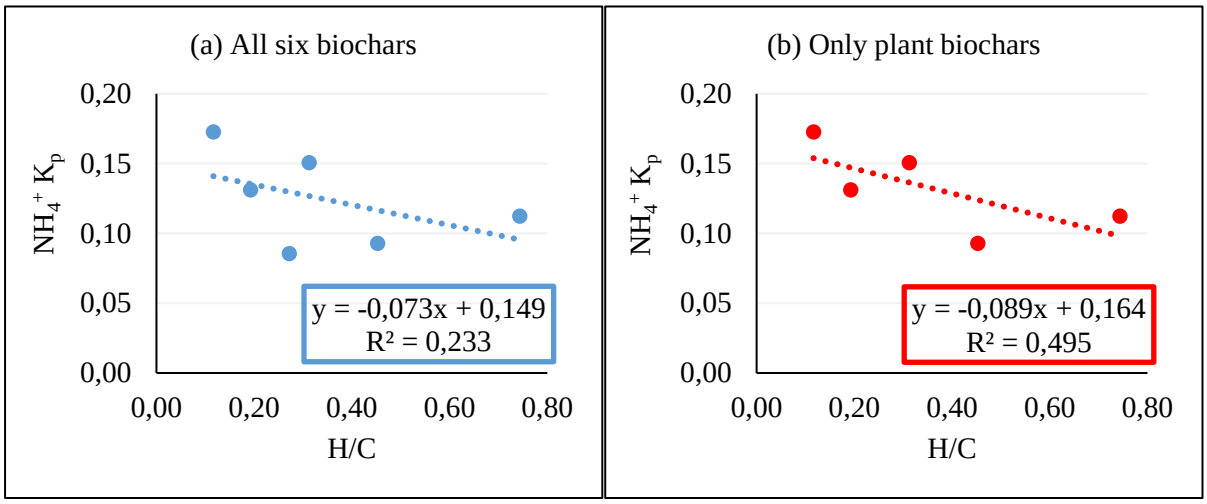

Figure 4. 8: Relationship between biochar H/C and ammonium partition coefficients comparing (a) all six biochars (including rubber tyre char) with (b) the biochars produced from plant biomass (excluding rubber tyre char).

These findings suggest that at least two mechanisms played a role regarding ammonium removal from solution by the biochars. The first being electrostatic adsorption of NH_4^+ to negatively charged carboxylic functional groups on the biochar surfaces (Cheng et al 2006; Yao et al 2012; Wang et al

2015a). Secondly, potential ammonia volatilisation could have occurred to a lesser extent. Therefore, it can be inferred that true adsorption of ammonium did not take place, but rather a combination of adsorption and volatilisation of ammonia.

The correlations for biochar pH in water with nitrate were slightly less weak (R^2 = 0.43) compared to those observed with ammonium (R^2 = 0.30) (Table 4.2). The weak negative correlation of nitrate adsorption with pH indicates that the lower the pH, the more nitrate is adsorbed (Figure 4.9). This relationship is probably related to negative surface charge on the biochar which increases as pH increases due to deprotonation of acidic functional groups.

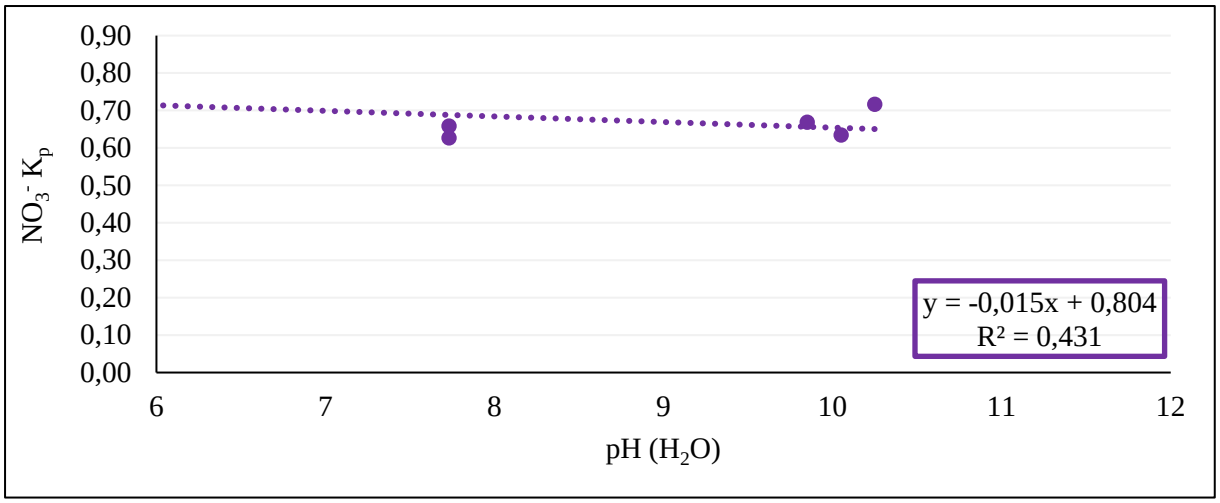

Figure 4. 9: Relationship between biochar pH in water and nitrate partition coefficients.

Although limited, it is possible that NH_4^+ removal from solution was influenced by potential NH_3 loss through volatilisation at higher pH values; especially at pH values above 8.0. As the biochar samples were highly diluted with solution (1:200) resulting in more neutralised pH readings (Table 4.3) a lot closer to water than the 1:20 (biochar to solution ratio) pH readings taken in Chapter 3, and furthermore, shaken in closed containers with small headspace, the volatilisation losses would have probably been very low.

Table 4. 3: pH of biochar samples measured at a 1:200 ratio.

Biochar	pH_{H2O}	pH_{KCl}	ΔpH
Maize stover	9.85	9.79	-0.06
Grape pip	10.05	9.92	-0.13
Grape skin	10.25	10.09	-0.16
Pine wood	7.73	7.27	-0.46
Rubber tyre	3.21	3.02	-0.20
Sugarcane pith	7.73	7.57	-0.16

Total zinc had a strong positive correlation with the nitrate partition coefficients (R^2 = 0.70) (Table 4.2) which was statistically significant ($P < 0.05$) (Appendix A). When Zn was compared with only the plant-derived biochars, the R^2 dropped dramatically to 0.48. The reason for this is that the rubber tyre biochar had a very high concentration of total Zn (2205 mg kg^{-1}) (Table 3.2) and it is the Zn that helped to reduce nitrate. The diammonium EDTA extractable Zn was also correlated with the sorption data to investigate the effect of exchangeable Zn. It was found that there was a strong positive correlation with the nitrate partition coefficients (R^2 = 0.66), however, it was not statistically significant ($P = 0.051$). Thus, it was suggested that Zn, a monometallic metal, was responsible for catalysing nitrate reduction in biochar. This was a surprising observation given that nitrate reduction is most commonly found in the presence of bimetallic catalysts such as rhodium-copper (Soares et al 2008) and palladium-copper (Yoshinaga et al 2002) supported by active carbon.

Contrary to the findings of Hollister et al (2013) where the biochar surface area was observed to influence sorption of nitrogen, the current study did not show any strong surface area correlations with ammonium (R^2 = 0.031) or nitrate (R^2 = 0.022) adsorption (Table 4.2).

4.5 Conclusions

The sorption experiments confirmed some of the results obtained through biochar characterisation. Most notably, the aromaticity of the biochars was useful in explaining the sorption results. All the biochars had a much higher affinity for nitrate (82-89%) than ammonium (33-39%). This is possibly because the biochars possess highly condensed aromatic ring structures which increase their capacity to potentially reduce nitrate, and subsequently promote reducing redox reactions.

The maize stover and grape skin biochars, which were previously found to be poorly pyrolysed (Chapter 3), adsorbed the most ammonium, 39 and 38%, respectively. This observation indicates that these biochars could possibly have higher cation exchange capacity than the other biochars. Furthermore, it was found that ammonium was moderately desorbed from the biochars as 53-60% of adsorbed NH_4^+ was desorbed with 2 M KCl after 24 h of extraction. This finding provided evidence that ammonium

adsorption is reversible. The mechanism for ammonium adsorption was thus largely cation exchange. This conclusion also correlates with the physico-chemical characteristics of the biochars of having net negative pH values. In addition, these results suggest that the biochars in the current study could function as slow-release ammonium-nitrogen fertilisers if the ammonium is bioavailable.

Although ammonium adsorption was found to be partially reversible, nitrate was not desorbable. Only 0.02-0.27% of the adsorbed NO_3^- was desorbed. Two possible reasons are suggested: Firstly, the nitrate may have been too strongly adsorbed to be extracted by 2 M KCl during the 24 h extraction time. Or, the nitrate may have reacted with biochar and changed speciation by being reduced to other nitrogenous compounds. This implies that nitrate adsorption may have not taken place, but reduction instead. However, it seems highly unlikely that within the short period of 24 h, nitrate could have reduced or undergone microbial denitrification. But, it is likely that reduction due to redox reactivity may have occurred.

The results from this research unit showed that the biochars primarily possess both ammonium adsorption and desorption properties, and nitrate adsorption characteristics. The suggested mechanism for the adsorption of ammonium and nitrate is physisorption. Physisorption is the simple ion exchange that occurs because of electrostatic and van der Waals forces. Furthermore, alternating redox reactions played a role in nitrate sorption due to the high capacity of the biochars to accept and donate electrons. Regarding ammonium, it was also found that NH_4^+ adsorption may have occurred together with volatilisation to a lower extent. Lastly, the total Zn concentration of the six biochars correlated significantly with the removal of nitrate. Since the biochars had a high affinity for nitrate adsorption, it follows that caution should be applied when using NO_3^- fertilisers together with biochar amended soils.

Chapter 5
Carbon and nitrogen mineralisation from different biochar types in a sandy soil

5.1 Introduction

Rising levels of atmospheric CO_2 and the sub-optimal use of inorganic N by soils are two examples of alarms perpetuated by modern day agricultural practices. The production and use of biochar, a carbon negative biofuel, as a means to remove carbon dioxide from the atmosphere has been widely proposed (Glaser 2007; Mathews 2008; Vaccari et al 2011; Anbar et al 2016). When biochar is incorporated into the soil, it stimulates soil microbes (Kuzyakov et al 2009), thus causing increases in soil microbial respiration (Smith et al 2010).

Soil respiration and net N mineralisation are inextricably related because C cycling controls N dynamics (Gruber and Galloway 2008). Recent studies have considered the complex relationship dynamics between C and N. For example, biochar has been shown to both have no net CO_2 mineralisation and reduce net CO_2 mineralisation (Prayogo et al 2014); reduce net N mineralisation (Castaldi et al 2011; Dempster et al 2012a; Prayogo et al 2014); increase net N mineralisation (Castaldi et al 2011; Bruun et al 2012); and also promote N immobilisation (Case et al 2012; Bruun et al 2012).

In a previous study, pine wood biochar was found to dramatically reduce mineral N leaching when the biochar was mixed with soil at rates between 0.5-10% biochar (w/w) and had 100 kg N ha^{-1} of NH_4NO_3 added (Sika and Hardie 2014). At the end of the 6 week incubation study, it was found that the amount of initial N in the leaching columns did not balance the sum of the amount of N leached and exchangeable by 2 M KCl (Sika and Hardie 2014). This means that although it is well established that some of the N was made less available because of biochar's influence during leaching, the question of what other reason was responsible persists. It was with this rationale that the idea of investigating the microbial immobilisation of biochar came about. This was done to assess whether microbial N immobilisation may also explain why N in biochar is less available. Furthermore, the effect of the physico-chemical properties of the biochar on C and N mineralisation was investigated.

Various models describing soil respiration have been proposed relating soil reaction to temperature and precipitation (Reichstein et al 2003; Yuste et al 2003; Yuste et al 2007). However, the soil respiration test is only a partial simulation of field conditions, since the primary producers are excluded from the system and C assimilation through photosynthesis does not occur. Such an experiment only describes the activity of the hierarchy of the consumptive part of the food chain. This process occurs at constant temperature and largely represents the reaction of soil community that survived the period of sample

drying. The reaction to addition of water is usually rapid and peak respiration is achieved within the first two days and should correspond to the largest proportion of soil biomass (both microbial and micro-faunal). Some parts of the detritovore/omnivore –predator chains are restored and after the peak of activity the total respiration starts to decline due to restrictions on food source availability/accessibility, which become more and more severe over time.

Such a system behaviour may be modelled by a set of two equations separately describing the "awakening" stage of rapid respiration growth followed by the stage of "population decline" manifested in reduced respiration. To our knowledge, no attempts have been made to describe the process with a single continuous function describing both processes, and this research aims to fill this gap in knowledge.

Yan et al (2014) observed an open system containing primary producers whereby a system behaviour in response to rain was investigated. The authors characterised the process with a complex exponential function, though similar soil system behaviour may be described by resilience functions (Todman et al 2016). The similarity of the function shape to underdamped oscillations were quite conspicuous, though fitting such complex functions with a large number of parameters may be quite challenging. A simplified version of a vapor pressure model or a rational function with linear and quadratic parts may be a simple fit describing the process with sufficient accuracy.

The current study investigates six locally produced biochars from different biomass feedstocks, including pine wood, and different pyrolytic processes. The soil used in this study was from the same location as the soil previously used in the MSc study, except that the topsoil, and not the subsoil was used. The soil chosen was based on the benefits it may gain from biochar amendment because it was highly leached with poor water and nutrient holding abilities, as is typical of soils found in the Western Cape, South Africa.

5.2 Objective

The objective of this study was to investigate which biochar properties affect short-term CO_2 respiration and N mineralisation in a sandy topsoil amended with the biochars.

5.3 Materials and Methods

5.3.1 Soil

The soil used in this study was collected from a fallow field in Brackenfell, Western Cape Province, South Africa (33°53' 43.08''S, 18°43' 24.24''E). Soil was collected from the top 15 cm of the soil surface, labelled the "topsoil", and then to a depth of 1 m from the 15 cm mark, labelled the "subsoil". According to the South African soil taxonomic system, the soil was classified as a Kroonstad soil form, in the Morgendal soil family (Soil Classification Working Group 1991). This soil was characterised by a thick topsoil A horizon, covered with kikuyu grass and weeds; and a bleached subsoil E horizon above a clay layer at a depth below 1 m with signs of wetness. According to the World Reference Base (IUSS Working Group WRB) soil classification system, this soil was classified as a Haplic Stagnosol (Albic). The soil was previously classified as a medium grade pure sand with 97.1% sand, 2.6% silt and 0.3% clay (Sika 2012). The topsoil was only used for the current experimental chapter on C and N mineralisation as a control (without biochar) and mixed at a rate of 2.5% (w/w) with the biochar materials, while the subsoil was used for the leaching experimental chapter (Chapter 6).

5.3.2 Soil pH

Soil pH was measured in a 1:2.5 w/v ratio using distilled water and 1 M KCl solution (White 1997). The soil was sieved to <2 mm and the oven dry weight equivalent was used for the measurement.

5.3.3 Determination of Heavy Metals in Soil

A 0.02 M diammonium EDTA extraction was used to test for the concentration of exchangeable metals in the soil (control) and soil-biochar mixtures (Non-affiliated Soil Analysis Work Committee 1990). Five grams of soil was used with 15 mL of extraction solution. The samples were first shaken in 100 mL stoppered centrifuge tubes for 60 minutes at 180 oscillations per minute. Thereafter, the samples were centrifuged using the Eppendorf 5810 R centrifuge (Eppendorf AG, Germany) in the same tubes for 5 minutes at 2000 rpm and immediately filtered through Whatman no. 40 filter paper. An inductively coupled plasma spectrometry was used to analyse the samples for the concentrations of metals.

5.3.4 Determination of C Respiration

Seven treatments comprising the control, with no biochar added, and the six biochars mixed with the topsoil sandy soil were used for this experiment. The oven dry equivalent of the soil and biochar were sifted through a < 2 mm sieve and mixed at a rate of 2.5% (w/w). Fifty grams of biochar treated soil was used for each treatment. All treatments were replicated three times.

Two series of experiments were carried out using 14-day incubation under optimum temperature (28 °C) and moisture conditions (field water capacity) to determine the CO_2 and inorganic N mineralisation

rates. A short-term (14-d) incubation period was chosen because fluxes are usually seen within the first few days or weeks, after which there are no differences from the control. Incubations were performed in an oven at 28°C. Samples were consistently maintained at field water capacity throughout the incubation by adding deionised water when necessary. Samples for CO_2 respiration and N mineralisation were taken at 12, 24, 48, 168 and 336 hours.

A closed system was used to assess CO_2 respiration. The CO_2 respiration set-up and analysis was as follows: A one-litre glass incubation vessel was used to hold the soil-biochar mixture. Fresh 0.05 M NaOH solution prepared with deionised water was placed in a 50 mL vial inside the vessel and tightly capped. The alkali adsorption method was used to estimate the amount of CO_2 trapped in the vials (Alef 1995). In summary, during each sampling point at the time intervals stated, the reacted NaOH in the vial was transferred into a polypropylene centrifuge tube and 0.5 M of $BaCl_2$ was immediately added to stop the CO_2 from reacting. The tube with the contents was centrifuged at 3000 rpm for 5 min using the Eppendorf 5810 R centrifuge. The centrifuged aliquot was then titrated with 0.05 M HCl and the rate of CO_2 respiration was calculated using the following equation:

$$mg\ CO_2\ d^{-1}\ kg^{-1} = \frac{(V_0 - V) \times 1.1}{d/kg} \qquad \text{Equation 5.1}$$

d: incubation time in hours

kg: amount of soil dwt (dry weight of 1 g moist soil) in grams

V_0: HCl used for titration (mL)

V: HCl used for control sample (mL)

1.1: conversion factor where 1 mL 0.05 M NaOH is equivalent of 1.1 mg CO_2

5.3.5 Determination of N Mineralisation

For the N mineralisation experimental set-up, the soil-biochar mixture was placed in a 100 mL beaker and covered with perforated Parafilm. The beaker was then incubated at the time intervals stated (Section 5.3.4). After the various incubation times had lapsed, a 2 M KCl extraction was performed on the samples for the determination of NH_4^+ and NO_3^- using the methods described in Section 4.4.3.

5.3.6 Soil respiration modelling

The Curve Expert version 1.4 software was used to fit a built-in vapor model function (Equation 5.2) and a custom rational function (Equation 5.3) assuming that the linear part of the equation had an intercept 0. The latter implies that no respiration occurred from an air-dry sample in storage.

Two types of equations, which may adequately describe the system behaviour were fitted to the experimental data per treatment. The first is the vapor pressure model function (Equation 2) first described by Riedel in 1954 (Vetere 1991) where:

$$\ln C_{CO2} = a + \frac{b}{t} + c \cdot ln\, t \text{ , t>0} \qquad \text{Equation 5.2}$$

ln C_{CO2} = vapor pressure of carbon dioxide (mmHg)

a, b, c = constants

t = temperature (°C)

The second model is the rational function (Equation 3) where:

$$C_{CO2} = \frac{at}{b+ct+ct^2} \text{ , t>0} \qquad \text{Equation 5.3}$$

C_{CO2} = CO_2 evolution (mg day^{-1})

a, b, c = constants

t = time (days)

5.3.7 Statistical analysis

The respiration and mineralisation data was analysed using the general linear model univariate analysis of variance (ANOVA) in order to determine statistically significant differences between the treatments. The data was tested for normal distribution and homogeneity before statistical analysis. For comparison of means, Fisher's Least Significant Difference (LSD) post hoc test with a $P < 0.05$ level of significance was used. Statistical analysis was performed using IBM SPSS (IBM SPSS Statistics for Windows, Version 24.0. Armonk, NY: IBM Corp.).

5.4 Results and Discussion

5.4.1 Soil pH

Mixing the near-neutral soil (pH 6.92) with the alkaline biochars and acidic rubber tyre biochar resulted in soil-biochar mixtures with a pH range between 5.62 and 8.86 (Table 5.1). All the soils had a net negative surface charge as indicated by negative delta pH values (Table 5.1). The alkaline biochars neutralised the slight soil acidity, while the acidic rubber tyre biochar decreased the soil pH. The pH results correlate with the total Ca content of the biochars (Table 3.2), where it was shown that the rubber tyre biochar had the least Ca contents (0.06%) compared to maize stover biochar which had the most Ca (2.25%).

Table 5. 1: The pH of soil-biochar mixtures.

Soil-biochar treatments	pH_{H2O}	pH_{KCl}	ΔpH
Control	6.92	6.16	-0.76
Soil+Maize stover	8.86	7.91	-0.96
Soil+Grape pip	7.74	6.82	-0.93
Soil+Grape skin	8.63	7.20	-1.44
Soil+Pine wood	7.23	6.36	-0.88
Soil+Rubber tyre	5.62	5.35	-0.27
Soil+Sugarcane pith	7.42	6.60	-0.82

5.4.2 Potentially bioavailable metals in biochar soil treatments

Table 5.2 shows the potentially bioavailable (EDTA-extractable) metal concentrations in the control soil and soil-biochar mixtures. Biochar application generally increased the EDTA extractable levels of Mn, Fe, Co, Ni and Cu (Table 5.2), which are generally considered to be essential elements, thus this would be beneficial for plants and microbes (Havlin et al. 2005). The application of the biochars generally reduced the availability of Pb (Table 5.2), probably due to the increase in soil pH (Table 5.1) which promotes the precipitation or adsorption of Pb (Jiang et al 2012). The exception was the rubber tyre char which decreased soil pH (Table 5.1), thus the slight decrease in availability could be due to adsorption or possibly precipitation with anions such as phosphate (Jiang et al 2012).

Based on the findings of the baseline concentration range of EDTA-extractable metals in South African soils and suggested threshold values by Herselman and Steyn (2001), the soil-biochar mixtures were either below or within the range of maximum permissible levels for Cd, Cr, Ni, Pb, Cu and Co. However, the Zn levels of soil mixed with rubber tyre char was above the suggested threshold value of

10 mg kg^{-1} (Table 5.2). Therefore, only the rubber tyre biochar could be of concern in soil application because of the high potentially bioavailable zinc level.

Table 5. 2: Diammonium EDTA extractable metal contents (mg kg^{-1}) of the soil and soil-biochar treatments.

Metal (mg kg^{-1})	Topsoil	Soil+Maize stover	Soil+Grape pip	Soil+Grape skin	Soil+Pine wood	Soil+Rubber tyre	Soil+Sugarcane pith
Al	113.96	134.07	122.05	149.44	86.97	71.56	117.20
Ti	2.62	3.57	3.02	4.20	1.77	1.08	2.90
V	0.32	0.41	0.38	0.42	0.31	0.25	0.63
Cr	0.05	0.07	0.10	0.14	0.05	0.18	0.16
Mn	7.39	11.66	8.57	8.03	10.10	8.84	17.13
Fe	110.54	124.06	123.96	133.94	119.35	115.91	210.60
Co	0.05	0.07	0.06	0.06	0.06	0.12	0.15
Ni	0.13	0.19	0.14	0.34	0.14	0.53	0.37
Cu	0.38	0.61	0.49	0.81	0.63	0.52	0.75
Zn	4.57	4.79	3.87	4.18	5.81	15.68	5.70
As	0.09	0.13	0.20	0.16	0.19	0.08	0.16
Se	0.08	0.08	0.08	0.08	0.09	0.07	0.09
Mo	0.01	0.02	0.02	0.03	0.01	0.01	0.02
Cd	0.01	0.01	0.01	0.01	0.01	0.01	0.02
Sb	0.00	0.00	0.00	0.00	0.00	0.00	0.01
Hg	0.00	0.00	0.00	0.00	0.00	0.00	0.00
Pb	2.38	1.52	1.38	1.32	2.26	1.97	1.79

5.4.3 Soil carbon and nitrogen contents

The addition of biochar to the (control) soil immediately increased the total carbon and nitrogen contents (Table 5.3). This demonstrates that amending soil with biochar increases its nutrient capacity. Furthermore, Table 5.3 shows that biochar affects potential soil mineralisation-immobilisation by altering the soil C/N ratios.

Table 5. 3: Total C and N contents of soil-biochar mixtures (expressed on dry wt. basis).

Soil-biochar treatments	%C	%N	C/N[a]
Control	1.42	0.08	17.25
Soil+Maize stover	2.25	0.12	18.21
Soil+Grape pip	4.88	0.30	16.07
Soil+Grape skin	3.45	0.08	44.67
Soil+Pine wood	4.67	0.13	34.88
Soil+Rubber tyre	7.95	0.19	42.92
Soil+Sugarcane pith	2.54	0.10	24.65

[a] = Mass ratio

5.4.4 Carbon mineralisation

The rate of CO_2 evolution from the control and biochar-amended soil treatments is shown in Figure 5.1. At the start of the experiment, the soil amended with rubber tyre char was at its peak and had almost three times the rate of CO_2 evolved compared to the soil and grape pip biochar treatment which measured the least CO_2 amount. This is because the soil plus rubber tyre biochar treatment had the highest %C (Table 5.3) and thus stimulated soil microbial activity the most due to the increased food source available for microbes. However, at the end of the study, the grape pip char released similar amounts of CO_2 compared to the rubber tyre char (Figure 5.2). This suggests that the rate of CO_2 evolution reached its maximum at day 2 for the remaining treatments primarily due to the enhanced microbial activity of the biochars' labile volatiles fraction (El-Naggar et al 2015). As expected, there was a decline in respiration on day 7 of the study in all the treatments (Figure 5.1) due to a reduction in soil microbial activity.

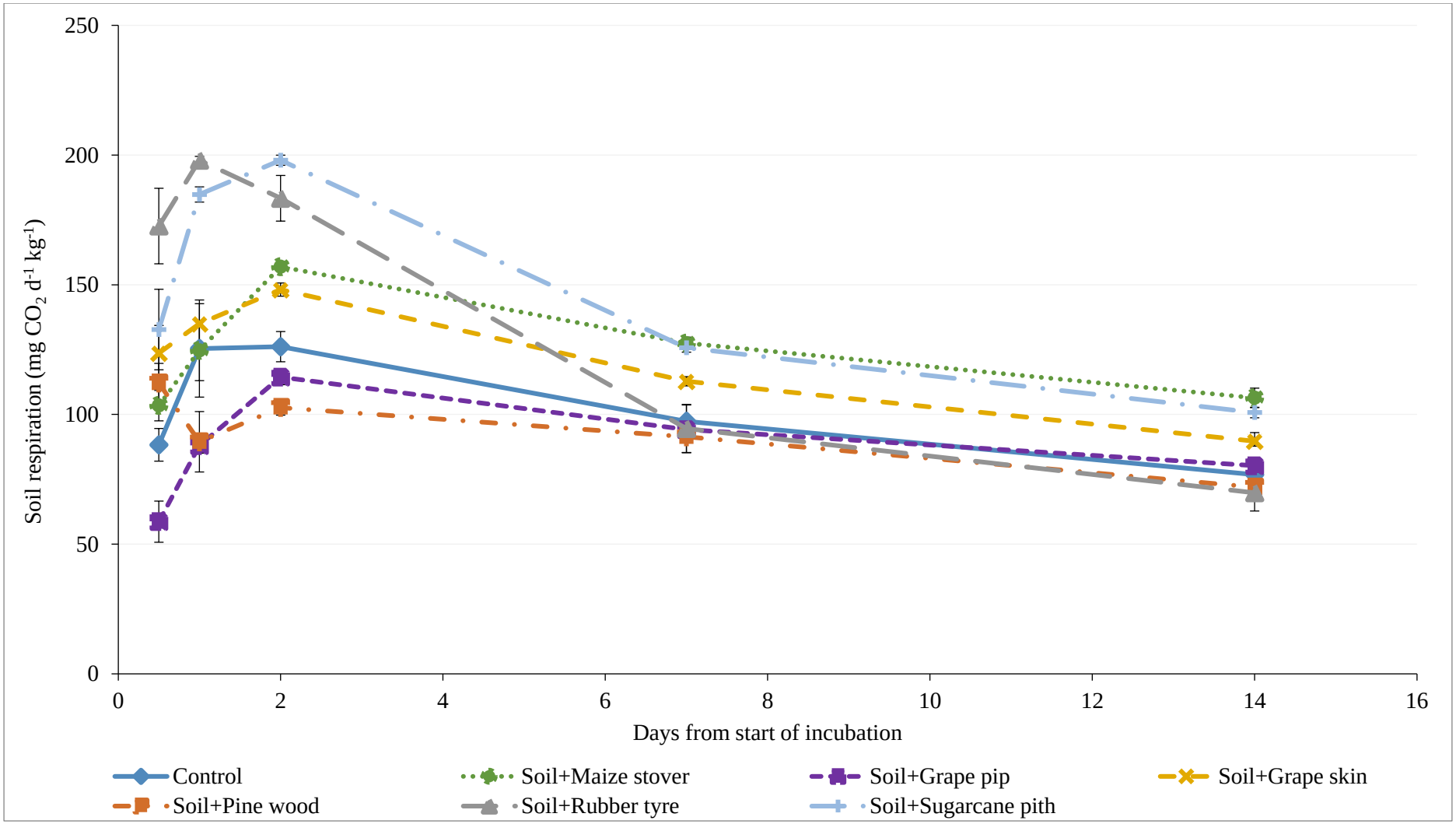

Figure 5. 1: Carbon dioxide evolution of soils treated with various biochars during the incubation study. Vertical bars represent the standard errors of the means (n = 3).

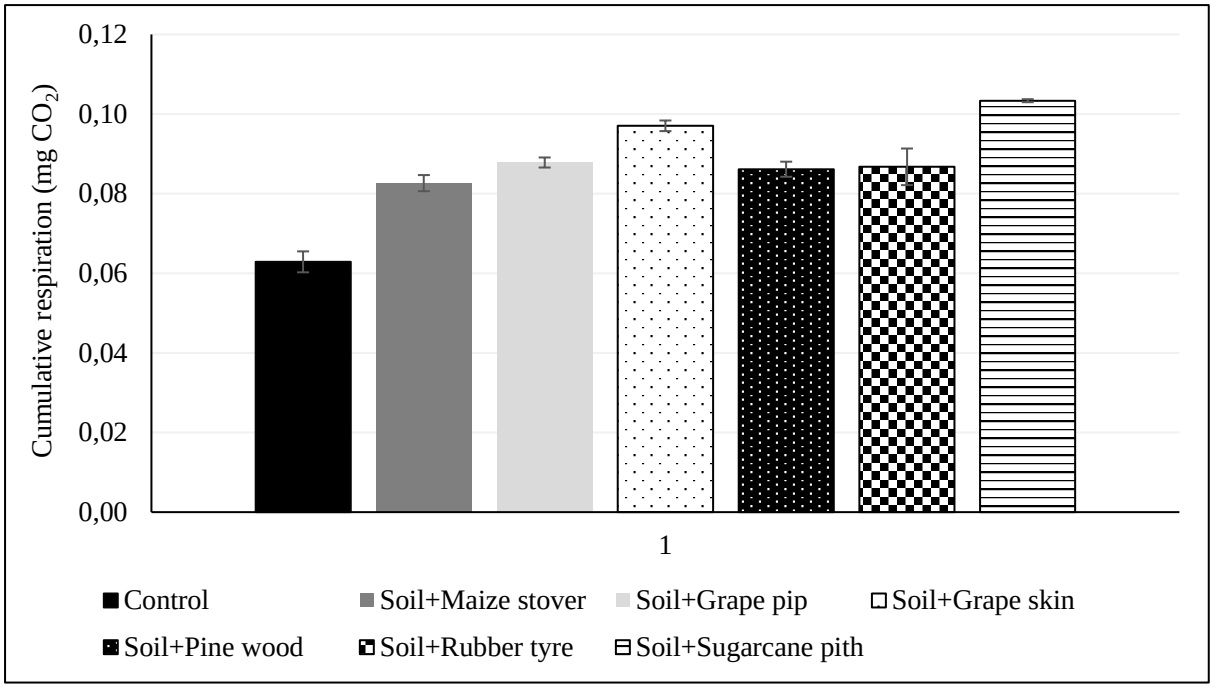

Figure 5.2: Carbon dioxide evolution of the final (unnormalised) cumulative (at 14 days) respiration of soils treated with various biochars. Vertical bars represent the standard errors of the means (n = 3).

The normalised (based on total C content) cumulative CO_2 respiration of all the biochar treatments is shown in Figure 5.3. All of the biochar-treatments respired relatively less than the control soil (Figure 5.3), ranging between 8-75% less C respired per gram of C added. This demonstrates that biochar C is generally less degradable than the soil organic matter C.

The order of relative C degradability in the biochar treated soils compared to the control soil was as follows: sugarcane pith (-8%) > maize stover (-17%) > grape skin (-36%) > pine wood (-58%) = grape pip (-59%) > rubber tyre (-75%) (Figure 5.3). Among the plant-derived biochars, there was a strong positive correlation between fixed C content and the relative decrease in cumulative respired respiration (R^2 = 0.86). The sugarcane pith and maize stover biochar amended soils had significantly the highest CO_2 production among the biochar treatments (Figure 5.3), due to their partially pyrolysed natures as indicated by their little or no fixed C contents of 15.6 and 0%, respectively (Table 3.3). Similar results were observed in a fast pyrolysis biochar with high CO_2 losses due to an un-pyrolysed carbohydrate fraction (Bruun et al 2012). These properties propose that the biochar had significant amounts of labile C that can be easily utilised by soil microorganisms within a short period (Smith et al 2010). Also, the least degradable plant biochars, pine wood and grape pip (Figure 5.3), contained the highest amount of fixed C (80.1 and 86.6 %, respectively) (Table 3.3). The rubber tyre biochar released 75% less cumulative CO_2 at the end of the study compared to the control, indicating that it was the least

degradable biochar in the short-term, despite not containing the highest fixed C content (68.2%) (Table 3.3). However, the rubber tyre biochar was the only biochar that decreased soil pH (Table 5.1) and also tripled soil EDTA-extractable Zn levels (Table 5.2) which could have led to suppressed microbial respiration.

To analyse the results from the CO_2 mineralisation experiments, multiple correlations were performed with the results from the biochar properties to investigate for trends. The results shown here were those of the correlations with the strongest relationships. Figure 5.4 shows the correlation of the fixed C contents of biochars with the amounts of CO_2 respired after 7 and 14 days. It shows that the fixed C was strongly negatively correlated with respiration. This means that there was less respiration with the pine wood and grape pip biochars which had higher fixed C contents (Table 3.4). Since the fixed C content represents the portion of biochar that is most stable, due to its condensed aromatic rings (Keiluweit et al 2010), it follows, then, that the pine wood and grape pip biochars could potentially be good for long term C sequestration (Lehmann et al 2006; Laird 2008).

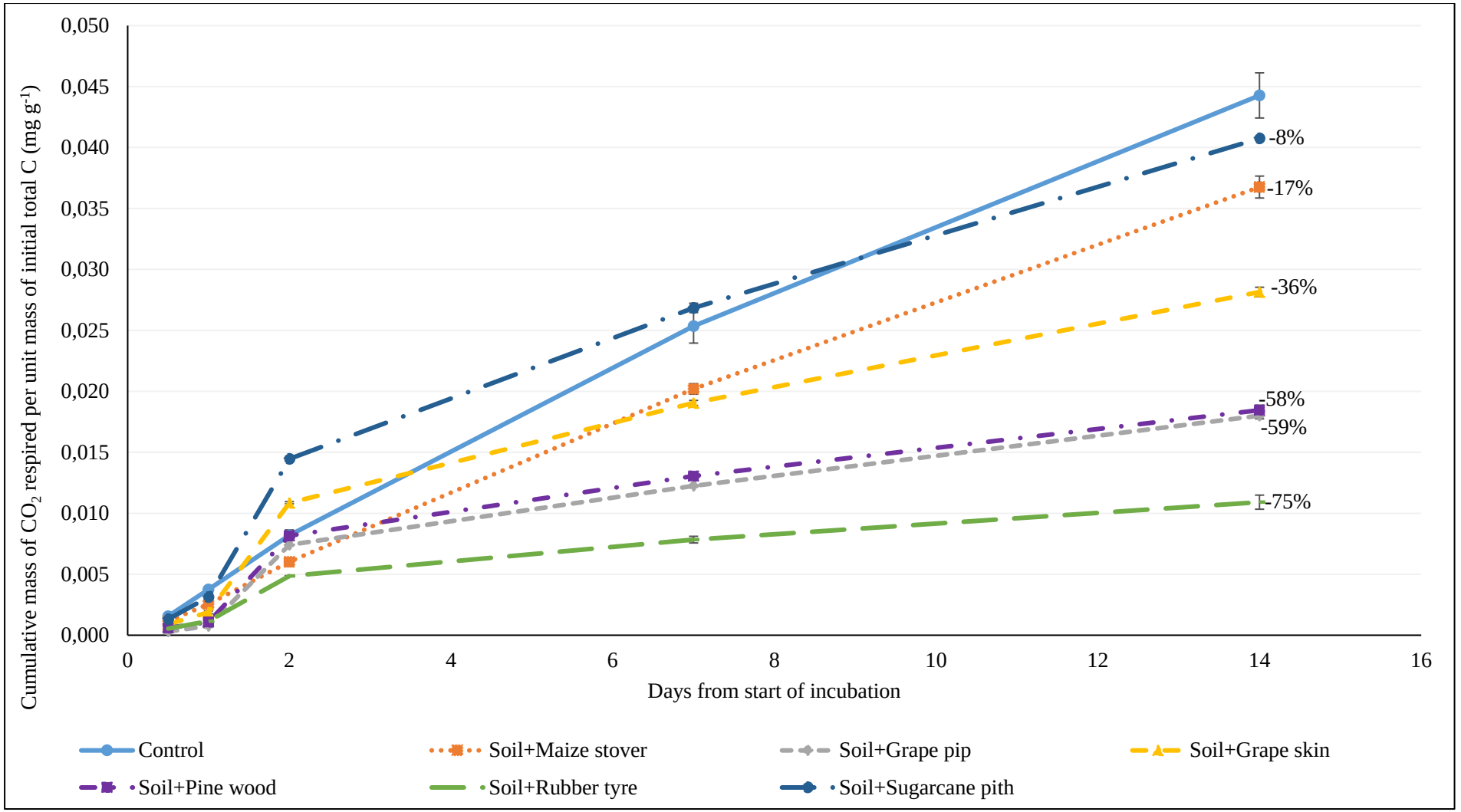

Figure 5. 3: Cumulative carbon dioxide respiration in soils normalised with the initial total C content of each treatment. The percentages indicate the relative % difference of CO_2 respiration from the control at 14 days. Vertical bars represent the standard errors of the means (n = 3).

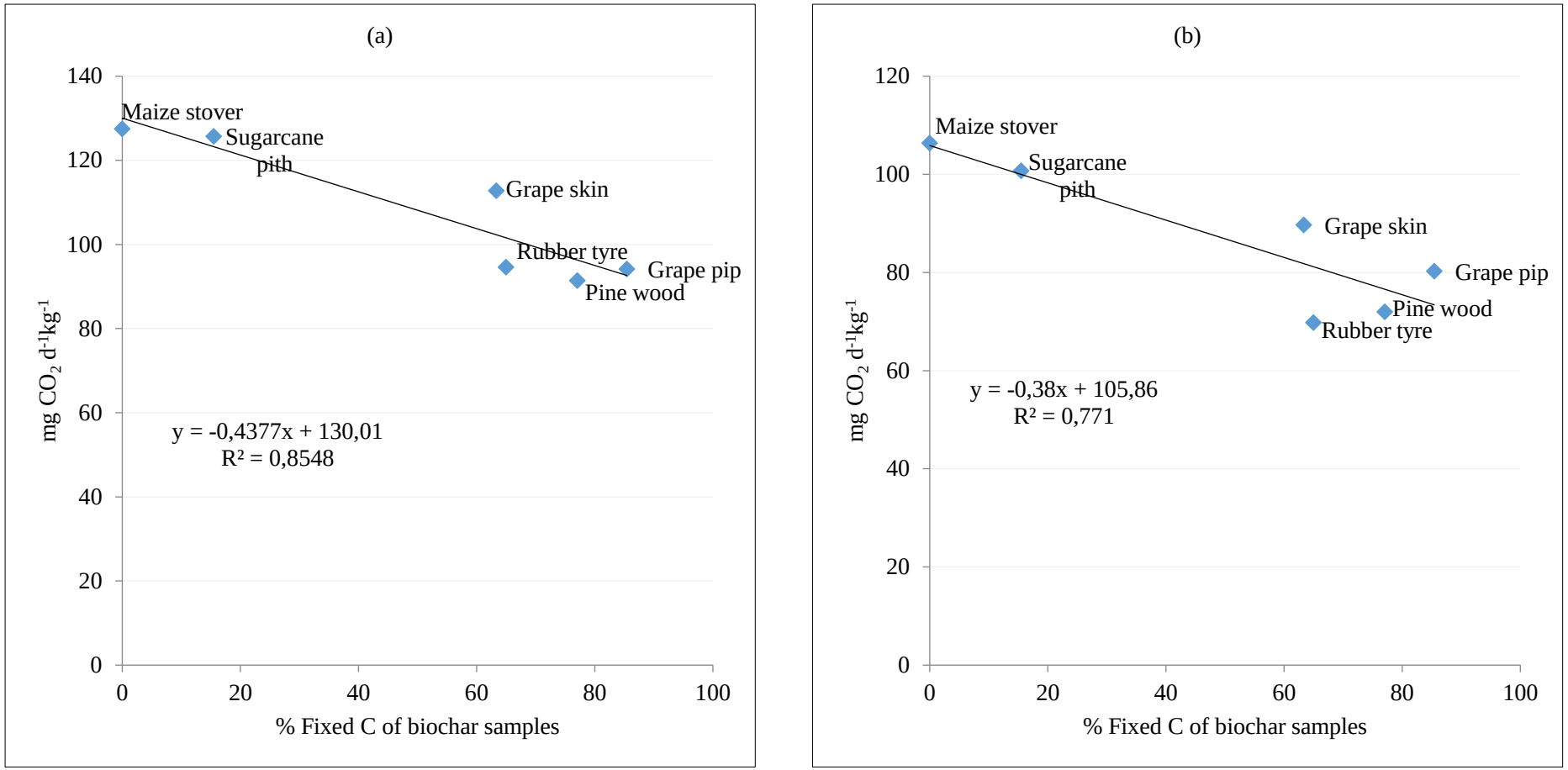

Figure 5. 4: Relationship between carbon contents of biochars with amount of carbon dioxide evolved after (a) 168 h (7 days) and (b) 336 h (14 days).

5.4.5 Nitrogen mineralisation

All of the plant-derived biochar treatments reached a maximum ammonium release on day 2 of the incubation, whereas, the rubber tyre biochar amended soil peaked on day 7 (Figure 5.5). A comparison of the plant-derived biochar treatments showed that they behaved similarly by measuring between 11 and 22 mg NH_4^+ kg^{-1} soil by day 7 and then sharply decreasing to between 11 and 14 mg NH_4^+ kg^{-1} soil at the end of the incubation period (Figure 5.5). At the end of the incubation study, the control and alkaline biochar amended soils measured much lower amounts of ammonium than the soil and rubber tyre biochar treatment (Figure 5.5).

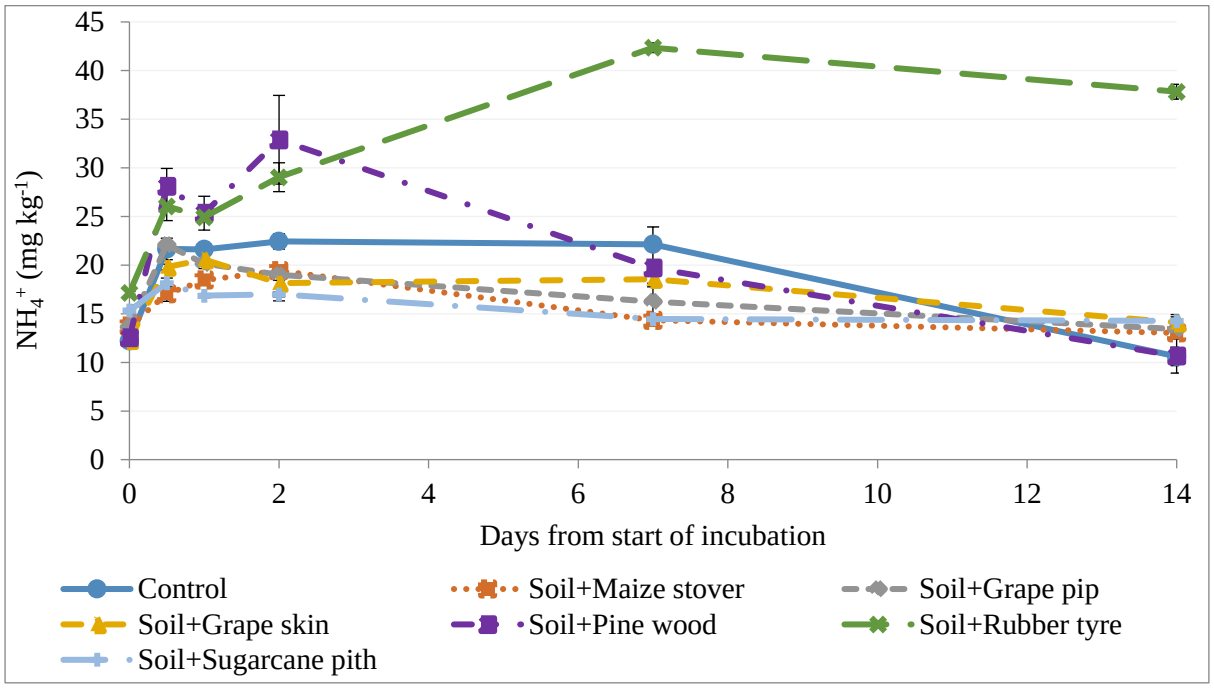

Figure 5. 5: Exchangeable ammonium (2 M KCl) concentration in control and biochar amended soil during 14-day incubation period. Vertical bars represent the standard errors of the means (n = 3).

The activity of soil microbes was the highest at the beginning of the incubation study. This is clearly seen as the carbon dioxide respiration pattern compares well with the N mineralisation pattern of the plant-derived biochars during the first 2 days of the incubation study (Figure 5.1). When the soil CO_2 levels reached their peak (Figure 5.1), the amount of ammonium released correspondingly increased (Figure 5.5), thus indicating a boost in N mineralisation.

The exchangeable nitrate measured was at least one order of magnitude less than that of the NH_4^+ levels (Figure. 5.6). This observation supports the finding in Chapter 4 that biochar has a much higher capacity

to irreversibly adsorb nitrate than ammonium. Therefore, any nitrate that was produced from the incubation study may have been immediately adsorbed by the biochars, thus leaving very little nitrate to be exchangeable.

Soil amended with rubber tyre biochar contained the least exchangeable nitrate at the end of the study (Figure 5.6). Rubber tyre biochar adsorbed the most nitrate (79%) of what was initially added at a concentration of 100 mg NO_3^- L^{-1} during the adsorption study (Figure 4.3). These observations correspond and indicate that nitrate was most strongly adsorbed by the rubber tyre biochar and thus least 2 M KCl exchangeable. Another possible reason why the rubber tyre biochar had the lowest NO_3^- concentration at the end of the incubation study compared to the other treatments is that in acid soil nitrification is slow. Grape skin biochar, however, had the most exchangeable NO_3^- at the end of the study. This suggests that nitrification is promoted when an acidic sandy soil is amended with a grape skin biochar, whereas N mineralisation is favoured by the rubber tyre char. Furthermore, because nitrates promote the uptake of cations, adding grape skin biochar to soil can promote the uptake of cations such as K^+, Ca^{2+} and Mg^{2+}.

Figure 5.7 shows the exchangeable (2M KCl) mineral N (NH_4^+-N + NO_3^--N) content normalised to the total N content of the treatments. The grape pip biochar treatment had the least inorganic N content throughout the 14-day incubation period indicating that the N was the least mineralisable or that immobilisation was favoured. Between day 2 and day 14, the treatment contained 0.06 and 0.05 mg inorganic N per g of pure soil, respectively. The control treatment mostly had the highest inorganic N content up until day 7 (0.30 mg g^{-1}), thereafter, it declined to 0.21 mg g^{-1} at day 14. These findings suggest that grape pip biochar was the least degradable treatment compared to the others.

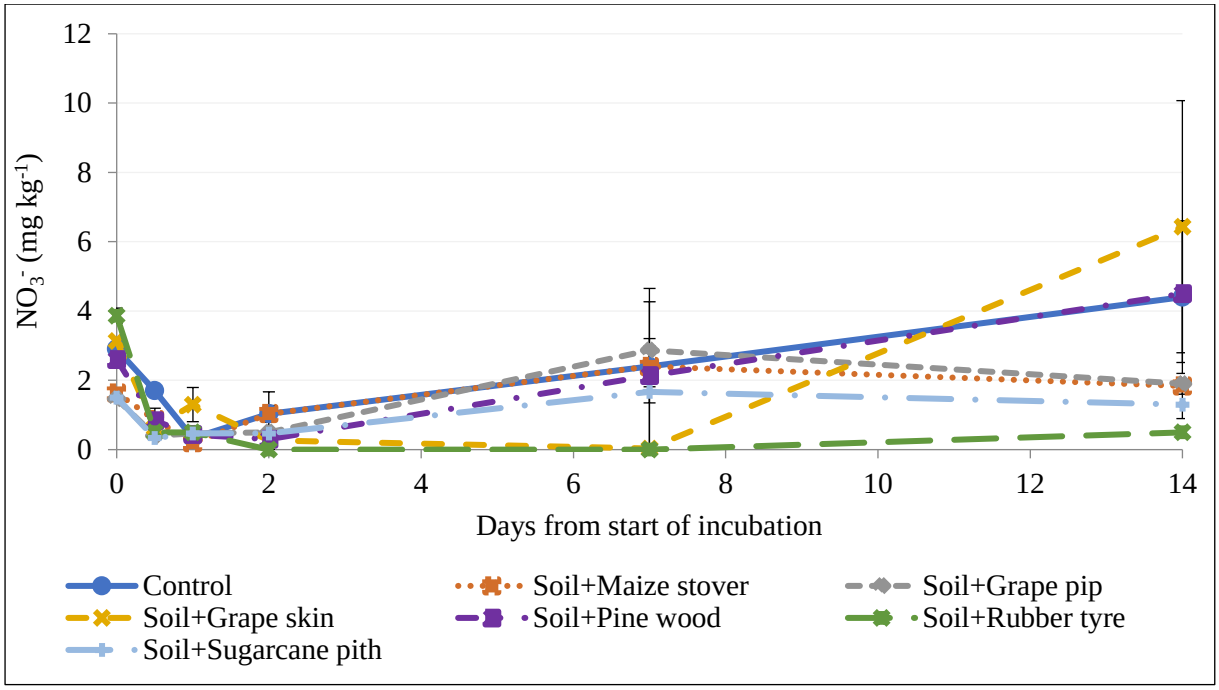

Figure 5. 6: Exchangeable nitrate (2 M KCl) concentrations in control and biochar amended soils during 14-day incubation period. Vertical bars represent the standard errors of the means (n = 3).

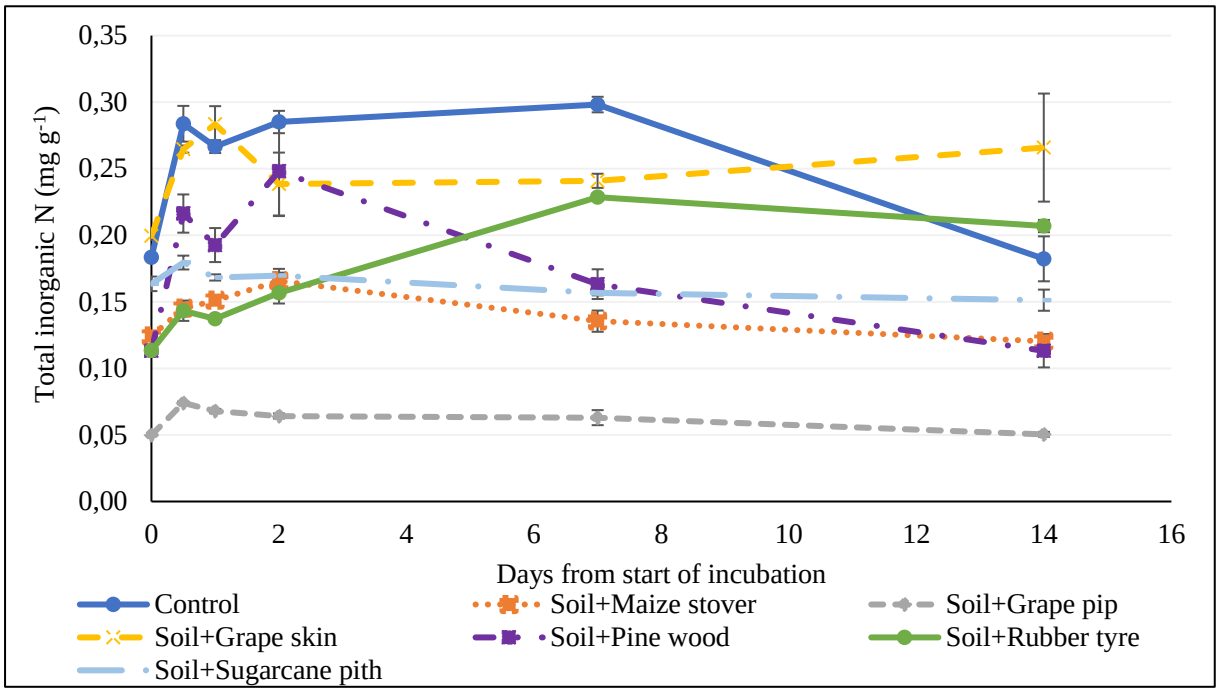

Figure 5. 7: Exchangeable mineral N (mg g^{-1}) normalised to the total N content of each treatment during the 14-d incubation period. Vertical bars represent the standard errors of the means (n = 3).

The total exchangeable mineral N (ammonium-N + nitrate-N) in each treatment at the various sampling points during the incubation study is shown in Table 5.4 in order to calculate the net amount of N mineralisation or immobilisation during the 14-day incubation at 28° C and at FWC. The total inorganic N content consisted largely of ammonium-nitrogen than nitrate-nitrogen (Figures 5.5 and 5.6). The initial measurement was indicated as day 0 and shows the pre-incubation N content conditions. The control treatment contained the lowest initial mineral N content (Table 5.4). This confirms that biochars contain some exchangeable inorganic N (Gaskin et al 2010; Mukherjee and Zimmerman 2013). The rubber tyre biochar amended soil contained the highest initial inorganic N content (14.18 mg N kg^{-1} soil) compared to the other soil-biochar treatments (Table 5.4).

Table 5. 4: Exchangeable inorganic N (mg g^{-1}) in soil-biochar treatments at each sampling point during the 14-d incubation study and the net change in inorganic N during the 14 days. Means in the same column followed by the same letter are not significantly different at P < 0.05 level based on the Least Significant Difference test.

Soil-biochar treatments	Sampling points (days)						
	0	0.5	1	2	7	14	Δ N
Control	10.13 e	17.20 b	16.86 b	17.65 b	17.74 b	9.23 c	-0.90 c
Soil+Maize stover	11.01 c	13.42 c	14.37 cd	15.32 b	11.67 e	10.53 bc	-0.48 c
Soil+Grape pip	10.94 cd	17.24 b	15.76 bc	14.87 b	13.27 de	10.85 bc	-0.09 c
Soil+Grape skin	10.24 e	15.52 bc	16.27 b	14.14 b	14.42 cd	12.39 b	+2.15 b
Soil+Pine wood	10.32 de	22.01 a	19.77 a	25.61 a	15.79 c	9.29 c	-1.03 c
Soil+Rubber tyre	14.18 a	20.34 a	19.46 a	22.55 a	32.88 a	29.49 a	+15.31 a
Soil+Sugarcane pith	12.24 b	14.16 c	13.19 d	13.30 b	11.61 e	11.37 b	-0.87 c

During the first sampling point, at 12 h, maize stover biochar amended soil released the least mineral N, whereas pine wood amended soil released the most N (22.01 mg N kg^{-1} soil) (Table 5.4). The release pattern at the 24 h and 48 h sampling points was similar. Soil amended with sugarcane pith biochar had the least N (13.19 and 13.30 mg kg^{-1}), respectively. While soil amended with pine wood biochar had the most N, 19.77 mg kg^{-1} at 24 h and 25.61 mg kg^{-1} at 48 h. The soil and rubber tyre biochar treatment reached a peak (32.88 mg N kg^{-1} soil) of N measured on day 7.

Only the rubber tyre biochar resulted in significant net N mineralisation during the 14-day incubation period, whereby the inorganic N was effectively doubled (Table 5.4). The grape skin biochar also resulted in a slight net inorganic N release during the 14 day period, while all the rest of the biochars resulted in net immobilisation. Therefore, this finding confirms that most of the plant-derived biochars can enhance N retention in soil through (possibly temporary) N immobilisation (Clough and Condron 2010; Van Zwieten et al 2010a). The control soil, pine wood and sugarcane pith biochars underwent the greatest net inorganic N immobilisation at the end of the incubation study (Table 5.4). There was no correlation between C/N ratio or any other chemical or physical properties of the biochars and net N mineralisation.

5.4.6 Soil respiration models

The respiration data fits the vapor pressure model (Equation 5.4) and rational function (Equation 5.5) with high R^2 values >90% (Table 5.5). Model fitting was done using the Curve Expert 1.4 Evaluation copy. The function shows the peak CO_2 production, which does occur within the first 2 days in the control and all soil-biochar treatments (Figures 5.8-5.14). The initial part of the function (Days 0-3) may be described as the phase of system awakening. This describes the active growth of microbial community. Since the soil ecosystem in this research unit did not include primary producers (because there is no photosynthetic C assimilation), thus the ecosystem is not resilient. Therefore, the second phase of the function (Days 4-14) rapidly falls into food source depletion.

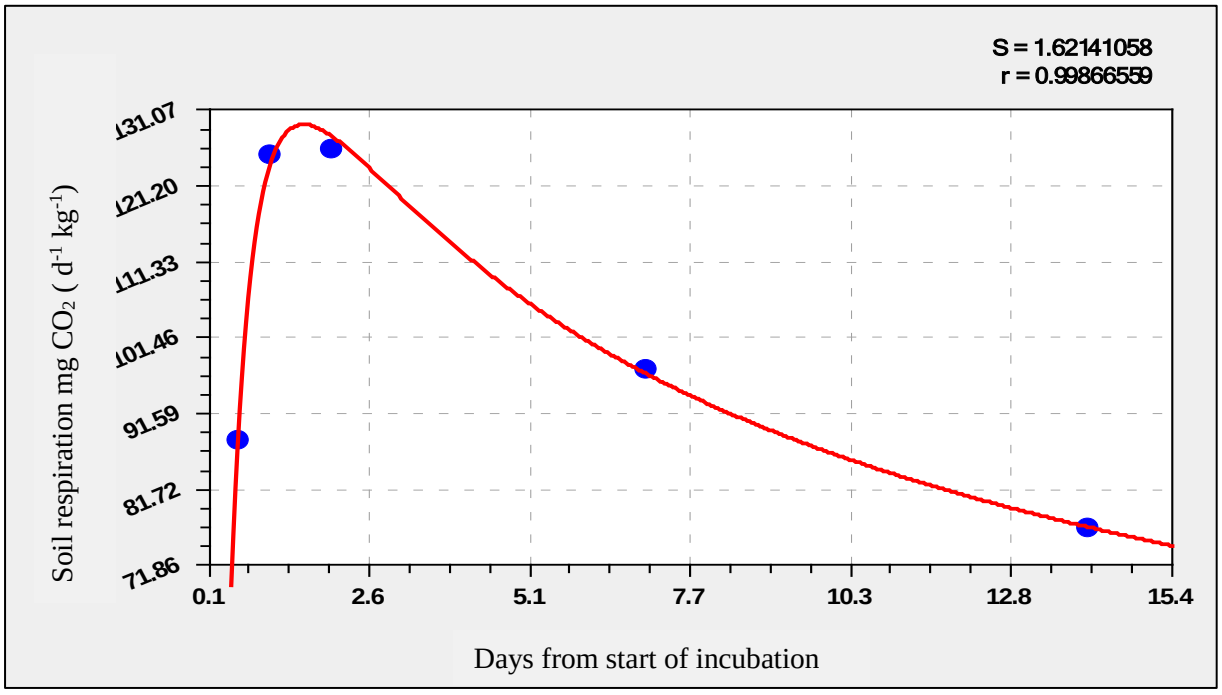

Figure 5. 8: Curve of the control respiration data fitted on the vapor pressure model.

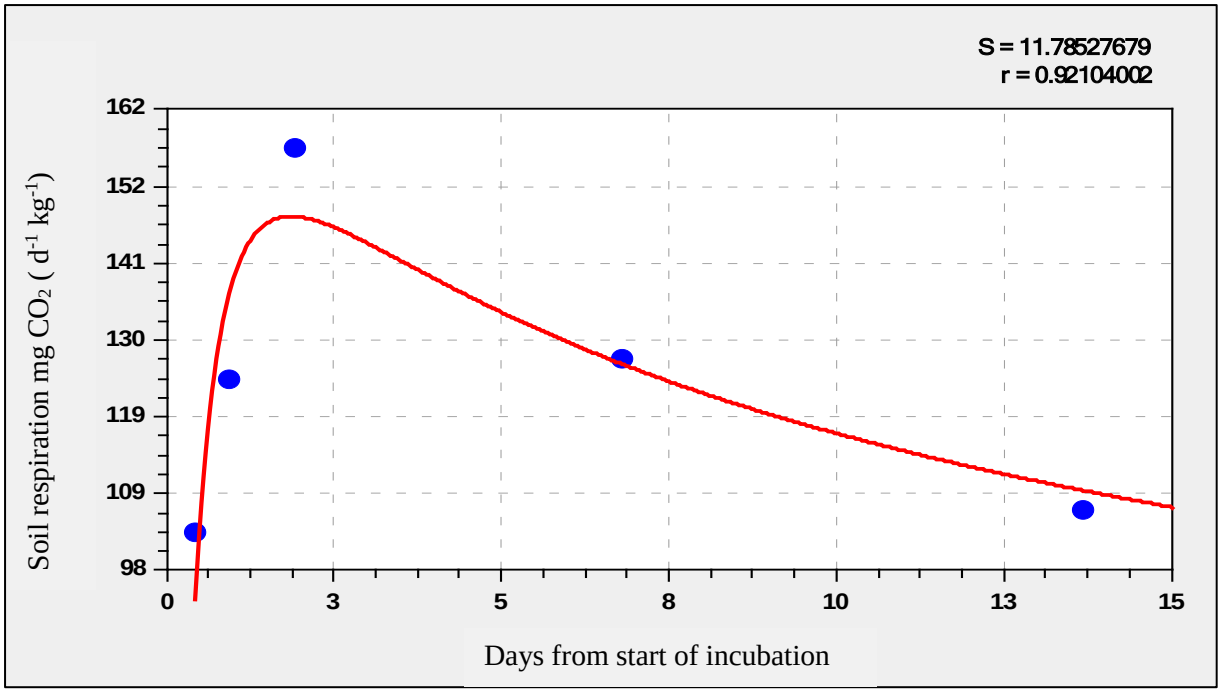

Figure 5. 9: Curve of the maize stover biochar respiration data fitted on the vapor pressure model.

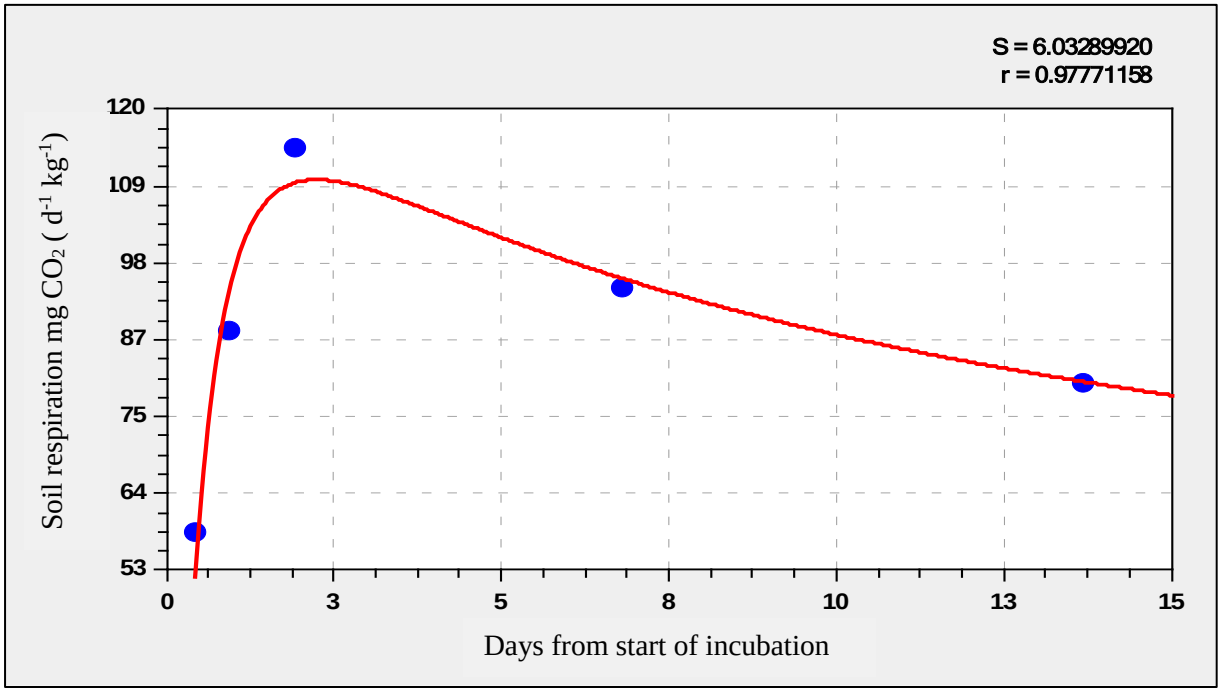

Figure 5. 10: Curve of the grape pip biochar respiration data fitted on the vapor pressure model.

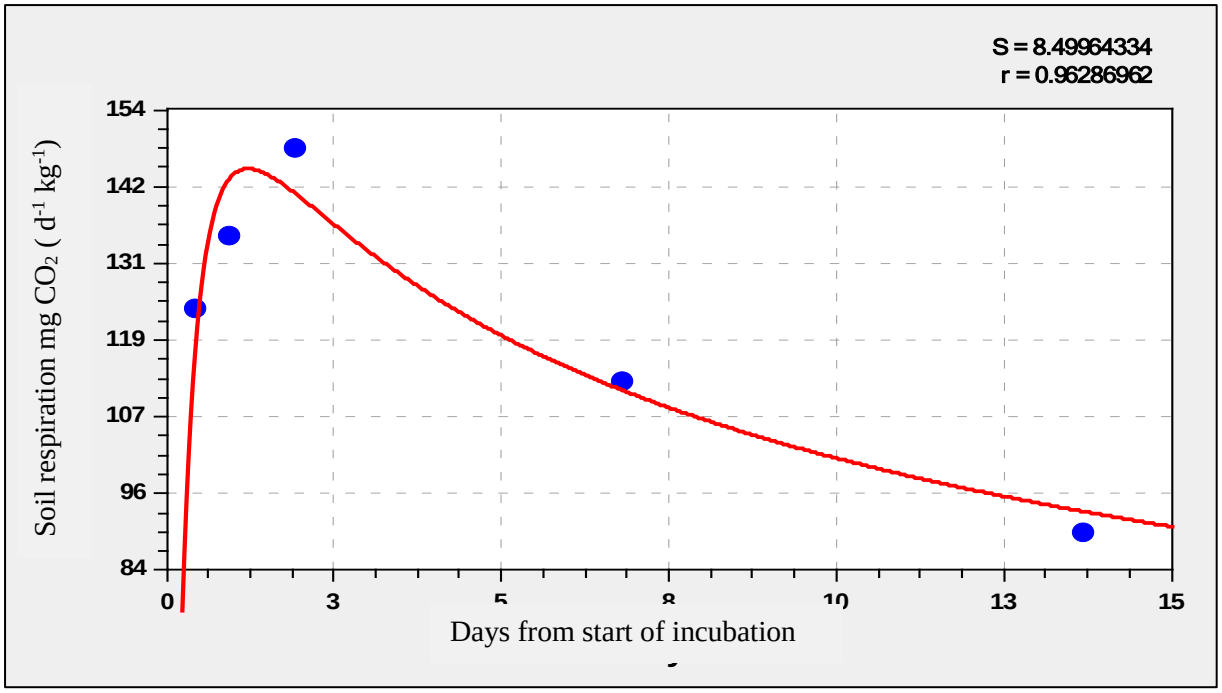

Figure 5. 11: Curve of the grape skin biochar respiration data fitted on the vapor pressure model.

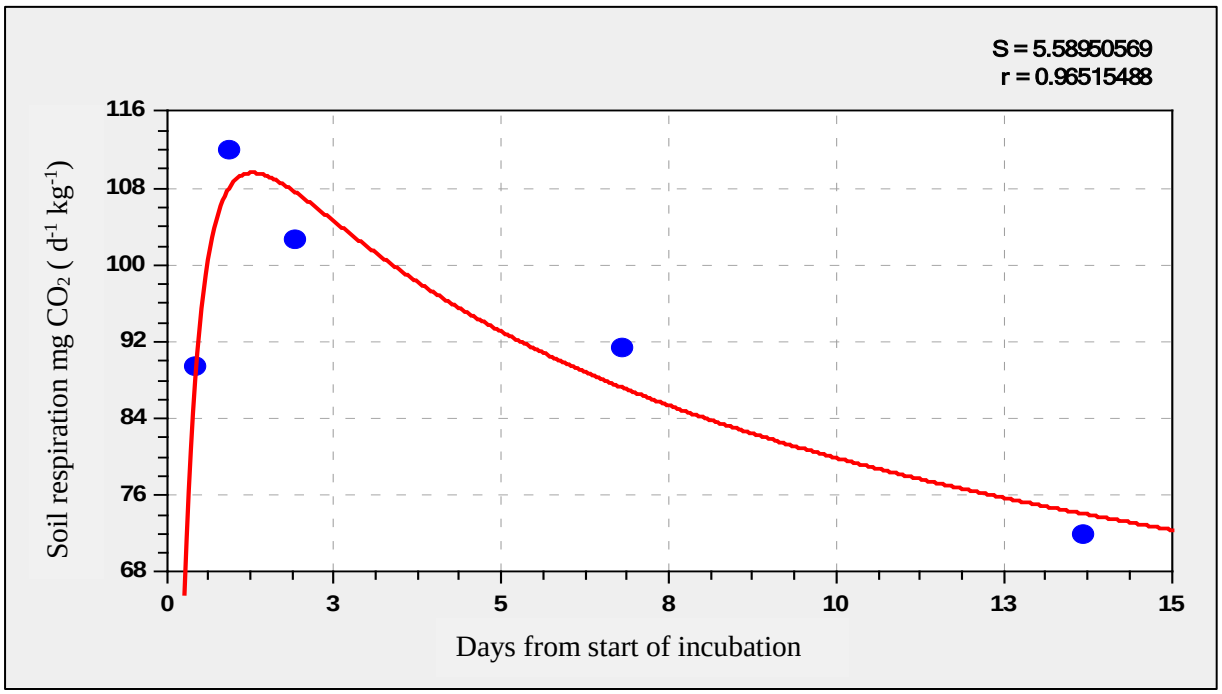

Figure 5. 12: Curve of the pine wood biochar respiration data fitted on the vapor pressure model.

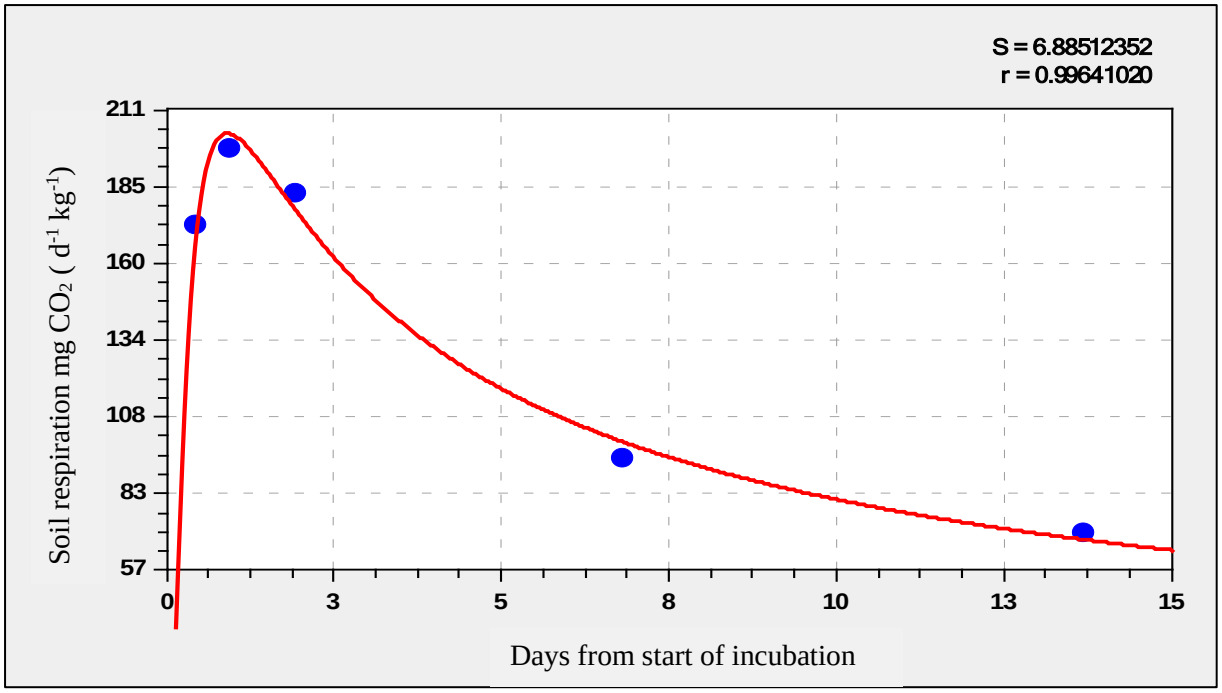

Figure 5. 13: Curve of the rubber tyre biochar respiration data fitted on the vapor pressure model.

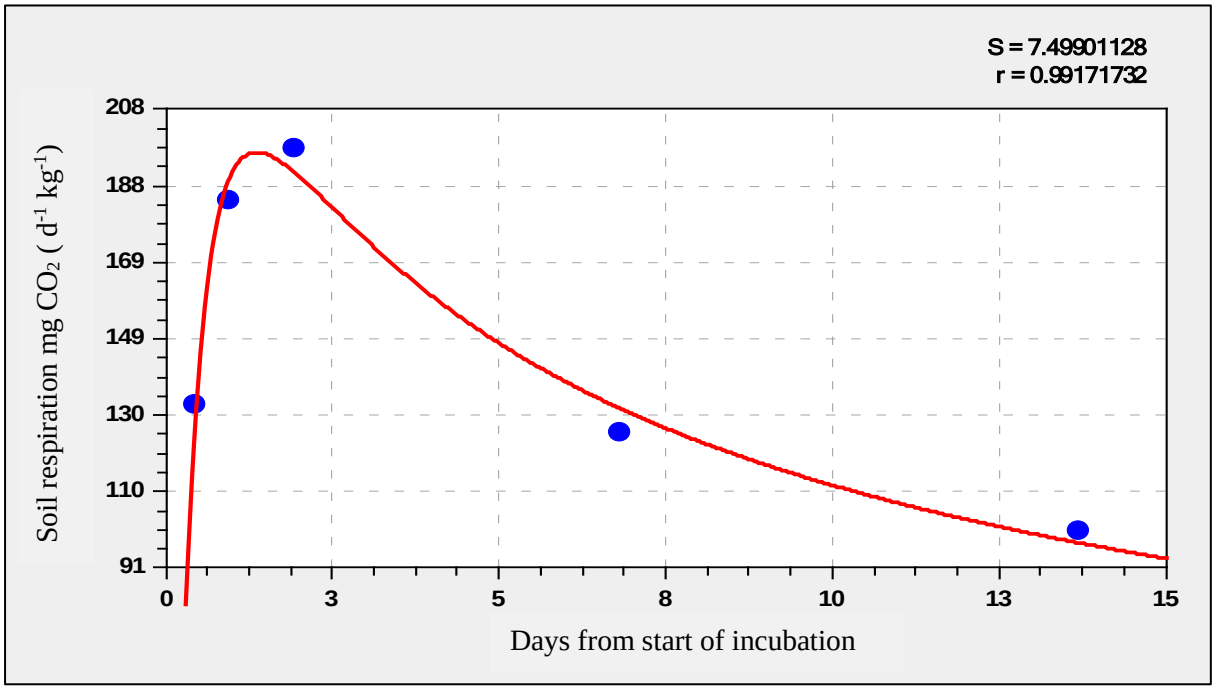

Figure 5. 14: Curve of the sugarcane pith biochar respiration data fitted on the vapor pressure model.

The values of the vapor pressure model parameters received for different biochars show strong similarity (Table 5.5). The large values of parameter "a" ranging from 5 to 6 largely determine the exponential growth phase for short time periods (usually t < 2 days). The negative values of parameters "b" and "c" allow us to rewrite the equation as,

$$\ln C_{CO2} = a - \frac{b}{t} - c \cdot ln\, t \qquad \text{Equation 5.4}$$

explicitly showing the effect of longer time spans on decline of CO_2 production. All three parameters (a, b and c) change with addition of biochar to the soil (control). The biochars may be a food source for some secondary consumers and CO_2 sorbent preventing CO_2 evolution into the atmosphere. These equation parameters were correlated to the biochar physico-chemical characteristics determined in Chapter 3. The ones with the strongest correlation coefficients are shown.

Table 5. 5: Respiration data coefficients of the control and six biochars from the vapor pressure model parameters.

Parameter	Control	Maize stover	Grape pip	Grape skin	Pine wood	Rubber tyre	Sugarcane pith
a	5.424	5.438	5.291	5.349	5.051	5.919	5.969
b	-0.605	-0.517	-0.746	-0.383	-0.367	-0.607	-0.723
c	-0.394	-0.268	-0.322	-0.300	-0.273	-0.631	-0.507
r^2	0.999	0.921	0.978	0.963	0.965	0.996	0.992

The plant-derived biochars had the strongest correlations when CO_2 respiration was correlated with the "a" parameter, which predicts the peak of the vapor pressure function against the biochar physico-chemical characteristics (Appendix B), especially with total C (R^2 = 0.918), but also with chromium (R^2 = 0.953), nickel (R^2 = 0.946) which in this case may be important biocatalysts of C oxidation (Shaheen and Rinklebe 2017). When all six biochars, including the rubber tyre char was correlated with cobalt, a very strong, positive relationship was observed (Figure 5.15). The reason for this was that the contents of cobalt was similar in all biochar samples, irrespective of biomass (Table 3.2).

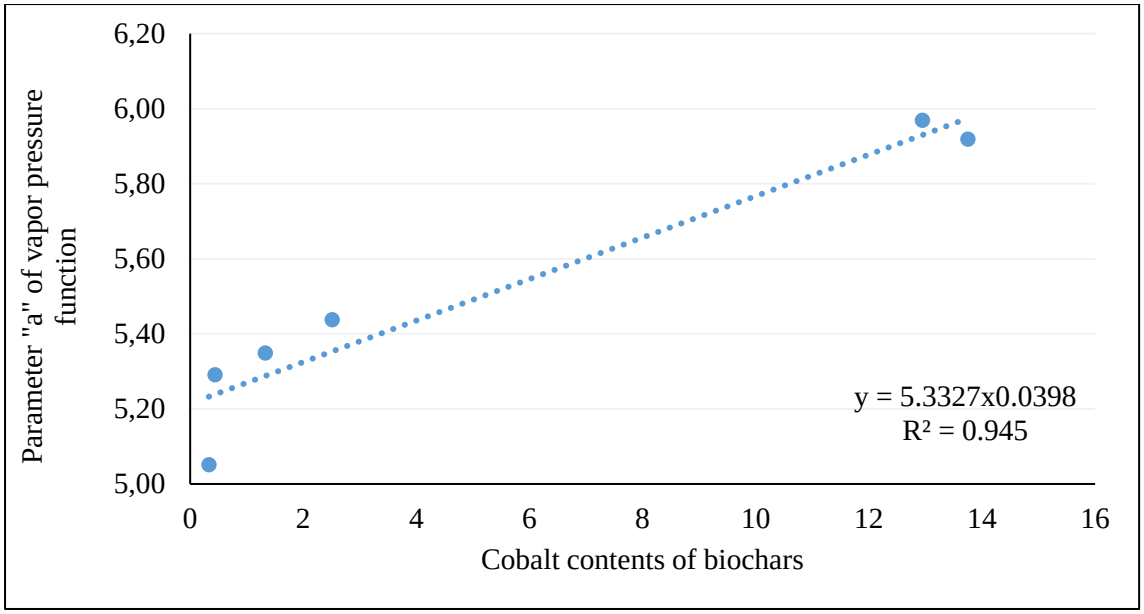

Figure 5. 15: Relationship between the cobalt contents of all six biochars with the "a" parameter of the vapor pressure function modelled against carbon dioxide respiration.

Another function that describes well the system behaviour in terms of R^2 and standard deviations is a rational function (Equation 5.5):

$$C_{CO2} = \frac{at}{b+ct+dt^2} \qquad \text{Equation 5.5}$$

The parameters “a” and “c” of the rational function model show strong variation with addition of different biochars (Table 5.6). However, correlation with the biochar physico-chemical characteristics resulted in no high correlation coefficients.

Table 5. 6: Respiration data coefficients of the control and six biochars from the rational function model parameters.

Parameter	Control	Maize stover	Grape pip	Grape skin	Pine wood	Rubber tyre	Sugarcane pith
a	38.737	47.103	29.596	65.065	53.005	85.769	54.484
b	0.101	0.118	0.162	0.079	0.078	0.099	0.113
c	0.205	0.224	0.156	0.360	0.405	0.256	0.157
d	0.023	0.016	0.016	0.027	0.024	0.082	0.032
r^2	0.969	0.948	0.995	0.985	0.987	0.956	0.977

5.4.7 Modelling Nitrogen dynamics

The net result of the N mineralisation experiment usually given as extractable N measured after 14 days of incubation: N_{14}-N_0 – the difference between the final and initial concentrations of extractable N given as mg N per kg of soil [mg kg^{-1}] divided by time (14 days) the average daily mineralisation rate is reported.

$$\frac{N_{14} - N_0}{14} = average\ net\ N\ mineralisation\ rate \qquad \text{Equation 5.6}$$

However, while monitoring the system behaviour over 14 days (with sampling at 0.5, 1, 2, 7 and 14 days) we can clearly see (Figure 5.16) that the N mineralisation process is not stationary with peak mineral N concentration commonly occurring between 0.5 and 2 days of mineralisation experiment. Some authors give it as the difference between the amounts of N extracted upon 14 days and 1 day of incubation recording N_{14}-N_1 as the net change (Hanselman et al 2004; Cai et al 2016).

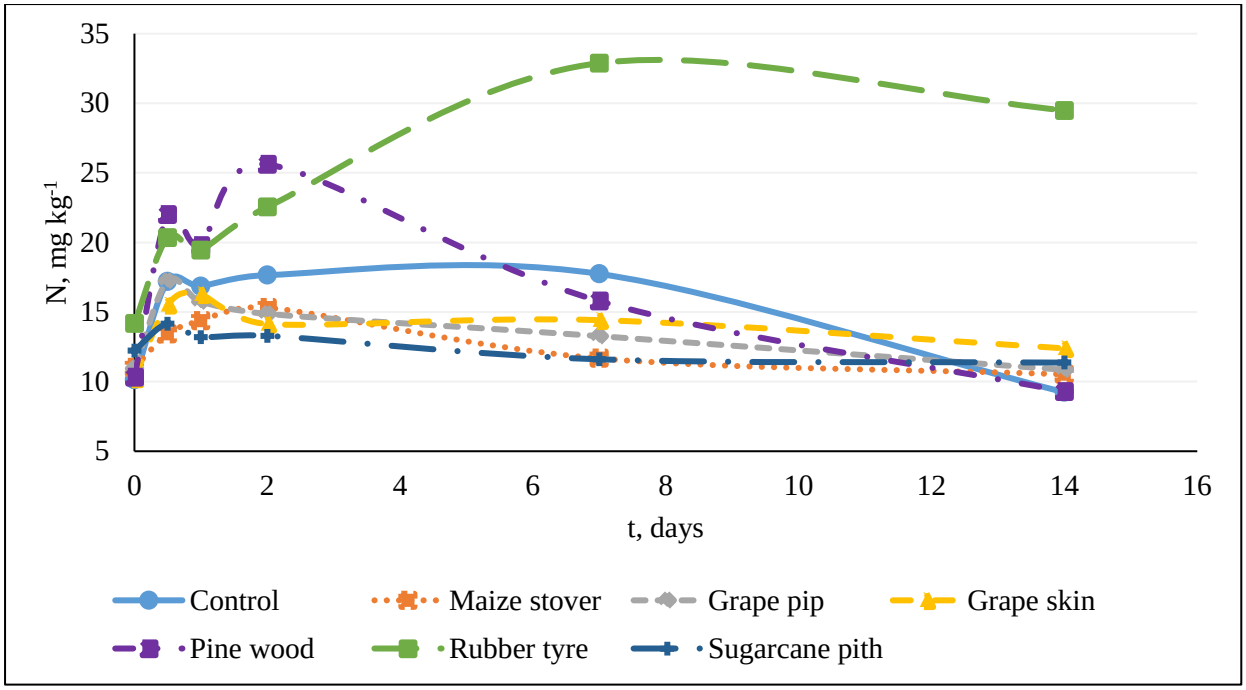

Figure 5. 16: Mineral N concentrations extracted upon sample incubation for a period of time (t) from the sandy soil amended with the different biochars.

Hence, we can say that there is a function that describes the rate of N mineralisation change such as:

$$\frac{dN}{dt} = f(t) \qquad \text{Equation 5.7}$$

Plotting the change in mineral N concentrations $(N_i\text{-}N_{i-1})/(t_i\text{-}t_{i-1})$ against time we see distinct periods of acceleration and deceleration in N mineralisation/immobilisation (Figure 5.17). The non-specific competing processes of mineral N release and consumption are probably related to population dynamics of various organisms involved. These fluctuations in N mineralisation rates are similar to damped oscillations ultimately tending towards 0 – a constant N mineralisation rate (Figure 5.17). We can attribute the initial surge in N mineralisation to wetting of the soil sample, which destabilised the microbial system and stimulated microbial activity.

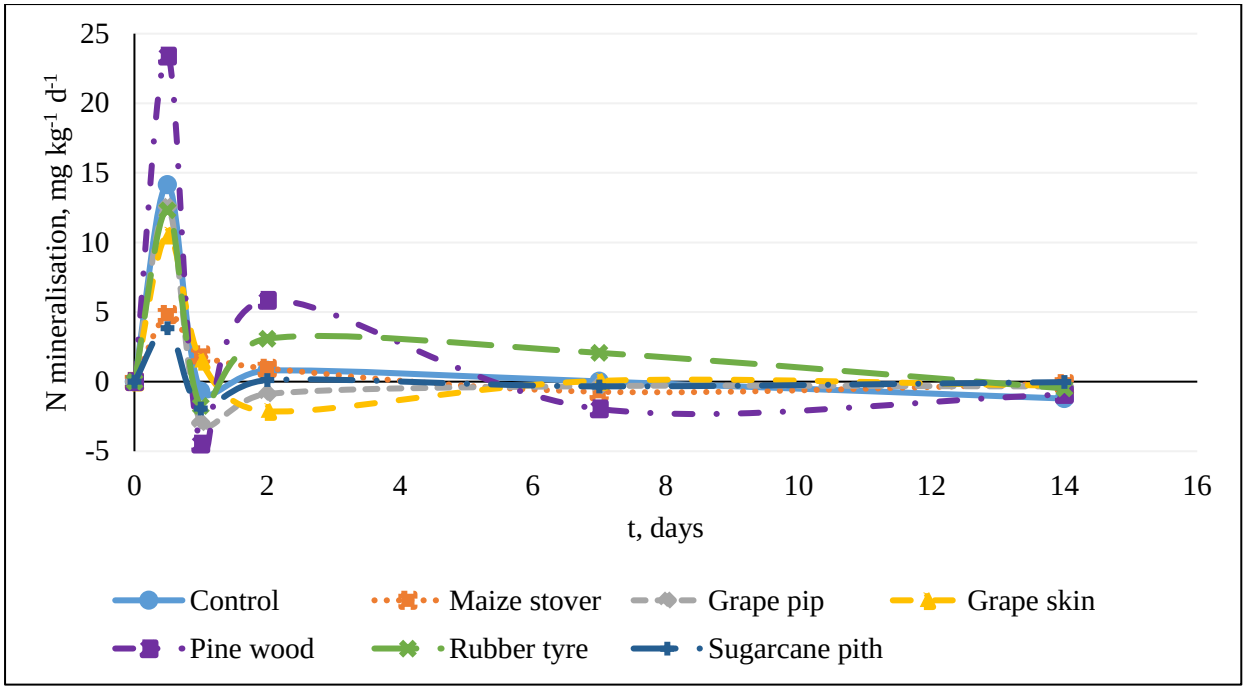

Figure 5. 17: Changes in N mineralisation rates over time resemble damped oscillations, where damping is influenced by the type of biochar addition.

Our attempts to model these oscillations have failed due to a small number of observations for such a complex system allowing for fitting of a wide variety of suitable functions that could be drawn through the observation points.

Still, it is clear that different biochars have a strong effect on system behaviour (Figure 5.17). The addition of pine wood and rubber tyre chars significantly underdamps the system showing the largest fluctuations of the mineralisation rates at the early stages of the process. On the contrary, the biochar produced from maize stover overdamps the system stabilising it shortly after two days. The magnitude of oscillations is significantly reduced with addition of grape skin, grape pip and sugarcane pith biochars.

Although it was impossible to model the differential behaviour of N mineralisation, it seems to be easier to model the cumulative net change in mineral N concentrations (Table 5.7) using a function similar to Equation 5.4.

Table 5. 7: Cumulative net change in mineral N concentrations and data coefficients of the control and six biochars from the vapor pressure model.

$\frac{N - N_0}{t}$	Control	Maize stover	Grape pip	Grape skin	Pine wood	Rubber tyre	Sugarcane pith
0.5	14.144	4.813	12.588	10.565	23.381	12.306	3.841
1	6.729	3.356	4.813	6.035	9.451	5.276	0.953
2	3.762	2.151	1.963	1.955	7.642	4.181	0.528
7	1.087	0.094	0.333	0.598	0.781	2.671	-0.090
14	-0.064	-0.035	-0.007	0.154	-0.074	1.093	-0.062
Parameter							
a =	1.916	1.963	1.551	2.727	2.182	1.183	-0.518
b =	0.020	-0.703	0.026	-0.939	0.186	0.572	0.536
c =	-0.999	-1.452	-1.340	-2.178	-0.851	-0.256	-1.141
r^2	0.999	0.993	1.000	1.000	0.987	0.992	0.997

The behaviour of the net change acceleration is a smoothened curve presented in Figure 5.18 for all the soils amended with different biochars.

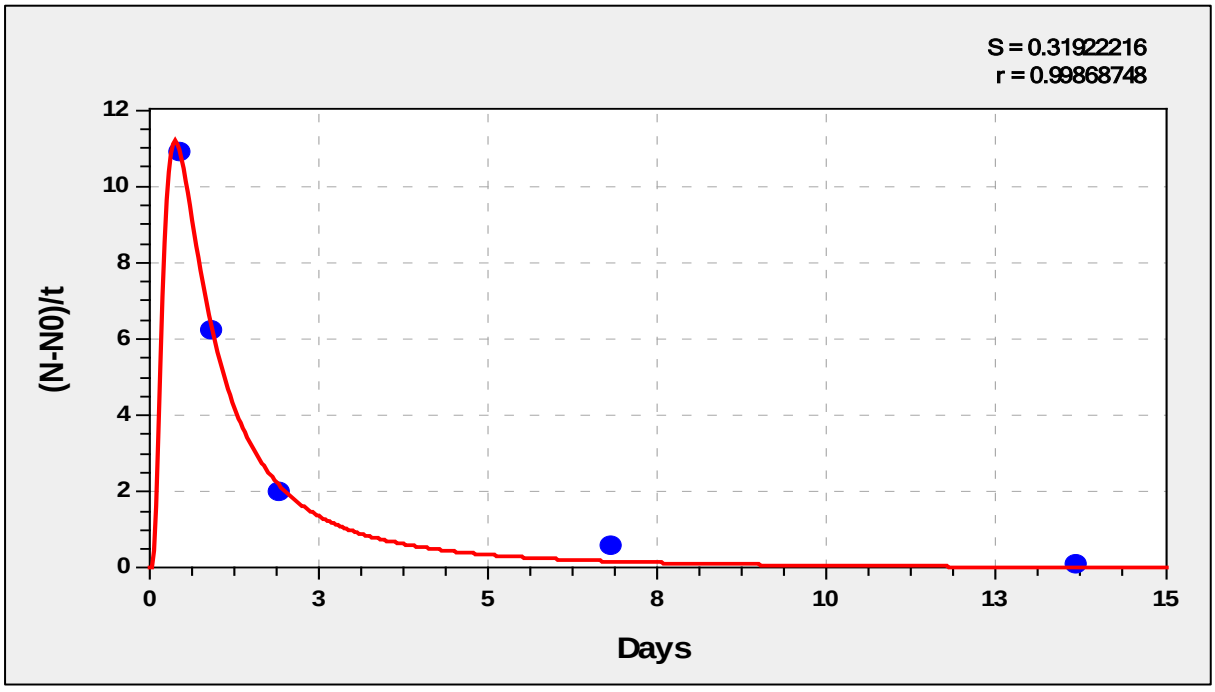

Figure 5. 18: Fitting a "vapor pressure model" to describe the behaviour of the change in the moving net N release in the control experiment.

No meaningful relationship was found between the equation parameters and biochar physico-chemical properties. It may be of interest though, that the curves describing carbon dioxide evolution and the curves describing the acceleration in net N mineralisation are of similar shape with peaks at the early stages of incubation. The correlation coefficient between parameter "a" in Equation 5.4 and Equation 5.8 is 0.64.

$$ln\frac{N-N_0}{t} = a - \frac{b}{t} - c \cdot ln\, t \qquad \text{Equation 5.8}$$

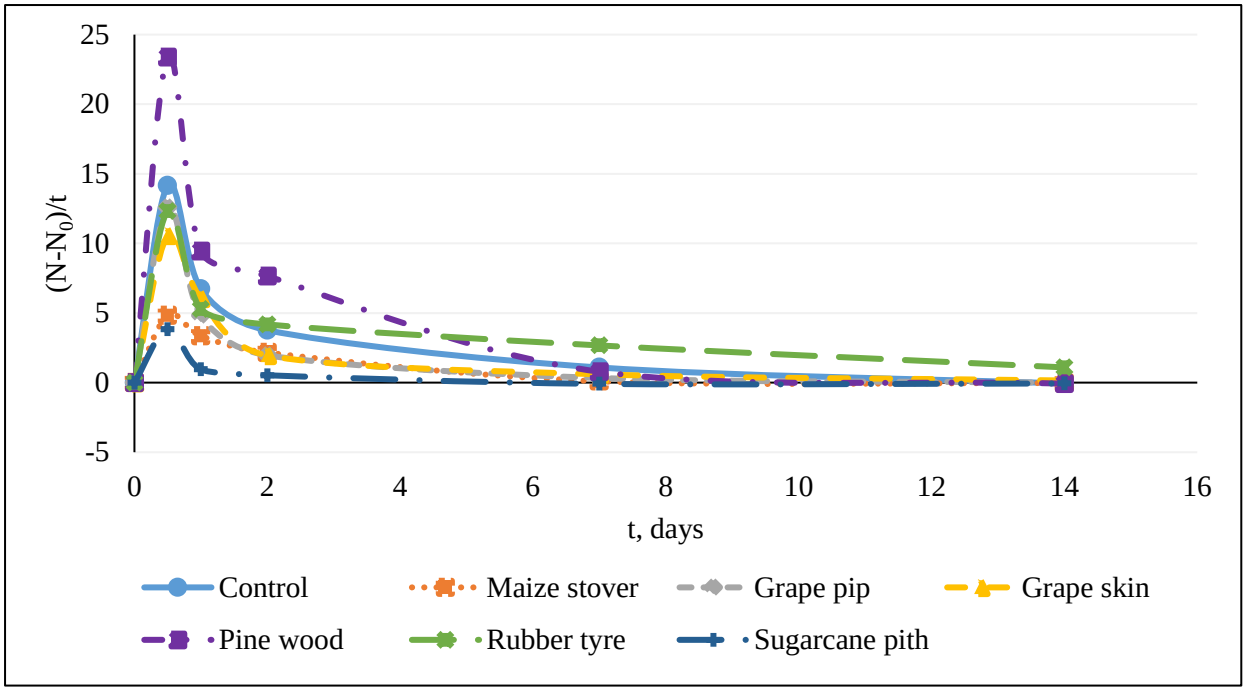

Figure 5. 19: Plot of $(N-N_0)/t$ behaviour.

Analysing Figure 5.19, it can be concluded that it is not the difference between days 14 and 0 (or 1) that describes best the steady state mineralisation, but rather the difference in mineral N concentrations between days 14 and 7. Longer experiments may be necessary to show that the system has stabilised, particularly in case of pine wood and rubber tyre biochar addition to the soil. The N mineralisation rates in all cases may be rather described as steady immobilisation (Figure 5.20) with rates in all cases being negative. Subsequently we may rather consider the effects of biochar on retarding immobilisation rather than accelerating mineralisation of nitrogen in soils.

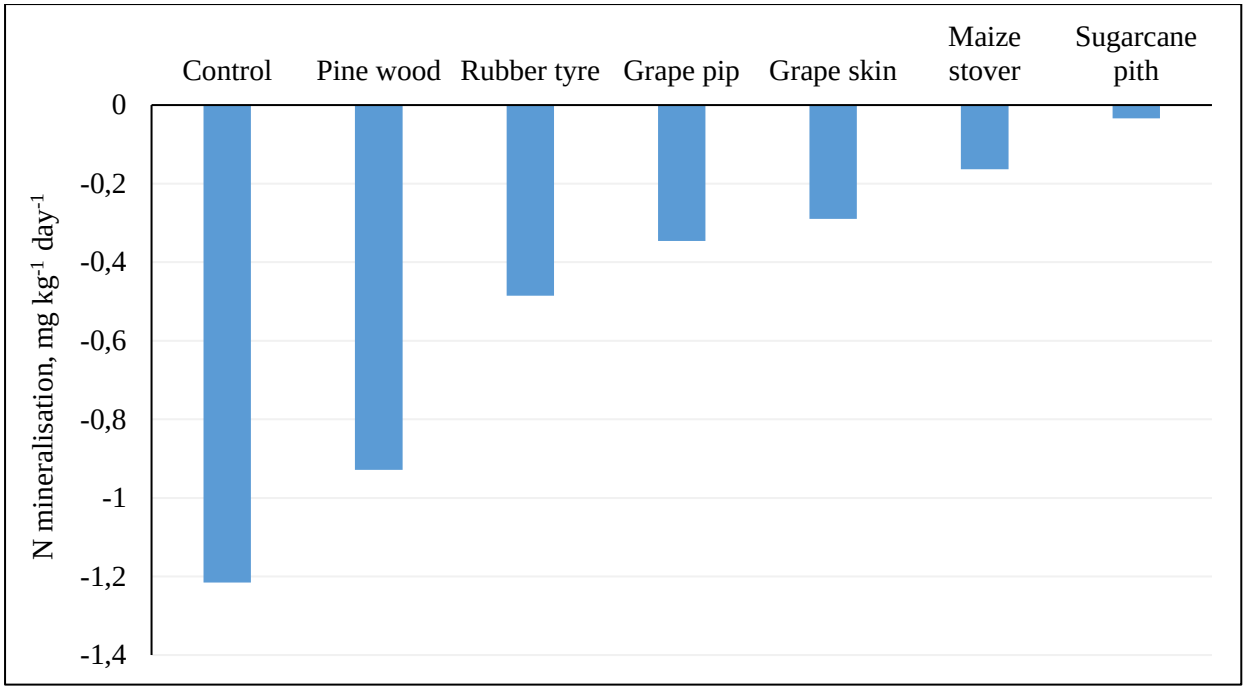

Figure 5. 20: Effects of biochar addition on steady-rate immobilisation of mineral N (days 7-14).

In the second week of the experiment (Figure 5.20) the system reached a state where N immobilisation became the dominant process. Here we see that all biochars have suppressed the N immobilisation rates compared to the control. This may be attributed to stable rates of microbial biomass production utilising the remainder of available nitrogen. In case of sugarcane pith biochar the system has almost completely stabilised by this time and mineralisation/immobilisation processes are almost balanced. The soil amended with pine wood biochar is closest to the behaviour of the control possibly due to poor biomass modification in the slow pyrolysis process.

Obviously, the continuous steady-rate N immobilisation is dependent on the initial presence of mineral N in the system, which was rather similar in all cases ranging from 10.13 mg in the control to 14.18 mg N per kg soil in the soil amended with rubber tyre biochar (Table 5.4). In most cases the initial mineral N concentration in the biochar-amended soils only slightly exceeded those observed in the control (except for rubber tyre and sugarcane pith biochars). Hence normalising the immobilisation rates by N_0 does not change the magnitude of the amendment effect on the steady rate of N immobilisation.

5.5 Conclusions

Biochar can serve as a sink for atmospheric carbon dioxide. It can also be a food source for soil microbes in the short-term. Total respiration was significantly lower in all the soils amended with various types of biochar. As per amount of initial carbon content in soil, the soils amended with the rubber tyre biochar

cumulatively released the least amount of CO_2 in 14 days. In contrast, the sugarcane pith char was not at all suitable for suppressing respiration. This means that biochar's fixed C content can act as an indicator for determining soil respiration behaviour. A very low fixed C content results in increased short-term CO_2 respiration, as was observed with the sugarcane pith biochar.

Two different models were fitted to describe the carbon dioxide respiration. The vapor pressure model showed strong positive correlations with the properties of the plant-derived biochars when correlated with the "a" parameter of the model, and cobalt had a strong influence for all six biochars. The rational function model on the other hand showed strong variation with the biochars, but no high correlation coefficients with any biochar physico-chemical properties. Of interest was the fact that modelling the C and N mineralisation data revealed that the curves describing the CO_2 evolution and curves showing the acceleration in net N mineralisation had similar shapes with peaks within the first 2 days in all the treatments. Furthermore, the results showed that all six biochars were an energy source for secondary carbon consumers. The biochars may have also acted as sorbents of carbon dioxide, thus being useful in limiting CO_2 emissions into the atmosphere.

Monitoring the incubated treatments closely at the beginning of the study showed that among the plant-derived biochars, the pine wood biochar amended soil released the most mineral N within 12 hours of observation; while the maize stover biochar addition resulted in the least N release. By the second day, pine wood biochar remained the highest N releasing plant-derived biochar, but the sugarcane pith char lost the least N. From the second day of measurements onwards, the rubber tyre biochar treated soil released a significant amount of N compared to all the other treatments due to N mineralisation.

Although several N transformation processes were identified in this experimental chapter, a steady-rate of nitrogen immobilisation was evident. Assessing the change in inorganic N concentrations against time revealed more specific periods of N release (mineralisation) and N consumption (immobilisation). In particular, nitrification was found to be promoted by the moderately alkaline (pH (H_2O) 8.63) grape skin biochar amended soil compared to the other treatments. Grape skin biochar was also shown to slightly increase N mineralisation. Whereas, the rubber tyre biochar significantly increased N mineralisation. All the plant-derived biochars, with exception to grape skin biochar, demonstrated that N immobilisation was the key mechanism for temporary N retention in the maize stover, grape pip, pine wood and sugarcane pith biochar-treated soils. These fluctuations in N mineralisation rates were like damped oscillations. The maize stover biochar caused an over-damping of the system, whereas the pine wood and rubber tyre chars resulted in an under-damping of the system. The remaining biochars caused a reduction in the magnitude of the oscillations compared to the control.

Considering the system behaviour (rapid mineralisation followed by immobilisation of N and several oscillations of these processes), we can conclude that the assessment of net mineralisation as a difference in N concentrations between days 14 and 0 of the incubation may be not the best way of estimating the N dynamics in amended soil systems. We can clearly see that the peak of mineralisation is achieved within the first 12 hours, while over longer time periods the system tends to stabilise, though at different rates. Subsequently, for overdamped systems (maize stover biochar-amended soils) we observe that stabilisation occurs quite rapidly (day two), while for underdamped systems (pine wood biochar-amended soils) the oscillations continue for the whole week one.

Among the plant-derived biochars, the grape pip biochar was found to be the least degradable in the short-term because it measured 59% lower cumulative CO_2 production per unit of initial carbon content than the control and had the least total N content (0.05-0.07 mg g^{-1}) released throughout 14-day incubation period.

Chapter 6
Leaching Study

6.1 Introduction

Leaching is a physico-chemical process associated with water drainage from the saturated section of soil. During this process, the input of water exceeds water loss by evapotranspiration (Lægreid et al 1999; Brady and Weil 2002), and mobile nutrients in soil solution are displaced by percolating water through the soil to an area outside the rooting zone; thus making the nutrients in soil solution out of reach for most crops (Major et al 2009).

Leaching of nutrients in agriculture is problematic because of the loss of nutrients meant for crop uptake, which seep into groundwater. Although nitrogen leaching in agriculture is common due to the inefficient use of N by crops, leaching of nitrate (NO_3^-), in particular, raises alarm. Nitrate leaching can adversely affect plant, animal and human health. It can contribute to the eutrophication of surface waters (Lægreid et al 1999) which negatively affects aquatic life. In humans, high levels of reduced nitrate, nitrite (NO_2^-), can be deadly because of the incidence of methaemoglobinaemia in infants and stomach cancer in adults (Addiscott 1996; Lægreid et al 1999). When the concentration of NO_3^- in drinking water exceeds 50 mg per litre, then the microbial reduction of NO_3^- to NO_2^- can cause methaemoglobinaemia in bottle-fed infants if milk is prepared with water containing nitrate levels above 50 mg L^{-1} (WHO 2006). Biochar, a product of pyrolysis technology, can be used to improve the state of the soil, the groundwater from which the soil leaches and ultimately, the water that people access for consumption.

Application of biochar has been shown to increase the capacity of soils to adsorb plant nutrients (Liang et al 2006; Cheng et al 2008b), which then reduces the loss of nutrients caused by leaching (Lehmann et al 2003; Major et al 2009). Usually, the potential of biochar to adsorb NO_3^- is possible when the pyrolysis temperature is at least 600°C and the amount adsorbed is feedstock and concentration dependent (Mizuta 2004; Kameyama et al 2012; Yao et al 2012; Dempster et al 2012b). However, unlike nitrate, the potential of biochar to adsorb ammonium has no apparent link to pyrolysis temperature, but, is also feedstock-dependent (Clough et al 2013). In addition to nutrient adsorption, biochar has been shown to retain plant available water (Tammeorg et al 2014). These positive effects on biochar nutrient and water use efficiency in a soil can help improve crop productivity (Glaser et al 2001; Liang et al 2006).

While several short-term studies have shown that biochar reduces N leaching and availability (Steiner et al 2008b; Knowles et al 2011; Zheng et al 2013b), little research has been conducted on what happens

to nitrogen in the soil-biochar environment after leaching. Stable N isotopes can be used to clarify this gap in knowledge. However, the chemical nature of soil N is highly controversial within the scientific community as various techniques leave a sizeable fraction of N unaccounted for. Much of the N is called "heterocyclic N" and this is used to account for the unidentified N fractions (Smernik and Baldock 2005). Thus, this study also focused on using labelled ^{15}N to trace the form and ultimate fate of the fertiliser N in the leached, biochar amended soils.

6.2 Objectives

This study focused on the effect that the different biochars had on reducing leaching of inorganic fertiliser N (ammonium and nitrate) and in quantifying the potentially exchangeable N remaining in the soil after intensive leaching.

6.3 Materials and Methods

In this research unit, the six biochars described in Chapter 3 and the and sandy subsoil described in Section 5.3.1 were used for the leaching study. The experimental layout of the leaching experiment is summarised in Figure 6.1. It demonstrates that soil-biochar mixtures were prepared and enriched (labelled) N fertiliser in the form of $^{15}NH_4{}^{15}NO_3$ was added to each column. The reason stable isotopes were used was because their signal can be tracked to determine the precise quantity of fertiliser mineral N not leached and distinguish them from mineral N present in the biochar or mineralised from soil organic matter.

6.3.1 Preparation of soil columns

Leaching columns for this experiment were constructed from polyvinyl chloride (PVC) pipes. The leaching column dimensions were as follows: 70 mm inner diameter (35 mm radius) and 150 mm length. Each column was fitted with a PVC end cap and drainage pipe at the bottom. The column tops were kept open to simulate a real field environment and to prevent anaerobic conditions from building up. The leaching columns were prepared by applying a thin coat of PVC weld on the inner column wall. Immediately thereafter, the inner wall was coated with the subsoil sample. This was done to help minimise preferential flow paths of percolating leachates. A small quantity of glass wool was fitted in the drain pipe opening at the base of each column to prevent losses of soil intermixed with biochar. Lastly, a 2 cm thick layer of quartz sand was placed at the bottom of each column to further prevent soil-biochar loss through the drain pipe opening.

The biochars and soil were passed through a 2 mm sieve prior to use. Each biochar was thoroughly mixed with the soil sample at 2.5% w/w (oven-dry equivalent) in plastic bags before packing in the

columns. There was also a control soil treatment (no biochar). Each column was packed with 0.5 kg of the soil-biochar mixture, packed to an initial bulk density of approximately 1.5 Mg m^{-3} and to a 12 cm soil layer height. Each treatment was replicated three times.

A single amount of 72 mg of 10 atom% $^{15}NH_4{}^{15}NO_3$ ammonium nitrate (AN) (Sigma Aldrich) was added to each column at the beginning of the leaching study (before leaching). This amount was chosen based on the typical N fertiliser recommendation of 100 kg N ha^{-1} for winter wheat in the Western Cape, South Africa, and the amount was adjusted for the dimensions of the soil column. The enriched ammonium nitrate was added by dissolving the pre-weighed chemical into clean plastic bottles with Milli-Q pore water (Millipore Corporation, France) and evenly applying to the soil surface in each column. The ammonium nitrate was the equivalent of 25.2 mg N per 0.5 kg soil in each column. This amount was calculated to be approximately 0.1 tons per ha. Unenriched AN treatments were also set-up to serve as a baseline for the ^{15}N isotopic study. Great care was taken to prevent cross-contamination by ensuring that different laboratory apparatus were used when working with the unlabelled and labelled treatments.

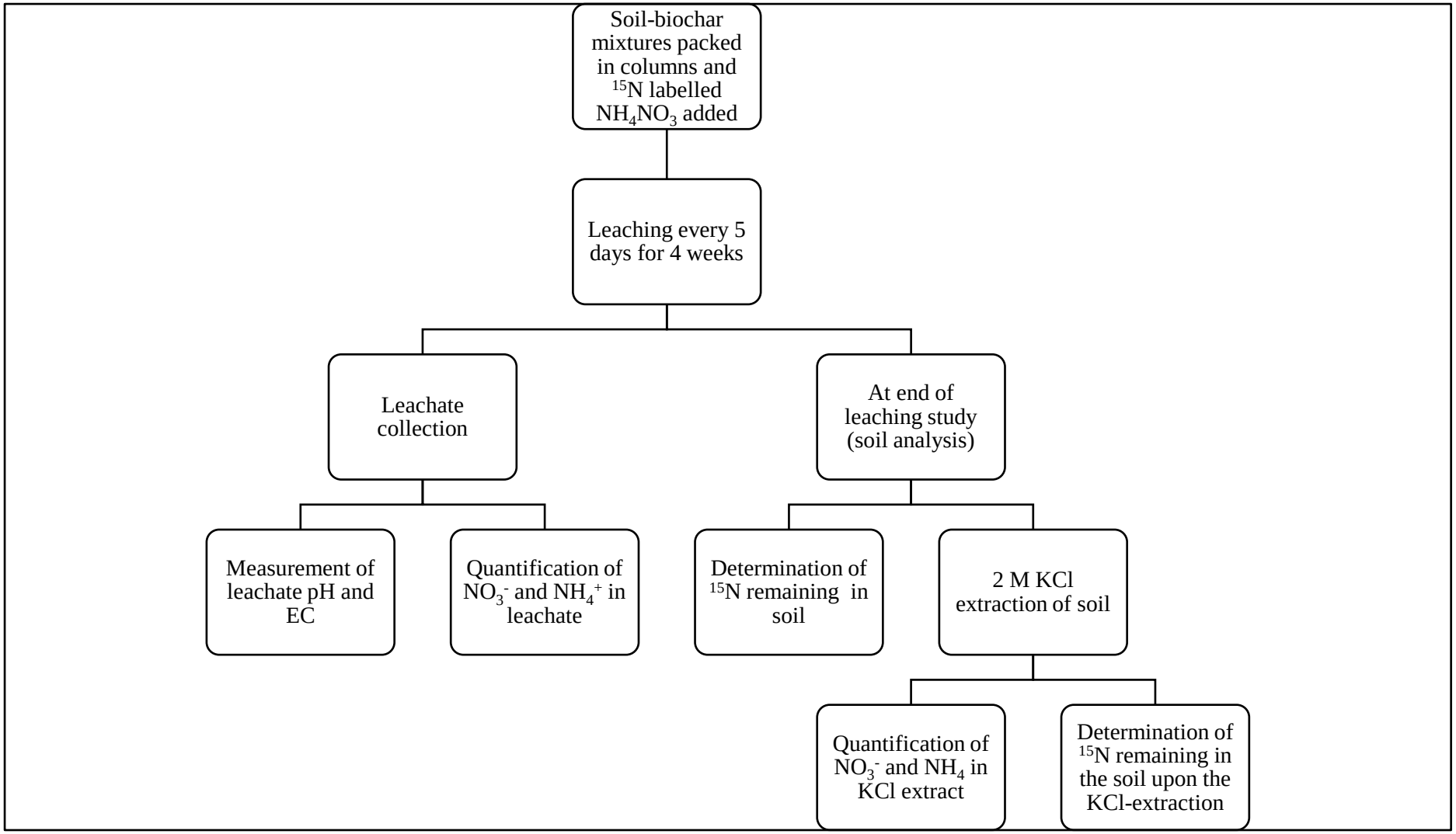

Figure 6. 1: Flow chart showing experimental layout used in leaching study.

6.3.2 Leaching study

Leaching columns were kept under ambient room temperature (approximately 23 °C) and humidity conditions. The leaching columns were erected above a series of tripod stands on a laboratory bench. Burette stands were used to mount 21 burettes above the columns. The burettes were positioned in the centre of leaching columns, without touching the soil. They were filled with Milli-Q pore water and allowed to drip during leaching events. Milli-Q pore water was used to leach the soil to eliminate the contribution of NO_3^- from tap water in the current experiment.

A total of six leaching events took place after every fifth day, allowing for 4 days of air drying between sample collections. An amount of 231 mL Milli-Q pore water was used during each leaching event (Appendix C). The amount of water used for each leaching event was calculated to apply 60 mm of water in 24 h period, simulating heavy winter rainfall in the Western Cape, South Africa (Sika and Hardie 2014). Leachates were collected in clean glass Erlenmeyer flasks, which were placed below the drain pipe opening situated below the centre of the tripod stand. The opening of the Erlenmeyer flasks were covered with Parafilm to minimise evaporative moisture loss. Leachates were allowed to collect in the Erlenmeyer flasks for 24 hours after leaching events. The flasks were covered with aluminium foil to prevent light interception into the liquid and thereby avoid algal growth.

6.3.3 Analysis of N in leachates

After collection of all the leachate from each leaching event, the volume of leachates were immediately measured gravimetrically and analysed. Leachate pH and electrical conductivity (EC) was measured at room temperature using a pH meter and EC meter, respectively. The leachates were then stored (frozen at -5°C) for NH_4^+ and NO_3^- analysis.

Leachate samples were defrosted and thoroughly shaken prior to inorganic N analysis. As clear samples are essential for colorimetric determinations, the samples were first centrifuged and vacuum filtered using 0.45 µm nylon membrane filter paper prior to N release rate measurements. The concentration of NH_4^+ in the leachates was determined colorimetrically using the salicylate method (Mulvaney 1996). In summary the procedure was undertaken as follows: the aliquot was mixed with a chelating agent, namely disodium salt of ethylenediaminetetraacetic acid (Na_2EDTA), to prevent precipitation; catalyst (sodium nitroprusside) which increases the rate and intensity of colour development; and finally, hypochlorite reagent. The sample was brought up to a volume of 25 mL and the colour was allowed to develop in a water bath set to 37°C. An ultra-violet/visible (UV/VIS) spectrophotometer was used to measure the intensity of the emerald green colour at 667 nm. The concentration of NH_4^+ was calculated based on the linear regression equation of the calibration curve prepared from the analyses of standards.

Nitrate in solution was measured using an auto analyser, high resolution digital colorimeter (SANS 13395 1996). In summary, the samples were put through a cadmium column and measured at a wavelength of 520 nm.

6.3.4 2 M KCl extraction of exchangeable inorganic N

At the end of the leaching study, the exchangeable (immediate plant available fraction) inorganic N (NH_4^+ and NO_3^-) was determined. The soil-biochar mixtures from each column were inverted and allowed to air dry. Representative soil samples (consisting of 10 g oven-dry weight equivalent soil and 100 mL 2 M KCl) were used for the extraction. The soil and KCl solution suspensions were shaken on the IKS ® KS basic shaker for 1 hour, then allowed to stand for 15 minutes before filtration using Whatman no. 2. The concentrations of NH_4^+ and NO_3^- in the filtrate were determined as described in Section 4.3.3.

6.3.5 Solid state ^{15}N CP-MAS-NMR of soil-biochar mixture

In order to establish whether ^{15}N was detectable in the soil-biochar sample at the end of the leaching study, an air-dried sample of soil with pine wood biochar was run using solid state ^{15}N nuclear magnetic resonance (NMR) spectroscopy. Solid state ^{15}N NMR was chosen because it is a non-invasive method that provides a tool for structural characterisation of soil organic matter. A standard of 10 atom% $^{15}NH_4{}^{15}NO_3$ was used as a reference.

The solid state NMR spectra were acquired using a Varian VNMRS 500 MHz two-channel spectrometer (Varian Inc., USA) using 6 mm zirconia rotors and a 6 mm Chemagnetics™ T3 HX MAS probe. The ^{15}N cross-polarisation (CP) spectra were recorded at ambient temperature with proton decoupling, a 6.0 μs 90° pulse and a recycle delay of 1 s. Magic-angle-spinning (MAS) was done at 5 kHz and ammonium nitrate was used as an external chemical shift standard where the downfield peak was referenced to –4.6 ppm. The power parameters were optimised for the Hartmann-Hahn match; the radio frequency fields were $\gamma_C B_{1N} = \gamma_H B_{1H} \approx 60$ kHz. The contact time for cross-polarisation was 1.5 ms. The free induction decay had 442 complex points and was Fourier transformed with 20 Hz line broadening.

6.3.6 Isotope analysis ($^{15}N/^{14}N$) of remaining fertiliser N in soil

At the termination of the leaching study, the leached soil and 2 M KCl extracted soil treatments were analysed to establish the amount of fertiliser N remaining in the soil-biochar mixtures after leaching. The reason this was done is because ^{15}N, which is least abundant, behaves exactly the same as ^{14}N which makes up 99.6% of N natural abundance. This means that the ^{15}N and ^{14}N fertilisers were likely

incorporated into the soil-biochar mixtures and leached similarly. Because the ratio of ^{15}N to ^{14}N in the fertiliser were known and the $^{15}N/^{14}N$ ratio in the soil was determined by mass spectrometry, it was possible to calculate the amounts of fertiliser N remaining in the soil-biochar mixtures.

The soil-biochar mixture samples were air-dried and carefully packaged in double 12 X 6 mm tin foil capsules weighing approximately 60 mg in size. Stable isotope analyses were done on a Flash HT Plus elemental analyser coupled to a Delta V Advantage isotope ratio mass spectrometer by a ConFloIV interface (all equipment supplied by ThermoFisher, Bremen, Germany). Carbon and nitrogen isotope values were corrected against an in-house standard (Merck gel). Laboratory standards and blanks were run after every 12 unknown samples.

6.3.7 Statistical analysis

The leaching data was analysed using the general linear model univariate analysis of variance (ANOVA) in order to determine statistically significant differences between the treatments. The data was tested for normal distribution and homogeneity before statistical analysis. For comparison of means, Fisher's Least Significant Difference (LSD) post hoc test with a $P < 0.05$ level of significance was used. Statistical analysis was performed using IBM SPSS (IBM SPSS Statistics for Windows, Version 24.0. Armonk, NY: IBM Corp.).

6.4 Results and Discussion

6.4.1 Soil-biochar mixtures

The pH of the subsoil (control pH 5.35, Table 6.1) was lower than the pH of the subsoil (Table 5.1). The addition of the alkaline plant-derived biochars, compared to the control, resulted in an immediate increase in the soil pH values by 1-5 pH units (Table 6.1). This demonstrated that biochar is a liming agent (Laird 2008). In contrast, the acidic rubber tyre char (Table 3.1) decreased the pH of the control soil by 2.5 units after mixing (before leaching). These observations in the pH changes correspond with the findings in Chapter 3 where each alkaline pH biochar (Table 3.4) had a corresponding high ash content (Table 3.3), with the exception of the pine wood biochar (ash content of 3.53%). Table 6.1 also showed that the soil pH had generally increased after leaching compared to before leaching during the 30-day leaching period. The reason for this is that there is an inversely proportional relationship between soil pH and EC. In the short-term when a soil has undergone excess leaching, the soil pH would be higher and the EC lower (Mohd-Aizat et al 2014).

Biochar acting as a liming agent is beneficial in acidic soil because the availability of Al in the acidic soil, which limits plant growth, is limited (Van Zwieten et al 2010b). The mechanism responsible for neutralising soil acidity is the dissolution of alkaline minerals in the biochar (Lehmann et al 2011). This was confirmed by the concentration of measured soluble salts (electrical conductivity measurements) in the leached soils, which were dramatically reduced compared to the non-leached (before leaching) soil-biochar mixtures (Table 6.1).

An acid soil that is over-limed is one where the pH measured in water is above pH 7.0 (Havlin et al 2014). Apart from the pine wood biochar amended soil, the remaining alkaline biochars caused the soil over-liming in the order: sugarcane pith > grape pip > grape skin > maize stover (Table 6.1). This means that only soil amended with pine wood biochar at a rate of 2.5% (w/w) is most suitable for plant production based on the pH after 2-weeks of leaching.

Table 6. 1: Measurements of pH and EC from the soil-biochar mixtures before and after leaching. Standard errors of the means in parentheses, n = 3).

Treatment	Before leaching			After leaching		
	pH(H_2O)	pH(KCl)	EC (dS m^{-1})	pH(H_2O)	pH(KCl)	EC (dS m^{-1})
Control	5.35 (0.01)	4.46 (0.01)	0.06 (1.29)	6.16 (0.02)	4.56 (0.04)	0.01 (0.39)
Maize stover	10.20 (0.03)	9.61 (0.01)	0.50 (7.00)	9.25 (0.02)	8.81 (0.14)	0.02 (0.01)
Grape pip	7.89 (0.04)	7.40 (0.04)	0.13 (7.71)	8.60 (0.03)	8.27 (0.12)	0.01 (0.31)
Grape skin	8.46 (0.05)	7.36 (0.31)	0.26 (3.46)	9.13 (0.12)	7.27 (0.03)	0.01 (1.03)
Pine wood	7.09 (0.02)	6.34 (0.03)	0.08 (2.07)	6.99 (0.10)	5.99 (0.12)	0.01 (0.56)
Rubber tyre	2.76 (0.01)	2.99 (0.01)	0.73 (3.48)	3.91 (0.01)	3.16 (0.01)	0.07 (1.68)
Sugarcane pith	7.12 (0.10)	6.47 (0.10)	0.13 (3.42)	7.13 (0.20)	6.21 (0.25)	0.01 (0.82)

6.4.2 Measurements from leachates

During the tenth and thirtieth days of the leaching study, between 80 and 100% of leachates were collected (Table 6.2). This shows a remarkable increase in the amount of leachates collected relative to the volume of leachates collected on Day 5. The increase in pore space may have occurred due to a shift in the air content and water retention capacity (Amonette and Joseph 2009) over time in the soil column. The main reason for incomplete soil wetting during the first leachate collection may be the presence of air-locked, discontinuous "blind" pores. Pore connectivity was improved after the first leaching rearrangement of particles had occurred. Further soil consolidation may have occurred until day 15, by which time the pore volume and connectivity had stabilised and 100±2 % of all the applied water was collected in subsequent leaching treatments.

When the amount of water leached through a soil is reduced, nutrient leaching will also be decreased (Glaser et al 2002). Further, this suggests that biochar porosity can affect nutrient retention capacity by binding cations and anions to its surfaces (Liang et al 2006). This reasoning is confirmed by the results found in our leaching experiment. The maize stover and pine wood biochar amended soils showed the least amount of water leached (Figure 6.2). This implies that more nutrients were retained in soils amended with maize stover and pine wood biochars. It is suggested that the reason for this is the comparatively higher surface areas (Table 3.6) for maize stover (160.53 m^2 g^{-1}) and pine wood (344.27 m^2 g^{-1}) biochars.

Table 6. 2: Percentage of leachate collected (relative to water supplied) after each leaching event.

Treatment	Days after start of leaching experiment					
	5	**10**	**15**	**20**	**25**	**30**
Control	46	87	103	101	99	97
Maize stover	26	98	96	74	98	98
Grape pip	48	98	95	87	98	94
Grape skin	47	85	102	102	100	98
Pine wood	42	85	97	86	96	91
Rubber tyre	58	89	100	99	98	98
Sugarcane pith	40	87	98	99	98	99

Table 6.2 further shows that 100±2 % of water was leached towards the end of the leaching experiment in all the treatments, showing that water movement within the soil from day 25 onwards occurred by saturated flow, largely due to macropores (Brady and Weil 2002).

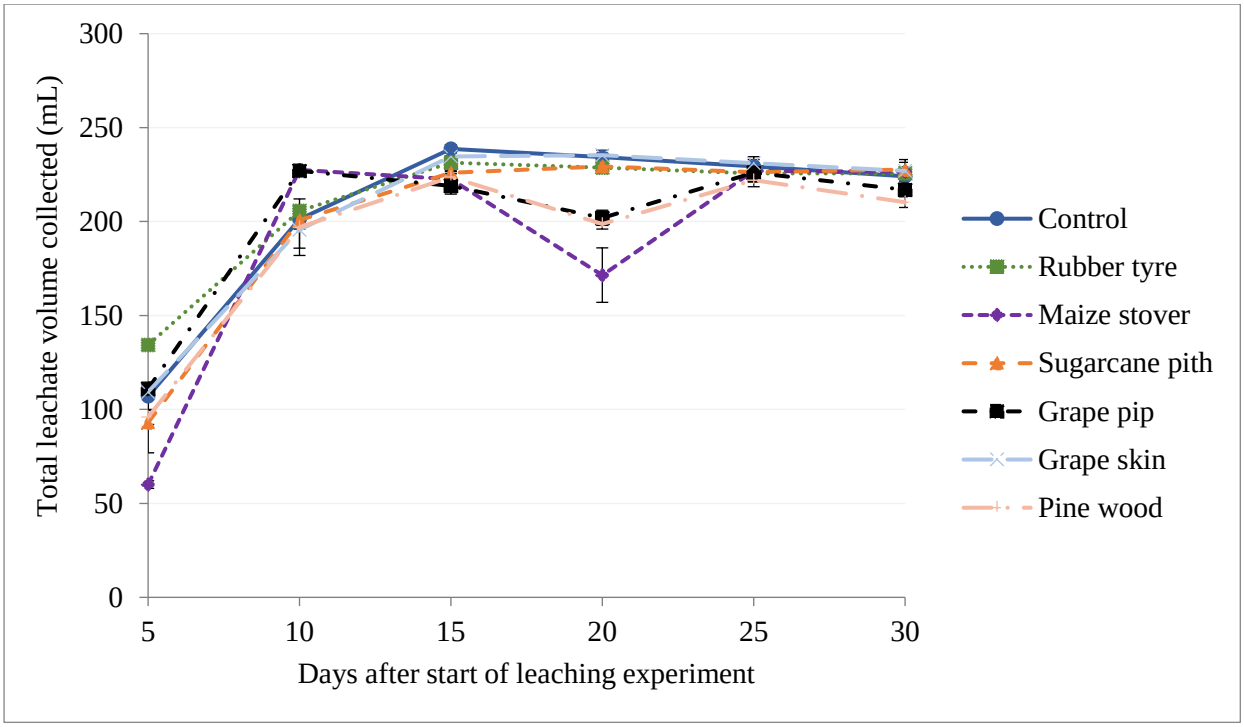

Figure 6. 2: Leachate volume collected at each leaching event from the biochar amended soils and control treatments.

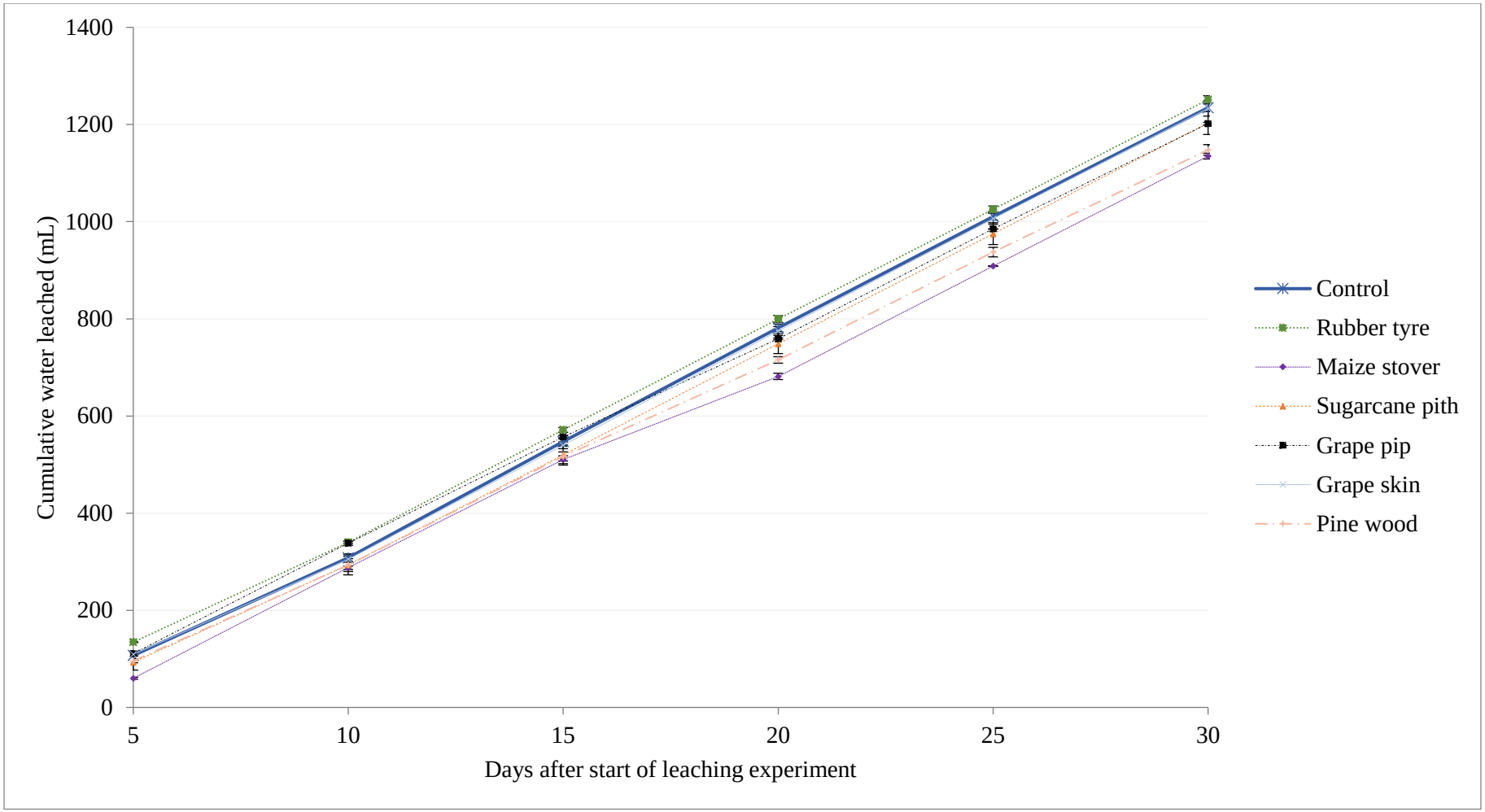

Figure 6. 3: Cumulative volume of water collected from biochar and control treatments over 30-day period.

6.4.2.1 Ammonium

The results obtained from the cumulative volume of water leached after the first leaching event on Day 5 (Figure 6.3) correlated with the high and low average concentrations of NH_4^+ leached from the rubber tyre and maize stover treatments, respectively (Figure 6.4). The rubber tyre had more than double the amount of NH_4^+ leached during the first leaching event compared to the other treatments. This was likely due to its inherently high total N content of 1.18% (Table 3.1). The amount of leached ammonium increased from the first to the second leaching event for the remaining treatments. After the second leaching event (Day 10), a decrease in the amount of NH_4^+ leached was observed for all treatments up to the fifth leaching event (Figure 6.4). There was no change in NH_4^+ leached between the fifth and sixth leaching events in all the treatments (Figure 6.4).

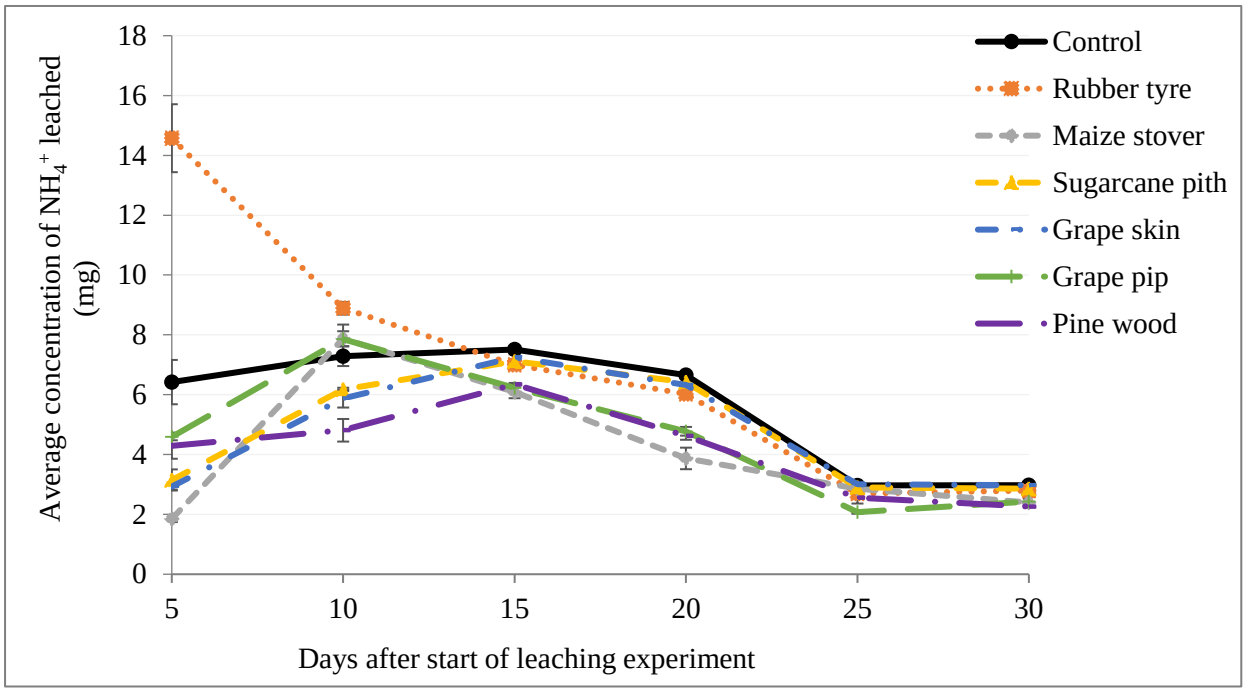

Figure 6. 4: Mean concentration of ammonium leached from the enriched treatments.

Biochar reduced the leaching of NH_4^+ relative to the control (by between 15 and 26%) in all treatments except for the rubber tyre char amended soil (Figure 6.5). It was observed that NH_4^+ was released from the rubber tyre char by up to 24% more than the control treatment. It was also previously reported that the rubber tyre biochar contained a relatively high amount (1.18%) of total N (Table 3.1) and released more mineral N compared to the other chars (Figure 5.5). This suggests that the rubber tyre char may have assisted in creating macropores with the soil in the leaching columns, thus increasing the infiltration rate. A similar finding was reported where organic waste materials used to amend a sandy clay loam ultisol caused an increase in the macroporosity as well as the total porosity as a result of reduced bulk density (Mbagwu 1989).

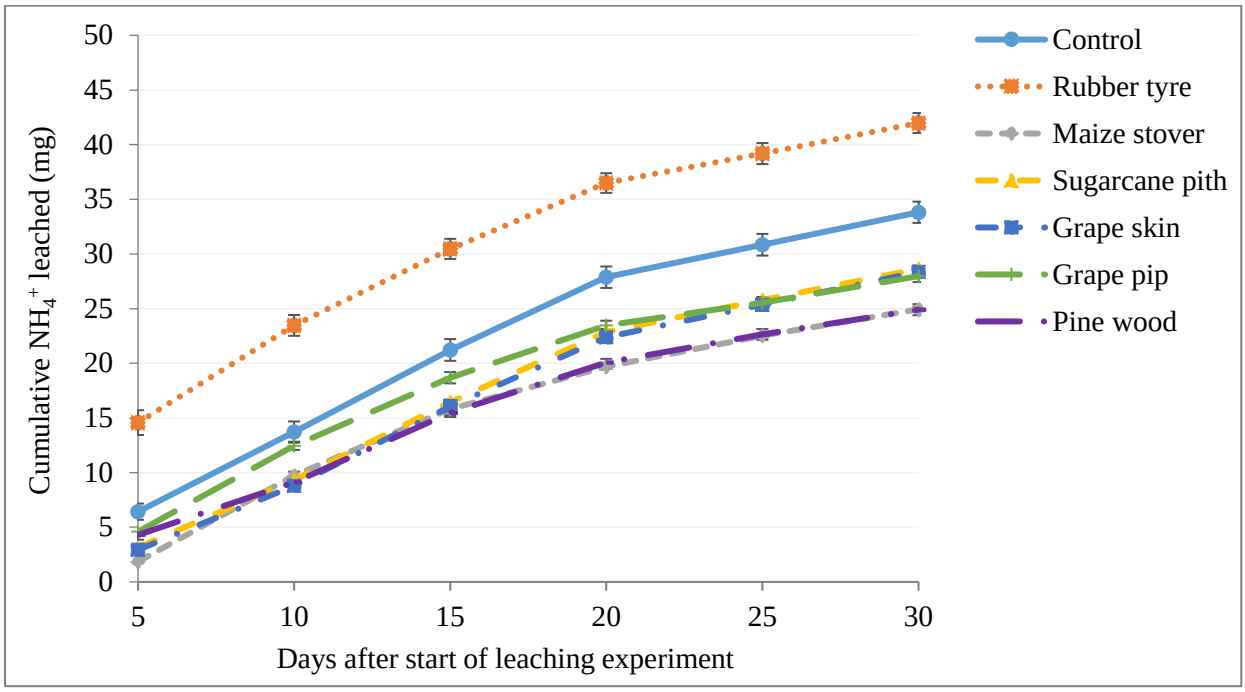

Figure 6. 5: Cumulative ammonium leaching losses from the biochar and control treatments.

6.4.2.2 Nitrate

The concentration of leached NO_3^- behaved differently compared to the ammonium leachates. The concentration of collected NO_3^- gradually declined and reached the stationary phase measuring NO_3^- levels between 0.03 and 0.94 mg L^{-1}, by day 20 of the experiment (Figure 6.6). This stationary phase was anticipated due to the highly mobile leaching character of nitrate (Brady and Weil 2002; Glaser et al 2002). Furthermore, it was previously reported (Figure 4.4) that the biochars had a very high adsorption capacity for nitrate (82-89%) and thus the amount of nitrate leached was especially reduced.

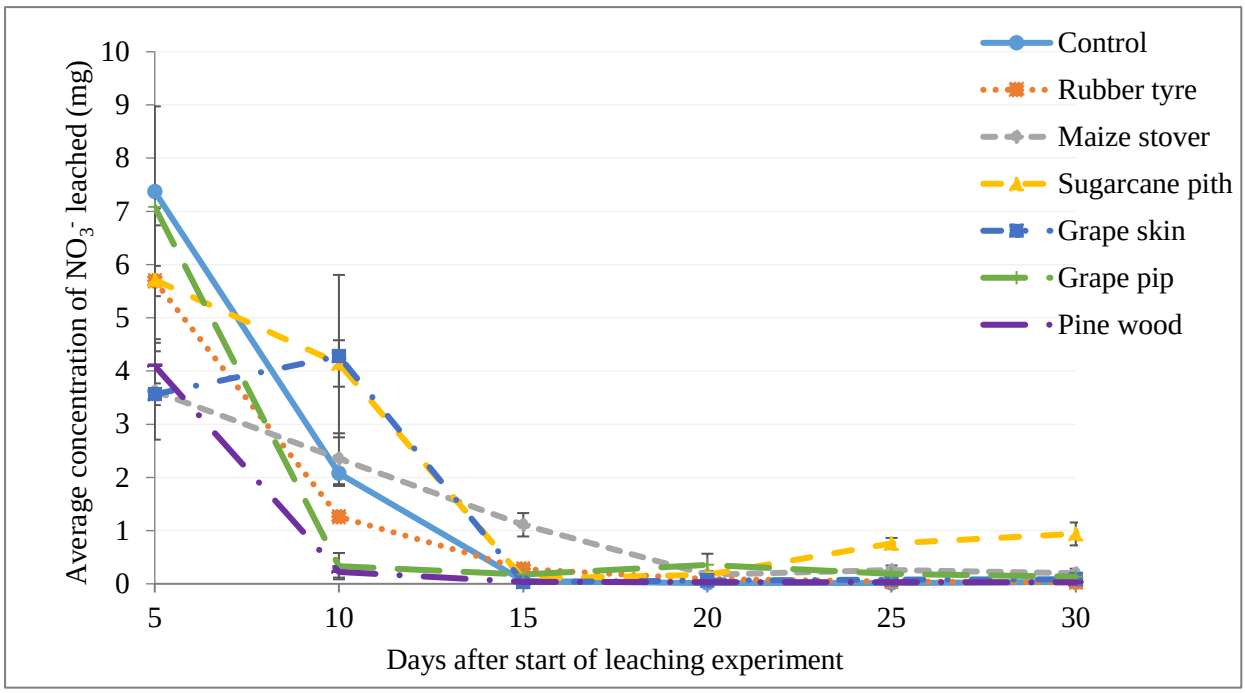

Figure 6. 6: Mean concentration of nitrate leached from the biochar and control treatments.

The rubber tyre biochar had the least NO_3^- concentration at the end of the incubation study relative to the other treatments (Figure 6.6). There are two possible reasons for this. Firstly, since the rubber tyre biochar adsorbed the most nitrate-N (Figure 4.3), it retained nitrate-N and therefore reduced the concentration of NO_3^- in the leachate. Secondly, because the rubber tyre amended soil is acidic, it may have inhibited nitrification. This suggestion is supported by the nitrate sorption study results in Chapter 4 where it was seen that the rubber tyre char adsorbed the most nitrate (79%, Figure 4.3) in a solution of 100 mg NO_3 per litre and therefore could not promote nitrification.

Biochar reduced the cumulative leaching of nitrate relative to the control (between 11 and 54%) in all treatments except for the sugarcane pith char (Figure 6.7). Instead, 23% more NO_3^- than was added was cumulatively leached from the sugarcane pith char treatment, while all the other char treatments resulted in a decrease in the amount of NO_3^- leached. The results suggested that the excess nitrate leached from

the sugarcane pith char was due to nitrification or mineralisation (Lægreid et al 1999).

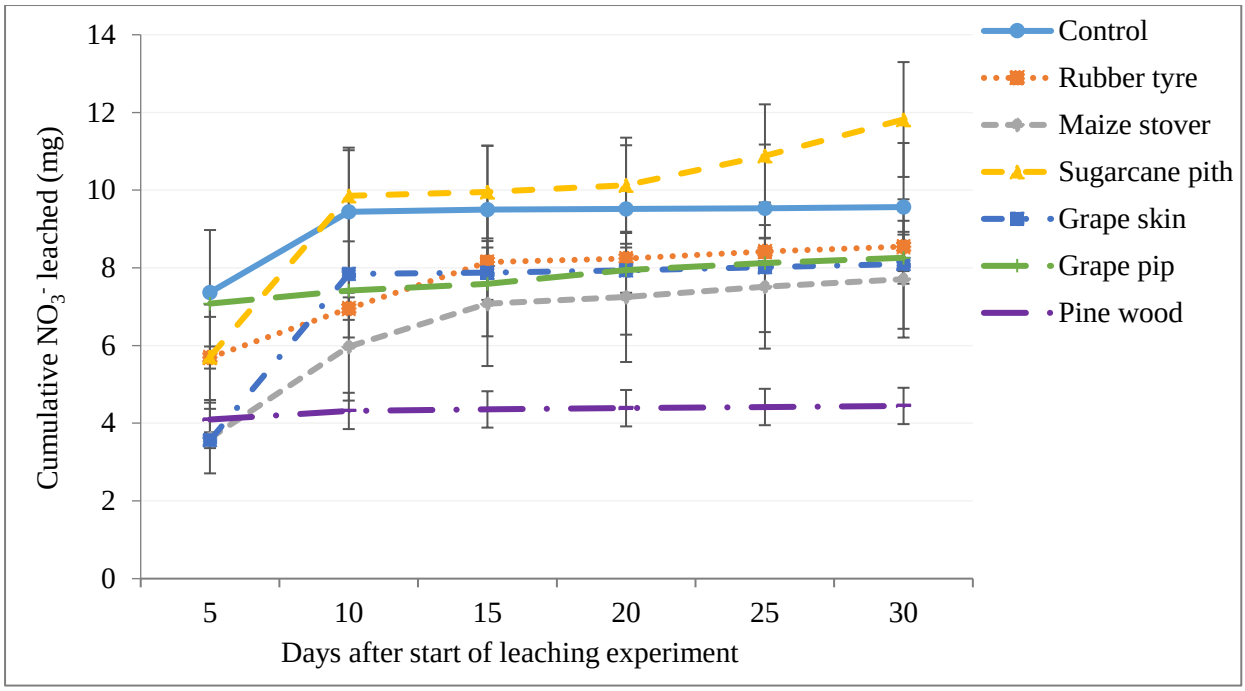

Figure 6. 7: Cumulative nitrate leaching losses from the biochar and control treatments.

Excess nitrate leached may have come from the mineralisation of organic matter fractions in the sugarcane pith. Since the fixed C percentage of sugarcane pith was below 50% (Table 3.3), it was previously suggested that it may not have been fully pyrolysed (Section 3.5.1). Based on the current experiment, the previous findings support the idea that perhaps the sugarcane pith char was indeed incompletely combusted. However, it is also likely that the reason more nitrate leached out of the sugarcane pith amended soil is because reduction of nitrate to nitrous oxide and N_2 gases did not take place to the same extent (if at all) as the other biochars due to the lower fixed C content (Figure 6.7).

Also, because the C/N ratio of the sugarcane pith char was the lowest relative to the other biochar samples (Table 3.1), mineralisation of the decomposable fractions of sugarcane pith may have resulted in the evolution of free N, resulting in more NO_3^- leaching than the inherent and originally added N.

Due to the maintenance of electro-neutrality in soil systems, when an anion leaches, a cation leaches too (Lægreid et al 1999; Brady and Weil 2002). This means that soils amended with rubber tyre and sugarcane pith chars are likely more at risk of being depleted of a range of nutrients, consequently negatively impacting crop production.

Several studies have also shown that biochar effectively reduces ammonium and nitrate leaching.

Similar to the observations found in the current study, Ding et al (2010) found that ammonium leaching was reduced by 15% when a sandy silt soil was amended with 0.5% (w/w) soil; and Dempster et al (2012b) reported that NH_4^+ leaching was reduced by 14% in a sandy soil amended with eucalyptus wood biochar. The reduction in nitrate leaching losses due to biochar application also varied; there was a reported 5% reduction by sugarcane bagasse biochar (Kameyama et al 2012), a 14% reduction by peanut hull biochar (Yao et al 2012), a 28% reduction by eucalyptus (hardwood) biochar (Dempster et al 2012b) and a 35% reduction by hardwood biochar (Yao et al 2012).

Nitrogen in the soil potentially available for crop uptake as nitrate, or ammonium, which soil microbes convert to nitrate (Brady and Weil 2002) is vulnerable of being leached out by heavy rainfall or irrigation events. Addiscott (1996) found that the critical period for N losses due to leaching is the first three weeks after fertiliser N application. This is because nitrate is highly water soluble (Brady and Weil 2002), and thus prone to leaching. To avoid nitrate losses in the soil solution, it is recommended that as little nitrate as possible is in the soil at any time (Addiscott 1996). For this reason, timely, split applications of N during the season are advised for sandy soils amended with biochar in heavy rainfall or high irrigation areas. The results indicate that all the biochars, except sugarcane pith can contribute to reduce nitrate losses (Figure 6.7). The pine wood biochar showed the greatest potential to reducing nitrate losses.

6.4.2.3 pH and EC of leachates

The pH measurements of the collected leachates showed little fluctuations throughout the leaching study (Figure 6.8). The slight decreases in pH were attributed to acidification caused by NH_4^+ (McBride 1994a) from the NH_4NO_3 fertiliser.

Soils amended with maize stover and rubber tyre biochars both had the highest amount of measured EC above 3.50 dS m^{-1} (Figure 6.9) after the first leaching event (at Day 5). After the third leaching event, 15 days after the start of the experiment, the soluble salts in the leachates had dramatically decreased to below 0.5 dS m^{-1} (Figure 6.9). The decline in measured EC was expected for all the treatments since it is well known that irrigation and rainfall slowly leach salts from a soil body. This finding also corresponds with the trend of soil pH and EC being indirectly proportional as observed in Table 6.1.

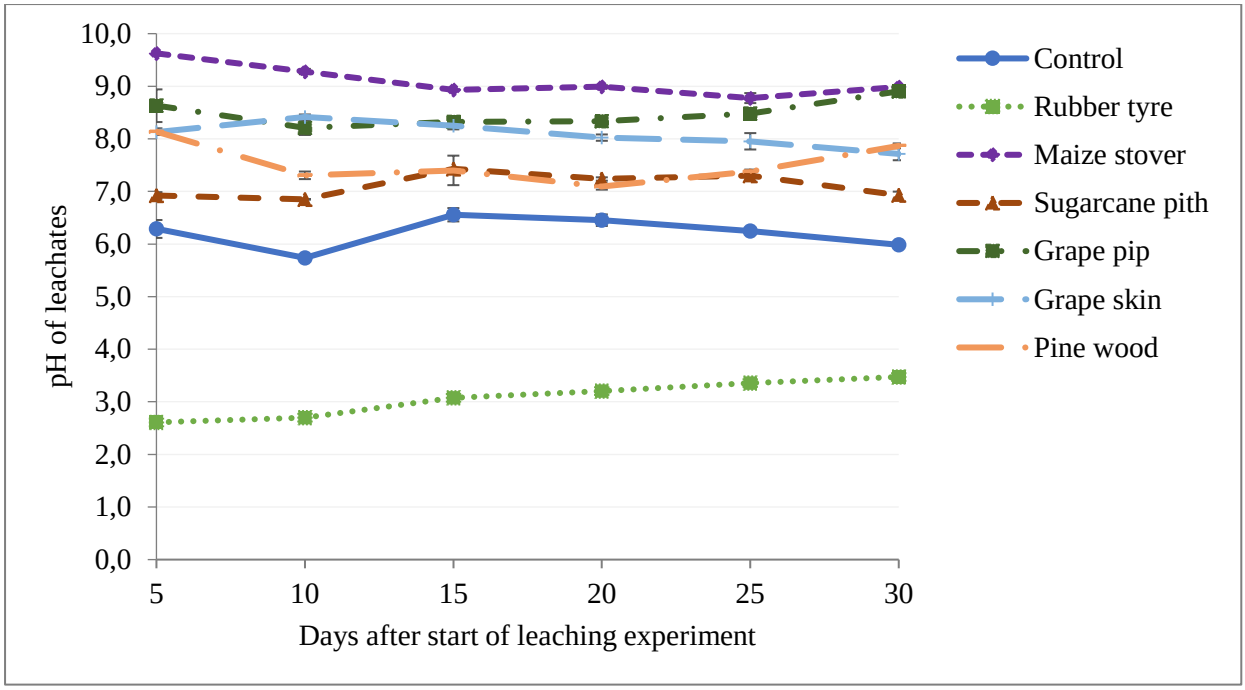

Figure 6. 8: Leachate pH values from control and biochar treatments during the 30-day leaching experiment.

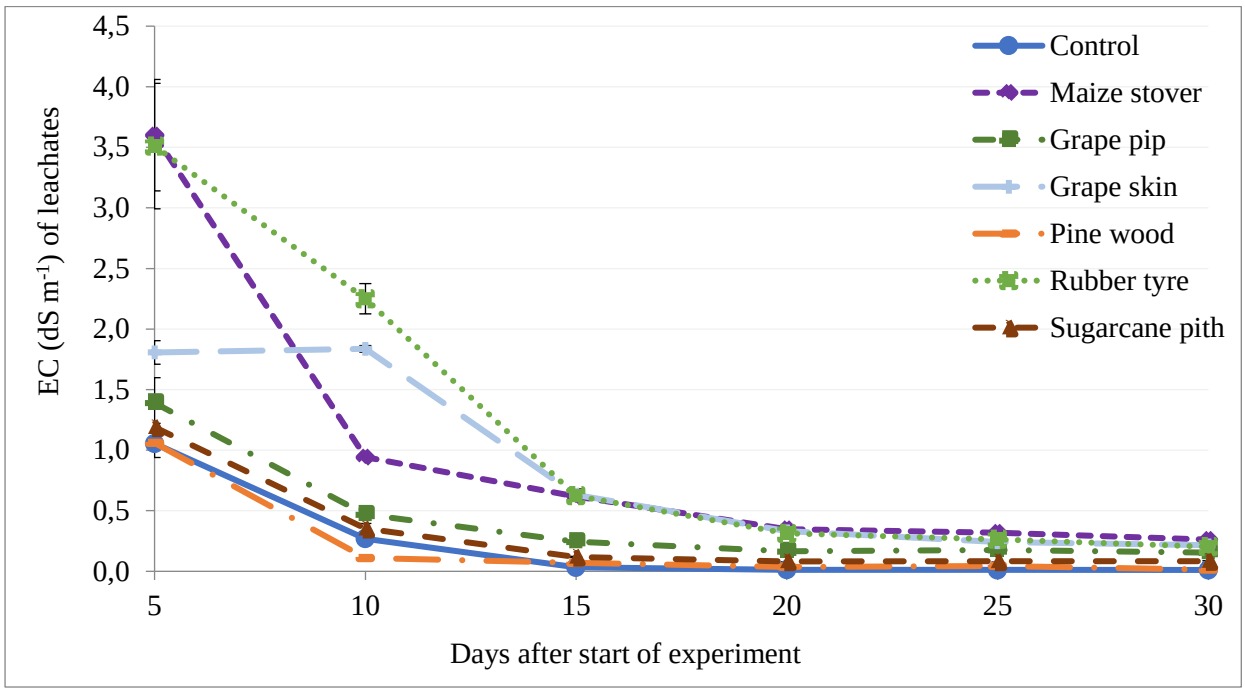

Figure 6. 9: Electrical conductivity measurements of leachates from the control and biochar treatments during the 30-day leaching experiment.

6.4.3 Ammonium-N and nitrate-N balance

Table 6.3 shows a summary of the amounts of exchangeable NH_4^+-N and NO_3^--N measured at the start of the leaching study, the amounts leached and the amounts still exchangeable after the leaching study in the control and biochar amended soils. A total of 25.20 mg (5.68 mg NH_4^+-N and 19.52 mg NO_3^--N) inorganic fertiliser N was added to each column. Amending the soils with various biochar materials reduced the leaching of ammonium and nitrate relative to the control in all the treatments except for the rubber tyre and sugarcane pith chars in the NH_4^+ and NO_3^- treatments, respectively. The excess ammonium-N leached from the rubber tyre char correlates with the results of the mineralisation study in Chapter 5 where it was shown that a significant amount of N was released (Figure 5.5), indicating that N mineralisation took place. There was no correlation between the nitrate leached from the sugarcane pith biochar and the mineralisation study. But, possible reasons for the excess NO_3^- leached from the sugarcane pith char were previously addressed in Section 6.4.2.2.

Although there were more statistically significant differences ($P < 0.05$) in the ammonium than the nitrate treatments (Table 6.3), pine wood biochar significantly reduced the amount of both ammonium and nitrate leached the most among all the treatments. This could be attributable to the fact that 89% nitrate was adsorbed by pine wood biochar, which was the highest adsorption capacity relative to the other chars (Figure 4.4). Furthermore, Table 5.4 showed that the pine wood biochar resulted in the highest amount of net N immobilisation and this corresponds with pine wood biochar's reduced leaching of mineral N. Thus, pine wood derived biochar can be used in reducing the leaching of ammonium and nitrate in sandy soil.

At the end of the leaching study, the soil in the columns was extracted with 2 M KCl to determine the amounts of exchangeable NH_4^+ and NO_3^- in the biochar amended soils. The amount of exchangeable NH_4^+ was between 6.11 and 7.77 mg, while that of NO_3^- was between 0.04 and 0.19 mg (Table 6.3).

Table 6. 3: Amount (mg) of ammonium-N and nitrate-N measured in 2.5% (w/w) soil-biochar mixtures in experimental columns. Standard errors of the means in parentheses, n = 3. Means in the same column followed by the same symbol are not significantly different at P < 0.05 level based on the Least Significant Difference test.

N-[NH_4^+] (mg)	Initial soil (2 M KCl + fertiliser) [a]	Total leached [b]	Exchangeable NH_4^+ after leaching [c]	Total recovered [d]	ΔN-[NH_4^+] (mg) [e]	Balance [f]
Control	15.87 (0.06) a	26.3 (0.76) b	6.7 (0.23) b	33 (0.86) b	17.12 (0.81) b	
Maize stover	12 (0.62) c	19.4 (0.18) d	6.78 (0.07) b	26.18 (0.25) e	14.18 (0.87) c	
Grape pip	12.82 (0.27) c	21.75 (0.42) c	7.61 (0.29) a	29.36 (0.28) c	16.54 (0.55) b	
Grape skin	12.26 (0.42) c	22.05 (0.07) c	6.33 (0.04) b	28.38 (0.1) cd	16.13 (0.35) bc	
Pine wood	12.04 (0.32) c	19.37 (0.39) d	7.77 (0.35) a	27.14 (0.43) de	15.09 (0.55) bc	
Rubber tyre	16.17 (0.25) a	32.65 (0.71) a	6.57 (0.29) b	39.22 (0.69) a	23.06 (0.88) a	
Sugarcane pith	14.26 (0.19) b	22.27 (0.24) c	6.11 (0.08) b	28.38 (0.17) cd	14.12 (0.23) c	
N-[NO_3^-] (mg)	**Initial soil (2 M KCl + fertiliser) [a]**	**Total leached [b]**	**Exchangeable NO_3^- after leaching [c]**	**Total recovered [d]**	**ΔN-[NO_3^-] (mg) [e]**	
Control	4.87 (0.02) ab	2.16 (0.37) a	0.04 (0) d	2.2 (0.37) a	-2.67 (0.39) ab	14.45(1.19) b
Maize stover	4.74 (0) c	1.74 (0.34) ab	0.19 (0.01) a	1.93 (0.33) ab	-2.8 (0.33) b	11.38(0.54) c
Grape pip	4.95 (0.02) a	1.87 (0.15) ab	0.17 (0) ab	2.04 (0.15) ab	-2.91 (0.17) b	13.63(0.67) bc
Grape skin	4.63 (0) d	1.83 (0.38) ab	0.06 (0) d	1.88 (0.38) ab	-2.74 (0.37) ab	13.38(0.69) bc
Pine wood	4.73 (0.01) c	1 (0.11) b	0.15 (0.01) b	1.16 (0.11) b	-3.57 (0.11) b	11.52(0.57) c
Rubber tyre	4.83 (0.05) b	1.93 (0.07) ab	0.05 (0) d	1.98 (0.07) ab	-2.84 (0.1) b	20.21(0.97) a
Sugarcane pith	4.65 (0.01) d	2.67 (0.33) a	0.12 (0.01) c	2.79 (0.33) a	-1.86 (0.32) a	12.26(0.4) bc

[a] Initial soil (2 M KCl extract) and added inorganic N fertiliser contents
[b] Total amount N cumulatively leached from columns
[c] Remaining exchangeable N extracted from soil in columns with 2 M KCl at the end of the leaching study
[d] The total recovered N values is the sum of the total N leached and the exchangeable N after leaching in the leached soils
[e] Change in N is the difference between N recovered and initial soil (2 M KCl + fertiliser) N added
[f] The sum of change (recovered-initial soil N) in ammonium-N and nitrate-N, which is the net assimilation of N in the soils

The total amounts of ammonium-N and nitrate-N collected from the leachates and 2 M KCl extracts was added together to quantify the total amounts of inorganic N recovered (Table 6.3). More NH_4^+ was recovered than what was initially exchangeable in the soil columns.

Table 6.3 also summarises the change in ammonium-N and nitrate-N derived from the difference between N recovered and the sum of the total N initially in the soil and added fertiliser. The under-recovery of N in NO_3^- was balanced by the over-recovery of ammonium N by less than the standard error (Table 6.3) in all cases except the rubber tyre biochar enriched soil. It is suggested that the inorganic N may have undergone transformation. Biological uptake of nitrate and subsequent excretion of ammonia is a common pathway, though abiotic transformations may also have occurred. Nitrate may have undergone reduction (Equations 6.1 and 6.2) and thus have contributed to the excess ammonium recovered (Table 6.3). The N in the soil-biochar system (from the soil/biochar/fertiliser) may have catalysed redox reactions associated with N transformation (Joseph et al 2015). The redox processes involving N may have included:

i. Reduction of NO_3^- to N_2 (g) under moderately reducing conditions (McBride 1994)

$$\frac{1}{5}NO_3^- + \frac{6}{5}H^+ + e^- = \frac{1}{10}N_{2\,(g)}\ \frac{3}{5}H_2O \qquad \text{Equation 6.1}$$

ii. Reduction of NO_3^- to NH_4^+ under exceptionally reducing conditions

$$NO_3^- + 10\,H^+ + 8e^- = NH_4^+ + 3H_2O \qquad \text{Equation 6.2}$$

This means that biochar represented the reductant and played the role of an electron donor; while nitrate represented the oxidant as the electron acceptor. In Klüpfel et al (2014), it was shown that biochar can reversibly accept and donate electrons, up to 2 mmol electrons per gram of char.

The high C/N ratio of the biochars (Table 3.1) indicate the potential for increased microbial immobilisation of the inorganic N. Kuzyakov et al (2000) reported that microbes immobilise N when residues have a C/N ratio greater than 32. This finding supports the results from the current study where the C/N ratio of the biochar materials is in the range of 38.0-372.3 (Table 3.1), giving evidence for the high probability of microbial immobilisation. Furthermore, previous results indicated that all the plant-derived biochars, except the grape skin char, possibly underwent temporary N immobilisation (Table 5.4) which further affected the availability of mineral N after leaching.

It was previously shown that the biochars in this research have a very strong adsorption capacity for nitrate (82-89%) which was not reversible (Figure 4.4b). Therefore, other possibilities for the under-recovery of nitrate-N are that the NO_3^- may have been physically absorbed due to the microporous

nature of biochar (Glaser et al 2002; Kameyama et al 2012), immobilised (Zavalloni et al 2011), or lost by denitrification (Wang et al 2001). However, biological denitrification is unlikely because the soil columns were open to the atmosphere to encourage aerobic conditions and freely draining throughout the leaching study. Based on these findings, it is evident that biochar amended soils are affected by multiple N pools. Therefore, the use of N tracer studies are useful to elucidate the gross mineralisation and immobilisation rates (Clough et al 2013).

6.4.4 ^{15}N labelled fertiliser study

In our previous study (Sika and Hardie 2014), we recommended the need to determine the chemical form of the immobilised N as this might help shed light on the mechanisms involved. In the present study, an attempt was made to determine the form of the fertiliser ^{15}N remaining in the soil-biochar mixtures after leaching using ^{15}N NMR spectroscopy. The spectrum of the ^{15}N enriched ammonium nitrate used as a standard reference showed five distinct chemical shifts of NH_4NO_3 (Figure 6.10). The two strongest resonances were observed at -4.6 ppm (non-protonated N, nitrate) and -358 ppm (protonated N, ammonium) (Figure 6.10). This confirms that the sensitivity of labelled N on the instrument was satisfactory. But the spectrum of the soil with biochar (Figure 6.11) did not show any peaks, only noise, because the N source was too dilute. Another attempt at determining the form of ^{15}N remaining after leaching was made by separating the biochar from the soil by flotation, picking, and air-drying. However, the investigation was unsuccessful again due to low concentration levels of ^{15}N in the samples. The spectra are shown in Appendix D.

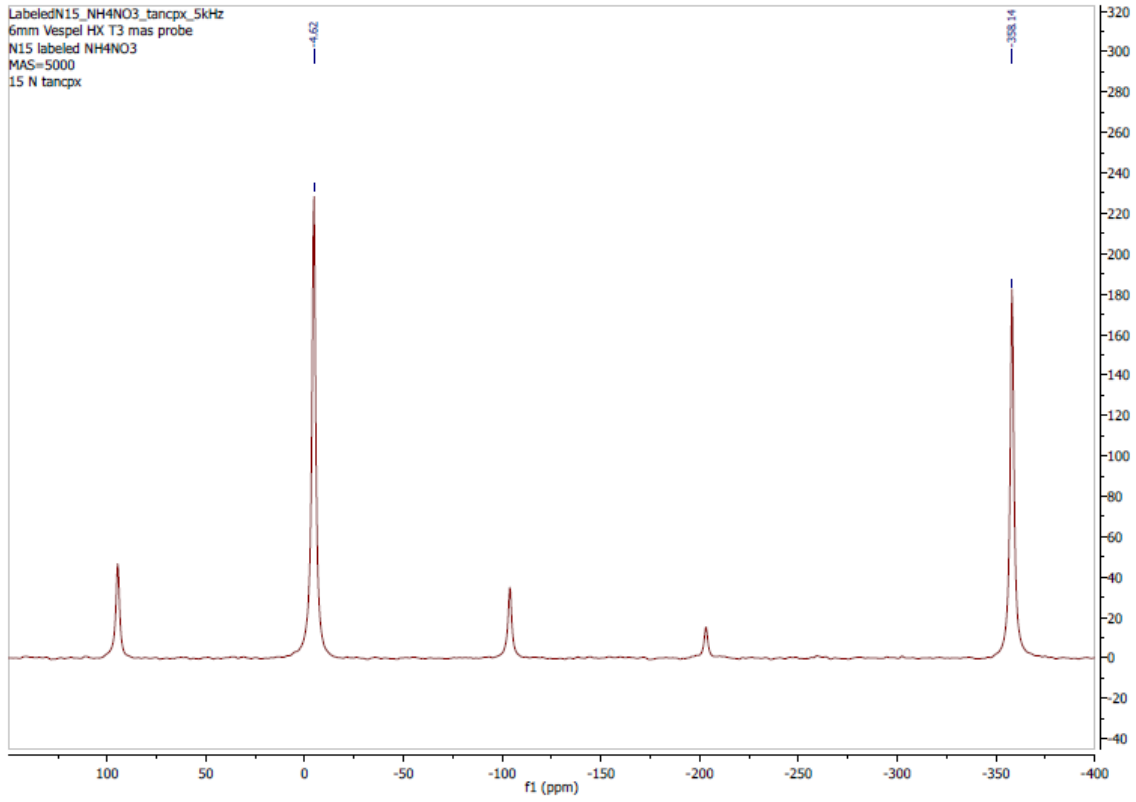

Figure 6. 10: Solid state NMR spectrum of enriched $^{15}NH_4{}^{15}NO_3$ sample used as a background for analysis.

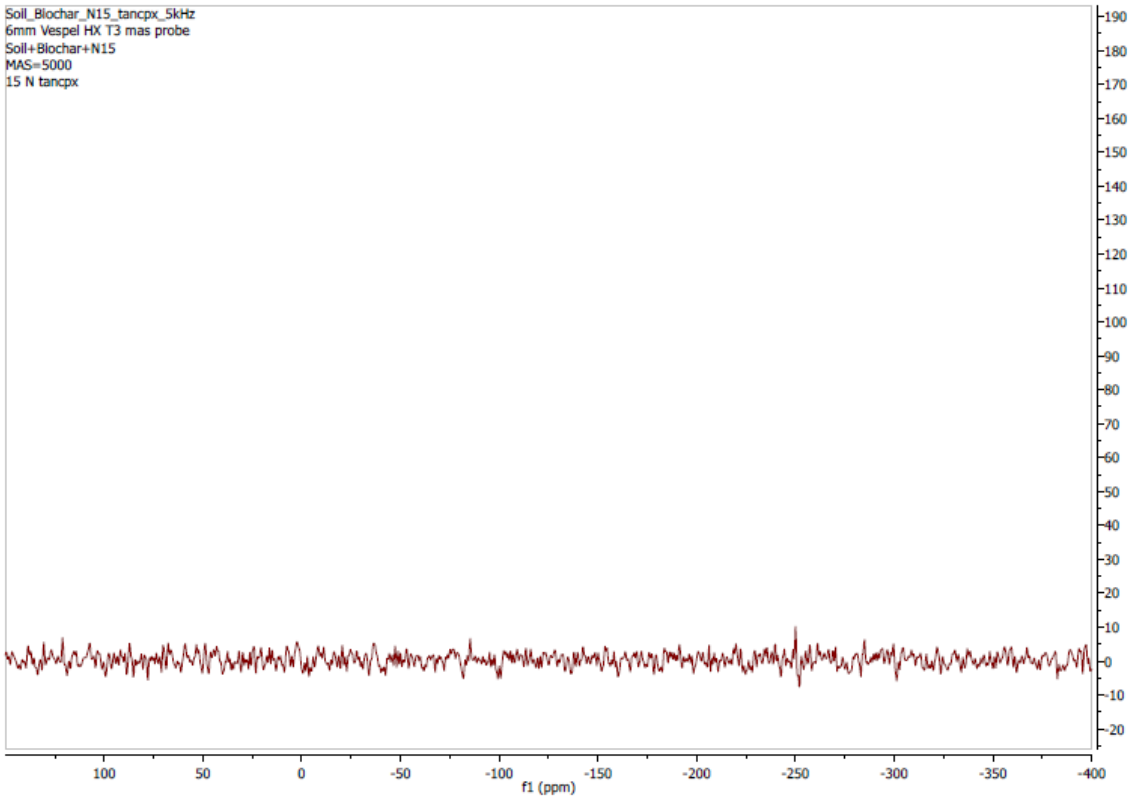

Figure 6. 11: Solid state NMR spectrum of leached and air-dried soil with pine wood biochar applied at 2.5% (w/w) and enriched with 10 atom% $^{15}NH_4{}^{15}NO_3$ after undergoing leaching for 30-days.

The amount of ^{15}N-labelled fertiliser remaining in the soil-biochar mixtures at the end of the leaching study was determined to try and further elucidate the soil-biochar N dynamics. The remaining fertiliser N in the soil-biochar mixtures was calculated based on the equation used by Steiner et al (2008) where:

$$Y = \frac{(N_f \times d^{15}N_f) - (N_f \times d^{15}N_c)}{d^{15}N_{NPK}} \qquad \text{Equation 6.3}$$

Y = amount of ^{15}N remaining in soil

N_f = soil nitrogen content of enriched N treatment (mg mg^{-1})

$d^{15}N_f$ = measured delta ^{15}N value of soil in enriched N treatment (‰)

$d^{15}N_c$ = measured delta ^{15}N value of soil in unenriched control treatment

$d^{15}N_{NPK}$ = delta ^{15}N value of NH_4NO_3 10 atom% ^{15}N excess = 29193.2 ‰

The N tracer study using labelled $^{15}NH_4{}^{15}NO_3$ revealed that between 0.77% and 10.81% of applied fertiliser N remained in the soil-biochar treatments after leaching (Figure 6.12, Table 6.4). Only the sugarcane pith char (157% relative increase compared to control) and pine wood biochar (136% relative increase compared to control) treatments significantly enhanced fertiliser N retention (10.81 and 9.97 % fertiliser N remaining, resp.) and compared to the control soil (4.21% fertiliser N remaining) or other char treatments (Figure 6.12). Whereas, the rubber tyre biochar significantly reduced fertiliser N retention (0.77% fertiliser N remaining) compared to the control or other biochar treatments. The amount of KCl-exchangeable fertiliser N of the grape pip and pine wood biochar amended soils could unfortunately not be analysed due to high ash contents of these samples (Figure 6.12, Table 6.4). Among the samples that could be analysed, the grape skin biochar treated soil had the highest amount of 2 M KCl exchangeable fertiliser N after leaching (2.30%) relative to the other treatments which could be measured, however it was not statistically significant form the control.

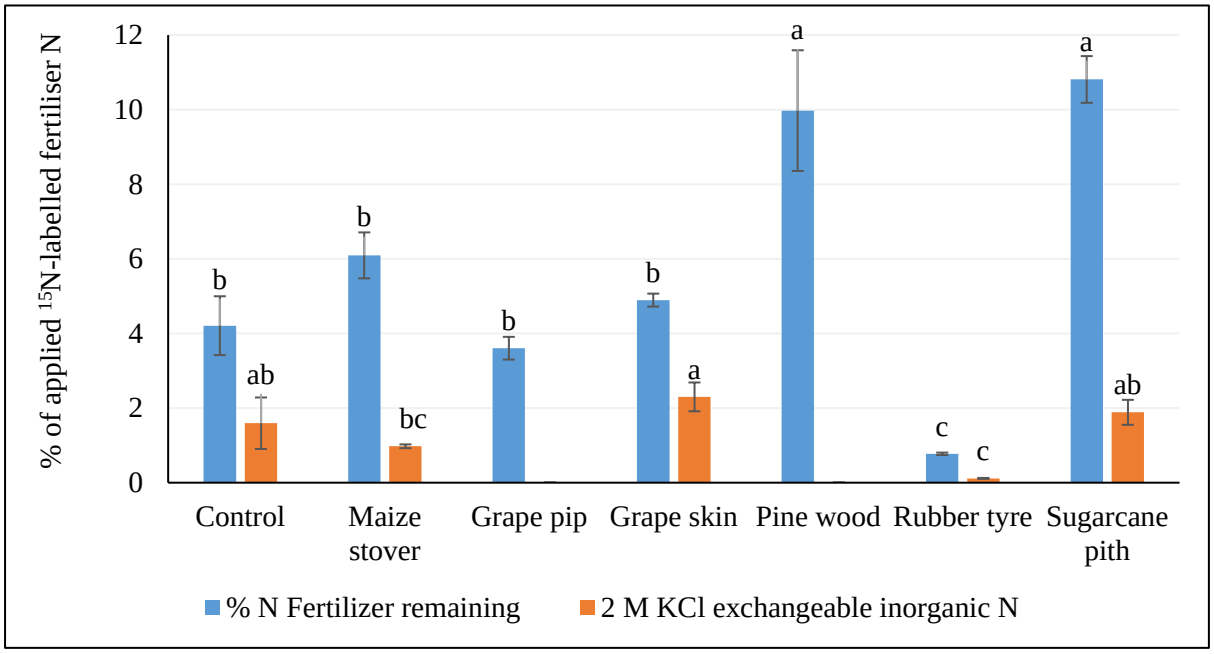

Figure 6. 12: Percentage of applied fertiliser N remaining after leaching and % extractable with 2 M KCl extraction post-leaching. Error bars represent standard deviation of the mean where n = 3. Letters indicate differences at P < 0.05 based on the Least Significant Difference test.

The observation that the pine wood and sugar cane pith biochars enhanced soil fertiliser N retention was consistent with previous studies investigating ^{15}N tracer recovery; for example, Zhao et al (2013) found that cropland soils amended with 5% (by weight) rice straw derived biochar produced at 500°C increased fertiliser N retention by between 5.6% and 26% when ^{15}N urea (10.25% enriched) was applied. Similarly, Zhou et al (2017) found that soil treated with biochars produced from solid anaerobic

digestate at different pyrolysis temperatures (250-600 °C) increased the percentage retention of the added 98 atom% $^{15}NH_4{}^{15}NO_3$ by an average of 39%.

Table 6.4 shows a summary of the source and fate of mineral N in the leaching column experiments, using total mineral N and^{15}N labelled mineral N experimental results to calculate which mineral N was derived from the soils. However it's important to take note that the quantity of fertiliser leached from the ^{15}N labelled fertiliser is an assumed value, since the fate of the fertiliser no longer detectable in the soil is unknown, and could also have included gaseous losses due to abiotic or biotic reactions. The results suggest that most of the nitrogen leached (22.48 mg-25.01mg) was from the fertiliser applied fraction compared to the mineral N fraction from soil-biochar mixtures (0 mg-9.53 mg) (Table 6.4). Furthermore, the calculated leached percentages of N from the soil-biochar mixtures fraction indicate that no soil-biochar derived mineral N was leached in the maize stover, grape pip, grape skin, and pine wood char treatments but was rather immobilised.

The soil mixed with pine wood biochar had the highest estimated remaining total mineral N (12.76 mg) followed by maize stover char (11.96 mg) compared to the other treatments (Table 6.4). The total exchangeable inorganic N extracted by KCl after leaching had very similar amounts between the treatments of between 6.38 and 7.91 mg N (Table 6.4). But, it was observed that the exchangeable N from the applied ^{15}N fertiliser fraction (Figure 6.12; 0-2.30%) was different to the calculated exchangeable N from the fertiliser (Table 6.4; 0-8.9%). the results in Table 6.4 are calculated approximations based on the difference between the remaining mineral N and residual N, thus serving as estimations.

The difference between N remaining after leaching and 2 M KCl extraction gives an estimation of the residual inorganic N which is non-exchangeable nor leached. It was observed that the rubber tyre char treated soil showed no residual N at the end of the leaching study. The reason for this is that the rubber tyre char enhanced N leaching of fertiliser by possibly creating macropores within the soil and thus a lot of N was lost via leaching. The other treatments had between 1.96 mg and 5.0 mg of total residual N at the end of the leaching experiment (Table 6.4). This fraction of residual N in the (maize stover > pine wood > sugarcane pith > grape skin > grape pip > control (soil)) treatments was most likely immobilised into the SOM, especially with the original structures of sugarcane pith material that remained intact (unpyrolysed) (Chapter 3).

Table 6. 4: Percentage (and absolute values, mg N ±standard error) of total inorganic N in experimental leaching columns. (n.d. = not determined)

N source	Soil/Char mixture	Initial, % (mg)	Leached, % (mg)	Remaining after leaching, % (mg)	Exchangeable, after leaching, % (mg)	Residual (non-exchangeable and not leached), % (mg)
Inorganic N, total	Control	100 % (37.1 ±0.06)	76.6 % (28.42 ±1.13)	23.4 % (8.69 ±1.18)	18.1 % (6.73 ±0.23)	5.3 % (1.96 ±1.42)
	Maize stover	100 % (33.07 ±0.5)	63.8 % (21.11 ±0.16)	36.2 % (11.96 ±0.66)	21.1 % (6.96 ±0.09)	15.1 % (5 ±0.75)
	Grape pip	100 % (34.1 ±0.28)	69.2 % (23.58 ±0.57)	30.8 % (10.52 ±0.85)	22.8 % (7.77 ±0.29)	8.1 % (2.75 ±1.14)
	Grape skin	100 % (33.22 ±0.42)	71.8 % (23.84 ±0.31)	28.2 % (9.38 ±0.73)	19.2 % (6.38 ±0.04)	9 % (3 ±0.76)
	Pine wood	100 % (33.1 ±0.32)	61.4 % (20.34 ±0.5)	38.6 % (12.76 ±0.81)	23.9 % (7.91 ±0.35)	14.7 % (4.85 ±1.17)
	Rubber tyre	100 % (37.32 ±0.29)	92.5 % (34.53 ±0.76)	7.5 % (2.79 ±1.05)	17.7 % (6.61 ±0.29)	-10.3 % (-3.83 ±1.34)
	Sugarcane pith	100 % (35.23 ±0.19)	70.7 % (24.9 ±0.55)	29.3 % (10.33 ±0.75)	17.6 % (6.22 ±0.08)	11.7 % (4.11 ±0.83)
Inorganic N, Fertiliser	Control	67.9 % (25.2 ±0)	95.8 % (24.14 ±0.2)	4.2 % (1.06 ±0.2)	3.3 % (0.83 ±0.29)	0.9 % (0.23 ±0.09)
	Maize stover	76.2 % (25.2 ±0)	93.9 % (23.66 ±0.16)	6.1 % (1.54 ±0.16)	5.1 % (1.29 ±0.17)	1 % (0.25 ±0.01)
	Grape pip	73.9 % (25.2 ±0)	96.4 % (24.29 ±0.08)	3.6 % (0.91 ±0.08)	n.d.	n.d.
	Grape skin	75.9 % (25.2 ±0)	95.1 % (23.97 ±0.04)	4.9 % (1.23 ±0.04)	3 % (0.75 ±0.05)	1.9 % (0.48 ±0.01)
	Pine wood	76.1 % (25.2 ±0)	90 % (22.69 ±0.41)	10 % (2.51 ±0.41)	n.d.	n.d.
	Rubber tyre	67.5 % (25.2 ±0)	99.2 % (25.01 ±0.01)	0.8 % (0.19 ±0.01)	0.7 % (0.17 ±0.01)	0.1 % (0.03 ±0)
	Sugarcane pith	71.5 % (25.2 ±0)	89.2 % (22.48 ±0.16)	10.8 % (2.72 ±0.16)	8.9 % (2.25 ±0.25)	1.9 % (0.48 ±0.09)
Inorganic N, Soil-Biochar	Control	32.1 % (11.9 ±0.06)	35.9 % (4.28 ±0.06)	64.1 % (7.63 ±0.12)	49.6 % (5.9 ±0.52)	14.5 % (1.73 ±0.64)
	Maize stover	23.8 % (7.87 ±0.62)	0 % (-2.56 ±0.5)	100 % (10.43 ±1.12)	72.1 % (5.68 ±0.25)	60.4 % (4.75 ±1.38)
	Grape pip	26.1 % (8.9 ±0.28)	0 % (-0.71 ±0.28)	100 % (9.61 ±0.56)	0 % (0 ±0.36)	0 % (0 ±0.92)
	Grape skin	24.1 % (8.02 ±0.42)	0 % (-0.12 ±0.42)	100 % (8.14 ±0.84)	70.2 % (5.63 ±0.09)	31.4 % (2.52 ±0.93)
	Pine wood	23.9 % (7.9 ±0.32)	0 % (-2.35 ±0.32)	100 % (10.25 ±0.64)	0 % (0 ±0.76)	0 % (0 ±1.4)
	Rubber tyre	32.5 % (12.12 ±0.29)	78.6 % (9.53 ±0.29)	21.4 % (2.59 ±0.58)	53.2 % (6.45 ±0.3)	-31.8 % (-3.86 ±0.88)
	Sugarcane pith	28.5 % (10.03 ±0.19)	24.2 % (2.43 ±0.19)	75.8 % (7.61 ±0.38)	39.6 % (3.97 ±0.33)	36.3 % (3.64 ±0.71)

Establishing the mechanism of N retention in biochar amended soils is complex. This is largely because biochars differ based on what they are produced from and how they are produced. The observations made in this study make for a classic example of this complexity. Only the pine wood and sugarcane pith chars significantly reduced fertiliser leaching compared to the control or other biochar treatments. The exact mechanism for retention are unknown, but could include immobilisation as both chars showed strong net N immobilisation (Table 5.4) during the 14 day incubation, but also the pine wood biochar showed strongest steady-state N immobilisation rate (Figure 5.20). Nitrogen retention by immobilisation has also been reported in other studies (Case et al 2012; Bruun et al 2012). Nitrogen retention by adsorption as investigated in Chapter 4 does not explain the observed behaviour, as neither pine wood nor sugarcane piths showed highest affinity for ammonium or nitrate adsorption (Table 4.1) compared to the other chars. Only the rubber tyre char significantly reduced the amount of fertiliser ^{15}N retained in the soil and showed the greatest amount of mineral N leaching compared to the other treatments (Table 6.4). This was highly likely since the rubber tyre char contained the most soil-biochar derived mineral N (12.12 mg) relative to the other treatments (Table 6.4), and demonstrated strongest initial net N mineralisation (Table 5.4)). Although not explicitly observed in this study, reduced NH_4^+ leaching and increased retention by biochar has also been observed in recent studies (Lehmann et al 2003; Mia et al 2017). A sandy soil (with 8% clay) treated with Eucalyptus biochar (pyrolysed at 550°C) increased the total ^{15}N recovery by an average of 12%, while the biochar effect with a higher (29%) clay content was not observed (Mia et al 2017). Other possible reported mechanisms of N retention involve lower gaseous or erosion N losses with biochar. Güereña et al (2013) reported a 39% recovery of applied $^{15}NH_4{}^{15}NO_3$ (10% enriched) in loam soil after maize stover biochar additions after one cropping season. The reason for the high recovered N was suggested to be due to N cycling through the soil microbial biomass and the retention of organic N.

6.5 Conclusions

Biochar properties affect inorganic N leaching and availability differently. In the current study, the soils amended with the plant-derived biochars significantly reduced the leaching of ammonium-N (between 15% and 26%) compared to the control (no biochar). However, the rubber tyre biochar did not reduce the leaching of NH_4^+-N. Instead, rubber tyre char, which contained the highest amount of inherent total inorganic N, leached significantly more NH_4^+-N compared to the other treatments. In addition, because rubber tyre char suppressed CO_2 respiration the most, this resulted in an upsurge in N mineralisation greater than the other biochars. Redox reactions were also suggested to play a role in the N dynamics in the soil-biochar systems created. Nitrate reduction reactions may have been responsible for the excess ammonium recovered, where biochar was the reductant, donating electrons; while nitrate accepted electrons as the oxidant. Nitrate leaching, relative to the control, was reduced in all the biochar

treatments (between 11% and 54%) except sugarcane pith. The possible reasons for the excess nitrate leached from the sugarcane pith biochar are its low fixed C content (15.60%) causing the reduction of nitrate to not have taken place completely (or at all) or its low C/N ratio (38.01) resulting in mineralisation of the sugarcane pith's degradable fractions. Overall, rubber tyre and sugarcane pith chars were not suitable for reducing leaching. Instead, pine wood biochar was found to be the better choice for reducing leaching losses of inorganic N in an acidic, sandy soil because it significantly had the least cumulative leaching losses of both ammonium and nitrate.

Determining the stable ^{15}N isotope amounts proved to be a unique opportunity to better understand N-cycling of biochars. A statistically significant amount of between 0.77% and 10.81% total inorganic ^{15}N fertiliser of what was initially applied remained in the soil-biochar treatments after leaching. In fact, the improvement of N fertiliser remaining in the sugarcane pith and pine wood biochars was effectively 136-157% the retention of fertiliser compared to the control. But, there was no significant improvement in remaining N after leaching in the soils amended with maize stover, grape pip and rubber tyre biochars. Although the mineral N remaining from the ^{15}N fertiliser was calculated to between 0.77% and 10.81% for the rubber tyre and sugarcane pith chars, respectively; the highest mineral N remaining from the total mineral N was found to be from the pine wood (38.6%) followed by the maize stover (36.2%) biochar treatments. The reason for this was that the remaining fertiliser N was estimated (Equation 6.3) after leaching and may have further been immobilised or lost via gaseous losses.

At the end of the leaching study, there was some 2 M KCl exchangeable fertiliser N and N from the soil-biochar fraction in all the treatments except grape pip and rubber tyre chars. There was no nitrogen remaining even after leaching and after 2 M KCl extraction (residual N) in the rubber tyre char. However, the remainder of the treatments had residual N which was likely immobilised. Overall, it was apparent that the fate of inherent and applied inorganic N in biochar amended soil is dependent on the biochar type and that the N can be adsorbed, mineralised, immobilised or even denitrified.

Chapter 7
General Discussion, Conclusions and Recommendations

7.1 Introduction

It was previously demonstrated that biochars can reduce N availability in soils. The main objective of this study was to characterise physical and chemical properties of six different biochars and use the findings to investigate how the biochar properties are responsible for affecting mineral N sorption and desorption, soil C and N mineralisation to ultimately understand how biochars reduce inorganic N fertiliser leaching from a sandy soil. To achieve this, a thorough laboratory analysis of the six readily-available commercially-produced biochars (maize stover, grape pip, grape skin, pine wood, rubber tyre and sugarcane pith) and acidic, sandy soil-biochar mixtures was performed. Laboratory experiments focusing on sorption and desorption, mineralisation and leaching were also carried out. The following sections summarise the findings of the research project and recommendations for future studies is given.

7.2 Characterisation of various biochar feedstocks

The six studied biochars showed a high variation in properties linked to precursor and production temperature, where the biochar produced from rubber (motor) tyres was dramatically different from plant-derived biochars.

Among the plant-derived biochars studied, the pine wood biochar appeared to have the most favourable properties for use in crop production, whereas the sugarcane pith biochar was the least favourite. This is because the sugarcane pith biochar had a very low total C content (27.9%) compared to pine wood (80.3%). The sugarcane pith char also showed characteristics of having lower stability (H/C = 0.74) and high chemical reactivity (O/C = 0.10) compared to all the other chars. Nonetheless, a benefit of using the sugarcane pith char in soil would be its high ash content (65.99%) which would act as a nutrient source.

A common consequence of biochar application to soil is a liming effect, which is controlled by the biochar ash content, basic cations content and biochar pH. The plant-derived (maize stover, grape pip, grape skin, pine wood and sugarcane pith) biochars used in this study were alkaline and had a pH(H_2O) reading between 8.0 and 10.7. However, the rubber tyre biochar was acidic (pH(H_2O) = 2.4) as a result of high content of acidic functional groups and low basic cation content.

7.3 Sorption – desorption behaviour of biochars

The biochars demonstrated a much higher effect on nitrate removal (>80%) compared to ammonium (<40%). However, the biochars showed no nitrate desorption (<0.3%), but ammonium desorption was found to be between 53% and 60%. It shows that approximately half of adsorbed ammonium was retained in exchangeable positions, while nitrate was immobilised in chemical and possible biochemical reactions associated with the biochar surface and its inhabitants. It was also found that the biochar properties responsible for controlling mineral nitrogen sorption reactions were cation exchange capacity and the aromaticity of the biochars which enhance nitrate reduction. The main mechanism responsible for ammonium adsorption was physisorption. It is recommended that nutrient sorption characteristics be studied prior to biochar application to soil. Redox reactions (possibly bio-assisted) were thought to have been involved in nitrate removal. This was further confirmed by the leaching study implemented here, but would require a dedicated study of mechanisms in future research.

7.4 Carbon and nitrogen mineralisation

The observation of carbon and nitrogen mineralisation in a 14-day incubation study has shown that the peak CO_2 evolution occurred within the first 2 days of incubation and can be described fairly well by a vapor pressure model, where the “a” parameter was strongly related to biochar composition and physico-chemical characteristics. The addition of biochar significantly increased soil respiration showing that the biochars added are in part biodegradable. However, respiration was reduced calculated per initial carbon content. This may be strongly related to immobilisation of nitrogen observed in the same experiment, which resulted in relative reduction of respiration. The N mineralisation/immobilisation system resembled damped oscillations, where the direction of the process (predominance of mineralisation or immobilisation) changes over time. The mineralisation process was not possible to model with the given observation frequency in differential terms. However, the moving net mineralisation rate was modelled successfully and showed a similar function to respiration rate.

The results from this research unit showed that the biochar properties that influence carbon and nitrogen mineralisation are fixed carbon and the concentration of cobalt, particularly when assessed against the vapor pressure model of C mineralisation. The maize stover and sugarcane pith biochars had the lowest fixed carbon contents (0% and 15.60%, respectively) and as a result suppressed the relative carbon dioxide respiration the least compared to the other biochars. The rubber tyre char suppressed the release of carbon dioxide the most compared to the plant-derived biochars. Thus, it was recommended that rubber tyre biochar may be used as a short-term soil carbon sink for CO_2 while also serving as a source of energy for soil microorganisms. The results from this study also demonstrated that the mechanism

for temporary N retention was net nitrogen immobilisation for all the plant-derived biochars except grape skin biochar.

7.5 Leaching study

Amendment of the sandy soil with plant-derived biochars at a rate of 2.5% (w/w) reduced the cumulative leaching of ammonium-N between 15% and 26% compared to the control. However, 24% more ammonium-N leached from the rubber tyre biochar compared to the control soils, probably due to its inherent high N content. More noticeable was the reduction of cumulative nitrate leaching in the range 11% to 54%, except in the sugarcane pith biochar where 23% more nitrate was leached. The excess ammonium-N leached could be due to mineralisation of inherent soil organic matter in the sandy soil. The excess nitrate-N leached could potentially be due to a low fixed C content which would inhibit nitrate reduction or a low C/N causing mineralisation. Thus rubber tyre and sugarcane pith biochars were not recommended for reducing leaching of NH_4^+ and NO_3^- in sandy soil, respectively. Instead, pine wood biochar was the most favourable char for the most reduction of cumulative ammonium and nitrate leaching. The pine wood and sugarcane pith biochars significantly enhanced ammonium nitrate fertiliser N retention by 136 and 157% respectively, compared to the control. The isotope analysis also showed that an estimated 0.7% to 8.9% fertiliser nitrogen was 2 M KCl exchangeable, and thus bioavailable, even after leaching.

7.6 Concluding remarks

The findings from this study suggest that the main goal of this study which was to determine the effects of different, locally-produced and easily available biochars on the nitrogen dynamics when applied to an acidic, sandy soil was met. One of the major findings from this research was being able to quantify the amount of inorganic N fertiliser remaining in the soil-biochar system even after leaching by using stable isotopes. The plant-derived biochars significantly reduced mineral N (ammonium-N plus nitrate-N) leaching. More so, 7.5-38.6% total mineral nitrogen remained in biochar-soil-fertiliser even after leaching. The leaching study also suggested that N availability is also reduced by denitrification, leading to gaseous losses into the atmosphere.

The grape pip, grape skin and pine wood biochars had the highest affinity for ammonium adsorption compared to the other chars and demonstrated that the mechanism for ammonium adsorption was cation exchange. The biochar property correlated with this observation was a net negative surface charge seen by negative delta pH values. The sorption study also demonstrated that 81.8-89.3% nitrate was adsorbed by all six biochars investigated in this study. Although to a lesser extent, the biochars had an adsorption ability for ammonium between 33.1% and 38.6%. In addition, the biochars demonstrated the fact that

ammonium adsorption was partially reversible (53.1-60.3%) compared to nitrate which was not desorbable (0.02-0.27%. The biochar properties with a correlation with this behaviour were the sodium concentration (which was statistically significant), where an increasing content was favoured; and volatile matter content, where a low content was favoured.

The C and N mineralisation study revealed that respiration from biochar-amended soil is primarily controlled by the biochar fixed carbon content. It was shown that the sugarcane pith biochar, which had a low fixed carbon content, had highest respiration rate. The results also showed that while some biochars, like rubber tyre char, significantly increased N mineralisation, there was a strong, steady rate of N immobilisation for all the biochar treatments, which further contributed to reducing the availability of N in biochars. There was no particular biochar property that correlated with N immobilisation, however, the inherent (initial) inorganic N content on the soil-biochar system suggested to have played a role.

This research has improved the understanding of why and how biochar reduces inorganic N availability through physical adsorption and immobilisation. This means that caution should be taken when an acidic sandy soil, fertilised with ammonium-N and nitrate-N, is amended with biochar because it may become temporarily unavailable. Also, although the grape pip, grape skin and pine wood biochars had a high ammonium-N capturing ability and could be used as a slow-release fertiliser, that is only possible if the NH_4^+-N is exchangeable.

7.7 Recommendations

Recommendations for further studies include:

- Investigating nitrate reduction and oxidation reactions, especially with regards to inorganic N adsorption and leaching.
- Quantifying the dynamics of reduction in N availability due to biochar application on soils which should be considered prior to biochar application in agricultural soils.
- To use the findings from this research as a contribution to establishing quality norms and standards for commercially-produced pyrolysis products in South Africa.

References

Abdulrazzaq H, Jol H, Husni A, Abu-Bakr R (2014) Characterization and stabilisation of biochars obtained from empty fruit bunch, wood and rice husk. Bioresources 9:2888–2898.

Addiscott TM (1996) Fertilizers and Nitrate Leaching. Issues Environ Sci Technol 5:1–26.

Ahmad M, Rajapaksha AU, Lim JE, et al (2014) Biochar as a sorbent for contaminant management in soil and water: a review. Chemosphere 99:19–33. doi: 10.1016/j.chemosphere.2013.10.071

Alburquerque JA, Calero JM, Barrón V, et al (2014) Effects of biochars produced from different feedstocks on soil properties and sunflower growth. J Plant Nutr Soil Sci 177:16–25. doi: 10.1002/jpln.201200652

Alef K (1995) Soil respiration. In: Alef K, Nannipieri P (eds) Methods Appl. soil Microbiol. Biochem. Academic Press, New York, pp 214–216

Amonette JE, Joseph S (2009) Characteristics of biochar: Microchemical properties. In: Lehmann J, Joseph S (eds) Biochar Environ. Manag. Sci. Technol. Earthscan, United Kingdom, pp 33–52

Anbar AD, Romaniello SJ, Allenby BR, Broecker WS (2016) Addressing the Anthropocene. Environ Chem 13:777–783. doi: 10.1071/en15115

Angin D (2013) Effect of pyrolysis temperature and heating rate on biochar obtained from pyrolysis of safflower seed press cake. Bioresour Technol 128:593–597. doi: 10.1016/j.biortech.2012.10.150

Angst TE, Six J, Reay DS, Sohi SP (2014) Impact of pine chip biochar on trace greenhouse gas emissions and soil nutrient dynamics in an annual ryegrass system in California. Agric Ecosyst Environ 191:17–26. doi: 10.1016/j.agee.2014.03.009

Artiola JF, Rasmussen C, Freitas R (2012) Effects of a biochar-amended alkaline soil on the growth of Romaine Lettuce and Bermudagrass. Soil Sci 177:561–570. doi: 10.1097/SS.0b013e31826ba908

ASTM standard 1762-84 (2007) Standard test method for chemical analysis of wood charcoal. American Society for Testing Materials (ASTM) International: Conshohocken, PA.

Baldock JA, Smernik RJ (2002) Chemical composition and bioavailability of thermally altered Pinus resinosa (Red pine) wood. Org Geochem 33:1093–1109. doi: 10.1016/S0146-6380(02)00062-1

Boateng AA (2007) Characterization and thermal conversion of charcoal derived from fluidized-bed

fast pyrolysis oil production of switchgrass. Ind Eng Chem Res 46:8857–8862.

Boehm HP (1994) Some aspects of the surface chemistry of carbon blacks and other carbons. Carbon N Y 32:759–769. doi: 10.1016/0008-6223(94)90031-0

Brady N, Weil R (2002) The Nature and Properties of Soils, 13th edn. Pearson Prentice Hall Upper Saddle River, New Jersey

Bridgwater A V., Meier D, Radlein D (1999) An overview of fast pyrolysis biomass. Org Geochem 30:1479–1493.

Bronick CJ, Lal R (2005) Soil structure and management: a review. Geoderma 124:3–22.

Brown R (2009) Biochar production technology. In: Lehmann J, Joseph S (eds) Biochar Environ. Manag. Sci. Technol. Earthscan, United Kingdom, London, pp 127–146

Brown RA, Kercher AK, Nguyen TH, et al (2006) Production and characterization of synthetic wood chars for use as surrogates for natural sorbents. Org Geochem 37:321–333.

Bruun EW, Ambus P, Egsgaard H, Hauggaard-Nielsen H (2012) Effects of slow and fast pyrolysis biochar on soil C and N turnover dynamics. Soil Biol Biochem 46:73–79. doi: 10.1016/j.soilbio.2011.11.019

Bruun EW, Hauggaard-Nielsen H, Ibrahim N, et al (2011) Influence of fast pyrolysis temperature on biochar labile fraction and short-term carbon loss in a loamy soil. Biomass and Bioenergy 35:1182–1189. doi: 10.1016/j.biombioe.2010.12.008

Butnan S, Deenik JL, Toomsan B, et al (2015) Biochar characteristics and application rates affecting corn growth and properties of soils contrasting in texture and mineralogy. Geoderma 237–238:105–116. doi: 10.1016/j.geoderma.2014.08.010

Cai A, Xu H, Shao X, et al (2016) Carbon and nitrogen mineralization in relation to soil particle-size fractions after 32 years of chemical and manure application in a continuous maize cropping system. PLoS One 11:1–14.

Cameron KC, Di HJ, Moir JL (2013) Nitrogen losses from the soil/plant system: A review. Ann Appl Biol 162:145–173. doi: 10.1111/aab.12014

Carrier M, Hardie AG, Uras Ü, et al (2012) Production of char from vacuum pyrolysis of South-African sugar cane bagasse and its characterization as activated carbon and biochar. J Anal Appl Pyrolysis

96:24–32. doi: 10.1016/j.jaap.2012.02.016

Case SDC, McNamara NP, Reay DS, Whitaker J (2012) The effect of biochar addition on N2O and CO2 emissions from a sandy loam soil - The role of soil aeration. Soil Biol Biochem 51:125–134. doi: 10.1016/j.soilbio.2012.03.017

Castaldi S, Riondino M, Baronti S, et al (2011) Impact of biochar application to a Mediterranean wheat crop on soil microbial activity and greenhouse gas fluxes. Chemosphere 85:1461–1471. doi: 10.1016/j.chemosphere.2011.08.031

Chan KYA, B LVZ, Meszaros IA, et al (2007) Agronomic values of greenwaste biochar as a soil amendment. 629–634.

Chan KY, Xu Z (2009) Biochar: nutrient properties and their enhancement. In: Lehmann J, Joseph S (eds) Biochar Environ. Manag. Sci. Technol. Earthscan, United Kingdom, pp 67–84

Chen B, Zhou D, Zhu L (2008) Transitional Adsorption and Partition of Nonpolar and Polar Aromatic Contaminants by Biochars of Pine Needles with Different Pyrolytic Temperatures. Environ Sci Technol 42:5137–5143. doi: 10.1021/es8002684

Cheng C-H, Lehmann J, Thies JE, Burton SD (2008a) Stability of black carbon in soils across a climatic gradient. J Geophys Res 113:1–10. doi: 10.1029/2007JG000642

Cheng CH, Lehmann J (2009) Ageing of black carbon along a temperature gradient. Chemosphere 75:1021–1027. doi: 10.1016/j.chemosphere.2009.01.045

Cheng CH, Lehmann J, Engelhard MH (2008b) Natural oxidation of black carbon in soils: Changes in molecular form and surface charge along a climosequence. Geochim Cosmochim Acta 72:1598–1610. doi: 10.1016/j.gca.2008.01.010

Cheng CH, Lehmann J, Thies JE, et al (2006) Oxidation of black carbon by biotic and abiotic processes. Org Geochem 37:1477–1488. doi: 10.1016/j.orggeochem.2006.06.022

Chintala R, Schumacher TE, Kumar S, et al (2014) Molecular characterization of biochars and their influence on microbiological properties of soil. J Hazard Mater 279:244–56. doi: 10.1016/j.jhazmat.2014.06.074

Choppala GK, Bolan NS, Megharaj M, et al (2012) The influence of biochar and black carbon on reduction and bioavailability of chromate in soils. J Environ Qual 41:1175–84. doi:

10.2134/jeq2011.0145

Clough TJ, Condron LM (2010) Biochar and the Nitrogen Cycle: Introduction. J Environ Qual 39:1218. doi: 10.2134/jeq2010.0204

Clough TJ, Condron LM, Kammann C, Müller C (2013) A review of biochar and soil nitrogen dynamics. Agron J 3:275–293. doi: 10.3390/agronomy3020275

Conte P, Hanke UM, Marsala V, et al (2014) Mechanisms of water interaction with pore systems of hydrochar and pyrochar from poplar forestry waste. J Agric Food Chem 62:4917–4923. doi: 10.1021/jf5010034

Conz RF, Abbruzzini TF, de Andrade CA, et al (2017) Effect of pyrolysis temperature and feedstock type on agricultural properties and stability of biochars. Agric Sci 8:914–933. doi: https://doi.org/10.4236/as.2017.89067

Czimczik CI, Masiello CA (2007) Controls on black carbon storage in soils. Global Biogeochem. Cycles 21:

Czimczik CI, Preston CM, Schmidt MWI, et al (2002) Effects of charring on mass, organic carbon, and stable carbon isotope composition of wood. Org Geochem 33:1207–1223.

Das O, Sarmah AK (2015) The love-hate relationship of pyrolysis biochar and water: A perspective. Sci Total Environ. doi: 10.1016/j.scitotenv.2015.01.061

Deenik JL, McClellan T, Uehara G, et al (2010) Charcoal Volatile Matter Content Influences Plant Growth and Soil Nitrogen Transformations. Soil Sci Soc Am J 74:1259. doi: 10.2136/sssaj2009.0115

DeLuca TH, MacKenzie MD, Gundale MJ, Holben WE (2006) Wildfire-produced charcoal directly influences nitrogen cycling in Ponderosa pine forests. Soil Sci 70:448–453. doi: 10.2136/sssaj2005.0096

Dempster DN, Gleeson DB, Solaiman ZM, et al (2012a) Decreased soil microbial biomass and nitrogen mineralisation with Eucalyptus biochar addition to a coarse textured soil. Plant Soil 354:311–324. doi: 10.1007/s11104-011-1067-5

Dempster DN, Jones DL, Murphy D V. (2012b) Clay and biochar amendments decreased inorganic but not dissolved organic nitrogen leaching in soil. Soil Res 50:216–221. doi: 10.1071/SR11316

Ding Y, Liu YX, Wu WX, et al (2010) Evaluation of biochar effects on nitrogen retention and leaching in multi-layered soil columns. Water Air Soil Pollut 213:47–55. doi: 10.1007/s11270-010-0366-4

Ding Y, Liu Y, Liu S, et al (2016) Biochar to improve soil fertility. A review. Agron for Sustain Dev 36:36. doi: 10.1007/s13593-016-0372-z

Donefer E (1986) Sugarcane pith (Sugar-fith) as animal feed. Rome, Italy

Downie A, Crosky A, Munroe P (2009) Physical Properties of Biochar. In: Lehmann J, Joseph S (eds) Biochar Environ. Manag. Sci. Technol. Earthscan, United Kingdom, pp 13–32

du Plessis J (2013) Maize production. Pretoria, South Africa

EBC (2012) European Biochar Certificate - Guidelines for a Sustainable Production of Biochar. doi: 10.13140/RG.2.1.4658.7043

El-Naggar AH, Usman ARA, Al-Omran A, et al (2015) Carbon mineralization and nutrient availability in calcareous sandy soils amended with woody waste biochar. Chemosphere 138:67–73. doi: 10.1016/j.chemosphere.2015.05.052

Enders A, Hanley K, Whitman T, et al (2012) Characterization of biochars to evaluate recalcitrance and agronomic performance. Bioresour Technol 114:644–53. doi: 10.1016/j.biortech.2012.03.022

Essington ME (2004) Soil and Water Chemistry: An intergrative approach. CRC Press, Boca Raton, Florida

Fernandez-Stark K, Bamber P, Gereffi G (2016) Peru in the Table Grape Global Value Chain: Opportunities for upgrading.

Fidel RB (2012) Evaluation and implementation of methods for quantifying organic and inorganic compounds of biochar alkalinity. Iowa State University

Fidel RB, Laird DA, Thompson ML (2013) Evaluation of Modified Boehm Titration Methods for Use with Biochars. J Environ Qual 42:1771–1778. doi: 10.2134/jeq2013.07.0285

Flematti GR, Ghisalberti EL, Dixon KW, Trengrove RD (2004) A compound from smoke that promotes seed germination. Science (80-) 305:977.

Fu P, Yi W, Bai X, et al (2011) Effect of temperature on gas composition and char structural features

of pyrolyzed agricultural residues. Bioresour Technol 102:8211–8219. doi: 10.1016/j.biortech.2011.05.083

Gai X, Wang H, Liu J, et al (2014) Effects of feedstock and pyrolysis temperature on biochar adsorption of ammonium and nitrate. PLoS One 9:1–19. doi: 10.1371/journal.pone.0113888

Gaskin JW, Speir A, Morris LM, et al (2007) Potential for pyrolysis char to affect soil moisture and nutrient status of a loamy sand soil. Proc. 2007 Georg. Water Resour. Conf. held March 27-29, 2007, Univ. Georg. pp 1–3

Gaskin JW, Speir RA, Harris K, et al (2010) Effect of peanut hull and pine chip biochar on soil nutrients, corn nutrient status, and yield. Agron J 102:623–633. doi: 10.2134/agronj2009.0083

Gaskin JW, Steiner C, Harris K, et al (2008) Effect of low-temperature pyrolysis conditions on biochar for agricultural use. Trans Asabe 51:2061–2069.

Gaunt J, Cowie A (2009) Biochar, greenhouse gas accounting and emissions trading. In: Lehmann J, Joseph S (eds) Biochar Environ. Manag. Sci. Technol., 1st edn. Earthscan, United Kingdom, London, pp 317–340

Girard P, Blin J, Bridgwater A V., Meier D (2006) An assessment of bio-oil toxicity for safe handling and transportation: Toxicological and ecotoxicological tests. In: Bridgwater A V., Boocook DGB (eds) Sci. Therm. Chem. Biomass Convers. Conversion CPL Press, Newbury, United Kingdom, p 27

Glaser B (2007) Prehistorically modified soils of central Amazonia: a model for sustainable agriculture in the twenty-first century. Philos Trans R Soc Lond B Biol Sci 362:187–196. doi: 10.1098/rstb.2006.1978

Glaser B, Birk JJ (2012) State of the scientific knowledge on properties and genesis of Anthropogenic Dark Earths in Central Amazonia (terra preta de Índio). Geochim Cosmochim Acta 82:39–51. doi: 10.1016/j.gca.2010.11.029

Glaser B, Haumaier L, Guggenberger G, Zech W (2001) The “Terra Preta” phenomenon: A model for sustainable agriculture in the humid tropics. Naturwissenschaften 88:37–41. doi: 10.1007/s001140000193

Glaser B, Lehmann J, Zech W (2002) Ameliorating physical and chemical properties of highly weathered soils in the tropics with charcoal - A review. Biol Fertil Soils 35:219–230. doi:

10.1007/s00374-002-0466-4

Glaser B, Woods WI (2004) Amazonian dark earths: explorations in space and time. Springer, Berlin

Gruber N, Galloway JN (2008) An earth-system perspective of the global nitrogen cycle. Nature 451:293–296. doi: 10.1038/nature06592

Güereña D, Lehmann J, Hanley K, et al (2013) Nitrogen dynamics following field application of biochar in a temperate North American maize-based production system. Plant Soil. doi: 10.1007/s11104-012-1383-4

Guo Y, Bustin RM (1998) FTIR spectroscopy and reflectance of modern charcoals and fungal decayed woods: implications for studies of inertinite coals. Int J Coal Geol 29–53.

Hale SE, Alling V, Martinsen V, et al (2013) The sorption and desorption of phosphate-P, ammonium-N and nitrate-N in cacao shell and corn cob biochars. Chemosphere 91:1612–1619. doi: 10.1016/j.chemosphere.2012.12.057

Hamer U, Marschner B, Brodowski S, Amelung W (2004) Interactive priming of black carbon and glucose mineralisation. Org Geochem 35:823–830. doi: 10.1016/j.orggeochem.2004.03.003

Hammes K, Schmidt MWI (2009) Changes of biochar in soil. In: Lehmann J, Joseph S (eds) Biochar Environ. Manag. Sci. Technol., 1st edn. Earthscan, United Kingdom, London, pp 169–178

Hanselman TA, Graetz DA, Obreza TA (2004) A comparison of in situ methods for measuring net nitrogen mineralization rates of organic soil amendments. J Environ Qual 33:1098–1105.

Hansen V, Müller-Stöver D, Ahrenfeldt J, et al (2014) Gasification biochar as a valuable by-product for carbon sequestration and soil amendment. Biomass and Bioenergy. doi: 10.1016/j.biombioe.2014.10.013

Harris PJF (2005) New perspectives on the structure of graphitic carbons. Crit Rev Solid State Mater Sci 30:235–253.

Havlin JL, Beaton JD, Tisdale SL, Nelson WL (2014) Soil Fertility and Fertilizers: An Introducton to Nutrient Management, 8th edn. Pearson Prentice Hall Upper Saddle River, New Jersey

Hedges JI, Eglinton G, Hatcher PG, et al (2000) The molecularly uncharacterized component of nonliving organic matter in natural environments. Org Geochem 31:945–958.

Herselman JE, Steyn CE (2001) Predicted concentration of trace elements in South African soils. Report no. GW/A/2001/14. Pretoria, South Africa

Hofrichter M, Ziegenhagen D, Sorge S, et al (1999) Degradation of lignite (low-rank-coal) by lignolytic basidiomycetes and their peroxidase system. Appl Microbiol Biotechnol 52:78–84.

Hollister CC, Bisogni JJ, Lehmann J (2013) Ammonium, Nitrate, and Phosphate Sorption to and Solute Leaching from Biochars Prepared from Corn Stover (Zea mays L.) and Oak Wood (Quercus spp.). J Environ Qual 42:137. doi: 10.2134/jeq2012.0033

Hoornweg D, Bhada-Tata P (2012) What a waste: A global review of solid waste management. Urban Development Series Knowledge Papers

IBI (2015) Standardized Product Definition and Product Testing Guidelines for Biochar That Is Used in Soil -Version 2.1.

Jiang J, Xu R, Jiang T, Li Z (2012) Immobilization of Cu(II), Pb(II) and Cd(II) by the addition of rice straw derived biochar to a simulated polluted Ultisol. J Hazard Mater 229–230:145–150.

Jindo K, Mizumoto H, Sawada Y, et al (2014) Physical and chemical characterization of biochars derived from different agricultural residues. Biogeosciences 11:6613–6621.

Johnston CT, Aochi YO (1996) Fourier Transform Infrared and Raman Spectroscopy. In: Sparks DL (ed) Methods soil Anal. Part 3 Chem. methods. Soil Science Society of America, Madison, WI, pp 269–322

Jones DL, Rousk J, Edwards-Jones G, et al (2012) Biochar-mediated changes in soil quality and plant growth in a three year field trial. Soil Biol Biochem 45:113–124. doi: 10.1016/j.soilbio.2011.10.012

Joseph S, Husson O, Graber ER, et al (2015) The Electrochemical Properties of Biochars and How They Affect Soil Redox Properties and Processes. Agron J 5:322–340. doi: 10.3390/agronomy5030322

Joseph S, Peacocke C, Lehmann J, Munroe P (2009) Developing a biochar classification and test methods. In: Lehmann J, Joseph S (eds) Biochar Environ. Manag. Sci. Technol. Earthscan, United Kingdom, London, pp 107–126

Kameyama K, Miyamoto T, Iwata Y, Shiono T (2016) Influences of feedtock and pyrolysis temperature

on the nitrate adsorption of biochar. Soil Sci Plant Nutr 62:180–184. doi: 10.1080/00380768.2015.1136553

Kameyama K, Miyamoto T, Shiono T, Shinogi Y (2012) Influence of Sugarcane Bagasse-derived Biochar Application on Nitrate Leaching in Calcaric Dark Red Soil. J Environ Qual 41:1131–1137. doi: 10.2134/jeq2010.0453

Kammann CI, Schmidt H-P, Messerschmidt N, et al (2015) Plant growth improvement mediated by nitrate capture in co-composted biochar. Sci Rep 5:1–12. doi: 10.1038/srep11080

Keiluweit M, Nico PS, Johnson MG, Kleber M (2010) Dynamic molecular structure of plant biomass-derived black carbon (biochar). Environ Sci Technol 44:1247–1253. doi: 10.1021/es9031419

Kercher AK, Nagle DC (2003) Microstructural evolution during charcoal carbonization by x-ray diffraction analysis. Carbon N Y 41:15–27.

Khan S, Reid BJ, Li G, Zhu Y-G (2014) Application of biochar to soil reduces cancer risk via rice consumption: a case study in Miaoqian village, Longyan, China. Environ Int 68:154–61. doi: 10.1016/j.envint.2014.03.017

Klüpfel L, Keiluweit M, Kleber M, Sander M (2014) Redox properties of plant biomass-derived black carbon (biochar). Environ Sci Technol 48:5601–5611. doi: 10.1021/es500906d

Knowles OA, Robinson BH, Contangelo A, Clucas L (2011) Biochar for the mitigation of nitrate leaching from soil amended with biosolids. Sci Total Environ 409:3206–3210. doi: 10.1016/j.scitotenv.2011.05.011

Krull ES, Baldock JA, Skemstad JO et al (2009) Characteristics of biochar: Organo-chemical properties. In Biochar for environmental management: Science and Technology. Eds. J Lehmann and S Joseph 53-65 Earthscan.

Kuzyakov Y, Friedel J., Stahr K (2000) Review of mechanisms and quantification of priming effects. Soil Biol Biochem 32:1485–1498. doi: 10.1016/S0038-0717(00)00084-5

Kuzyakov Y, Subbotina I, Chen H, et al (2009) Black carbon decomposition and incorporation into soil microbial biomass estimated by 14C labeling. Soil Biol Biochem 41:210–219. doi: 10.1016/j.soilbio.2008.10.016

Laborda F, Redondo MF, Luna N, Monistrol IF (1995) Characterization of liquefaction/solubilization

mechanisms of Spanish coals by newly isolated microorganisms. Coal Sci Technol 24:1387–1390.

Lægreid M, Bøckman OC, Kaarstad O (1999) Agriculture, Fertilizers and the Environment. CABI Publishing, Oslo, Norway

Laird DA (2008) The charcoal vision: A win-win-win scenario for simultaneously producing bioenergy, permanently sequestering carbon, while improving soil and water quality. Agron J 100:178–181. doi: 10.2134/agronj2007.0161

Laird DA, Brown RC, Amonette JE, Lehmann J (2009) Review of the pyrolysis platform for coproducing bio-oil and biochar. Biofuels, Bioprod Biorefining 3:547–562. doi: 10.1002/bbb.169

Laird DA, Fleming P, Davis DD, et al (2010a) Impact of biochar amendments on the quality of a typical Midwestern agricultural soil. Geoderma 158:443–449. doi: 10.1016/j.geoderma.2010.05.013

Laird DA, Fleming P, Wang B, et al (2010b) Impact of biochar amendments on the quality of a typical Midwestern agricultural soil. Geoderma 158:436–442. doi: 10.1016/j.geoderma.2010.05.012

Laird DA, Rogovska NP, Garcia-Perez M, et al (2010c) Pyrolysis and Biochar - Opportunities for distributed production and soil quality enhancement. In: Braun R, Karlen D, Johnson D (eds) Sustain. Altern. Fuel Feed. Oppor. Challenges Roadmaps Six U.S. Reg. Proc. Sustain. Feed. Adv. Biofuels Work. pp 257–281

Laird D, Fleming P, Wang B, et al (2010d) Biochar impact on nutrient leaching from a Midwestern agricultural soil. Geoderma 158:436–442.

Lee JW, Kidder M, Evans BR, et al (2010) Characterization of biochars produced from cornstovers for soil amendment. Environ Sci Technol 44:7970–7974. doi: 10.1021/es101337x

Lee Y, Eum P-R-B, Ryu C, et al (2013) Characteristics of biochar produced from slow pyrolysis of Geodae-Uksae 1. Bioresour Technol 30:345–350.

Lehmann J, da Silva Jr JP, Rondon M, et al (2002) Slash- and -char- A feasible alternative for soil fertility management in the central Amazon? 17th World Congr. Soil Sci. Bangkok, Thailand, pp 1–12

Lehmann J, Gaunt J, Rondon M (2006) Bio-char sequestration in terrestrial ecosystems - A review. Mitig Adapt Strateg Glob Chang 11:403–427. doi: 10.1007/s11027-005-9006-5

Lehmann J, Joseph S (2009) Biochar for envinronmental management: an introduction. In: Lehmann J,

Joseph S (eds) Biochar Environ. Manag. Sci. Technol., 1st edn. Earthscan, United Kingdom, London, pp 1–12

Lehmann J, Pereira J, Steiner C, et al (2003) Nutrient availability and leaching in an archaeological Anthrosol and a Ferralsol of the Central Amazon basin : fertilizer , manure and charcoal amendments. 343–357.

Lehmann J, Rillig MC, Thies J, et al (2011) Biochar effects on soil biota – A review. Soil Biol Biochem 43:1812–1836. doi: 10.1016/j.soilbio.2011.04.022

Li H, Dong X, da Silva EB, et al (2017) Mechanisms of metal sorption by biochars: Biochar characteristics and modifications. Chemosphere 178:466–478. doi: 10.1016/jchemosphere.2017.03.072

Liang B, Lehmann J, Solomon D, et al (2006) Black Carbon Increases Cation Exchange Capacity in Soils. Soil Sci Soc Am J 70:1719. doi: 10.2136/sssaj2005.0383

Liang B, Lehmann J, Solomon D, et al (2008) Stability of biomass-derived black carbon in soils. Geochim Cosmochim Acta 72:6069–6078. doi: 10.1016/j.gca.2008.09.028

Liu Z, Chen X, Jing Y, et al (2014) Effects of biochar amendment on rapeseed and sweet potato yields and water stable aggregate in upland red soil. CATENA 123:45–51. doi: 10.1016/j.catena.2014.07.005

Lua AC, Yang T, Guo J (2004) Effects of pyrolysis conditions on the properties of activated carbons prepared from pistachio-nut shells. J. Anal. Appl. Pyrolysis 72:

Lusiba S, Odhiambo J, Ogola J (2016) Effect of biochar and phosphorus fertilizer application on soil fertility: soil physical and chemical properties. Arch Agron Soil Sci 1–14. doi: 10.1080/03650340.2016.1218477

Major J, Lehmann J, Rondon M, Goodale C (2010) Fate of soil-applied black carbon: downward migration, leaching and soil respiration. Glob Chang Biol 16:1366–1379. doi: 10.1111/j.1365-2486.2009.02044.x

Major J, Steiner C, Downie A, Lehmann J (2009) Biochar effects on nutrient leaching. In: Lehmann J, Joseph S (eds) Biochar Environ. Manag. Sci. Technol. Earthscan, United Kingdom, London, pp 271–287

Manyà JJ (2012) Pyrolysis for biochar purposes: A review to establish current knowledge gaps and research needs. Environ Sci Technol 46:7939–7954.

Masiello CA (2004) New directions in black carbon organic geochemistry. Mar Chem 92:201–213.

Mathews JA (2008) Carbon negative biofuels. Energy Policy 36:940–945. doi: 10.1016/j.enpol.2007.11.029

Mbagwu JSC (1989) Effects of organic amendments on some physical properties of a tropical Ultisol. Biol Wastes 28:1–13.

McBride MB (1994a) Soil Acidity. Environ. Chem. Soils. Oxford University Press, New York, pp 169–206

McBride MB (1994b) Environmental Chemistry of Soils. Oxford University Press, New York

Mia S, Singh B, Dijkstra FA (2017) Aged biochar affects gross nitrogen mineralization and recovery: a 15N study in two contrasting soils. Glob Chang Biol Bioenergy 9:1196–1206. doi: 10.1111/gcbb.12430

Mizuta K (2004) Removal of nitrate-nitrogen from drinking water using bamboo powder charcoal. 95:255–257. doi: 10.1016/j.biortech.2004.02.015

Mohan D, Pittman Jr. CU, Steele, Philip H (2006) Pyrolysis of wood/biomass for bio-oil: a critical review. Energy & Fuels 20:848–889.

Mohan D, Sarswat A, Ok YS, Pittman CU (2014) Organic and inorganic contaminants removal from water with biochar, a renewable, low cost and sustainable adsorbent--a critical review. Bioresour Technol 160:191–202. doi: 10.1016/j.biortech.2014.01.120

Mohd-Aizat A, Mohamad-Roslan MK, Sulaiman WNA et al (2014) The relationship between soil pH and selected soil properties in 48 years logged-over forest. International Journal of Environmental Sciences 4 (6): 1129-1140.

Mukherjee A, Zimmerman AR (2013) Organic carbon and nutrient release from a range of laboratory-produced biochars and biochar–soil mixtures. Geoderma 193–194:122–130. doi: 10.1016/j.geoderma.2012.10.002

Mukherjee A, Zimmerman AR, Harris W (2011) Surface chemistry variations among a series of laboratory-produced biochars. Geoderma 163:247–255. doi: 10.1016/j.geoderma.2011.04.021

Mukome FND, Zhang X, Silva LCR, et al (2013) Use of chemical and physical characteristics to investigate trends in biochar feedstocks. J Agric Food Chem 61:2196–2204. doi: 10.1021/jf3049142

Mulvaney RL (1996) Nitrogen - Inorganic Forms. Methods soil Anal. Part 3 Chem. methods. Madison, WI, pp 1123–1187

Nelson DW, Sommers LE (1996) Total carbon, organic carbon, and organic matter. In: Sparks DL (ed) Methods soil Anal. Part 3 Chem. methods. ASA and SSSA, Madison, WI, pp 961–1010

Neves EG, Peterson JB, Bartone RN, da Silva CA (2003) Historical and socio-cultural origins of Amazonian Dark Earths. In: Lehmann J, Kern DC, Glaser B, Woods WI (eds) Amaz. Dark Earths Orig. Prop. Manag. Kluwer Academic Publishers, Netherlands, pp 29–49

Non-affiliated Soil Analysis Work Committee (1990) Handbook of standard soil testing methods for advisory purposes. Pretoria, South Africa

Novak JM, Busscher WJ, Laird DL, et al (2009) Impact of Biochar Amendment on Fertility of a Southeastern Coastal Plain Soil. Soil Sci 174:105–112.

Oh SY, Cha DK, Chiu PC (2004) Reduction of nitroglycerin with cast iron: Pathway, kinetics, and mechanisms. Environ Sci Technol 38:3723–3730.

Oh SY, Chiu PC (2009) Graphite- and soot-mediated reduction of 2,4-dinitrotoluene and hexahydro-1,3,5-trinitro-1,3,5-triazine. Environ Sci Technol 43:6983–6988.

Oh SY, Son JG, Lim OT, Chiu PC (2012) The role of black carbon as a catalyst for environmental redox transformation. Environ Geochem Heal 34:105–113. doi: 10.1007/s10653-011-9414-0

OIV (2015) Global economic vitiviniculture data. Organ Int la Bigne du Vin 1–5.

Paris O, Zollfrank C, Zickler GA (2005) Decomposition and carbonisation of wood biopolymers - a microstructural study of softwood pyrolysis. Carbon N Y 43:53–66.

Pietikäinen J, Kiikkilä O, Fritze H, et al (2000) Charcoal as a habitat for microbes and its effect on the microbial community of the underlying humus. Oikos 89:231–242. doi: 10.1034/j.1600-0706.2000.890203.x

Pituello C, Francioso O, Simonetti G, et al (2014) Characterization of chemical–physical, structural and morphological properties of biochars from biowastes produced at different temperatures. J Soils

Sediments. doi: 10.1007/s11368-014-0964-7

Podgorski DC, Hamdan R, McKenna AM, et al (2012) Characterization of pyrogenic black carbon by desorption atmospheric pressure photoionization fourier transform ion cyclotron resonance mass spectrometry. Anal Chem 84:1281–1287. doi: 10.1021/ac202166x

Powlson DS, Whitmore AP, Goulding KWT (2011) Soil carbon sequestration to mitigate climate change: a critical re-examination to identify the true and the false. Eur J Soil Sci 62:42–55. doi: 10.1111/j.1365-2389.2010.01342.x

Prayogo C, Jones JE, Baeyens J, Bending GD (2014) Impact of biochar on mineralisation of C and N from soil and willow litter and its relationship with microbial community biomass and structure. Biol Fertil Soils 50:695–702. doi: 10.1007/s00374-013-0884-5

Puga AP, Abreu CA, Melo LCA, Beesley L (2015) Biochar application to a contaminated soil reduces the availability and plant uptake of zinc, lead and cadmium. J Environ Manage 159:86–93. doi: 10.1016/j.jenvman.2015.05.036

Rafatullah M, Sulaiman O, Hashim R, Ahmad A (2010) Adsorption of methylene blue on low-cost adsorbents: a review. J Hazard Mater 177:70–80.

REDISA (2011) REDISA integrated industry waste tyre management plan. In: Submitt. terms Regul. 9 Waste Tyre Regul. Publ. Gov. Gaz. No. 31901 13 Febr. 2009. http://www.redisa.org.za. Accessed 8 Dec 2016

Reichstein M, Rey A, Freibauer A, et al (2003) Modeling temporal and large-scale spatial variability of soil respiration from soil water availability, temperature and vegetation productivity indices. Global Biogeochem. Cycles 17:

Rowell DL (1994) Soil science: methods & applications. Longman Scientific & Technical, Longman Group UK Ltd, Essex, UK

Roy C, Chaala A, Darmstadt H (1999) The vacuum pyrolysis of used tires: End-uses for oil and carbon black products. J Anal Appl Pyrolysis 51:201–221. doi: 10.1016/s0165-2370(99)00017-0

Roy C, Labrecque B, de Caumia B (1990) Recycling of scrap tires to soil and carbon black by vacuum pyrolysis. Resour Conserv Recycl 4:203–213.

SANS 13395 (1996) Water quality: Determination of nitrite and nitrate nitrogen and the sum of both

by flow analysis and spectrometric detection.

Sarma NS (2004) Etymology as an aid to understanding chemistry concepts. J Chem Educ 81:1437–1439.

SASA (2017) South African Sugar Association. http://www.sasa.org.za/HomePage1.aspx. Accessed 17 Jan 2017

Schimmelpfennig S, Glaser B (2012) One step forward toward characterization: Some important material properties to distinguish biochars. J. Environ. Qual. 41:

Sevilla M, Fuertes AB (2009) The production of carbon materials by hydrothermal carbonization of cellulose. Carbon N Y 47:2281–2289. doi: 10.1016/j.carbon.2009.04.026

Shah J, Rasul Jan M, Mabood F, Shahid M (2006) Conversion of Waste Tyres into Carbon Black and their Utilization as Adsorbent. J Chinese Chem Soc 53:1085–1089.

Shaheen SM, Rinklebe J (2017) Sugar beet factory lime affects the mobilization of Cd, Co, Cr, Cu, Mo, Ni, Pb, and Zn under dynamic redox conditions in a contaminated floodplain soil. J Environ Manage 186:253–260.

Shenbagavalli S, Mahimairaja S (2012) Characterization and effect of biochar on nitrogen and carbon dynamics in soil. Intern J Adv Biol Res 2:249–255.

Sika MP (2012) Effect of biochar on chemistry, nutrient uptake and fertilizer mobility in sandy soil. Stellenbosch

Sika MP, Hardie AG (2014) Effect of pine wood biochar on ammonium nitrate leaching and availability in a South African sandy soil. Eur J Soil Sci 65:113–119. doi: 10.1111/ejss.12082

Silverstein RM, Bassler GC, Morrill TC (1991) Spectrometric identification of organic compounds, 5th editio. Wiley, New York

Singh B, Singh BP, Cowie AL (2010) Characterisation and evaluation of biochars for their application as a soil amendment. Aust. J. Soil Res. pp 516–525

Sjöström E (1993) Wood Chemistry: Fundamentals and Applications, 2nd edn. Academic Press, San Diego, United States

Smernik RJ, Baldock J a. (2005) Does Solid-state 15N NMR Spectroscopy Detect all Soil Organic

Nitrogen? Biogeochemistry 75:507–528. doi: 10.1007/s10533-005-2857-8

Smith JL, Collins HP, Bailey VL (2010) The effect of young biochar on soil respiration. Soil Biol Biochem 42:2345–2347. doi: 10.1016/j.soilbio.2010.09.013

Soares OSGP, Órfão JJM, Pereira MFR (2008) Activated Carbon Supported Metal Catalysts for Nitrate and Nitrite Reduction in Water. Catal Letters 126:253–260.

Sohi SPP, Krull E, Lopez-Capel E, Bol R (2010) A review of biochar and its use and function in soil. Adv Agron 105:47–82. doi: 10.1016/S0065-2113(10)05002-9

Sollins P, Homann P, Caldwell BA (1996) Stabilization and destabilization of soil organic matter: mechanisms and controls. Geoderma 74:65–105.

Song W, Guo M (2012) Quality variations of poultry litter biochar generated at different pyrolysis temperatures. J Anal Appl Pyrolysis 94:138–145. doi: 10.1016/jaap.2011.11.018

Spokas KA (2010) Review of the stability of biochar in soils : predictability of O : C molar ratios. 1:289–303.

Spokas KA, Cantrell KB, Novak JM, et al (2012) Biochar: A synthesis of its agronomic impact beyond carbon sequestration. J Environ Qual 41:973–989. doi: 10.2134/jeq2011.0069

Srinivasan P, Sarmah AK, Smernik R, et al (2015) A feasibility study of agricultural and sewage biomass as biochar, bioenergy and biocomposite feedstock: Production, characterization and potential applications. Sci Total Environ 512–513C:495–505. doi: 10.1016/j.scitotenv.2015.01.068

Steiner C, Das KC, Garcia M, et al (2008a) Charcoal and smoke extract stimulate the soil microbial community in a highly weathered xanthic Ferralsol. Pedobiologia (Jena) 51:359–366.

Steiner C, Glaser B, Teixeira WG, et al (2008b) Nitrogen retention and plant uptake on a highly weathered central Amazonian Ferralsol amended with compost and charcoal. J Plant Nutr Soil Sci 171:893–899. doi: 10.1002/jpln.200625199

Stevenson FJ, Cole MA (1999) Cycles of soil: Carbon, Nitrogen, Phosphorus, Sulfur, Micronutrients, 2nd edn. John Wiley & Sons, New York

Streubel JD, Pierce FJ (2011) Biochar: Its characterization and utility for recovering phosphorus from anaerobic digested dairy effluent. ProQuest Diss Theses Doctor of:159.

Tammeorg P, Simojoki A, Mäkelä P, et al (2014) Short-term effects of biochar on soil properties and wheat yield formation with meat bone meal and inorganic fertiliser on a boreal loamy sand. Agric Ecosyst Environ 191:108–116. doi: 10.1016/j.agee.2014.01.007

Thies JE, Rillig MC (2009) Characteristics of biochar: Biological properties. In: Lehmann, J, and Joseph S (ed) Biochar Environ. Manag. Sci. Technol. Earthscan, United Kingdom, pp 85–105

Todman LC, Fraser FC, Corstanie R, et al (2016) Defining and quantifying the resilience of responses to disturbance: a conceptual and modelling approach from soil science. Sci. Rep. 6:

Tsechansky L, Graber ER (2014) Methodological limitations to determining acidic groups at biochar surfaces via the Boehm titration. Carbon N Y 66:730–733.

Umeugochukwu OP (2016) Mitigation of soil and ground water pollution caused by on-land disposal of olive mill wastewater. Stellenbosch, South Africa

United Nations (2015) World Population Prospects: The 2015 Revision Key findings and advance tables. New York

Uras-Postma Ü, Carrier M, Knoetze J (Hansie) (2014) Vacuum pyrolysis of agricultural wastes and adsorptive criteria description of biochars governed by the presence of oxides. J Anal Appl Pyrolysis 107:123–132. doi: 10.1016/j.jaap.2014.02.012

Uras Ü, Carrier M, Hardie AG, Knoetze JH (2012) Physico-chemical characterization of biochars from vacuum pyrolysis of South African agricultural wastes for application as soil amendments. J Anal Appl Pyrolysis 98:207–213. doi: 10.1016/j.jaap.2012.08.007

Uzoma KC, Inoue M, Andry H, et al (2011) Influence of biochar application on sandy soil hydraulic properties and nutrient retention. J Food, Agric Environ 9:1137–1143.

Vaccari FP, Baronti S, Lugato E, et al (2011) Biochar as a strategy to sequester carbon and increase yield in durum wheat. Eur J Agron 34:231–238. doi: 10.1016/j.eja.2011.01.006

Van Zwieten L, Kimber S, Downie A, et al (2010a) A glasshouse study on the interaction of low mineral ash biochar with nitrogen in a sandy soil. Aust. J. Soil Res. pp 569–576

Van Zwieten L, Kimber S, Morris S, et al (2010b) Effects of biochar from slow pyrolysis of papermill waste on agronomic performance and soil fertility. Plant Soil 327:235–246. doi: 10.1007/s11104-009-0050-x

Vetere A (1991) The Riedel Equation. Ind Eng Chem Res 30:168–173.

Wang B, Lehmann J, Hanley K, et al (2015a) Adsorption and desorption of ammonium by maple wood biochar as a function of oxidation and pH. Chemosphere 138:120–126. doi: 10.1016/j.chemosphere.2015.05.062

Wang WJ, Chalk PM, Chen D, Smith CJ (2001) Nitrogen mineralisation, immobilisation and loss, and their role in determining differences in net nitrogen production during waterlogged and aerobic incubation of soils. Soil Biol Biochem 33:1305–1315.

Wang Z, Guo H, Shen F, et al (2015b) Biochar produced from oak sawdust by Lanthanum (La)-involved pyrolysis for adsorption of ammonium (NH4(+)), nitrate (NO3(-)), and phosphate (PO4(3-)). Chemosphere 119:646–53. doi: 10.1016/j.chemosphere.2014.07.084

White RE (1997) Principle and practice of soil science: The soil as a natural resource. Blackwell science, Oxford, UK

WHO (2006) World Health Organization Guidelines for drinking-water quality: First addendum to third edition. Volume 1, Recommendations.

Williams PT (2013) Pyrolysis of waste tyres: A review. Waste Manag 33:1714–1728.

Wirawan R, Sapuan SM, Robiah Y, Khalina A (2010) Flexural properties of sugarcane bagasse pith and rind reinforced poly(vinyl chloride). IOP Conf Ser Mater Sci Eng. doi: 10.1088/1757-899X/11/1/012011

Woods WI, McCann JM (1999) The Anthropogenic Origin and Persistence of Amazonian Dark Earths. Yearb Conf Lat Am Geogr 25:7–14. doi: 10.2307/25765871

Wu W, Yang M, Feng Q, et al (2012) Chemical characterization of rice straw-derived biochar for soil amendment. Biomass and Bioenergy 47:268–276. doi: 10.1016/j.biombioe.2012.09.034

Yan L, Chen S, Xia J, Luo Y (2014) Precipitation regime shift enhanced the rain pulse effect on soil respiration in a semi-arid steppe. PLoS One 9:

Yang H, Yan R, Chen H, et al (2007) Characteristics of hemicellulose, cellulose and lignin pyrolysis. Fuel 86:1781–1788.

Yang HI, Lou K, Rajapaksha AU, et al (2017) Adsorption of ammonium in aqueous solutions by pine sawdust and wheat straw biochars. Environ. Sci. Pollut. Res.

Yao Y, Gao B, Zhang M, et al (2012) Effect of biochar amendment on sorption and leaching of nitrate, ammonium, and phosphate in a sandy soil. Chemosphere 89:1467–1471. doi: 10.1016/j.chemosphere.2012.06.002

Yoshinaga Y, Akita T, Mikami I, Okuhara T (2002) Hydrogenation of nitrate in water to nitrogen over Pd-Cu supported on active carbon. J Catal 207:37–45. doi: 10.1006/jcat.2002.3529

Yuan JH, Xu RK, Wang N, Li JY (2011) Amendment of Acid Soils with Crop Residues and Biochars. Pedosph An Int J 21:302–308. doi: 10.1016/S1002-0160(11)60130-6

Yuan Y, Yuan T, Wang D, et al (2013) Sewage sludge biochar as an efficient catalyst for oxygen reduction reaction in an microbial fuel cell. Bioresour Technol 144:115–20. doi: 10.1016/j.biortech.2013.06.075

Yuan Y, Bolan N, Prévoteau A, Vithanage M, Biswas JK, Ok YS, Wang H, et al (2017) Applications of biochar in redox-mediated reactions. Bioresour Technol 246:271-281. doi:10.1016/j.biortech.2017.06.154

Yuste JC, Baldocchi DD, Gershenson A, et al (2007) Microbial soil respiration and its dependency on carbon inputs, soil temperature and moisture. Glob Chang Biol 13:2018–2035. doi: 10.1111/j.1365-2486.2007.01415.x

Yuste JC, Janssens IA, Carrara A, et al (2003) Interactive effects of temperature and precipitation on soil respiration in a temperate maritime pine forest. Tree Physiol 23:1263–1270.

Zavalloni C, Alberti G, Biasiol S, et al (2011) Microbial mineralization of biochar and wheat straw mixture in soil: A short-term study. Appl Soil Ecol 50:45–51. doi: 10.1016/j.apsoil.2011.07.012

Zhang H, Voroney R P, Price GW (2015) Effects of temperature and processing conditions on biochar chemical properties and their influence on soil C and N transformations. Soil Biol Biochem. 83:19-28. doi:10.1016/j.soilbio.2015.01.006

Zhang H, Voroney R P., Price GW (2017) Effects of temperature and activation on biochar chemical properties and their impact on ammonium, nitrate, and phosphate sorption. J Environ Qual. doi: 10.2134/jeq2017.02.0043

Zhang T, Walawender WP, Fan LT, et al (2004) Prepartion of activated carbon from forest and agricultural residues through CO2 activation. Chem Eng J 105:53–59.

Zhao B, Nartey OD (2014) Characterization and evaluation of biochars derived from agricultural waste biomass from Gansu, China. 2014 World Congr. Adv. Civil, Environ. Mater. Res. (ACEM14), August 24-28, 2014

Zhao X, Yan X, Wang S, et al (2013) Effects of the additon of rice-straw-based biochar on leaching and retention of fertilizer N in highly fertilized cropland soils. Soil Sci Plant Nutr 59:771–782. doi: 10.1080/00380768.2013.830229

Zheng H, Wang Z, Deng X, et al (2013a) Characteristics and nutrient values of biochars produced from giant reed at different temperatures. Bioresour Technol 130:463–471. doi: 10.1016/j.biortech.2012.12.044

Zheng H, Wang Z, Deng X, et al (2013b) Impacts of adding biochar on nitrogen retention and bioavailability in agricultural soil. Geoderma 206:32–39. doi: 10.1016/j.geoderma.2013.04.018

Zhou Y, Berruti F, Greenhalf C, et al (2017) Increased retention of soil nitrogen over winter by biochar application: Implications of biochar pyrolysis temperature for plant nitrogen availability. Agric Ecosyst Environ 236:61–68. doi: 10.1016/j.agee.2016.11.011

Appendix A

Table A. 1: Results of Pearson's statistical test (r-value and p-value) from the correlation coefficients associated with various physico-chemical properties of the six biochars.

Ion sorbed	Biochar properties	Pearson's r-value	p-value	Ion sorbed	Biochar properties	Pearson's r-value	p-value
Ammonium	%C	0.212	0.687	Nitrate	%C	0.383	0.454
	%N	0.136	0.798		%N	0.296	0.568
	%H	0.573	0.234		%H	0.166	0.754
	%S	0.496	0.316		%S	0.491	0.322
	%O	0.338	0.513		%O	0.093	0.862
	%Ash	0.182	0.731		%Ash	0.363	0.479
	C/N	0.158	0.764		C/N	0.180	0.733
	H/C	0.482	0.333		H/C	0.454	0.365
	O/C	0.555	0.253		O/C	0.138	0.795
	%P	0.483	0.331		%P	0.314	0.545
	%Ca	0.073	0.890		% Ca	0.496	0.317
	%Mg	0.353	0.492		% Mg	0.410	0.419
	%K	0.444	0.378		%K	0.042	0.937
	Fe (mg kg^{-1})	0.314	0.545		Fe (mg kg^{-1})	0.272	0.602
	Mn (mg kg^{-1})	0.238	0.650		Mn (mg kg^{-1})	0.538	0.271
	Cu (mg kg^{-1})	0.358	0.486		Cu (mg kg^{-1})	0.253	0.629
	Zn (mg kg^{-1})	0.576	0.231		Zn (mg kg^{-1})	0.839	0.037
	Co (mg kg^{-1})	0.640	0.171		Co (mg kg^{-1})	0.374	0.465
	B (mg kg^{-1})	0.662	0.152		B (mg kg^{-1})	0.110	0.836
	Mo (mg kg^{-1})	0.665	0.149		Mo (mg kg^{-1})	0.319	0.537
	Na (mg kg^{-1})	0.833	0.039		Na (mg kg^{-1})	0.231	0.660
	Si (mg kg^{-1})	0.292	0.574		Si (mg kg^{-1})	0.167	0.752
	Al (mg kg^{-1})	0.144	0.785		Al (mg kg^{-1})	0.396	0.438
	Se (mg kg^{-1})	0.046	0.932		Se (mg kg^{-1})	0.558	0.249
	Ba (mg kg^{-1})	0.248	0.635		Ba (mg kg^{-1})	0.184	0.728
	Sr (mg kg^{-1})	0.357	0.488		Sr (mg kg^{-1})	0.164	0.757
	Cr (mg kg^{-1})	0.715	0.110		Cr (mg kg^{-1})	0.450	0.370
	As (mg kg^{-1})	0.687	0.132		As (mg kg^{-1})	0.592	0.216
	Ni (mg kg^{-1})	0.607	0.202		Ni (mg kg^{-1})	0.186	0.724
	Pb (mg kg^{-1})	0.333	0.519		Pb (mg kg^{-1})	0.273	0.600
	Cd (mg kg^{-1})	0.266	0.611		Cd (mg kg^{-1})	0.350	0.497
	Sb (mg kg^{-1})	0.457	0.362		Sb (mg kg^{-1})	0.470	0.347
	Hg (mg kg^{-1})	0.496	0.317		Hg (mg kg^{-1})	0.439	0.383
	%Volatiles	0.683	0.134		%Volatiles	0.036	0.946
	%Fixed C	0.495	0.318		%Fixed C	0.233	0.657
	pH (H_2O)	0.546	0.263		pH (H_2O)	0.657	0.157
	pH (KCl)	0.516	0.294		pH (KCl)	0.646	0.166
	Surface acidity	0.667	0.148		Surface acidity	0.624	0.185
	Surface alkalinity	0.332	0.520		Surface alkalinity	0.625	0.184
	BET	0.175	0.740		BET	0.149	0.778

Table A. 2: Correlations coefficients associated with various physico-chemical properties of the plant-derived biochars (excluding rubber tyre char).

Ion sorbed	Biochar properties	K_p	R^2	Ion sorbed	Biochar properties	K_p	R^2
Ammonium	%C	0.001	0.268	Nitrate	%C	0.000	0.034
	%N	0.014	0.038		%N	0.022	0.077
	%H	0.030	0.358		%H	0.033	0.323
	%S	0.025	0.778		%S	0.013	0.167
	%O	0.002	0.099		%O	0.000	0.003
	%Ash	0.001	0.245		%Ash	0.000	0.013
	C/N	0.000	0.000		C/N	0.000	0.018
	H/C	0.089	0.495		H/C	0.087	0.372
	O/C	0.368	0.551		O/C	0.056	0.010
	%P	0.029	0.060		%P	0.053	0.158
	%Ca	0.030	0.438		% Ca	0.005	0.011
	%Mg	0.060	0.669		% Mg	0.005	0.003
	%K	0.005	0.065		%K	0.015	0.574
	Fe (mg kg^{-1})	0.000	0.158		Fe (mg kg^{-1})	0.000	0.229
	Mn (mg kg^{-1})	0.000	0.260		Mn (mg kg^{-1})	0.000	0.329
	Cu (mg kg^{-1})	0.000	0.036		Cu (mg kg^{-1})	0.000	0.023
	Total Zn (mg kg^{-1})	0.000	0.228		Total Zn (mg kg^{-1})	0.001	0.447
	EDTA Zn (mg kg^{-1})	0.000	0.044		EDTA Zn (mg kg^{-1})	0.000	0.119
	Co (mg kg^{-1})	0.003	0.190		Co (mg kg^{-1})	0.003	0.231
	B (mg kg^{-1})	0.001	0.381		B (mg kg^{-1})	0.001	0.595
	Mo (mg kg^{-1})	0.020	0.416		Mo (mg kg^{-1})	0.006	0.032
	Na (mg kg^{-1})	0.000	0.564		Na (mg kg^{-1})	0.000	0.447
	Si (mg kg^{-1})	0.000	0.007		Si (mg kg^{-1})	0.000	0.143
	Al (mg kg^{-1})	0.000	0.124		Al (mg kg^{-1})	0.000	0.135
	Se (mg kg^{-1})	0.005	0.044		Se (mg kg^{-1})	0.021	0.531
	Ba (mg kg^{-1})	0.000	0.062		Ba (mg kg^{-1})	0.001	0.232
	Sr (mg kg^{-1})	0.000	0.008		Sr (mg kg^{-1})	0.001	0.417
	Cr (mg kg^{-1})	0.000	0.293		Cr (mg kg^{-1})	0.000	0.247
	As (mg kg^{-1})	0.008	0.314		As (mg kg^{-1})	0.005	0.113
	Ni (mg kg^{-1})	0.000	0.252		Ni (mg kg^{-1})	0.000	0.112
	Pb (mg kg^{-1})	0.001	0.151		Pb (mg kg^{-1})	0.001	0.313
	Cd (mg kg^{-1})	0.032	0.141		Cd (mg kg^{-1})	0.052	0.296
	Sb (mg kg^{-1})	1.288	0.643		Sb (mg kg^{-1})	0.751	0.171
	Hg (mg kg^{-1})	0.445	0.733		Hg (mg kg^{-1})	0.202	0.118
	%Volatiles	0.001	0.616		%Volatiles	0.000	0.001
	%Fixed C	0.001	0.580		%Fixed C	0.000	0.009
	pH (H_2O)	0.003	0.013		pH (H_2O)	0.014	0.270
	pH (KCl)	0.001	0.002		pH (KCl)	0.012	0.233
	Surface acidity	0.037	0.203		Surface acidity	0.056	0.365
	Surface alkalinity	0.031	0.087		Surface alkalinity	0.037	0.095
	BET	0.000	0.006		BET	0.000	0.002

Table A. 3: Results of Pearson's statistical test (r-value and p-value) from the correlation coefficients associated with various physico-chemical properties of the plant-derived biochars (excluding rubber tyre char).

Ion sorbed	Biochar properties	Pearson's r-value	p-value	Ion sorbed	Biochar properties	Pearson's r-value	p-value
Ammonium	%C	0.518	0.371	Nitrate	%C	0.185	0.766
	%N	0.195	0.753		%N	-0.278	0.651
	%H	-0.598	0.287		%H	-0.569	0.317
	%S	0.882	0.048		%S	0.409	0.494
	%O	-0.315	0.605		%O	-0.055	0.930
	%Ash	-0.495	0.397		%Ash	-0.116	0.853
	C/N	-0.004	0.995		C/N	0.134	0.830
	H/C	-0.704	0.185		H/C	-0.610	0.275
	O/C	-0.742	0.151		O/C	-0.100	0.873
	%P	0.244	0.692		%P	0.397	0.508
	%Ca	-0.662	0.224		% Ca	0.106	0.865
	%Mg	-0.818	0.091		% Mg	-0.055	0.930
	%K	0.255	0.679		%K	0.758	0.138
	Fe (mg kg^{-1})	-0.398	0.507		Fe (mg kg^{-1})	-0.478	0.415
	Mn (mg kg^{-1})	-0.510	0.380		Mn (mg kg^{-1})	-0.574	0.312
	Cu (mg kg^{-1})	0.189	0.761		Cu (mg kg^{-1})	0.151	0.809
	Total Zn (mg kg^{-1})	-0.478	0.416		Total Zn (mg kg^{-1})	-0.669	0.217
	EDTA Zn (mg kg^{-1})	-0.210	0.735		EDTA Zn (mg kg^{-})	-0.345	0.569
	Co (mg kg^{-1})	-0.436	0.463		Co (mg kg^{-1})	0.481	0.413
	B (mg kg^{-1})	0.617	0.267		B (mg kg^{-1})	0.771	0.127
	Mo (mg kg^{-1})	-0.645	0.240		Mo (mg kg^{-1})	0.179	0.773
	Na (mg kg^{-1})	0.751	0.144		Na (mg kg^{-1})	0.668	0.218
	Si (mg kg^{-1})	-0.086	0.891		Si (mg kg^{-1})	-0.378	0.530
	Al (mg kg^{-1})	-0.352	0.562		Al (mg kg^{-1})	-0.367	0.544
	Se (mg kg^{-1})	-0.210	0.735		Se (mg kg^{-1})	-0.729	0.162
	Ba (mg kg^{-1})	0.248	0.687		Ba (mg kg^{-1})	0.481	0.412
	Sr (mg kg^{-1})	0.089	0.887		Sr (mg kg^{-1})	0.646	0.239
	Cr (mg kg^{-1})	-0.541	0.347		Cr (mg kg^{-1})	-0.497	0.394
	As (mg kg^{-1})	0.560	0.326		As (mg kg^{-1})	-0.337	0.579
	Ni (mg kg^{-1})	-0.502	0.389		Ni (mg kg^{-1})	-0.335	0.582
	Pb (mg kg^{-1})	-0.388	0.519		Pb (mg kg^{-1})	-0.559	0.327
	Cd (mg kg^{-1})	-0.376	0.533		Cd (mg kg^{-1})	-0.544	0.343
	Sb (mg kg^{-1})	-0.802	0.103		Sb (mg kg^{-1})	-0.414	0.489
	Hg (mg kg^{-1})	-0.856	0.064		Hg (mg kg^{-1})	-0.343	0.572
	%Volatiles	-0.785	0.116		%Volatiles	-0.031	0.961
	%Fixed C	0.762	0.135		%Fixed C	0.094	0.880
	pH (H_2O)	0.113	0.857		pH (H_2O)	0.519	0.370
	pH (KCl)	0.049	0.938		pH (KCl)	0.483	0.410
	Surface acidity	-0.450	0.447		Surface acidity	-0.604	0.281
	Surface alkalinity	0.296	0.629		Surface alkalinity	-0.309	0.613
	BET	0.076	0.904		BET	0.048	0.939

Appendix B

Table B. 1: Correlation coefficients of the CO_2 respiration vapor pressure model associated with various physico-chemical properties of the biochars.

Biochar properties	All six biochars		Plant-derived biochars	
	Gradient	R^2	Gradient	R^2
%C	-0.010	0.309	-0.016	0.918
%N	0.326	0.165	0.139	0.033
%H	0.065	0.010	0.011	0.000
%S	-0.130	0.143	-0.222	0.532
%O	0.033	0.188	-0.040	0.39
%Ash	0.008	0.271	0.012	0.866
C/N	-0.002	0.447	-0.001	0.408
H/C	0.914	0.316	1.095	0.64
O/C	0.886	0.019	-0.529	0.01
%P	0.019	0.000	0.619	0.234
%Ca	-0.027	0.003	0.225	0.207
%Mg	0.128	0.022	0.431	0.293
%K	-0.083	0.16	-0.038	0.038
Fe (mg kg^{-1})	0.000	0.599	0.000	0.906
Mn (mg kg^{-1})	0.001	0.34	0.001	0.891
Cu	0.004	0.114	0.008	0.515
Total Zn	0.000	0.349	0.007	0.853
EDTA Zn	0.000	0.342	0.000	0.058
Co	0.055	0.923	0.060	0.903
B	-0.004	0.118	0.002	0.045
Mo	0.224	0.319	0.178	0.270
Na	0.000	0.096	0.000	0.001
Si	0.003	0.772	0.003	0.740
Al	0.000	0.396	0.000	0.009
Se	0.133	0.165	0.182	0.428
Ba	-0.008	0.161	-0.007	0.188
Sr	-0.007	0.402	-0.005	0.233
Cr	0.002	0.922	0.002	0.953
As	-0.075	0.221	-0.039	0.065
Ni	0.009	0.929	0.008	0.946
Pb	0.019	0.594	0.019	0.838
Cd	0.787	0.502	0.841	0.829
Sb	9.922	0.248	14.821	0.727
Hg	2.736	0.181	4.302	0.585
%Volatiles	0.003	0.020	0.002	0.017
%Fixed C	-0.004	0.192	-0.006	0.477
pH(H_2O)	-0.081	0.353	-0.067	0.064
pH(KCl)	-0.105	0.646	-0.105	0.646
Surface acidity	0.402	0.713	0.822	0.865
Surface alkalinity	0.145	0.036	0.694	0.365
BET surface area	-0.001	0.201	-0.001	0.176

Appendix C

Current study *designed* to simulate Swartland winter rainfall patterns of heavy rainfall events of 60 mm (Agricultural Research Council, Agromet – Institute for Soil, Climate and Water).

Since, 1mm rainfall = 1L water per m^2

Then, 60L rainfall per m^2 X surface area of a circle = amount rainfall

Surface area of leaching column (cylinder) used:

With radius of 3.5cm

Area of a circle is:

$A = pi\ r^2$

$A = (3.14159)*(3.5cm)^2$

Then	38.48451001	cm^2
Therefore,	0.003848451	m^2
And amount rainfall on this surface area is:	0.23	L
	231	**mL**

Appendix D

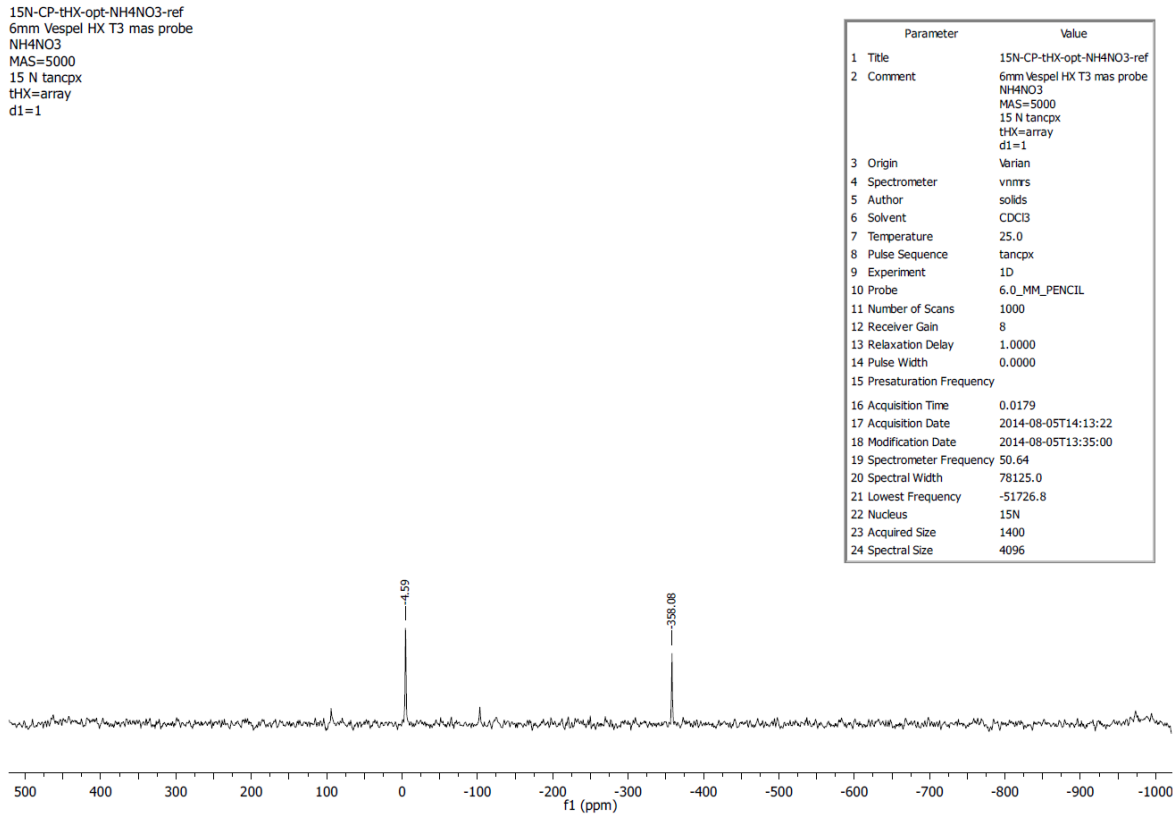

Figure D. 1:Solid state NMR spectrum of enriched $^{15}NH_4{}^{15}NO_3$ sample used as a background for analysis.

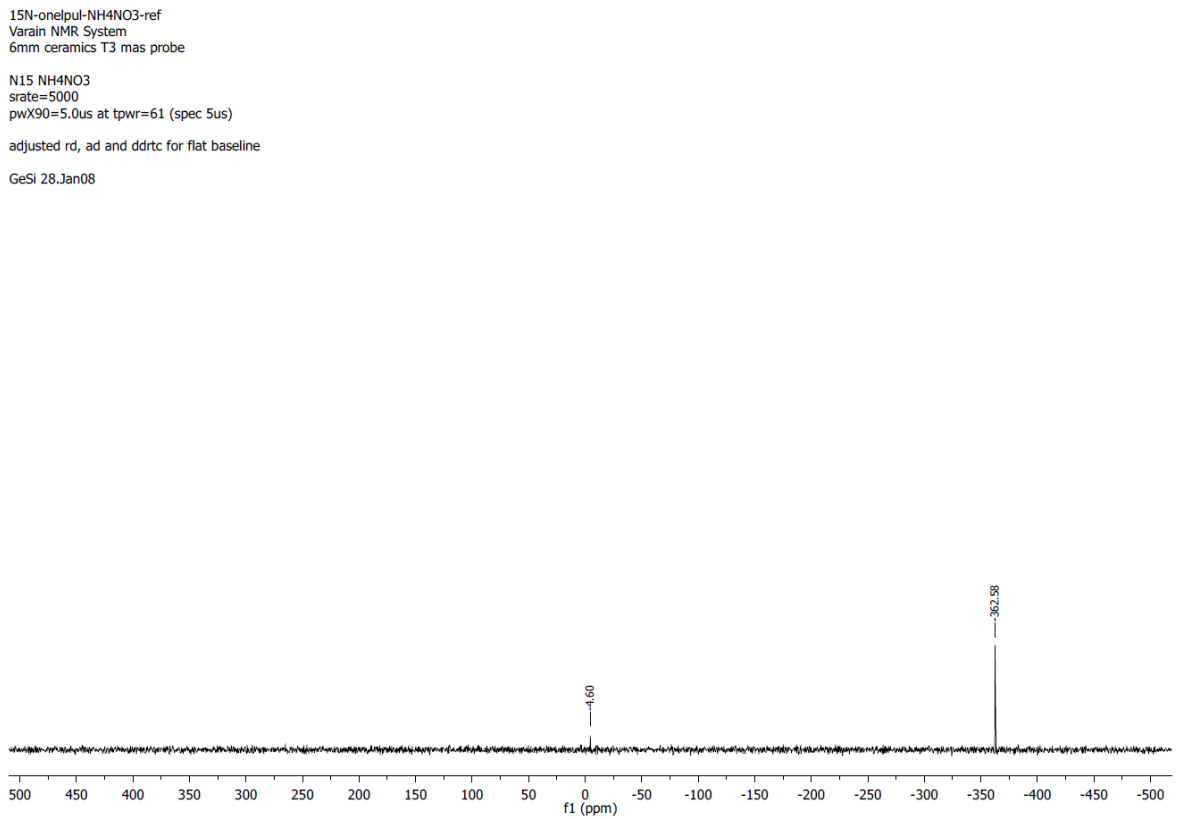

Figure D. 2: Baseline corrected solid state NMR spectrum of enriched $^{15}NH_4{}^{15}NO_3$ sample used as a background for analysis.

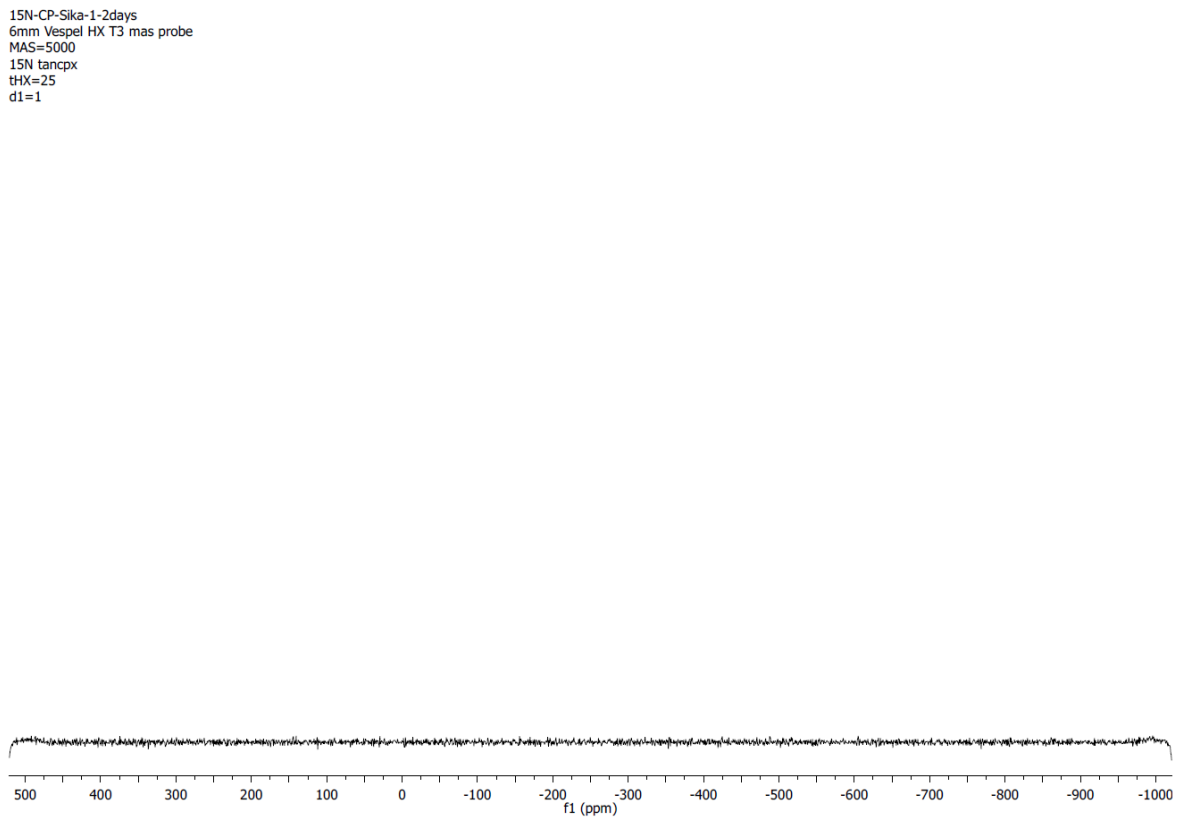

Figure D. 3: Solid state NMR spectrum of leached and air-dried pine wood biochar with enriched 10 atom% $^{15}NH_4{}^{15}NO_3$ after undergoing leaching in a column with a soil-biochar mixture for 30-days.